# University of KwaZulu-Natal

## College of Agriculture, Engineering and Science

### Howard College Campus

# INVESTIGATION OF THE EFFECTS OF THE PROCESS AND EQUIPMENT PARAMETERS ON THE SEPARATION EFFICIENCY OF A VIBRATING PLATE EXTRACTOR

Pavanisha Naidoo

This MSc. in Chemical Engineering Dissertation is submitted in fulfilment of the requirements for the MSc. (Engineering) in Chemical Engineering Degree, College of Engineering at the University of KwaZulu-Natal.

**Supervisor:** Prof. M. Carsky

**Co-supervisor**: Dr. S. Rathilal

**Date of Submission:** 14 December 2012

# UNIVERSITY OF KWAZULU-NATAL

## COLLEGE OF AGRICULTURE, ENGINEERING AND SCIENCE

## DECLARATION

I, ……. Pavanisha Naidoo ……., declare that

1. The research reported in this dissertation, except where otherwise indicated, is my original research.

2. This dissertation has not been submitted for any degree or examination at any other university.

3. This dissertation does not contain other persons' data, pictures, graphs or other information, unless specifically acknowledged as being sourced from other persons.

4. This dissertation does not contain other persons' writing, unless specifically acknowledged as being sourced from other researchers.  Where other written sources have been quoted, then:

   a. Their words have been re-written but the general information attributed to them has been referenced

   b. Where their exact words have been used, then their writing has been placed in italics and inside quotation marks, and referenced.

5. This dissertation does not contain text, graphics or tables copied and pasted from the Internet, unless specifically acknowledged, and the source being detailed in the dissertation and in the References sections.

Signature: ……………………….          Date: 14/12/2012

As the candidate's supervisor, I, Prof. M. Carsky, have approved this MSc. dissertation for submission.

Signature: ……………………….          Date: 14/12/2012

# ACKNOWLEDGEMENTS

# ABSTRACT

In the industrial world where many different types of separation processes are available, liquid-liquid extraction is gaining increasing attention, since it offers many advantages over distillation especially for heat sensitive and azeotropic compounds. Liquid-liquid extraction is an essential separation method that applies to the chemical, petroleum, metallurgy, biotechnology, nuclear and waste management related industries. This separation technique also offers potential means of saving energy, thus making extraction a more economical separation process.

The effectiveness of a vibrating plate extractor was previously investigated however limited research was conducted on the effect of tray spacing, solvent-to-feed ratio and agitation level on a vibrating plate extraction column. These parameters affect the hydrodynamics and mass transfer in a vibrating plate extraction column therefore the determination of the optimum process parameters is important in achieving the highest efficiency for the column and this is sought after for a vibrating plate extractor. A toluene-acetone-water system was selected for experimental work to be conducted on the vibrating plate extraction column. This test system for liquid-liquid extraction is a standard system proposed by the European Federation of Chemical Engineering.

The research aimed at testing the effect of tray spacing, agitation level (product of amplitude and frequency of vibration), and the ratio of flow rates of the phases on the number of stages in order to optimise the efficiency of a vibrating plate extraction column.

For the hydrodynamic experiments the dispersed phase holdup, drop size distribution and Sauter mean diameter were evaluated for varying parameters. For the mass transfer experiments the percentage acetone extracted, number of equilibrium stages, mass transfer coefficient and overall efficiency were determined as well as the dispersed phase holdup, drop size distribution and the Sauter mean diameter for varying parameters.

A decrease in the holdup occurred for an increase in the solvent-to-feed ratio and an increase in the agitation level resulted in a decrease in the Sauter mean diameter. Results indicated that lower tray spacing resulted in a higher extraction of acetone. Backmixing in the dispersed phase resulted in higher number of stages.

# TABLE OF CONTENTS

# LIST OF FIGURES

# List of Photographs

# LIST OF TABLES

# LIST OF SYMBOLS

| Symbol | Definition | Units |
|--------|-----------|-------|
| $\beta$ | Separation Factor | Dimensionless |
| $\mu$ | Viscosity | Pa.s |
| $\rho$ | Phase Density | kg/m$^3$ |
| $\bar{\rho}$ | Mean Density of Dispersion | kg/m$^3$ |
| $\Delta\rho$ | Density Difference, $(\rho_c - \rho_d)$ | kg/m$^3$ |
| $\Delta p$ | Pressure Drop | N/m$^2$ |
| $\delta$ | Plate Thickness | m |
| $\sigma$ | Interfacial Tension | N/m |
| $\varphi$ | Fractional Open Area of Plates | Dimensionless |
| $\psi$ | Power Dissipation per Unit Volume of Dispersion | W/m$^3$ |
| $\epsilon$ | Mechanical Power Dissipation per Unit Mass | W/kg |
| $\phi$ | Volume Fraction Holdup of Dispersed Phase | Dimensionless |
| $\emptyset 1$ | Constant | Dimensionless |

## Subscripts

| Symbol | Definition |
|--------|-----------|
| A | Carrier |
| c | Continuous Phase |
| C and B | Solute |
| d | Dispersed Phase |
| E | Extract Phase |
| e | Effective |
| F | Feed |
| R | Raffinate Phase |

# **NOMENCLATURE**

| Symbol | Definition | Units |
|---|---|---|
| $A_{in}$ | Interfacial Surface Area | m$^2$ |
| $a$ | Vibration Amplitude (Half-Stroke) | m |
| $a_i$ | Specific Interfacial Area | m$^2$ |
| C$^*$ | Solute Concentration at Equilibrium | mol/m$^3$ |
| C$^\circ$ | Solute Concentration in a Phase in Equilibrium with Other Phases in the System | mol/m$^3$ |
| C$_E$ | Solute Concentration in Bulk Extract Phase | mol/m$^3$ |
| C$_i$ | Solute Concentration in a Phase Adjacent to the Interface | mol/m$^3$ |
| C$_o$ | Discharge Coefficient Through the Perforations | Dimensionless |
| $C_\Pi$ | Parameter in Equation 2.21 | Dimensionless |
| $C_\Psi$ | Parameter Allowing for the Effect of Mass Transfer on the Drop Size | Dimensionless |
| $C_\Omega$ | Parameter in Equation 2.21 | Dimensionless |
| C$_R$ | Solute Concentration in Bulk Raffinate Phase | mol/m$^3$ |
| D$_C$ | Column Diameter | m |
| d | Drop Equivalent Sphere Diameter | m |
| d$_{32}$ | Sauter (Volume-Surface) Mean Drop Diameter | m |
| d$_o$ | Plate Perforations Diameter | m |
| E | Extarction Factor | Dimensionless |
| e | Fractional Free Cross Sectional Area | Dimensionless |
| $f$ | Vibration Frequency | Hz |
| F$_A$ | Mass or Molar Feed Rate of Carrier (Component A) | kg/h or kmol/h |
| g | Gravitational Acceleration | m/s$^2$ |
| $H_{ox}$ | True Height of a Transfer Unit | m |
| HETS | Height Equivalent to a Theoretical Stage | m |
| h | Plate Spacing (Centre to Centre) | m or mm |
| K | Overall Mass Transfer Coefficient | m/s |
| K$_A$ | Distribution Coefficient of Component A in Equilibrium | Dimensionless |
| K$_C$ | Distribution Coefficient of Component C in Equilibrium | Dimensionless |
| $K'_{D_\iota}$ | Equilibrium Ratio in Mole/Mass Ratio Compositions for Liquid-Liquid Equilibria | Dimensionless |
| $K_1$ | Drop Circulation Constant | Dimensionless |
| $K_D$ | Equilibrium Ratio for Liquid-Liquid Equilibria | Dimensionless |
| $k_E$ | Film Mass Transfer Coefficient for Extract Phase | m/s |
| K$_{eq}$ | Equilibrium Ratio | Dimensionless |
| $k_R$ | Film Mass Transfer Coefficient for Raffinate Phase | m/s |
| L | Ratio (U$_d$/U$_c$) | Dimensionless |

| | | |
|---|---|---|
| $m1$ | Index | Dimensionless |
| n | Index | Dimensionless |
| $N_f$ | Solute Flux | m/s |
| $N_{ox}$ | True Overall Number of Transfer Units based on $x$ Phase | Dimensionless |
| $N_{oxm}$ | Measured Number of Transfer Units based on $x$ Phase | Dimensionless |
| $N_{oxp}$ | Apparent Number of Transfer Units based on $x$ Phase | Dimensionless |
| $n1$ | Index | Dimensionless |
| q | Backmixing Coefficient Between Adjacent Stages | Dimensionless |
| $q_e$ | Effective Coefficient of Longitudinal Mixing | Dimensionless |
| Re | Reynolds Number | Dimensionless |
| S | Solvent Flow Rate | kg/h or kmol/h |
| t | Coefficient | m/s |
| $U_c$ | Superficial Velocity of Continuous Phase | m/s |
| $U_d$ | Superficial Velocity of Dispersed Phase | m/s |
| $U_*$ | Velocity | m/s |
| $u_k$ | Characteristic Velocity | m/s |
| $u_s$ | Slip Velocity | m/s |
| $v_s$ | The superficial velocity of the continuous phase relative to the dispersed phase | m/s |
| X | Mass or Mole Ratio | Dimensionless |
| $x$ | Mass or Mole Fraction | Dimensionless |
| $x_A$ | Mass or Mole Fraction of Component A | Dimensionless |
| $x_C$ | Mass or Mole Fraction of Component C | Dimensionless |
| z or H | Column Height | m or mm |

# CHAPTER 1: INTRODUCTION

In an industrial world where many different types of separation processes are available, liquid-liquid extraction is gaining increasing attention, since it offers many advantages over distillation especially for heat sensitive and azeotropic compounds (Rocha et al., 1986). Liquid-liquid extraction is a key separation method that applies to the chemical, petroleum, metallurgy, biotechnology, nuclear and waste management associated industries, (Usman et al., 2008 and Tsouris et al., 1994). This separation technique also offers potential means of saving energy, thus making extraction more economical separation process (Usman et al., 2008).

Liquid-liquid extraction is a mass transfer operation in chemical engineering, which is also known as solvent extraction. Liquid-liquid extraction utilizes an added substance (solvent) as a method of separating components of a solution (Treybal, 1963). The extraction process depends on the transfer of solute by diffusion from the feed mixture into the pure solvent. The solute transfer is completed once thermodynamic equilibrium is achieved between the two phases (Camurdan, 1986).

The first reciprocating plate extraction column was developed in 1935 by Van Dijck (1935) for the liquid-liquid extraction separation process. Prochazka and his co-workers (Lo & Prochazka, 1983) developed (industrially in Czechoslovakia) the vibrating plate extraction (VPE) column which is a type of reciprocating plate extraction column that has a different plate design. The vibrating plate extraction column features small perforations and a downcomer, in order to facilitate the movement of the continuous phase. The VPE plates compared to the other types of reciprocating plate extraction columns can operate at higher frequencies and lower amplitudes (Lo et al., 1992).

The effectiveness of a vibrating plate extractor was previously investigated however limited research was conducted on the effect of tray spacing, solvent-to-feed ratio and agitation level (product of amplitude and frequency of vibration) on a vibrating plate extraction column (Rathilal, 2010). These parameters affect the hydrodynamics and mass transfer in a vibrating plate extraction column. Therefore the determination of the optimum process parameters is important in achieving the highest efficiency for the column and this is sought after for a vibrating plate extractor.

The research aim and objective was to test the effect of tray spacing, frequency and amplitude of plate vibrations, and the ratio of flow rates of the phases on the number of stages in order to optimise the efficiency of a vibrating plate extraction column. The effects of the agitation level, solvent to feed ratio, and the plate spacing on the mass transfer in the vibrating plate extractor was investigated experimentally and the results were compared with the recently published correlations.

This research project on the investigation of the effects of the process and equipment parameters on the separation efficiency of a vibrating plate extractor focuses on the literature review pertaining to the research topic, the experimental work conducted and the results obtained from the experimental work as well as a discussion of the results.

# CHAPTER 2: LITERATURE REVIEW

## 2. Liquid-Liquid Extraction

### 2.1. Introduction to Liquid-Liquid Extraction

Liquid-liquid extraction is a mass transfer operation in chemical engineering, which is also known as solvent extraction. Liquid-liquid extraction utilizes an added substance (solvent) as a method of separating components of a solution. This type of separation technique is attractive compared to other separation techniques due to the ability of liquid-liquid extraction to make separations according to chemical type (Treybal, 1963).

The liquid-liquid extraction process is operated at near atmospheric pressure and ambient temperature (Humphrey & Keller, 1997). For liquid-liquid extraction to be feasible the following are required (Humphrey & Keller, 1997):

- The component to be removed from the feed mixture must preferentially distribute in the solvent.
- The feed and solvent phases must be considerably immiscible.

### 2.2. Industrial Applications of Liquid-Liquid Extraction in Chemical Processes

Liquid-liquid extraction is an important separation method that applies to the chemical, petroleum, metallurgy, biotechnology, nuclear and waste management related industries (Tsouris et al., 1994 and Usman et al., 2008).

Liquid-liquid extraction is of use in the following cases (Treybal, 1963 and Humphrey & Keller, 1997):

- An alternative means of separation when distillation, evaporation or forms of crystallization are costly or when these separation techniques are impractical.
- For the separation of close-boiling liquids.
- For the separation of liquids of poor relative volatility.
- An alternative to high-vacuum or molecular distillation, for mixtures that can only be separated in this manner due to the extremely high boiling points.
- An alternative for expensive evaporation and fractional crystallization.
- Effective for the separation of heat sensitive substances.
- Separation of mixtures that form azeotropes.
- Separation of mixtures according to chemical type, in cases where boiling points overlap.

## 2.3. <u>Advantages of Liquid-Liquid Extraction</u>

The following show advantages of liquid-liquid extraction (Humphrey & Keller, 1997 and Schulz, 2009):

- ➢ Used to separate azeotropes and components with overlapping boiling points.
- ➢ Reasonably large capacities are probable with low energy consumption (for example: separation of paraffin's and aromatics in the oil industry).
- ➢ Selectivity, especially when other common separation techniques (such as rectification) are unsuccessful or require expensive equipment or incur additional energy costs.
- ➢ Heat sensitive products (in food and pharmaceutical industries) are produced at ambient or moderate temperatures.
- ➢ Separation of small materials with high boiling impurities, generally in aqueous solutions. In the normal thermal separation technique, the complete water content has to be withdrawn by a very energy-intensive evaporation process.

## 2.4. <u>Disadvantages of Liquid-Liquid Extraction</u>

The following indicate disadvantages of liquid-liquid extraction (Treybal, 1963 and Humphrey & Keller, 1997):

- ➢ The added substance (solvent) is chemically different, due to the requirement that it be insoluble with the original solution, therefore the solvent complicates the selection of materials of construction to ensure corrosion resistance.
- ➢ Large capital expenses incurred as a result of large quantity of solvent required.
- ➢ Cost expenses incurred for a solvent-recovery system.
- ➢ Contamination of the ultimate product since it contains the solvent.

## 2.5. <u>Counter-Current Extraction</u>

The most basic extraction system comprises of the following components (Fair & Humphrey, 1983 and Seader & Henley, 2006):

*Solute* – Is a liquid component to be separated from a liquid mixture.

*Solvent* – Is a pure compound, which is miscible with one of the components in the feed mixture. The solvent is used to selectively extract a component from a liquid mixture.

*Carrier* – Non-solute portion of the liquid mixture to be separated.

The following diagram depicts a basic counter-current extraction process with a feed mixture comprising of liquid components A (Solute) and B (Carrier), and a pure solvent (S):
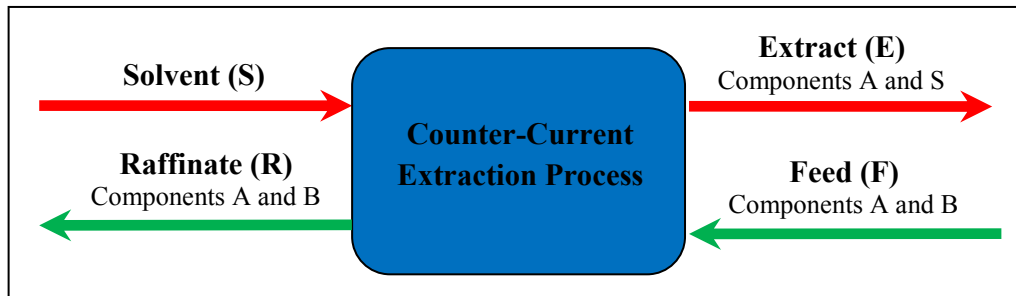


***Figure 2.1: Basic counter-current extraction process (Adapted from Seader & Henley, 2006).***

The extraction process depends on the transfer of solute by diffusion from the feed mixture into the pure solvent. The solute transfer is completed once thermodynamic equilibrium is achieved between the two phases. When the two phases are separated, the original feed mixture which is now lean in solute concentration is referred to as the raffinate and the phase which is rich in solute concentration is referred to as the extract (Camurdan, 1986).

*Light phase*: is regarded as the phase with the lower density. The light phase flows up the extraction column and accumulates at the top of the extraction column (Rathilal, 2010).

*Heavy phase*: is regarded as the phase with a higher density. The heavy phase flows down the extraction column and accumulates at the bottom of the extraction column (Rathilal, 2010).

In a liquid-liquid extraction column two phases are distinguishable, the dispersed and continuous phases. The dispersed phase is the phase that flows through a distributor/sparger which produces droplets in the column. The continuous phase is the phase that flows in bulk without the formation of droplets. The continuous and dispersed phases are both depicted in Figure 2.2. (Baird & Lane, 1973 and Shen et al., 1985).
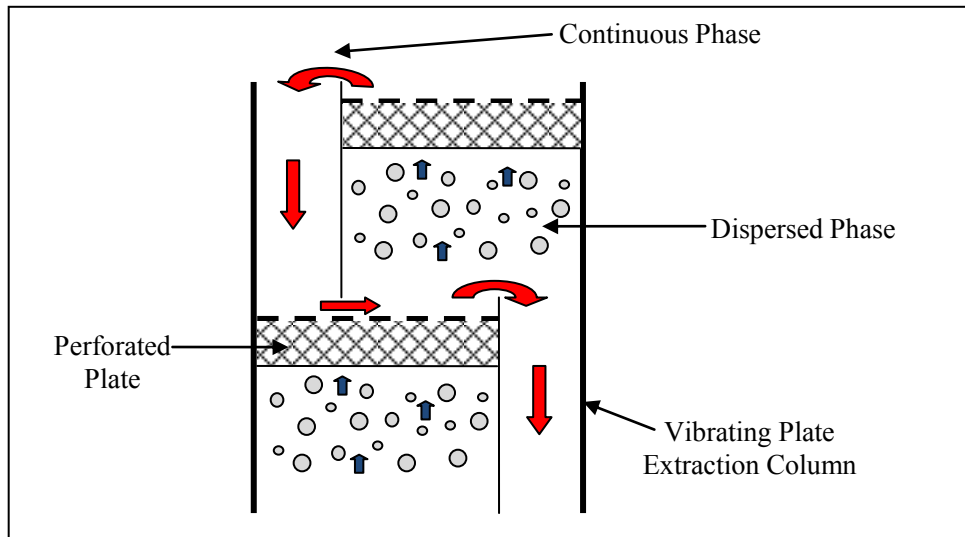
***Figure 2.2: Counter-current flows of two phases across perforated plates in an extraction column (Adapted from Fair & Humphrey, 1983).***

The wettability of a liquid with the internals of the extraction column determines which liquids from the standard test system would be considered as the continuous and dispersed phases in the separation process. The organic phase (dispersed phase) has a preferred wettability to Teflon, whereas the aqueous phase (continuous phase) has a preferred wettability to stainless steel as indicated by investigations conducted by Baird & Lane, (1973) and Shen et al., (1985).

Lisa et al., (2003) recommend that the phase which contains the lowest equilibrium concentration (which is the phase with higher resistance) should be selected as the continuous phase, since it would result in more intensive mixing.

## 2.6. **Thermodynamic and Mass Transfer Principles**

### 2.6.1. **Thermodynamic Principles**

The separation of components by liquid-liquid extraction is dependent on the distribution of the solute between two liquids, which includes the solvent and carrier. Thus the solute transfer is concluded after thermodynamic equilibrium is established between the two phases (Schweitzer, 1997 and Camurdan, 1986)

Ternary phase diagrams are plotted on Gibbs equilateral triangle, where the vertices of the triangle represent the pure components of the test system, the edges characterise the binary mixtures and the points within the ternary phase diagram indicate the ternary mixture (Thornton, 1992).

Five different ternary phase systems exist (Novak et al., 1987), but three were selected to be discussed in detail; the simplest ternary system is Type I system depicted in Figure 2.3, for this system the carrier and the solvent are immiscible, while the carrier-solute and solvent-solute pairs are miscible. Figure 2.3 (Type I system) indicates two different regions: a single-phase and two-phase region. In order to obtain feasible extraction, compositions must lie within the two-phase envelope (Fair & Humphrey, 1983; Thornton, 1992 and Humphrey & Keller, 1997).

The plait point is the critical point where the two branches of the phase boundary (binodal curve) meet. Therefore the plait point is the intersection of the raffinate phase and extract phase boundary curve. At the plait point, no separation can be achieved. The tie lines connect the extract and raffinate equilibrium compositions and therefore used to determine the equilibrium ratio, $K_{eq}$ and separation factors (Fair & Humphrey, 1983; Thornton, 1992 and Humphrey & Keller, 1997).

The concept of the separation factor is thus used, where this factor utilizes the equilibrium ratio, $K_{eq}$. The separation factor is similar to the relative volatility required for distillation processes. The separation factor is therefore indicated by Equation (2.1) (Thornton, 1992):

$$\beta_{CA} = \frac{K_C}{K_A} \qquad \qquad \text{... (2.1)}$$

$K_{eq}$ represents the equilibrium ratio, where $K_C$ and $K_A$ indicates the distribution of the solute in equilibrium and the distribution of the carrier in equilibrium respectively. The equilibrium ratios for the solute and the carrier are given by Equation (2.2).

$$K_C = \frac{x_{C\,(extract)}}{x_{C\,(raffinate)}} \qquad \text{and} \qquad K_A = \frac{x_{A\,(extract)}}{x_{A\,(raffinate)}} \qquad \text{...(2.2)}$$
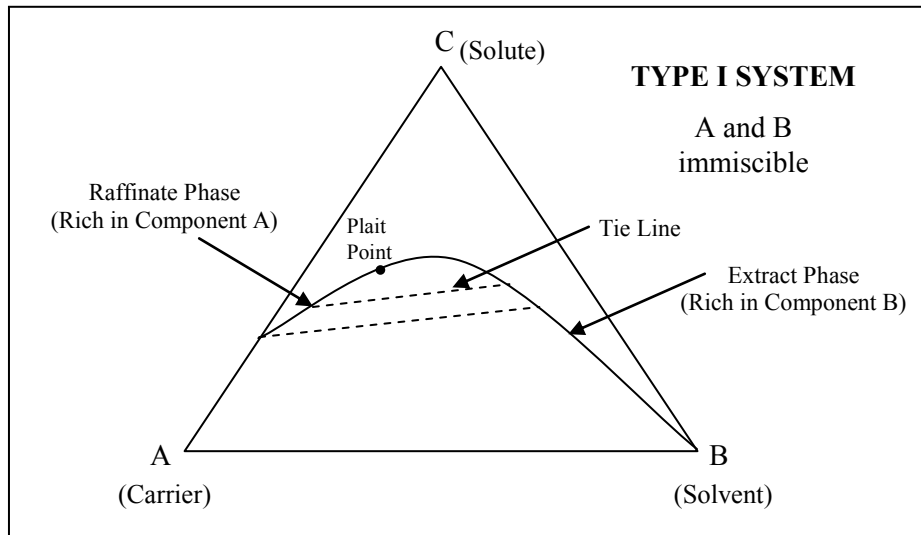
***Figure 2.3: Ternary liquid-liquid Type I system. (Adapted from Fair & Humphrey, 1983).***

The Type II system is another type of ternary liquid-liquid system in which there are two partially miscible binary pairs, (where there are immiscibility's between the solvent and the solute and between the solvent and carrier). Figure 2.4 shows tie lines and no plait point, with this type of ternary liquid-liquid system; it is possible to obtain an extract that is free of carrier, which is not achievable with Type I systems (Thornton, 1992 and Fair & Humphrey, 1983).
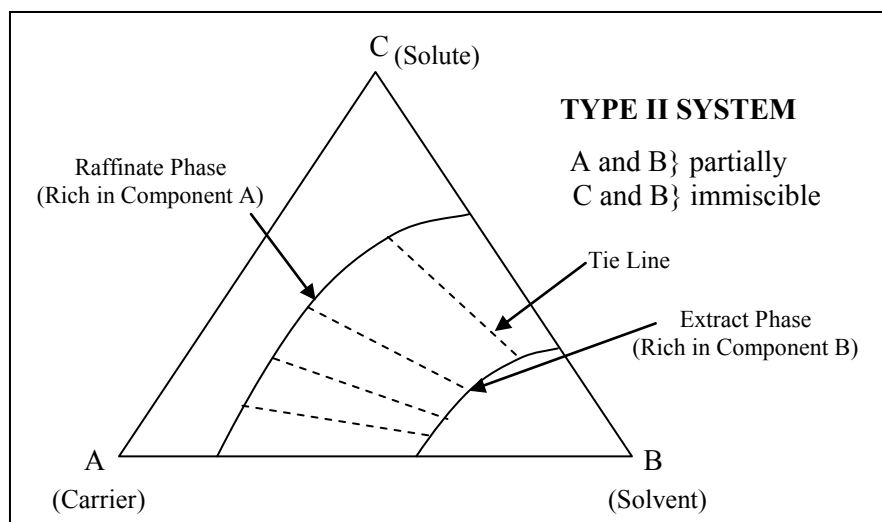


***Figure 2.4: Ternary liquid-liquid Type II system (Adapted from Fair & Humphrey, 1983).***

Lastly there is Type III system, in which immiscibility's exist among all three pairs, but Type III systems are relatively rare in extraction process design (Fair & Humphrey, 1983).

## 2.6.2. **Mass Transfer Principles**

### 2.6.2.1. **Two-Film Theory**

For the process of liquid-liquid separation, mass transfer resistances in both phases need to be considered. Therefore the two-film theory is used to explain the mass transfer mechanism in the extraction process, where the solute is transferred between two liquid phases (raffinate and extract phases). This mass transfer theory suggests that each thin film layer presents a resistance to mass transfer and that the two phases are in equilibrium at the liquid-liquid interface, therefore there is no resistance to mass transfer at the liquid-liquid interface. Due to eddy and molecular diffusion, the concentrations in the bulk phases are assumed to be uniform. Figure 2.5 illustrates the concentration gradients in interphase mass transfer (Humphrey & Keller, 1997; Schweitzer, 1997 and Seader & Henley, 2006).
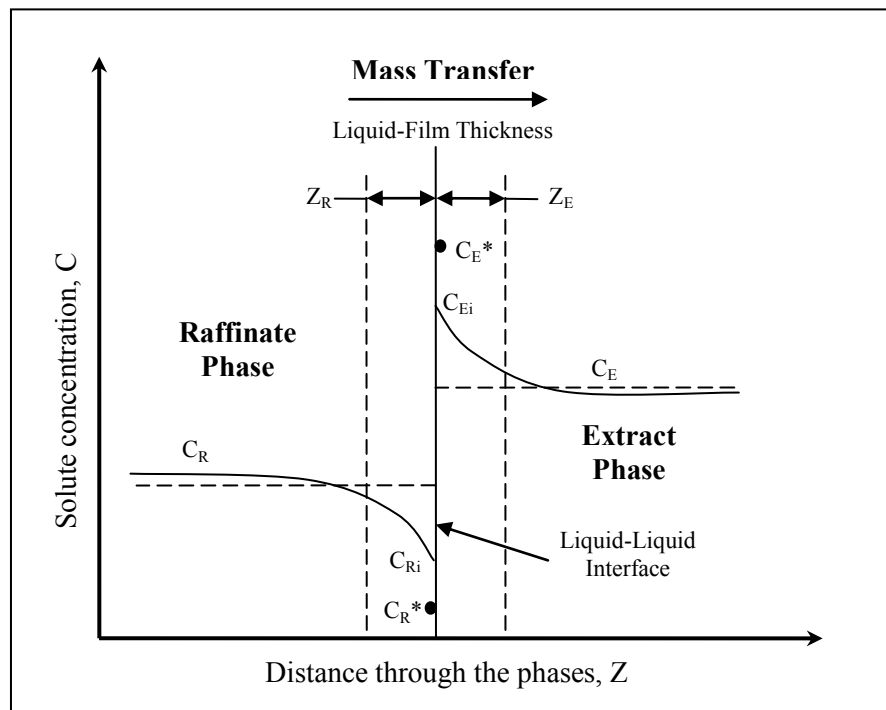


*Figure 2.5: Concentration profiles in interphase mass transfer (Adapted from Schweitzer, 1997).*

Lisa et al., (2003) research involved using an improved Lewis extraction cell to establish the existence of interfacial resistances and established that for the water-acetone-toluene system a significant resistance around the magnitude of $10^4$ s/cm exists. The research conducted thus indicates that an interfacial resistance does exist.

2.6.2.2. **Rate of Mass Transfer**

The following Equations (2.3) and (2.4) describe the rate of mass transfer of the solute from the bulk solution of A to the bulk solution of B, using $k$, which is the film mass transfer coefficient for a particular phase (Schweitzer, 1997):

$$N_f = k_R A_{in}(C_R - C_{Ri}) = k_E A_{in}(C_{Ei} - C_E) \qquad \qquad ... (2.3)$$

$$N_f = k_R A_{in}(C_R - C^{\circ}_R) = k_E A_{in}(C^{\circ}_E - C_E) \qquad \qquad ... (2.4)$$

Equation (2.5) was established by combining Equations (2.3) and (2.4), where m is the slope of the equilibrium curve. This equation relates the overall mass transfer coefficient to the individual film mass transfer coefficients (Schweitzer, 1997).

$$\frac{1}{K_R} = \frac{1}{k_R} + \frac{1}{mk_E} \qquad \qquad ... (2.5)$$

The precise mechanism describing the interphase mass transfer for liquid-liquid extraction is more complex than the simplified approach described above, since the rate of mass transfer in extraction columns is greatly influenced by other factors.

These factors include the hydrodynamics of interfacial turbulence, droplet coalescence and re-dispersion. Nevertheless, the two-film theory still applies, in order to obtain the parameters affecting the rate of mass transfer in the extraction separation process (Pratt, 1983a; Laddha & Degaleesan, 1983 and Schweitzer, 1997).

### 2.6.2.3. __Factors Affecting Rate of Mass Transfer__

a) _Mass Transfer Coefficients_

The following factors influence the mass transfer coefficient (Lo & Baird, 1994 and Schweitzer, 1997):

- Phase Composition: govern the diffusivity and results in interfacial turbulence
- Temperature: affects the diffusion rates
- Degree and Type of Agitation: affects the film thickness and the interfacial turbulence
- Direction of Mass Transfer: depends on the dispersed phase
- Physical Properties of the components of the Test System: some of these include the densities, viscosities, interfacial tension, etc.

b) _Interfacial Area_

The interfacial area relies on the following factors (Lo & Baird, 1994 and Schweitzer, 1997):

- Phase Composition: which affects the phase densities and interfacial tension
- Temperature: influences the interfacial tension
- Degree and Type of Agitation: by generating a more intimate dispersion of two phases
- Phase Ratio
- Physical Properties of the System: example, interfacial tension, etc.

c) _Concentration Driving Force_

The following factors affect the concentration driving force (Lo & Baird, 1994 and Schweitzer, 1997):

- The solute bulk concentration of the two phases
- Distribution Coefficient: affects $C_{Ri}$ and $C_{Ei}$
- Temperature: influences the distribution coefficient

### 2.6.2.4. **Mass Transfer Equations and Balances**

The following Figure 2.6 depicts the counter-current flow for a ternary liquid-liquid system which is used to develop the equations for mass transfer.
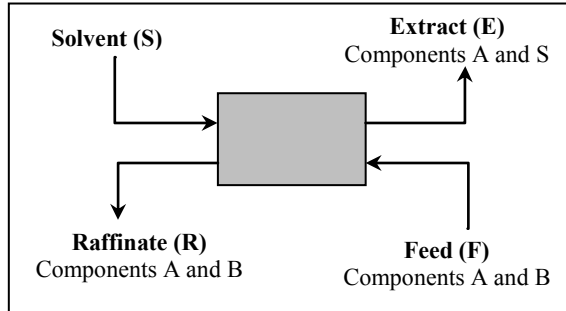


*Figure 2.6:Counter-current flow for a ternary liquid-liquid system (Adapted from Seader and Henley, 2006).*

*Component A represents the carrier and component B represents the solute.*

For the ternary liquid-liquid system mass balance, a mass or mole ratio of component $i$, $X_i$ is used which is related to the mass or mole fractions, $x_i$, as indicated in Equation (2.6) (Seader & Henley, 2006).

$$X_i = \frac{x_i}{(1-x_i)} \qquad\qquad ... (2.6)$$

Using Figure 2.6, the solute (component B) material balance is given by the following Equation (2.7) (Seader & Henley, 2006):

$$X_B{}^{(F)} F_A = X_B{}^{(E)} S + X_B{}^{(R)} F_A \qquad\qquad ... (2.7)$$

At equilibrium the distribution of solute is indicated by Equation (2.8), where the distribution coefficient of the solute, $K'_{D_i}$, relates $K_D$ and the mass/mole fractions given by Equation (2.9), (Seader & Henley, 2006).

$$X_B{}^{(E)} = K'_{D_B} X_B{}^{(R)} \qquad\qquad ... (2.8)$$

$$K'_{D_i} = \frac{x_i{}^{(1)}/(1-x_i{}^{(1)})}{x_i{}^{(2)}/(1-x_i{}^{(2)})} = K_D \left(\frac{1-x_i{}^{(2)}}{1-x_i{}^{(1)}}\right) \qquad ... (2.9)$$

By substituting Equation (2.8) into Equation (2.7), $X_B^{(E)}$, the mass or mole ratio for the solute in the extract phase is eliminated, thus resulting in the following Equation (2.10) (Seader & Henley, 2006):

$$X_B^{(R)} = \frac{X_B^{(F)} F_A}{F_A + K_{D_B}' S} \qquad \text{... (2.10)}$$

For convenience, an extraction factor for the solute, E, is introduced which is shown in Equation (2.11) (Seader & Henley, 2006). A larger value for the extraction factor, results in a greater extent to which the solute is extracted. Large extraction factor values are due to large distribution coefficient values or due to large solvent to carrier ratios (Seader & Henley, 2006).

$$E_B = \frac{K_{D_B}' S}{F_A} \qquad \text{... (2.11)}$$

The fraction of solute (component B) that is not extracted is given by Equation (2.12), by substituting Equation (2.11) into Equation (2.10). This Equation (2.12) indicates that the larger the extraction factor of the solute, the smaller the fraction of solute not extracted (Seader & Henley, 2006).

$$\frac{X_B^{(R)}}{X_B^{(F)}} = \frac{1}{1 + E_B} \qquad \text{... (2.12)}$$

## 2.7. <u>**Commercial Extractors**</u>

### 2.7.1. <u>**Classification of Commercial Extractors**</u>

Extractors or contactors can be categorised according to the techniques applied for the interdispersing phases and creating the counter-current flow configuration. Both of these conditions, can be attained either by gravity acting on the density difference between the phases or by applying a centrifugal force (Lo & Baird, 1994). Thus Figure 2.7 shows the classification of major types of commercial liquid-liquid extractors.
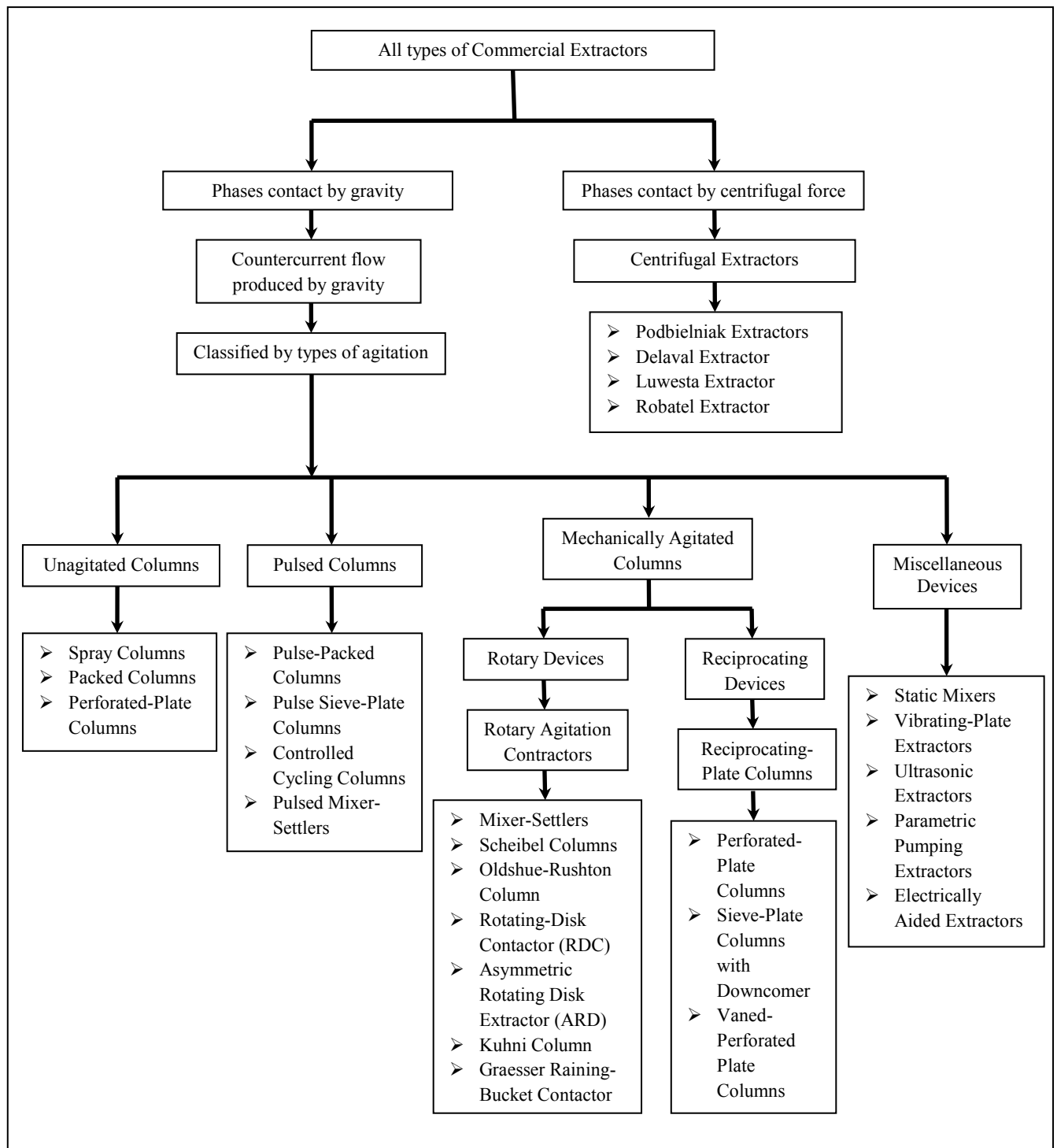
*Figure 2.7: Classification of Commercial Extractors. (Adapted from Lo & Baird, 1994).*

For liquid-liquid extraction processes, various types of commercial extractors exist. Some of these extractors include discrete-stage mixer-settlers in which the phases for extraction are repeatedly mixed and separated; differential columns in which the concentration gradients are continuous; then there are multi-compartment cell-type columns with and without agitation; and centrifugal contactors, which may be either a mixer-settler or differential type to name a few (Thornton, 1992).

Brief classification of different types of commercial extractors is given in Table 2.1, together with general indications of the range of industrial applications of each type of extractor (Adapted from Thornton, 1992).

*Table 2.1: Classification and Range of Applications of Different Commercial Extractors*

| Classification and Type | Industrial Applications* |
|---|---|
| **A. Gravity-Separated Extractors** | |
| a. Continuous-Contact (i.e. Differential) | |
|    *1. Non-Mechanical Columns* | |
|      (i) Spray columns | CR |
|      (ii) Baffle-Plate Columns | C, P |
|      (iii) Packed Columns | C, P, N |
|    *2. Mechanically-Agitated Columns* | |
|      (i) Pulsed Packed Columns | C, P |
|      (ii) Raining Bucket (Graesser RTL) Contactor | C |
| b. Discontinuous (i.e. Stagewise) Contact, no interstage settling | |
|    *1. Rotary Agitated Columns* | |
|      (i) Rotary Disc Column (RDC) | C,P |
|      (ii) Multi-impeller Columns | C, P, M |
|    *2. Reciprocating Types* | |
|      (i) Pulsed Perforated Plate Column | C, P, Ph, M, N |
|      (ii) Oscillating Plate (Karr) Column | C, P, Ph |
| c. Discontinuous (Stagewise) Contact, with interstage settling | |
|    *1. Partial Settling* | |
|      (i) Scheibel Column | C, Ph |
|      (ii) Asymmetric Rotary Disc Column (ARDC) | C, Ph |
|    *2. Total Settling* | |
|      (i) Perforated Plate Column (with Downcomers or Risers) | P, C |
|      (ii) Rotary Film Column | M |
|      (iii) Vertical Mixer-Settlers | P, C, M |
|      (iv) Horizontal Mixer-Settlers | P, C, M, N |
| **B. Centrifugally-Separated Extractors** | |
| a. Continuous Contact | |
|    *1. Perforated Plate (Podbialniak)* | C, Ph, (N) |
|    *2. Film-Flow (de Laval)* | C, Ph, (N) |
| b. Mixer-Settler | |
|    *1. Luwesta* | C, Ph |
|    *2. Robatel* | C, Ph |

*Key for Industrial applications: C = Chemical Manufacture; CR = Fast Homogeneous Chemical Reaction Only; P = Petroleum Refining, Petrochemicals; Ph = Pharmaceutical; M = Hydrometallurgy; N = Nuclear

2.7.2. **Advantages and Disadvantages of Different Extractors**

Table 2.2 lists the advantages and disadvantages of various different types of extractors (Adapted from Lo, 1975; Schweitzer, 1997 and Seader & Henley, 2006).

*Table 2.2: Advantages and Disadvantages of Different Extractors*

| Class of Extractors | Advantages | Disadvantages |
|---|---|---|
| Mixer-Settlers | • Good contacting<br>• High-stage efficiency<br>• Handles wide flow ratio<br>• Low headroom<br>• Many stages available<br>• Consistent scale-up<br>• Good Flexibility<br>• Operable for high viscosity liquids | • Large holdup<br>• Large floor space<br>• High power costs<br>• High investment<br>• Interstage pumping may be required |
| Continuous, Counter-current Flow Contactors (No Mechanical Agitation) | • Low initial costs<br>• Low operating costs<br>• Simplest construction | • High headroom<br>• Sometimes low efficiency<br>• Difficult scale-up<br>• Limited throughput with small density difference<br>• Cannot handle high flow ratio |
| Continuous, Counter-current Flow Contactors (Mechanical Agitation) | • Reasonable costs<br>• Good dispersion<br>• Many stages possible<br>• Relatively easy scale-up | • Cannot handle emulsifying systems<br>• Cannot handle high flow ratio<br>• Limited throughput with small density difference |
| Centrifugal Extractors | • Low holdup volume<br>• Short holdup time<br>• Low space requirements<br>• Handles low-density difference between phases<br>• Small inventory of solvent | • High operating costs<br>• High initial costs<br>• High maintenance costs<br>• Limited number of stages in a single unit |

### 2.7.3.    **Comparison of Commercial Extractors Performance**

Stichlmair (1980) conducted an investigative comparative analysis of ten different counter-current extraction columns for a toluene-acetone-water system. Figure 2.8 illustrates his findings in terms of two key parameters: the apparent number of stages per unit length related to the extractor capacity ($m^3/m^2$.h).
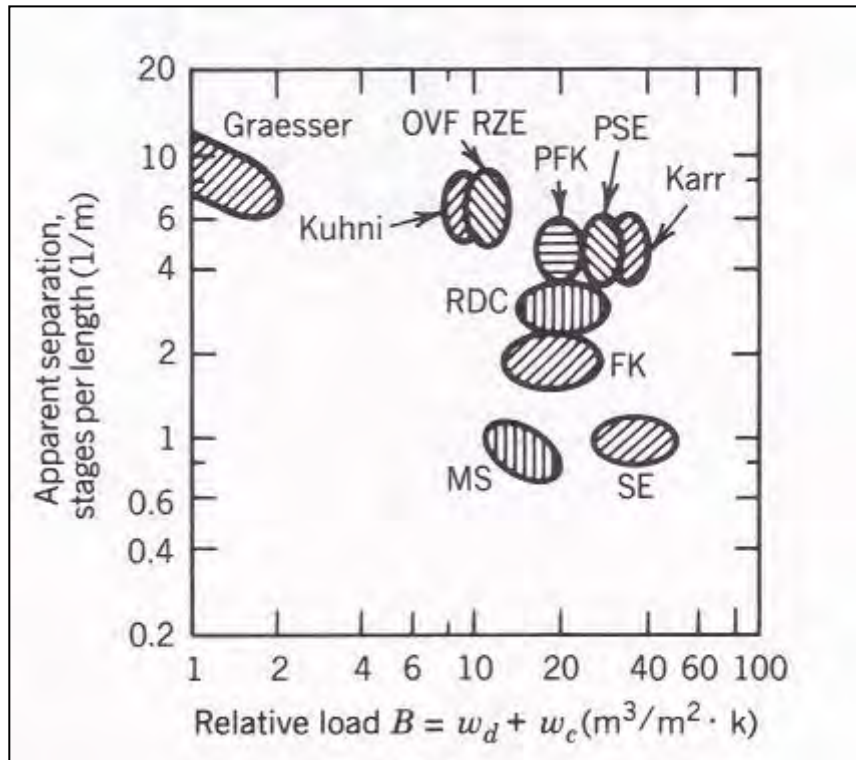


***Figure 2.8: A comparative performance of different extraction columns for a toluene-acetone-water system (Adapted from Stichlmair, 1980 and Rousseau, 1987).***

From Figure 2.8, results for the mixer-settler indicate that the system was operating at approximately 100% efficiency. The Karr extraction column (type of reciprocating plate extraction column) and the static perforated plate column was found to give the highest capacities for this ternary liquid-liquid system, but results also indicated that the Karr extraction column exhibited significantly lower HETP values. The performance of the other types of mechanically agitated extraction columns were found to be close to that of the Karr extraction column, but with slightly lower capacities.

The following Table 2.3 gives the HETP values of several types of mechanically aided extraction columns (Holmes et al., 1987; Karr and Ramanujam, 1987 and Humphrey & Keller, 1997).

*Table 2.3: Efficiencies of Mechanically Aided Extractors.*

| Type of Extractor | Chemical System | HETP (ft) |
|---|---|---|
| Reciprocating Plate | Toluene-Acetone-Water | 0.5 – 1 |
| Reciprocating Plate | Methyl isobutyl ketone-Phenol-Water | 2 – 6 |
| Rotating-Disc Contactor | Toluene-Acetone-Water | 0.5 – 2 |
| York-Scheibel | Toluene-Acetone-Water | 0.3 – 0.8 |
| Centrifugal | Toluene-Acetone-Water | 0.6 |

Humphrey & Keller (1997) also illustrates a graph similar to Figure 2.8 shown in Figure 2.9 that relates the efficiency to the total flow for numerous types of liquid-liquid extraction columns. Humphrey & Keller (1997) indicate that when six or more stages are required, mechanically aided extractors should be considered.



Total Flow ($U_c + U_d$) (ft/h)
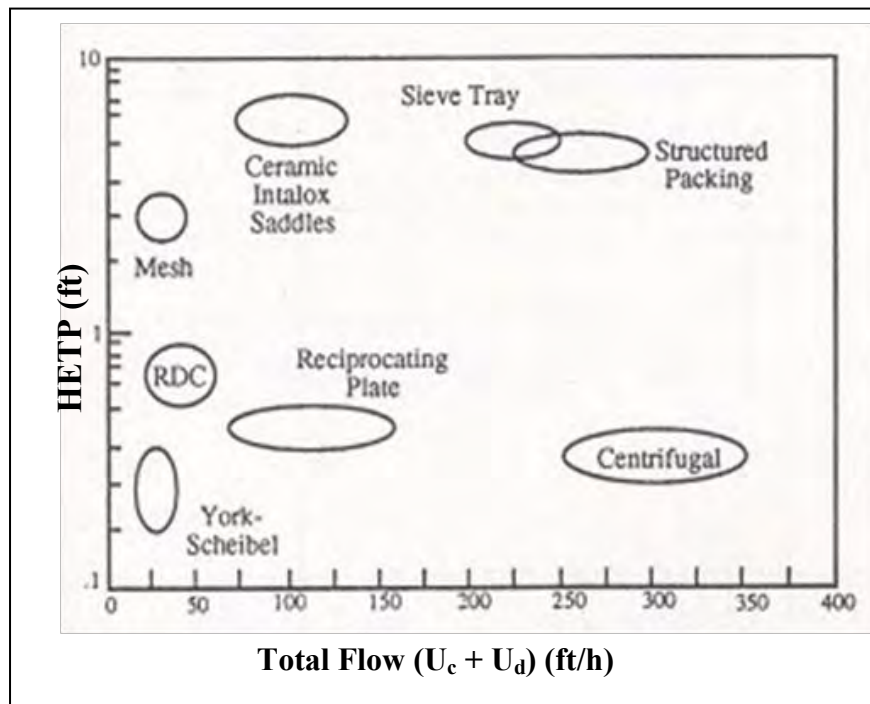
***Figure 2.9: Efficiency versus Total Flow (Capacity) for several extractors (Adapted from Humphrey and Keller, 1997).***

## 2.8. <u>**Vibrating Plate Extraction Columns (VPE)**</u>

The first reciprocating plate extraction column (RPC) was developed in 1935 for the liquid-liquid extraction separation process and in industry three different types of RPC's are used (Van Dijck, 1935). The Union of Soviet Socialist Republics developed the Karr column, the vibrating plate extraction column and the vaned-perforation plate column (KRIMZ and GIAP).

All three types of reciprocating plate columns operate on the same principles, but they vary in terms of their design characteristics. The reciprocating plate extraction columns have a stack of perforated plates mounted on an upright shaft driven by a vibrating motor above the vibrating plate extraction column as a common feature (Lo et al., 1992)

### 2.8.1. <u>**Introduction to Vibrating Plate Extraction Columns**</u>

Prochazka and his co-workers developed industrially in Czechoslovakia the vibrating plate extraction (VPE) column which is type of reciprocating plate extraction column that has a different plate design (Lo & Prochazka, 1983). The vibrating plate extraction column features small perforations and a downcomer, in order to facilitate the movement of the continuous phase as depicted in Figure 2.10. The Prochazka RPC plate has a fractional open plate area around 0.04 to 0.3 excluding the downcomer and perforation diameter around 2 to 5 mm (Lo et al., 1992)
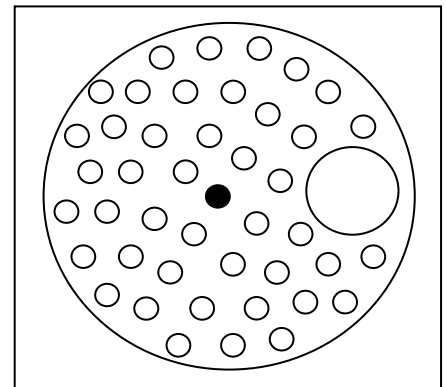


*Figure 2.10: Prochazka RPC Plate (Adapted from Lo et al., 1992).*

Figure 2.11 indicates the other types of RPC plates used in industry besides the Prochazka plate shown in Figure 2.10. A tube or an opened section of the plate represents the downcomer, (Lo et al., 1992). The vibrating plate extractor which is also known as the Prochazka plate functions in the mixer-settler hydrodynamic regime or, if the VPE is operated at greater agitation rates, operates in the emulsion hydrodynamic regime (Lo et al., 1992).

The VPE plates compared to the other types of reciprocating plate extraction columns can operate at higher frequencies and lower amplitudes. These types of RPC's have been ustilised in industry in columns up to 1.2 m in diameter.

| a) Karr RPC Plate | b) KRIMZ RPC Plate | c) GIAP II RPC Plate |
|---|---|---|
| *Fractional Open Plate Area =0.5 to 0.6* | *Fractional Open Plate Area ≈ 0.45* | *Fractional Open Plate Area ≈ 0.45* |
| *Perforation Diameter = 10 to 16mm* | *Vaned Rectangular Perforations* | *(excluding downcomer)* |
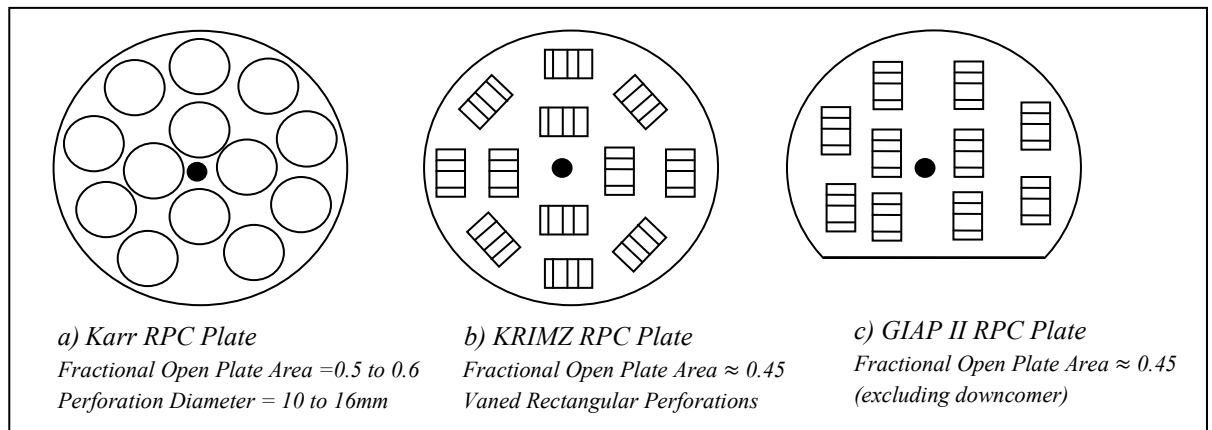
***Figure 2.11: Other two types of RPC plates used in industry. (Adapted from Lo et al., 1992).***

The RPC with perforated plates and downcomers (VPE) could use a segmental downcomer for large columns instead of the tubular downcomer. Prochazka et al., (1971) research reports that as a result of drops formed from the small perforations a considerably uniform dispersion is formed.

The amplitude and frequency of vibration and the perforations diameter determines the drop size. Axial dispersion is reduced for the VPE column since the drops are evenly dispersed through the column (Prochazka et al., 1971).

### 2.8.2. <u>Advantages of Vibrating Plate Extraction Columns</u>

The following indicate the advantages of a vibrating plate extraction column (Prochazka et al., 1971 and Lo et al., 1992):

➢ Operates at high flow rates thus attaining a high efficiency
➢ The extractions column ability to adapt to an extensive array of system properties
➢ Ease with regards to the construction and the maintenance of VPE columns
➢ Easy modification to variations in conditions
➢ Simple scale-up

### 2.8.3. <u>Disadvantages of Vibrating Plate Extraction Columns</u>

The following indicate the disadvantages of a vibrating plate extraction column (Rama Rao et al; 1991 and Takacs et al., 1993):

➢ Entrainment problems due to fine droplets
➢ For larger energy contributions, axial mixing is increased, thus reducing overall effectiveness of the column.
➢ Vibrating plate extraction column is sensitive to impurities, not suitable for liquid mixtures containing solid materials.

### 2.8.4. <u>**Applications of Vibrating Plate Extraction Columns**</u>

The following Table 2.4 shows the applications for extraction in vibrating plate extraction columns (Prochazka et al., 1971 and Lo et al., 1992).

*Table 2.4: Extraction Separation Applications of Vibrating Plate Extraction Columns*

| System | Direction of Mass Transfer | Dispersed Phase | Diameter (m) | Length (m) | $(U_c + U_d) \times 10^2$ (m/s) | Yield (%) |
|---|---|---|---|---|---|---|
| Water-Caprolactam-Trichloroethylene | W→O | W | 0.500 | 6.8 | 1.89 | 99.8 |
| | O →W | O | 0.500 | 8.0 | 1.40 | 99.9 |
| Water-Caprolactam-Benzene | W→O | W | 0.085 | 4.0 | 1.61 | 99.7 |
| | O →W | O | 0.085 | 4.0 | 1.83 | 98.6 |
| Water-Phenols-Butylacetate | W→O | O | 0.085 | 4.0 | 2.74 | 97.3 |
| Water-Phenols-Diisoproplethers | W→O | O | 0.050 | 4.0 | 1.34 | 98.8 |
| Fermentation broth-Ketol-Butylacetate | W→O | O | 0.600 | 7.0 | 1.25 | 90.0 |
| Fermentation broth-Erythromycine-Butylacetate | W→O | W | 0.050 | 4.0 | 1.04 | 98.0 |
| Water-Acrylic acid-Isopropylacetate | W→O | W | 0.085 | 4.0 | 1.35 | 99.1 |

## 2.9. <u>Hydrodynamic Characteristics in Extraction Columns</u>

### 2.9.1. <u>Hydrodynamic Regime</u>

Nemecek and Prochazka (1974) investigated three flow regimes that distinctly display different characteristics of longitudinal mixing by focusing mainly on the effect of the dispersed phase flow.

The three different hydrodynamic regimes are defined as follows:

1) *Mixer-Settler Flow Regime*

In the mixer-settler flow regime a level of concentrated dispersed phase accumulates on the plate, where the thickness of the layer changes. One of the liquid phases is continuously projected into the other liquid phase, resulting in the formation of a cluster of drops as depicted in Figure 2.12. The holdup of the dispersed phase in the remaining volume is considered negligible. Groups of large drops pass through the last part of the plate. There is no back flow of the dispersion through the perforated plate (Nemecek & Prochazka, 1974 and Lo et al; 1992).
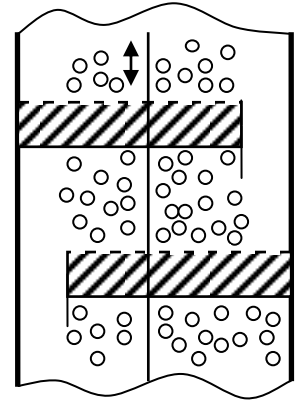


***Figure 2.12: Mixer-settler regime with downcomer (Adapted from Lo et al., 1992).***

2) *Dispersion Flow Regime*

In the dispersion flow regime a compact layer of drops on the plate develops over the height of the stage but a section of low local holdup near the dispersed phase inlet as well as a section of higher local holdup near the outlet is observed. The drops characteristics are fairly large and uniform and predominantly move in a vertical direction. Through the plate no back flow of the dispersed phase is noted (Nemecek & Prochazka, 1974).

3) *Emulsion Flow Regime*

In the emulsion flow regime the dispersed phase is evenly distributed over the height of the stage. The drops display the following characteristics, being relatively small and the drops move unsteadily through the plate. This erratic motion results in back flow through the plate. Figure 2.13 describes the emulsion regime, where the drop dispersion moves backward and forward through the perforations of the plate. As a result of the flow through the perforations, a turbulent energy is dissipated causing a fine dispersion to be maintained (Nemecek & Prochazka, 1974 and Lo et al., 1992).
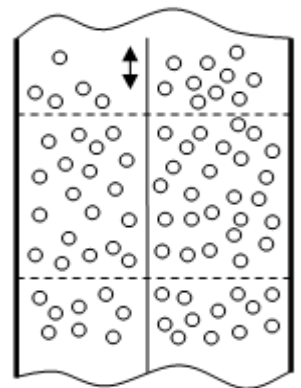


***Figure 2.13: Emulsion regime (Adapted from Lo et al., 1992).***

In reciprocating plate type columns, the flow is intermittent, thus small pulses of fluid are moved axially in either direction. In the mixer-settler flow regime there is an intermittent formation of drops, while in the emulsion flow regime an intermittent flow of two-phase dispersion is displayed (Lo et al., 1992).

### 2.9.2.  **Drop Size and Drop Size Distribution**

A basic characteristic required for the calculation and creation of liquid-liquid extraction columns is the Sauter mean drop diameter. The Sauter mean drop diameter is established on the mean size of drops formed in turbulent liquid-liquid dispersions (Boyadzhiev and Spassov, 1982).

The understanding of the drop size is of fundamental significance as it affects the dispersed phase hold-up, the residence time of the dispersed phase and the acceptable throughputs. The drop size together with the hold-up is used to determine the interfacial area available for mass transfer and also affects the mass transfer coefficients for both the continuous and dispersed phases (Kumar & Hartland, 1996).

Through the application of the Kolmogoroff - Obukhov theory of local structure of turbulent vibrations under certain assumptions, the Sauter (volume surface) mean drop diameter could be estimated (Kolmogorov, 1941 and Obukhov, 1941). The theory was adapted to the liquid-liquid dispersion formation, considering that the drop break-up is controlled by forces acting on the process.

Investigations conducted by Boyadzhiev and Spassov (1982) calculated the Sauter mean drop diameter using the given Equation (2.13):

$$d_{32} = \frac{\sum_{i=1}^{n} n_i d_i^3}{\sum_{i=1}^{n} n_i d_i^2} \qquad \qquad ...\ (2.13)$$

The research carried out by Boyadzhiev and Spassov (1982) established the following correlation to predict the Sauter mean drop diameter in a vibrating plate column within 20% accuracy for systems with different physical properties ($805 < \rho_c < 1000$; $816 < \rho_d < 1595$; $0.008 < \sigma < 0.0515$) and plates with different design characteristics ($0.002 < d_o < 0.0127$; $0.052 < \varphi < 0.55$). The Sauter mean drop diameter correlated by Boyadzhiev and Spassov (1982) is shown in Equation (2.14):

$$d_{32} = (0.57 \pm 0.11).\left(\frac{\sigma}{\rho_c}\right)^{3/5} . \frac{\varphi^{4/5} d_o^{2/5}}{(2af)^{6/5}} \qquad \qquad ...\ (2.14)$$

The Sauter mean droplet diameter, $d_{32}$, developed by Baird and Lane (1973) is calculated based on the agitation rate and the interfacial tension and is given by Equation (2.15).

$$d_{32} = 0.36 \frac{\sigma^{0.6}}{\bar{\rho}^{0.2}\psi^{0.4}} \qquad \text{... (2.15)}$$

The power dissipation is calculated using Equation (2.16), for a fraction open area $\varphi$ and orifice coefficient Co of 0.6 each (Camurdan et al., 1989).

$$\psi = \frac{2\pi^2}{3}\left(\frac{1-\varphi^2}{hC_o{}^2\varphi^2}\right)\bar{\rho}(af)^3 \qquad \text{... (2.16)}$$

The average dispersion density used to calculate the Sauter mean droplet diameter is calculated by Equation (2.17) (Camurdan et al., 1989):

$$\bar{\rho} = \rho_d\phi + (1-\phi)\rho_c \qquad \text{... (2.17)}$$

Research conducted by Rama Rao et al; (1991) deduced that for efficient liquid-liquid extraction large interfacial areas are required thus agitation is effective since it generates turbulence which results in the breaking up of dispersed phase droplets which increases the interfacial area. Unfortunately agitation has consequences, the first being that very fine droplets form at lower size distribution ranges which causes entrainment losses. Secondly, due to large energy inputs there is an increase in axial mixing which may diminish the overall effectiveness of the extraction column (Rama Rao et al., 1991).

Therefore a counter-current extraction column having acceptable mass transfer efficiency by means of low axial mixing and even drop sizes is sought after. Rama Rao et al., (1991) research indicated a considerably stronger effect on the droplet size by the frequency of vibration than the amplitude of vibration. The following Equation (2.18) was correlated which included the effects of other variables indicated in Equation (2.19) (Rama Rao et al., 1991).

$$d_{32} = 0.001 \, exp(-X) \qquad \text{... (2.18)}$$

where:

$$X = 8.98 \times 10^{-5} af^2 d_o{}^{0.5} U_c{}^{-1.2} U_d{}^{-1.5} \Delta\rho^{-1}\sigma^{-0.4} \qquad \text{... (2.19)}$$

Equation (2.18) applies to both the mixer-settler regime and the emulsion regime. The mixer-settler hydrodynamic regime exists, at no and low levels of agitation, with the dispersed phase establishing a distinct layer beneath each plate (Rama Rao et al., 1991).

Kumar and Hartland (1996) investigated different types of extraction columns including the Karr reciprocation plate column and developed unified correlations to predict the drop size in these liquid-liquid extraction columns.

Hafez and Baird (1978) proposed an equation for the calculation of $\epsilon$ for Karr reciprocating plate extraction columns, given by Equation (2.20), which is used in the unified correlation developed by Kumar and Hartland (1996) for the Sauter mean diameter shown in Equation (2.21).

$$\epsilon = \frac{2\pi^2(1-e^2)}{3hC_o^2e^2}(af)^3 \qquad \qquad ...(2.20)$$

$$d_{32} = C_\Psi e^n \left[ \frac{1}{\left[C_\Omega\left(\frac{\sigma}{\Delta\rho g}\right)^{0.5}\right]^2} + \frac{1}{\left[C_\Pi \epsilon^{-0.4}\left(\frac{\sigma}{\rho_c}\right)^{0.6}\right]^2} \right]^{1/2} \qquad \qquad ...(2.21)$$

The parameter, $C_\Psi$ used in the unified correlation in Equation (2.21) allows for the effect of mass transfer on drop size. In the case were no mass transfer occurs, $C_\Psi = 1$. Table 2.5 contains the parameter values for Equation (2.21) and the error in drop size for this correlation (Kumar and Hartland, 1996). AARE is the average absolute value of the relative error, given by Equation (2.22), which is used to relate the predicted results with the experimental data (Kumar and Hartland, 1996).

$$AARE = \frac{1}{NDP}\sum_{i=1}^{NDP}\frac{|predicted\ value - experimental\ value|}{experimental\ value} \qquad \qquad ...(2.22)$$

NDP value represents the number of data points.

Table 2.5:Parameter values for Equation 2.21 and Error in Drop Size.

| Column Type | $C_\Psi$ | | $C_\Omega$ | $C_\Pi$ | n | AARE (%) |
|---|---|---|---|---|---|---|
| | c → d | d → c | | | | |
| Karr | 0.95 | 1.48 | 1.30 | 0.67 | 0.50 | 19.7 |

Kumar and Harland (1996) found that although Equation (2.21) provided reasonable estimates of the drop size, it was possible to improve the association between the experimental data and the predicted values. A dimensionless correlation for the drop size, given by Equation (2.23), was developed that involves the use of plate spacing, h and gravitational acceleration, g.

$$\frac{d_{32}}{h} = \frac{C_\Psi e^{0.32}}{\frac{1}{1.55\left(\frac{\sigma}{\Delta\rho gh^2}\right)^{1/2}} + \frac{1}{0.42\left[\left(\frac{\epsilon}{g}\right)\left(\frac{\Delta\rho}{\sigma g}\right)^{1/4}\right]^{-0.35}\left[h\left(\frac{\Delta\rho g}{\sigma}\right)^{1/2}\right]^{-1.15}}} \qquad \text{... (2.23)}$$

Equation (2.23) was developed using values of $C_\Psi = 1$ for no mass transfer, $C_\Psi = 0.92$ for mass transfer from c→d and $C_\Psi = 1.67$ for mass transfer from d→c. The average absolute value of the relative error is now reduced to 16.1% (Kumar and Hartland, 1996).

Kumar and Hartland (1996) unified correlations for mechanically agitated columns is comprised of two terms, at low agitation levels the interfacial tension divided by the buoyancy forces and at higher agitation levels, the concept of isotropic turbulence. Equation (2.23) was developed since the theory of isotropic turbulence was found to not be suitable for describing the breakup of drops. Therefore the disruptive energy due to continuous phase turbulence is determined by the density difference, rather than the continuous phase density (Kumar & Hartland, 1996).

Shen et al., (1985) research explains that the direction of mass transfer has a major impact on the drop size, since the drops were found to be twice as large for mass transfer from d→c as compared to the mass transfer from c→d. As a result of the combination effects the drop size was expected to be larger for mass transfer from d→c. It should also be noted that the magnitude of the coalescence effect depends very much on the liquid-liquid system used (Shen et al., 1985).

### 2.9.3. **Dispersed Phase Holdup**

In an extraction column an important hydrodynamic variable is the holdup. The holdup is the volume fraction of the phase in the active part of the column (Camurdan, 1986). The following Equation (2.24) relates the specific area to the holdup and the Sauter mean droplet diameter (Lo et al; 1992).

$$a_i = \frac{6\emptyset}{d_{32}} \qquad \ldots (2.24)$$

Research conducted by Camurdan (1986) indicates that an increase in the dispersed phase holdup is due to a higher frequency of vibration. Also for Karr reciprocating plate columns, a nonlinear relationship exists between the holdup and the agitation rate (product of amplitude and frequency of vibration) depicted in Figure 2.14.

At a constant amplitude of vibration, with an escalation in the vibration frequency, the turbulence level increases, which causes smaller droplet sizes. Therefore the drag force acting on the drops increases in relation to the buoyancy and the droplets velocity decreases. This results in the droplets having a higher residence time, thus leading to an increase in the holdup (Taylor et al., 1982 and Camurdan, 1986).

Besides the frequency of vibration, the holdup is also found to be dependent upon the operating conditions of the extraction column. This includes the dispersed and continuous phase flow rates along with the physical and chemical properties of the test system used.
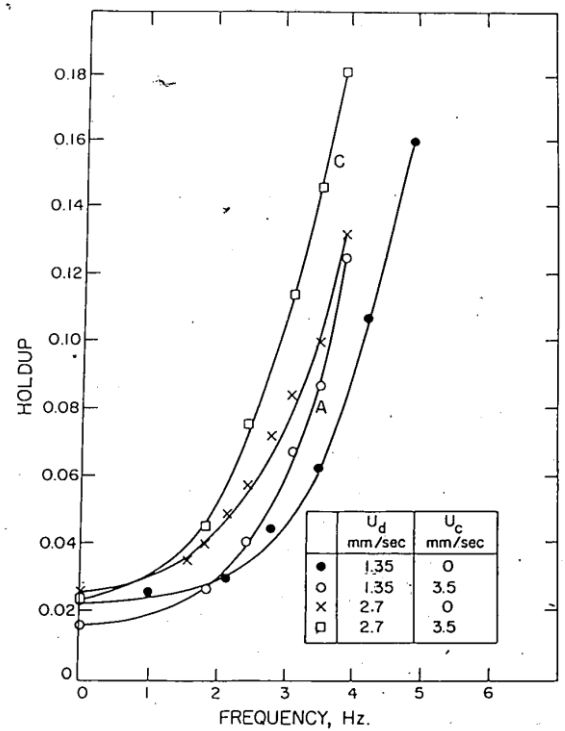


***Figure 2.14: Holdup versus Frequency of vibration (Adapted from Taylor et al., 1982).***

The outcome of the dispersed and continuous phase flow rates plus the physical and chemical properties on the holdup are indicated below (Taylor et al., 1982 and Camurdan, 1986):

***The Dispersed Phase Flow Rate***: A higher dispersed phase flow rate leads to an increase in the number density of the droplets thus increasing the holdup.

***The Continuous Phase Flow Rate***: A higher continuous phase flow increases the drag force on the droplet. Hence residence time of the droplets increase, therefore increasing the holdup.

***The Continuous Phase Viscosity:*** Has a similar affect as increasing the flow rate of the continuous phase.

***Density Difference***: The higher the difference in densities, the higher the buoyancy forces, thus causing the droplets to rise faster, leading to a decrease in the holdup.

***Interfacial Tension***: A high interfacial tension leads to the formation of droplets with large diameters and hence holdup values are low.

Baird and Lane (1973) proposed the first model for the holdup in reciprocating plate extraction columns, by utilizing the Ergun equation, given by Equation (2.25).

$$\left(\frac{\Delta p}{z}\right)\frac{d(1-\phi)^3}{\rho_c v_s^2 \phi} = \frac{150\phi}{Re} + 1.75 \qquad \text{... (2.25)}$$

The superficial velocity of the continuous phase in relation to the droplets of the dispersed phase, $v_s$, is described in Equation (2.26).

$$v_s = u_s(1-\phi) = \left(\frac{1-\phi}{\phi}\right)U_d + U_c \qquad \text{... (2.26)}$$

Similar to fluidised beds, the pressure drop in Equation (2.25) was given in relation to the net weight of the dispersed phase; this relation is depicted in Equation (2.27) as follows:

$$\left(\frac{\Delta p}{z}\right) = \phi\Delta\rho g \qquad \text{... (2.27)}$$

By substituting Equation (2.27) into Equation (2.25), the following correlation shown in Equation (2.28) for the holdup is established. Therefore in order to calculate the holdup, the phase velocities, physical properties as well as the drop size is required to be known.

$$\frac{d(1-\phi)^3 \Delta\rho g}{\rho_c v_s{}^2} = \frac{150\phi}{Re} + 1.75 \qquad \ldots (2.28)$$

Baird and Shen (1984) modified the correlation shown in Equation 2.28, by approximating that the right hand side of Equation (2.28) is proportional to $Re^{-0.5}$ as seen in Equation (2.29). Thereafter the slip velocity was solved for from Equation (2.29), which resulted in Equation (2.30).

$$\frac{d(1-\phi)^3 \Delta\rho g}{\rho_c v_s{}^2} = K_1 \left(\frac{\phi}{Re}\right)^{0.5} \qquad \ldots (2.29)$$

$$u_s = \frac{(1-\phi)d_{32}}{K_1{}^{2/3}\phi^{1/3}} \left[\frac{g^2 \Delta\rho^2}{\rho_c \mu_c}\right]^{1/3} \qquad \ldots (2.30)$$

The modified relation, under agitation conditions, between the slip velocity and a velocity, $U_*$, similar to the characteristic velocity for Karr columns was established by Baird and his colleagues shown in Equations (2.31) and (2.32) (Baird et al, 1971; Baird & Lane, 1973; Hafez et al., 1979 and Baird & Shen, 1984). The modified relation depicted in Equation (2.31) becomes impractical as the holdup approaches zero, but the slip velocities are consistent with the observations under normal operating range of holdups. The circulation parameter $K_1$ in the equations is taken to be 30 for rigid drops and a value of 15 for circulating drops (Baird et al, 1971).

$$U_c = \frac{U_*(1-\phi)^2}{(1-L)\phi^{1/3} + L\phi^{-2/3}} \qquad \ldots (2.31)$$

$$U_* = d_{32}\left[\frac{g^2 \Delta\rho^2}{\rho_c \mu_c}\right]^{1/3} K_1{}^{-2/3} \qquad \ldots (2.32)$$

The holdup for counter-current flow can be related to the dispersed and continuous phase superficial velocities via the slip velocity, for the emulsion flow regime, as shown in Equation (2.33) (Kumar & Hartland, 1988 and Rama Rao et al., 1991).

$$u_s = \frac{U_c}{1-\phi} + \frac{U_d}{\phi} \qquad \qquad \text{... (2.33)}$$

Research conducted by Gayler et al., (1953); Kumar et al., (1980) and Kumar & Hartland (1985) shows that the slip velocity is related to the drop size and physical properties of the liquid-liquid ternary system and it also depends on the holdup itself.

Slip velocity in relation to the dispersed phase holdup and characteristic velocity ($u_k$) was suggested by Thornton (1956), shown in Equation (2.34), where $u_k$ is approximately the terminal velocity of a particular drop, at low holdup values.

$$u_s = u_k(1 - \phi) \qquad \qquad \text{... (2.34)}$$

Correlations relating the slip velocity with the dispersed phase holdup have generally been used to describe the hydrodynamics of liquid-liquid extraction columns. Slater (1985) suggests that the following Equation (2.35) for the slip velocity has a very wide applicability.

Where the second term ($t\phi^n$) of the equation applies for large $\phi$ values, $m1$ and $u_k$ are obtained for $\phi <$ 0.2, and estimations are required for $t$ and $n1$.

$$u_s = u_k(1 - \phi)^{m1} + t\phi^{n1} \qquad \qquad \text{... (2.35)}$$

Equation (2.35) is reduced to the following expression given by Equation (2.36), when $t\phi^{n1}$ term is eliminated, since it applies for large values of holdup and since it reflects the effects of coalescence resulting in larger drops (Slater, 1985).

$$u_s = u_k(1 - \phi)^{m1} \qquad \qquad \text{... (2.36)}$$

Slater (1985) discovered that the value of $m1$ decreases as the agitation rate increases, and for reciprocating plate columns it was deduced that a linear relation exists between $m1$ and the drop size, as indicated in Equation (2.37).

$$m1 = 2.4 \times 10^3 d_{32} \qquad \qquad \text{... (2.37)}$$

Research pertaining to the holdup was carried out by Bensalem et al., (1985) who used a toluene-acetone-water test system. Bensalem et al., (1985) found that the holdup increased rapidly when the rate of agitation was increased, particularly in the case were the flooding point was being approached.

The holdup was also found to increase as the dispersed phase superficial velocity increased while the effect of the continuous phase superficial velocity has a less pronounce effect on the holdup.

With regards to the mass transfer, a higher holdup was noticed for the transfer of the solute from the continuous phase to the dispersed phase (c→d). However the holdup was lower for the transfer of the solute from the dispersed phase to the continuous phase (d→c), as compared to the holdup attained when no mass transfer took place.

The following Equations (2.38), (2.39) and (2.40) were proposed by Bensalem et al., (1985) for the situation of no mass transfer, mass transfer from (c→d) and mass transfer from (d→c) respectively.

*No mass transfer*

$$\phi = 9.99(af + U_c)^{0.3}U_d^{0.606} \qquad \text{... (2.38)}$$

*Mass transfer from (c → d)*

$$\phi = 330.40(af + U_c)^{0.91}U_d^{0.87} \qquad \text{... (2.39)}$$

*Mass transfer from (d→c)*

$$\phi = 27.38(af + U_c)^{0.437}U_d^{0.807} \qquad \text{... (2.40)}$$

Kumar and Hartland (1985) suggested the following Equation (2.41) for the holdup and slip velocity, which is applicable to all cases of counter-current flow.

$$\frac{4d_{32}g\Delta\rho(1-\phi)}{3\rho_c u_s^2(1+4.56\phi^{0.73})} = 0.53 + \frac{24\mu_c}{d_{32}u_s\rho_c} \qquad \text{... (2.41)}$$

Equation (2.41) can be rearranged, as expressed by Equation (2.42) to solve for the continuous phase superficial velocity, where $\beta_1$ and $\gamma$ expressions are described by Equations (2.43) and (2.44) respectively.

$$U_c = \frac{\left[-\beta_1 + \left(\frac{\beta_1{}^2 + 4\gamma(1-\phi)}{1+4.56\phi^{0.73}}\right)^{0.5}\right]\phi(1-\phi)}{2[\phi + L(1-\phi)]} \qquad \dots (2.42)$$

$$\beta_1 = \frac{24\mu_c}{0.53 d_{32}\rho_c} \qquad \dots (2.43)$$

$$\gamma = \frac{4d_{32}g\Delta\rho}{1.59\rho_c} \qquad \dots (2.44)$$

### 2.9.4. **Flooding**

Flooding is deemed to take place, if there is a further increase in the frequency of vibration, which leads to a rise in the holdup (Camurdan et al., 1989 and Lo et al., 1992)

Thornton (1959) anticipated that flooding comes about when either $U_d$ or $U_c$ approaches a maximum with respect to the holdup as shown by Equations (2.45) and (2.46).

$$\frac{dU_c}{d\phi} = 0 \qquad \dots (2.45)$$

$$\frac{dU_d}{d\phi} = 0 \qquad \dots (2.46)$$

Flooding conditions for a liquid-liquid extraction column can be predicted using the following conditions indicated by the equations above.

Slater (1985) established the following Equations (2.47) and (2.48), for the flooding conditions in an extraction column, which are only valid for $\phi_f < 0.2$.

$$U_{df} = (1 + m1)U_k(1 - \phi_f)^{m1}\phi_f{}^2 \qquad \dots (2.47)$$

$$U_{cf} = U_k(1 - \phi_f)^{m1+1}(1 - (m1+1)\phi_f) \qquad \dots (2.48)$$

## 2.10.  <u>Axial Mixing in Extraction Columns</u>

### 2.10.1. <u>Introduction to Axial Mixing</u>

In the development of liquid-liquid extraction columns, in the past an ideal or plug flow has been assumed in the prediction of the height of an extraction column for a specified separation. This assumption has been incorrect in predicting the performance of extraction columns. The continuous phase axial dispersion (also referred to as axial mixing or backmixing) has been found to be a major deviation from plug flow. Axial dispersion is a non-uniform movement of the continuous phase through the extraction column that leads to a drop in the driving force for mass transfer (Stella & Pratt, 2006).

Axial dispersion or axial mixing is likely to lessen the effectiveness of any counter-current mass transfer process, by levelling in each phase the axial concentration gradients and consequently decreasing the available overall driving force. Liquid-liquid extraction columns such as reciprocating plate columns are particularly prone to axial mixing effects because of fairly low superficial velocities of the flowing streams (Baird, 1974 and Stella & Pratt, 2006).

Axial dispersion also affects the scale-up of extraction columns, for example the axial dispersion effects may increase with the column diameter causing a poorer large scale performance (Rosen and Krylov, 1974).

The following are contributing factors to the continuous phase axial dispersion (Stella & Pratt, 2006):
- The entrainment of the continuous phase in the wake of the dispersed phase droplets.
- The energy dissipation of droplets causing a circulatory movement of the continuous phase.
- The molecular and turbulent eddy diffusion, also channelling and stagnant flow effects.

## 2.10.2. **Effect of Axial Mixing on Extraction Efficiency**

Extractor designs are established on the basis of plug flow pattern of each phase, in practice, this assumption is incorrect, as a result of deviations caused by axial mixing. Axial mixing thus results in a decrease in the concentration driving force, with in turn causes an increase in the HTU or HETS values. Figure 2.15 depicts the effect of axial mixing on the concentration profiles in a counter-current extraction column (Schweitzer, 1997).
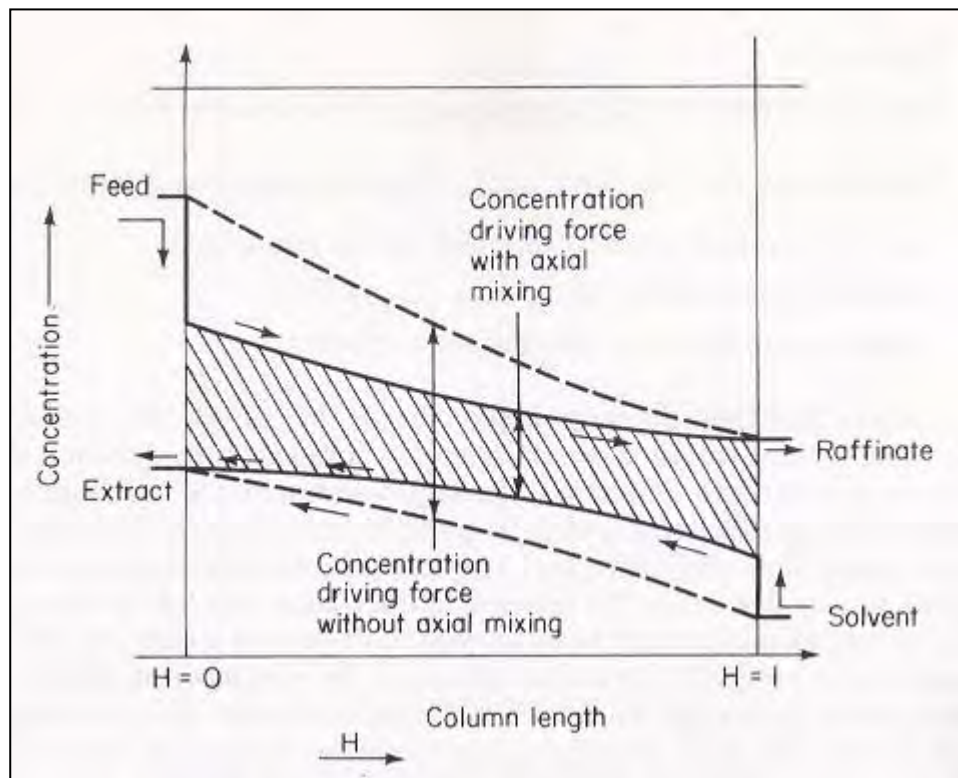


*Figure 2.15: Effect of Axial Mixing on Concentration Profiles in a Counter-Current Extraction Column (Adapted from Schweitzer, 1997).*

Axial mixing in a liquid-liquid extraction separation process can be contributed to a combination of factors which vary according to the type of extractor used and the liquid flow conditions within that type of extractor.

Investigations conducted by Sleicher (1959) suggest that axial mixing in the continuous phase may be due to the sum of the following two effects:

1.  The true molecular diffusion and turbulent flow in the axial direction, which may be as a result of the following (Sleicher, 1959 and Schweitzer, 1997):
    -   Vertical circulation current
    -   Mixing of eddies from the wakes of the dispersed droplets
    -   Dispersed phase entrainment of the continuous phase
    -   Turbulence in the extractor or the effect of pulsation or vibrating causes forced back-mixing action.
    -   As a result of a particular type of extractor or the packing geometry, a channelling flow could form.
2.  Eddy diffusion in extractors with no or a small degree of mechanical agitation, example spray column; thus results in non-uniform and subsequent radial mixing or Taylor diffusion.

Axial mixing also affects the dispersed phase, but the effect is generally not appreciable unless the extraction column is operated close to the flooding point of the column. Axial mixing in the dispersed phase may be due to the following (Schweitzer, 1997):

-   Continuous phase local velocity eddies carrying droplets counter-current to the main direction of the dispersed phase flow.
-   Size distribution of droplets cause forward mixing.
-   The distribution of droplet size and the distribution in rising velocities for droplets lead to the distribution residence time in the droplet swarm.
-   As a result of a particular type of extractor or the packing geometry, channelling effects are experienced.

2.10.3. **Axial Mixing Correlations**

Many research studies, including those investigations conducted by Miyauchi & Oya (1965) and Kumar & Hartland (1989 and 1999) focused on the prediction of axial mixing coefficients in the continuous phase, since backmixing in the dispersed phase is not considered to be of much importance (Dongoankar et al., 1991 and 1993).

Novotny et al. (1970) and thereafter Nemecek & Prochazka (1974) were first researchers to investigate the effects of longitudinal axial mixing in a reciprocating plate and pulsed perforated-plate columns for single phase flow. The model developed by these researchers was centred on the backflow model. The backflow model assumes that axial dispersion is caused by both backflow of the liquid through the perforated plate and by axial mixing between neighbouring plates in the extraction column.

Nemecek & Prochazka (1974) afterwards investigated the role that axial dispersion played in a vibrating plate extraction column for two phase flow, which outlined the influence of the dispersed phase on axial dispersion in the continuous phase.

The following Equation (2.49) for the effective backmixing coefficient was developed, where $\emptyset 1$ is calculated using Equation (2.50) (Nemecek & Prochazka, 1974). The correlation depicted by Equation (2.49) considered the axial dispersion coefficient to be in terms of the single phase dispersion and an increment as a result of the dispersed phase.

$$q_e = \frac{U_c + U_d}{U_c}\left(\frac{\emptyset 1}{\pi} - \frac{1}{2} + \frac{2af}{U_c + U_d}\cos(\emptyset 1)\right) + \frac{U_d}{U_c}(1 + q_d) \qquad \text{... (2.49)}$$

$$\emptyset 1 = arcsin\left(\frac{U_c + U_d}{2\pi af}\right) \qquad \text{... (2.50)}$$

Kim and Baird (1976) developed the following correlation for the axial dispersion coefficient for a two phase system, given by Equation (2.51).

$$\acute{E} = 5.62a^{1.41}f^{0.73}h^{-0.88} \qquad \text{... (2.51)}$$

From the investigation conducted by Kim and Baird (1976) it was found that as the agitation increased, the axial mixing increased which resulted in a drastic reduction in the concentration

driving force and offsets any increase in the mass transfer rates which is as a result of a higher interfacial area.

The following Table 2.6 contains different correlations developed for axial mixing in reciprocating plate columns (Novotny et al., 1970; Nemecek & Prochazka, 1974; Kim and Baird, 1976; Hafez et al., 1979; Kostanyan et al., 1980; Parthasarathy et al, 1984 and Bensalem, 1985).

*Table 2.6: Axial Dispersion Correlations*

| *System* | *Axial Dispersion Correlation* | *Source* |
|---|---|---|
| Karr (RPC) Column (Single phase system) | $q_c = \left\{ \left(1 + \dfrac{1}{q}\right) exp\left[6.6(h - 4.5)\dfrac{\varphi^{3/2}U_c}{d_o af}\right]\right\}^{-1}$ <br><br> $q = \dfrac{\alpha}{\pi} - \dfrac{1}{2} + \dfrac{2af}{U_c}$ <br><br> $\alpha = arcsin\left(\dfrac{U_c}{2\pi af}\right)$ | Novotny et al. (1970) |
| Vibrating Plate Column (Two phase system) | $q_c = \dfrac{U_c + U_d}{U_c}\left(\dfrac{\emptyset 1}{\pi} - \dfrac{1}{2} + \dfrac{2af}{U_c + U_d}\cos(\emptyset 1)\right) + \dfrac{U_d}{U_c}(1 + q_d)$ <br><br> $\emptyset 1 = arcsin\left(\dfrac{U_c + U_d}{2\pi af}\right)$ | Nemecek & Prochazka (1974) |
| Karr Column (Two phase system) | $\acute{E} = 5.62a^{1.41}f^{0.73}(h/1000)^{-0.88}$ | Kim and Baird (1976) |
| Karr Column (Two phase system) | $\acute{E} = 5.56a^{1.77}f^{1.0}(h/1000)^{-1.32}$ | Hafez et al. (1979) |
| Vibrating Plate Column (Two phase system) | $q_c = \dfrac{h}{1000}\left\{\dfrac{1}{0.5U_c + af} + 8\left(\dfrac{\delta}{d_o}\right)^{1/3}\left(\dfrac{\left(\frac{h}{1000}\right) + D_C}{D_C}\right)^{4/3}\dfrac{\varphi^{2/3}}{af}\right\}^{-1}$ | Kostanyan et al. (1980) |
| Karr Column (Two phase system) | $\dfrac{\acute{E}_c}{U_c H_c} = Pe^{-1} = (4.22 \times 10^{-2})a^{0.457}f^{0.344}U_c^{-0.37}d_o^{0.274}\varphi^{-0.68}(h/1000)^{-0.687}$ | Parthasarathy et al. (1984) |
| Karr Column (Two phase system) | $\acute{E}_c = 28.04(af)^{-0.009}U_c^{1.95}U_d^{-0.82}\phi^{0.555}$ d→c <br><br> $\acute{E}_c = 11.05(af)^{-0.223}U_c^{0.22}U_d^{0.06}\phi^{0.473}$ c→d | Bensalem (1985) |

## 2.11. <u>**Number and Heights of Transfer Units**</u>

The mass transfer effectiveness for liquid-liquid extraction is represented as the height of a transfer unit ($H_{ox}$) and is correlated taking into account axial mixing. It depends on the phase flow rates, the agitation level and the mass transfer direction (Shen et al., 1985).

Investigations conducted by Shen et al., (1985) indicates that the mass transfer is more effective, which implies that a low height of transfer unit was achieved for mass transfer from the continuous to the dispersed phase.

Smoot and Babb (1962) have defined three different types of number of transfer units depending on the nature of the concentration profile along the extraction column. Chilton and Colburn (1935) developed the correlation for the true number of transfer units depicted by Equation (2.52) as follows, where $a$ is the interfacial area per unit volume of the column ($m^2/m^3$).

$$N_{ox} = \frac{K_c a H}{U_c} \qquad \qquad \text{... (2.52)}$$

For the piston model, the measured number of transfer units is described by Equation (2.53) (Usman et al., 2006). The outlet and inlet molar concentrations in the continuous phase, mol/L, is represented by $x_o$ and $x_i$ respectively, while $x_e$ is the equilibrium molar concentration in the aqueous phase and $x$, the molar concentration in the continuous phase at any point in the extraction column. The measured number of transfer units can be established by graphical or numerical integration using the known concentration profile along the column (Usman et al., 2006).

$$N_{oxm} = \int_{x_i}^{x_o} \frac{1}{x_e - x} \, dx \qquad \qquad \text{... (2.53)}$$

By integrating Equation (2.53) and taking the operating and equilibrium curves as straight lines the apparent number of transfer units can be determined from Equation (2.54) (Usman et al., 2006). The inlet and outlet molar concentrations in the dispersed phase, mol/L is represented by $y_o$ and $y_i$ respectively, while $m$ indicates the slope of the equilibrium curve.

$$N_{oxp} = \frac{1}{\left[\frac{(y_i - y_o)}{m(x_i - x_o)}\right] - 1} \ln \frac{(y_i - mx_o)}{(y_o - mx_i)} \qquad \qquad \text{... (2.54)}$$

Shen et al. (1985) introduces the concept of true heights of a transfer unit, $H_{ox}$, which is described by Equation (2.55) as follows, where H is the height of the active part of the extraction column.

$$H_{ox} = \frac{H}{N_{ox}} \qquad \qquad \text{... (2.55)}$$

Baird and Shen (1984) indicates that the true height of a transfer unit, $H_{ox}$, is considerably larger for mass transfer from d→c than for mass transfer from c→d. The mass transfer combination effects in the d→c case is the cause of large drop sizes, lower holdup and greatly decreases the mass transfer performance. Thus this indicates that the mass transfer is less capable per unit height of dispersion in the case of mass transfer from d→c (Baird and Shen, 1984 and Shen et al., 1985).

Investigations conducted on Karr extraction columns by researchers have deduced that the HETS decreases with an increase in the frequency, thus the extraction column should be operated near its flooding point.

Investigations by Camurdan (1986) indicates that it would be very economical if the holdup was set at a constant value, thus in this way the extraction column can be operated around the minimum HETS value, which in turn results in an increase in the extraction column efficiency. This occurs by extracting the solute from the feed mixture at the maximum possible amount for a certain column height. From the investigations of Camurdan (1986) it was also discovered that a minimum HETS can be reached at agitation levels below the flooding point. This is due to serious axial mixing effects occurring at high agitation levels.

Investigations on vibrating plate extraction columns conducted by Rathilal (2010) led to the development of a model for the estimate of the number of transfer units, (NTU). Rathilal (2010) indicates that the agitation level, which is a product of the amplitude and frequency of vibration, the solvent to feed ratio as well as the tray spacing are some of the dependent variables for the determination of the number of transfer units. The research investigation also indicates that the NTU remains fairly constant in the mixer-settler regime, but as the dispersion flow regime is approached there is an exponential increase in the NTU.

The following NTU correlation shown by Equation (2.56) was developed by Rathilal (2010) for the data collected from experimental work conducted on the vibrating plate extraction column.

$$N_{oxm} = \left[ 5.5 + \left(1.8e^{0.258(af)} - 5.5\right) u \right] \times L \times \left(\frac{100}{h}\right) \qquad \dots (2.56)$$

From Equation (2.56), L represents the feed to solvent ratio, which is the reciprocal of S/F, h represents the tray spacing in units of mm and u is a unit step function. Based on which regime the extraction column operated at a specific unit step value was used as indicated below.

$u = 0$  for $(af)$ < 3.75 mm/s     (Mixer-settler Regime)

$u = 1$  for $(af)$ ≥ 3.75 mm/s     (Dispersion Flow Regime)

Equation (2.56) developed by Rathilal (2010) was unfortunately only tested for a tray spacing of 100 mm, therefore the correlation is required to be verified for different tray spacings. However for the tray spacing tested with the utilisation of the developed correlation in Equation (2.56), the correlation seems to predict fairly well with a close approximation to the actual NTU values being achieved.

The NTU correlation developed by Rathilal (2010) could also be used for the prediction of HTU or HETS by substituting Equation (2.57) into Equation (2.56) thus resulting in Equation (2.58) as indicated as follows. HTU represents the height of a transfer unit and H as the actual height of the extraction column.

$$HTU = \frac{H}{N_{oxm}} \qquad\qquad \dots (2.57)$$

$$\frac{H}{HTU} = \left[ 5.5 + \left(1.8e^{0.258(af)} - 5.5\right)u \right] \times L \times \left(\frac{100}{h}\right) \qquad\qquad \dots (2.58)$$

## 2.12.    **Efficiency for Extraction Columns**

In order to relate the performance of a real stage to that of an ideal theoretical stage, the stage efficiency is used for extraction columns with continuous flow. The following accounts only pertain to the case where a single solute is present, since the situation becomes extremely complicated once two or more solutes are present (Thornton, 1992).

### 2.12.1.  **Overall Efficiency**

Pratt (1983b) defined the overall efficiency, $E_o$, of an extraction column as the ideal number of stages divided by the number of real stages required to achieve the same duty, which is the same concentration change with the given flows. Equation (2.59) indicates the overall efficiency as follows, where $N_s$ represents the number of stages:

$$E_o = \frac{N_S(Ideal)}{N_S(Real)} \qquad \dots (2.59)$$

The overall efficiency is significant only for a linear equilibrium relation, even though Equation (2.59) is convenient to use for design purposes (Pratt, 1983b).

### 2.12.2.  **Murphree Efficiency**

Pratt (1983b) defines the Murphree efficiency as the actual concentration change of that phase within the stage divided by the concentration change that would have occurred if equilibrium had been achieved, with the Murphree efficiency being expressed in terms of either the X (Dispersed Phase) or Y (Continuous Phase) phase. The following Equations (2.60) and (2.61) indicate the Murphree efficiency for both phases using the mass fractions.

$$E_{Mx} = \frac{x_{n-1} - x_n}{x_{n-1} - x_n^*} \qquad \dots (2.60)$$

$$E_{My} = \frac{y_n - y_{n+1}}{y_n^* - y_{n+1}} \qquad \dots (2.61)$$

The Murphree efficiency was derived using the following Figure 2.16, where $x_{n-1}$ and $y_{n+1}$ are the concentrations for the streams entering the stage, $x_n$ and $y_n$ are the concentrations for the streams leaving the stage and $x_n{}^*$ as well as $y_n{}^*$ represents the concentrations at equilibrium conditions (Pratt, 1983b).
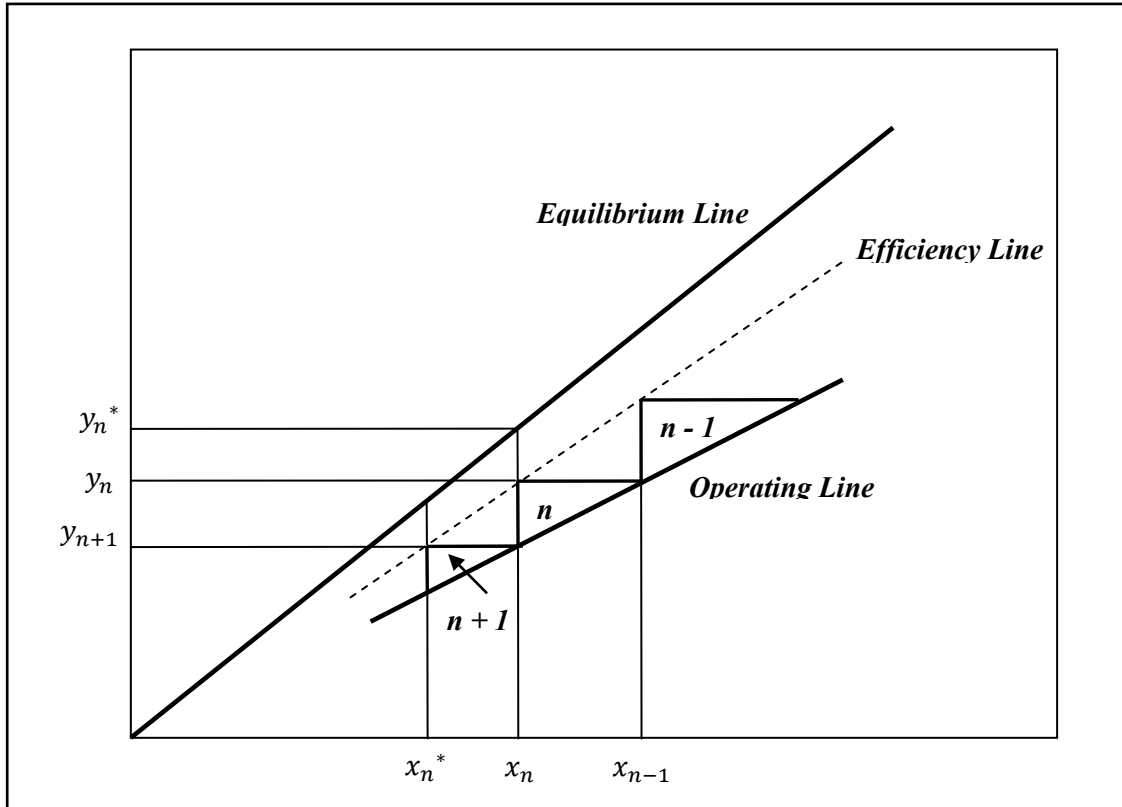


*Figure 2.16: x-y Plot for the determination of the Murphree Efficiency (Adapted from Pratt, 1983b).*

# CHAPTER 3: EXPERIMENTAL WORK

## 3.1. Experimental Test System

A toluene-acetone-water system was selected for experimental test work to be conducted on the vibrating plate extraction column. This test system for liquid-liquid extraction is a standard system proposed by the European Federation of Chemical Engineering (EFCE, 1985 and Steiner et al., 1990). The toluene-acetone-water system was chosen since this standard test system has a high interfacial tension (Misek et al., 1985). The selected standard liquid-liquid test system is also favoured due to its high precision and repeatability when utilizing gas chromatography for the investigation of the extraction process (Saien et al., 2006).

Liquid-liquid counter-current extraction is the separation technique that was employed in order to extract acetone (solute) from acetone-toluene feed using water as the solvent. Water (solvent), which is the continuous phase, flowed down the column, while the acetone-toluene feed was dispersed from the bottom into the extraction column.

## 3.2. Properties of the Test Systems Constituents

### 3.2.1. General Description of Test System Constituents

#### 3.2.1.1. Toluene

Toluene is a colourless liquid, which has a similar smell to benzene. It is a flammable liquid and its vapours can be easily ignited. It is immiscible in water and spreads on its surface. Toluene evaporates rapidly and the vapours produce explosive mixtures with air. These vapours are ignited on heated surfaces, by a spark or an open flame. At high concentrations the vapours irritate breathing organs while in liquid state toluene irritates the eyes and skin (EFCE, 1985).

#### 3.2.1.2. Acetone

Acetone is a clear, colourless liquid that has a sweet aromatic odour. Similarly to toluene, acetone is also flammable and its vapours can be easily ignited. It is completely miscible in water. Acetone is also known to evaporate rapidly and its vapours produce explosive mixtures with air. The vapours are also ignited on heated surfaces, by a spark or an open flame. In both liquid and gaseous states acetone has been found to irritate the eyes and skin (EFCE, 1985).

### 3.2.1.3. **Water**

Water is a clear, colourless, tasteless liquid that can be found in all three physical states (liquid, solid and gas). It has a neutral pH, is highly cohesive and is not a conductor of electricity (USGS, 2012).

*For fire and safety properties of the constituents of the test system please refer to Appendix E, Table E1.1. Please refer to Appendix F for Acetone and Toluene Material Safety Data Sheets.*

### 3.2.2. **Physical Properties of the Toluene-Acetone-Water Ternary System**

Equilibrium data obtained from Walton and Jenkins (1923) was used in order to develop the equilibrium phase diagram for the toluene-acetone-water test system which is depicted in Figure 3.1.
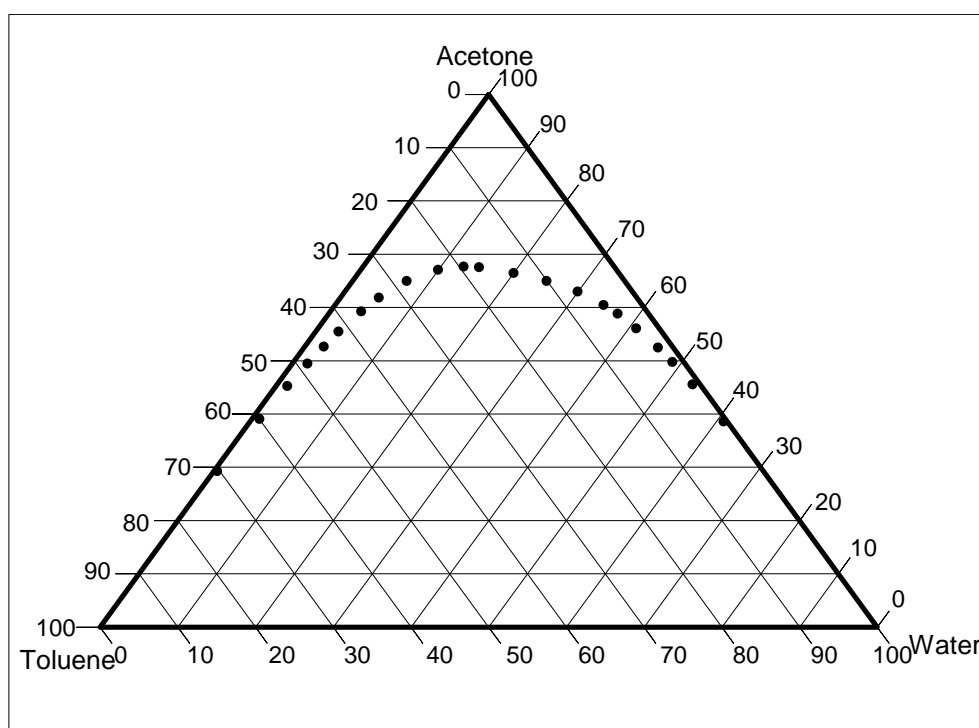


***Figure 3.1: Equilibrium Phase Diagram for Toluene-Acetone-Water Ternary System (Graham & Midgley, 2000).***

The physical properties of the pure coponents and the test system is described in Table 3.1 and Table 3.2 respectively.

*Table 3.1: Physical Properties of Pure Components at 20˚C.*

|  | Toluene | Acetone | Water |
|---|---|---|---|
| Density (kg/m$^3$) | 866.9 | 790.5 | 998.0 |
| Viscosity (g/m.s) | 0.6712 | 0.3976 | 1.0118 |
| Interfacial Tension (mN/m) | 36.1 | - | - |
| Diffusion Coefficient in Water ($1\times10^{-6}$ m/s) | - | $10.93 \pm 2.9\%$ | - |
| Diffusion Coefficient in Toluene ($1\times10^{-6}$ m/s) | - | $25.51 \pm 2.3\%$ | - |

(Brodkorb et al., 2003)

The chemical purity of acetone and toluene used for the experimental work were both 99% and the refractive index of acetone and toluene at 20˚C from literature were 1.359 and 1.497 respectively (Wikipedia, 2013).

*Table 3.2: Physical Properties of Liquid-Liquid Extraction System Toluene-Acetone-Water at 20˚C.*

|  | Dispersed Phase | Continuous Phase |
|---|---|---|
| Density (kg/m$^3$) | 864.192 | 993 |
| Viscosity (Pa.s) | $0.573\times10^{-3}$ | $1.11\times10^{-3}$ |
| Diffusivity (m$^2$/s) | $2.55\times10^{-9}$ | $1.09\times10^{-9}$ |

(Saien et al., 2006; Bahmanyar et al., 2008)

Enders et al. (2007) investigated the surface tension properties of the ternary system toluene-acetone-water and established from experimental work the surface tension behaviour at different temperatures for acetone-water and acetone-toluene mixtures. The experimental work concluded that there is an exponential decrease in the surface tension for the acetone-water mixture as the concentration of acetone increased. For the acetone-toluene mixture it was found that the surface tension decreased linearly as the acetone concentration was increased. From the experimental data obtained from Enders et al. (2007) the surface tension for the constituents of the toluene-acetone-water test system can be found in Table 3.3.

*Table 3.3: Surface Tension Data for Constituents of Test System at 20˚C.*

|  | Toluene | Acetone | Water |
|---|---|---|---|
| Surface Tension (mN/m) | 27.76 | 23.02 | 71.98 |

(Enders et al., 2007)

## 3.3. **Experimental Aims and Objectives**

The experimental research aims and objectives are to investigate the effect of the following on the number of stages and mass transfer coefficient:

- The tray spacing
- The product of frequency and amplitude of plate vibrations (Agitation Level)
- The solvent to feed ratio

The effect of these parameters on the number of theoretical stages and the mass transfer coefficient was investigated experimentally in order to optimise the performance of a vibrating plate extraction column. The experimental results obtained from the experimental research were thereafter compared with recently published correlations.

## 3.4. **Methodological Approach**

A Toluene-Acetone-Water system was selected for experimental work to be conducted on the vibrating plate extraction column. In the extraction separation process, water (aqueous phase) was used as the continuous phase, entering from the top and flowing down the vibrating plate extraction column, while for the dispersed phase, toluene-acetone feed (organic phase) was utilised, entering from the bottom and flowing up the vibrating plate extraction column  (Figures 3.2 and 3.3). The experimental work was conducted at a temperature of 25°C, (ambient conditions).

The experimental work involves varying the tray spacing, solvent to feed ratio and frequency of vibrations, while keeping the amplitude of vibrations constant. Thereafter the experimental procedure for the extraction process, which is explained in greater detail later, is followed through (Please refer to Experimental Procedures). After the system had achieved steady state, samples were withdrawn from along the length of the column along with samples from the extract and raffinate settling tanks and were then analysed using a gas chromatograph.

Finally using the data obtained from the extraction experiment, the number/height of transfer units (which gives an indication of the separation efficiency of the column) as well as the mass transfer coefficient was calculated and compared with various existing correlations.

## 3.5. **Experimental Set-up**

### 3.5.1. **Process Flow Diagram of the Experimental Set-Up**

The following Figure 3.2 illustrates the experimental set-up equipped with experimental apparatus and ancillaries for the liquid-liquid extraction process.



| Equipment List | | | |
|---|---|---|---|
| Unit No. | Description | Unit No. | Description |
| BST 101 | Bottom Settling Tank | T 101 | Toluene /Acetone Feed Tank |
| CA 101 | Compressed Air | T 102 | Extract Tank |
| FD 101 | Feed Distributor | T 103 | Water Tank |
| LC 101 | Level Controller | T 104 | Raffinate Tank |
| P 101 | Toluene /Acetone Feed Pump | TST 101 | Top Settling Tank |
| P 102 | Extract Pump | V 101 | Feed Valve |
| P 103 | Water Pump | V 102 , V 103 and V 107 | Inlet Air Valves |
| R 101 | Feed Rotameter | | |
| R 102 | Water Rotameter | V 104 | Distribution Valve |
| ST 101 | 1st Feed Surge Tank | V 105 | Extract Valve |
| ST 102 | 2nd Feed Surge Tank | V 106 and V 108 | Water Valves |
| ST 103 | Water Surge Tank | | |

*Figure 3.2: Process Flow Diagram for the Liquid-Liquid Extraction Process.*

**3-Dimensional Process Flow Diagram of the Experimental Set-Up**
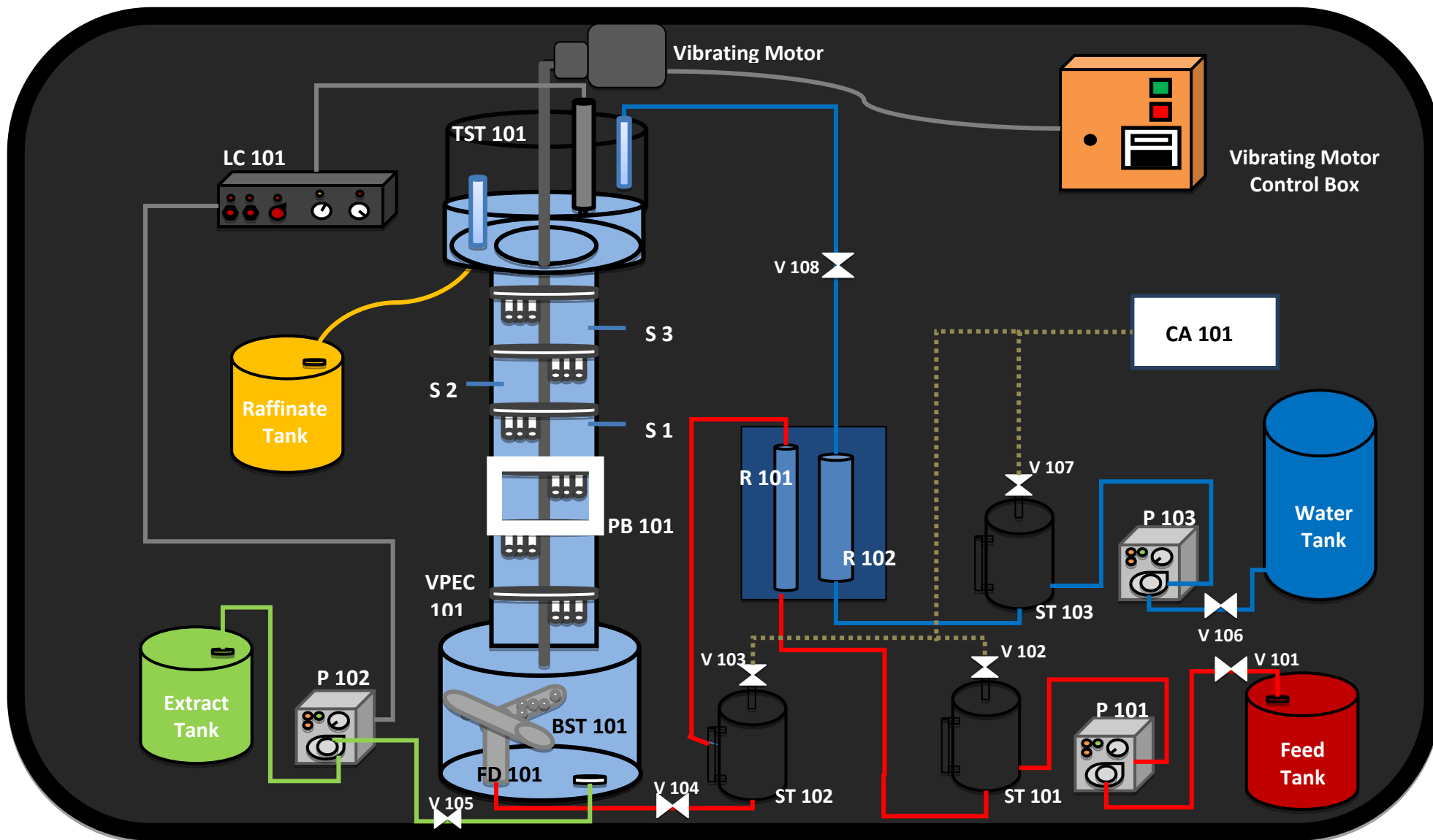


*Figure 3.3: 3-Dimensional Process Flow Diagram for the Liquid-Liquid Extraction Process.*

### 3.6. <u>Description of Experimental Equipment and Ancillaries</u>

### 3.6.1. <u>Extraction Column</u>

The extraction column consisted of 8 flanged glass sections and Table 3.4 indicates the extraction columns specifications.

| Table 3.4: Extraction Column Specifications. | |
|---|---|
| Inner Diameter (mm) | 47.7 |
| Outer Diameter (mm) | 58.7 |
| Thickness (mm) | 5.7 |
| Number of sections | 8 |
| Length of each section (mm) | 550 |
| Effective Height of the Column (m) | 4.76 |
| Cross Sectional Area of the Column (m$^2$) | $1.787 \times 10^{-3}$ |

### 3.6.2. <u>Perforated Plates</u>

Stainless steel perforated plates were attached to a central shaft in the vibrating plate extraction column. The perforated plates had small perforations to allow for the movement of the dispersed phase and three downcomers to allow for the flow of the continuous phase as depicted in Figure 3.4. Table 3.5 contains the specifications for each perforated plate in the vibrating plate extraction column.
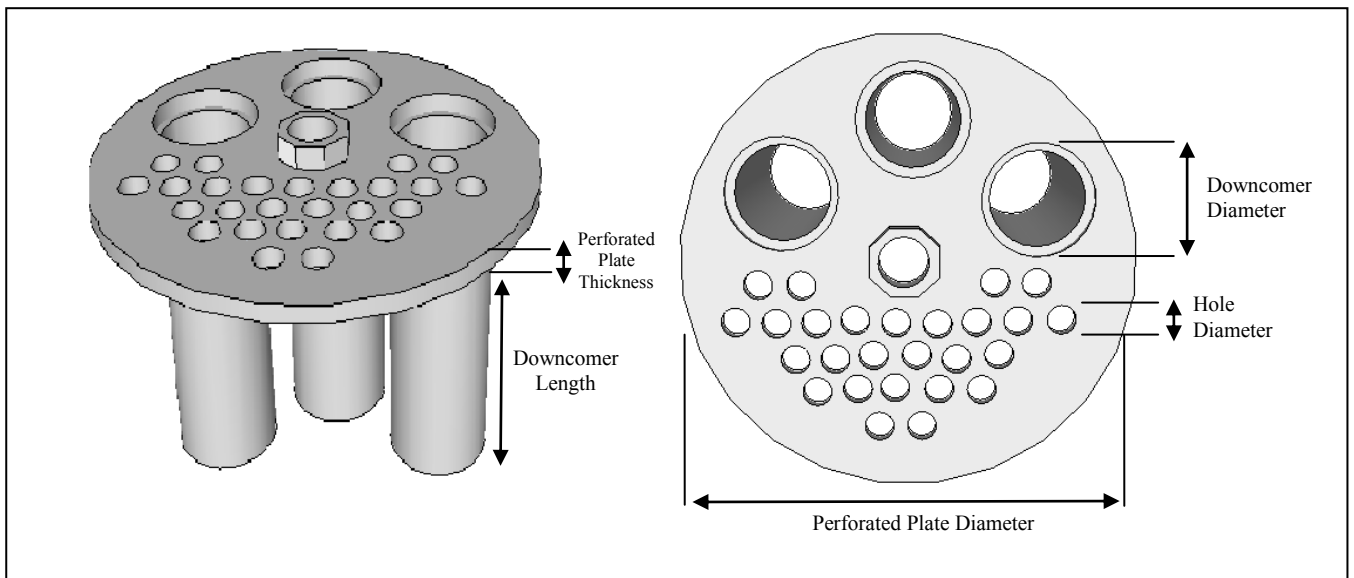


***Figure 3.4: Perforated Plates with Perforated Holes and Downcomers.***

**Table 3.5: Perforated Plate Specifications.**

| | |
|---|---|
| Perforated Plate Diameter (mm) | 47.4 |
| Perforated Plate Thickness (mm) | 2 |
| Number of small holes | 26 |
| Hole Diameter (mm) | 2.98 |
| Number of Downcomers per Perforated Plate | 3 |
| Downcomer Diameter (mm) | 10.9 |
| Downcomer Length (mm) | 43.3 |
| Number of Perforated Plates (h=10 cm) | 46 |
| Number of Perforated Plates (h=15 cm) | 31 |
| Number of Perforated Plates (h=20 cm) | 23 |

Table 3.6 contains additional specifications for the perforated plates.

**Table 3.6: Additional Perforated Plate Specifications.**

| | |
|---|---|
| Cross Sectional Area of Perforated Plate (m$^2$) | $1.764 \times 10^{-3}$ |
| Total Area of Holes (m$^2$) | $0.181 \times 10^{-3}$ |
| Free Area for Dispersed Phase (%) | 10.3 |
| Total Area of Downcomers (m$^2$) | $0.280 \times 10^{-3}$ |
| Free Area for Continuous Phase (%) | 15.9 |

The small perforations on the perforated plates allow for the dispersed phase to pass through and re-disperse after passing through each perforated plate. The downcomers on the perforated plates were attached and arranged on the central shaft and placed into the extraction column, in order for consecutive perforated plates to have the downcomers at opposite ends as depicted in Figure 3.5. This arrangement of the perforated plates in the extraction column allows for the continuous phase to move across the perforated section of the perforated plate.

The wettability of a liquid with the internals of the extraction column determines which liquids from the standard test system would be considered as the continuous and dispersed phases in the separation process.
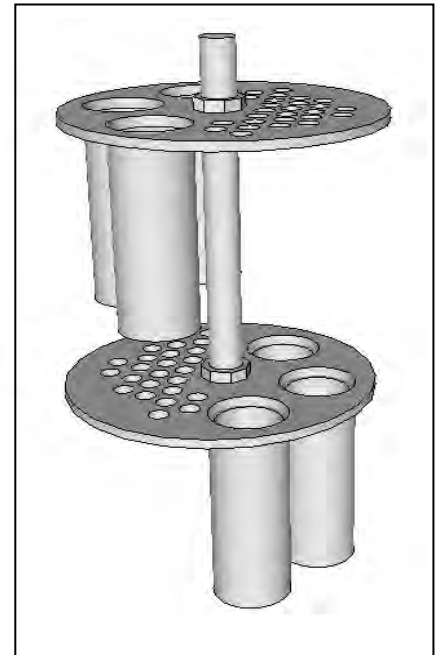


*Figure 3.5: Arrangement of perforated plates in the vibrating plate extraction column.*

The organic phase (dispersed phase) has a preferred wettability to Teflon, whereas the aqueous phase (continuous phase) has a preferred wettability to stainless steel as indicated by investigations conducted by Baird & Lane (1973) and Shen et al., (1985). Since the perforated plates are made of stainless steel there is a greater wettability by water and water is chosen as the continuous phase.

## 3.6.3. <u>Settling Tanks</u>

The vibrating extraction column has two identical settling tanks one above and the other below the extraction column. The settling tanks were used in order to allow for the separation of phases.

The bottom settling tank contained the feed distributor for the dispersion of the dispersed phase. The top settling tank was required in order to maintain the liquid-liquid interface between the aqueous and organic phases as depicted in Figure 3.6.

Figure 3.6 below illustrates the location of the inlet water tube, outlet organic phase tube and the conductivity probe as well as the central shaft, onto which the perforated plates are attached.
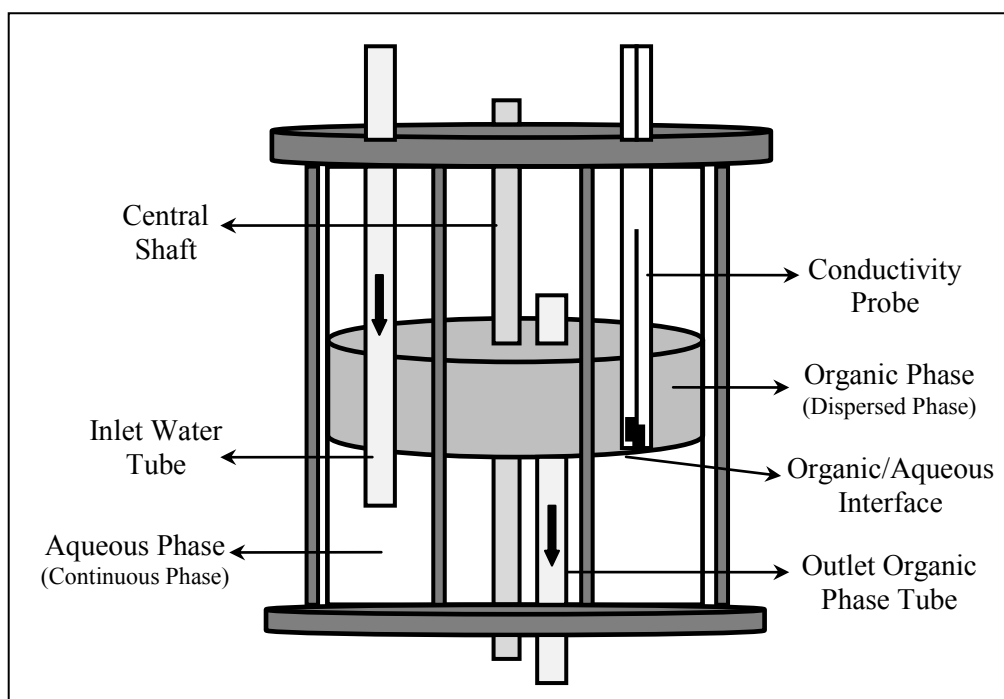


*Figure 3.6: Top settling tank, indicating the liquid-liquid interface.*

The Table 3.7 below indicates the specifications of the extraction column's settling tanks.

| *Table 3.7: Settling Tanks Specifications.* | |
| --- | --- |
| Inner Diameter (mm) | 150 |
| Outer Diameter (mm) | 160 |
| Thickness (mm) | 5 |
| Length (mm) | 250 |
| Cross Sectional Area (m$^2$) | $17.671 \times 10^{-3}$ |

### 3.6.4. **Surge Tanks**

For the liquid-liquid extraction experimental set-up three stainless steel surge tanks were required, a single surge tank is illustrated in Figure 3.7. The surge tank had the following specifications:

| *Table 3.8: Surge Tanks Specifications.* | |
| --- | --- |
| Outer Diameter (mm) | 115 |
| Height (mm) | 265 |
| Maximum Capacity (L) | 2 |

The surge tanks were required to dampen flow fluctuations which were caused by peristaltic motion of the pumps and by vibrating perforated plates in the extraction column. Therefore surge tanks were introduced into the experimental set-up in order to easily obtain constant reading on the rotameter.

Each surge tank was pressurized with compressed air from the top of the surge tank and the surge tanks were equipped with transparent tubing at the side in order to observe the level of the liquid in the tank, as illustrated in Photograph 3.1.
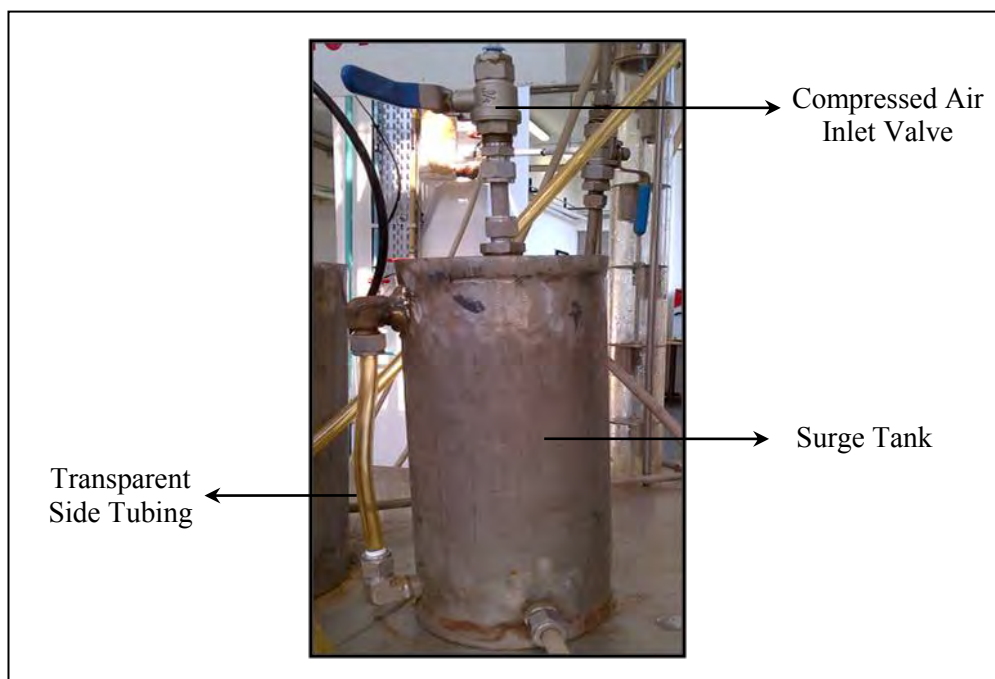
***Photograph 3.1: Surge tank, fitted with transparent side tubing.***

### 3.6.4.1. **Location of the surge tanks**:

One of the surge tanks was on the water line and this tank was placed between the water peristaltic pump and the water rotameter (Please refer to Process Flow Diagram in Figures 3.2 and 3.3). The water surge tank was located here since the peristaltic pump caused a fluctuating water flow rate which was difficult to read on the rotameter. The water surge tank thus considerably reduced the water rotameter fluctuations and resulted in steady water flow rates.

More flow fluctuations were encountered on the organic feed line thus two surge tanks were placed on this line in the experimental set-up. The peristaltic motion of the pump and the vibration of the perforated plate vibration in the extraction column resulted in a pressure variation in the bottom settling tank where the dispersed phase entered. The first feed surge tank was thus placed between the feed pump and the feed rotameter in order to try and overcome flow fluctuations caused by the feed peristaltic pump. The second surge tank was placed between the feed rotameter and the feed distributor in order to reduce flow fluctuations caused by the vibration of the perforated plates in the extraction column (refer to Process Flow Diagram in Figures 3.2 and 3.3) Both the surge tanks on this line hence allowed for stable rotameter readings to be taken on the rotameter.

### 3.6.5. **Water, Feed, Extract and Raffinate Tanks**

A 280 L water tank of height 117 cm, inner diameter 45 cm and outer diameter 56 cm was used to hold sufficient tap water (solvent) for two complete runs at maximum flow rate as well as for washing the extraction column between runs.

The feed, extract and raffinate tanks were 20 L steel tanks and were required in order to store the feed and product for the entire duration of the experiments.

### 3.6.6. **Vibration Motor**

The stainless steel perforated plates which were attached to a central shaft, were attached to an adjustable yoke above the extraction column, which is driven by the vibration motor. Therefore the perforated plates in the extraction column were reciprocated using a variable speed vibration motor with the following specifications: 220 V; frequency of 50 Hz; power of 0.75kW, 1430 min$^{-1}$ and 3.37 amp.

The amplitude of vibration could be varied by changing the spacing between the shafts connection point and the motor's centre through the adjustable yoke. The frequency of vibration could be altered by regulating the speed of the vibration motor. Please refer to Appendix AA for the vibration motor calibration graphs.

### 3.6.7. **Perspex Box**

A 130 by 135 by 250 mm, perspex box was positioned on the outer side of the vibrating plate extraction column, towards the middle section of the extraction column, between plates 14 and 15, when the plate spacing was 100 mm, counting from the bottom of the extraction column. The purpose of the perspex box, which is filled with water, was to eliminate refractive distortions due to the curvature of the extraction column, during the photography of the droplets (Baird & Lane, 1973 and Rama Rao et al., 1991). As illustrated in Photograph 3.2, the perspex box was opened at the top. The perspex box was illuminated from either side by floodlights to allow high contrast photographs of the droplets to be taken.
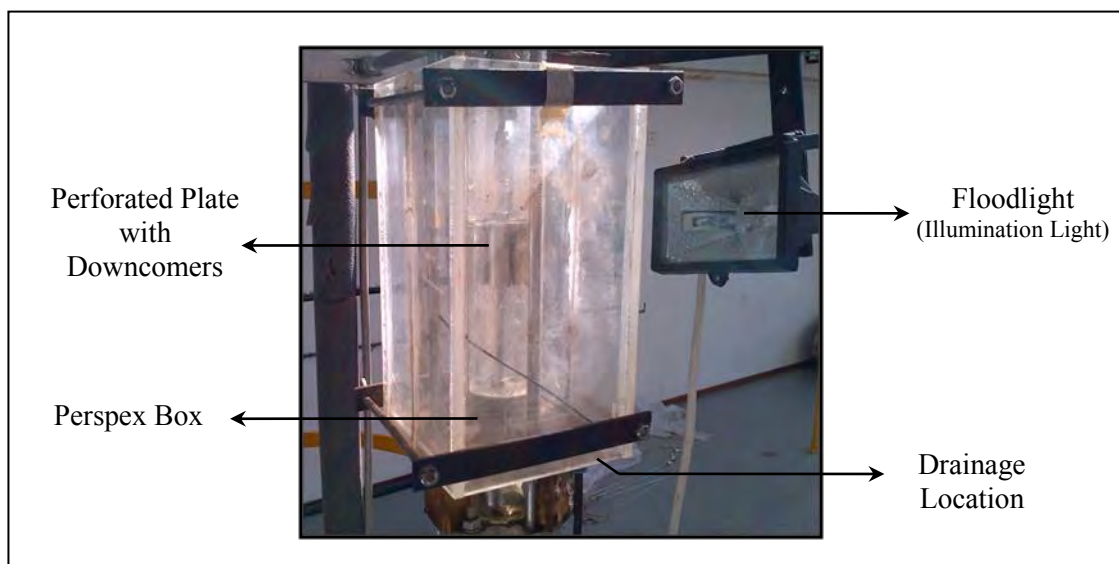
*Photograph 3.2: Perspex box, with floodlights.*

## 3.6.8. <u>**Samplers**</u>

Along the length of the extraction column, three sets of two samplers were located to withdraw each of the phases individually from different locations in the extraction column. Thereafter these samples were evaluated to determine the concentration at these locations in the extraction column.

The continuous phase samplers had a stainless steel tip and the tip was fitted to face upwards since the continuous phase flows down the column. The wetting preference of stainless steel is the aqueous phase and it was possible to remove just the aqueous phase using the sampler. The sampler for the dispersed phase had a Teflon tip and was faced downwards opposing the dispersed phase flow direction. Teflon has a favoured wettability for the organic phase (toluene) and therefore it was possible to withdraw only the dispersed phase from that sampler (Rathilal, 2010).

Photograph 3.3 shows the sampler type used to obtain samples of the two phases in the extraction column.
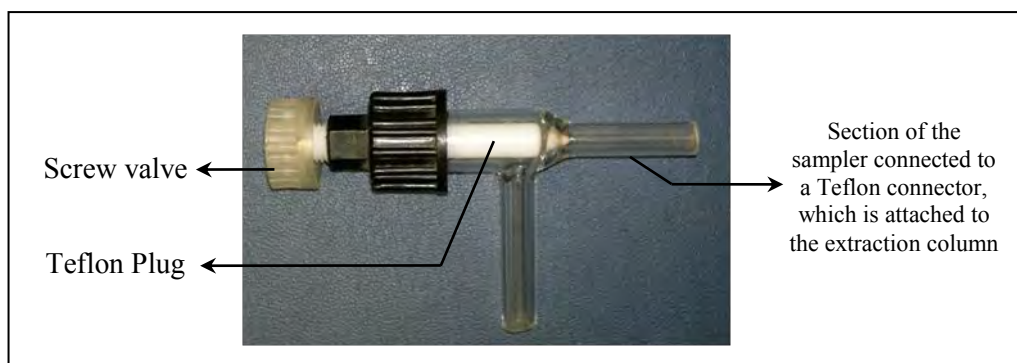


*Photograph 3.3: Sampler.*

Table 3.9 indicates the location of the three pairs of samplers along the extraction column for a plate spacing of 10 cm.

*Table 3.9: Sampler Locations.*

| Samplers | 1 | 2 | 3 |
|---|---|---|---|
| Distance (m) | 2.03 | 3.22 | 4.42 |
| **Sampler Location on the Extraction Column** *(in terms of the number of plates counted from the bottom of the extraction column)* | | | |
| Plate Spacing of 10 cm | 18-19 | 30-31 | 42-43 |
| Plate Spacing of 15 cm | 11-12 | 19-20 | 27-28 |
| Plate Spacing of 20 cm | 8-9 | 14-15 | 20-21 |

## 3.6.9. **Peristaltic Pumps**

Three peristaltic pumps were used in the experimental set-up, this includes a water pump, toluene/acetone feed pump and an extract pump. All three peristaltic pumps had the following specifications:

*Table 3.10: Peristaltic Pumps Specifications.*

| Name | Heidolph PD5106 |
|---|---|
| Minimum Speed (rpm) | 24 |
| Maximum Speed (rpm) | 600 |
| Maximum Flow Rate (l/h) | 160 |

Each peristaltic pump is a positive displacement pump that is operated by a rotor that controls the amount of liquid being pumped through silicon tubing.

Since the flow rates were changed by varying the speed of the pump these pumps were also variable speed pumps.

The peristaltic pumps could be operated in either a clockwise or an anticlockwise direction by changing the rotor direction on the pump itself.



*Photograph 3.4: Peristaltic Pump.*

### 3.6.10. **Rotameters**

Two rotameters were used in order to set the flow rates for the feed mixture and water (solvent) into the extraction column. Each rotameter was calibrated using the bucket/stopwatch technique in order to obtain the three readings on the rotameter that correspond to a flow rate of 10, 15 and 20 l/h.

### 3.6.11. **Level Controller**

The level controller was connected to the extract pump in order to regulate the interface level in the top settling tank. The level controller comprised of a conductivity probe and a control system box which contained the controller electronics which was connected to the variable speed extract peristaltic pump (Rathilal, 2010).

#### 3.6.11.1. **Operation of the Level Controller**

Since the conductivity probe operates on the basis of changes in electrical conductivity and knowing that the electrical conductivity of water is very low as compared to the electrical conductivity of toluene (hydrocarbon compound), this can be used to adjust the speed of the extract pump to control the aqueous-organic interface level.

In the case were the conductivity meter receives a low conductivity reading for the water the level controller would change the speed of the extract pump in order to increase the flow of the extract leaving the extraction column, thus resulting in a decrease in the interface in the top settling tank. The level controller also operates for the alternate case as well.

The operation of the level controller thus ensured that the interface level was kept at a stable and constant level. The level controller could also be adjusted so as to keep the speed of the extract pump at specific values corresponding to the high and low limits of the electrical conductivity readings. Since low flow rates were selected for the experimental work, the extract pumps lower speed limit was set at zero rpm.



*Photograph 3.5: Level controller.*

## 3.6.12. **Flame Ionization Detector Gas Chromatograph**

A gas chromatograph installed with a flame ionization detector (FID) was used to analyse the binary samples obtained from different locations along the length of the extraction column. The Shimadzu gas chromatograph depicted in Photograph 3.6 was used and the gas chromatograph has the following specifications as shown in Table 3.11.

A 0.5 $\mu$L sample from the extraction column was injected through the septum of the injector into the packed column in the gas chromatograph. The binary sample was carried through the packed column by nitrogen gas (carrier gas). The flame inside the gas chromatograph was kept ignited by the presence of hydrogen gas and air.



*Photograph 3.6: Shimadzu*
*FID Gas Chromatograph.*

| Table 3.11: Gas Chromatograph Specifications. | |
| --- | --- |
| Name: | Shimadzu GC-2014 |
| Injector Temperature(˚C): | 200 |
| Run Time (minutes): | 3 |
| Column Name: | Chromosorb WHP SE 30 |
| Column Pressure (kPa): | 0.4 |
| Column Flow (ml/min): | 25 |
| Column Temperature (˚C): | 90 |
| Column Length (m): | 3 |
| Column Inner Diameter (mm): | 2 |
| Detector Temperature (˚C): | 250 |

The FID gas chromatograph was utilised since it was able to detect the presence of hydrocarbons. The gas chromatograph was calibrated for two different binary systems, acetone-water and toluene-acetone, at varied concentrations of acetone.

The standard solutions prepared for both the binary systems contained a mass percentage of acetone ranging from 1 to 10 percent. Each of the standard solutions used for the calibration was analysed three times in order to obtain a satisfactory calibration plot.

For the toluene-acetone binary system two different peaks were identified by the gas chromatograph, thus the ratio of acetone and toluene peak areas was taken and plotted against the acetone mass percentage data. The gas chromatograph detector calibration for acetone in toluene is contained in Appendix A2, Figure A2.

Since the flame ionisation detector gas chromatograph detects only the presence of hydrocarbons, water was not detected by the GC, thus for the acetone-water binary system only one peak area of the acetone was obtained and plotted against the acetone mass percentage data. The gas chromatograph detector calibration for acetone in water is contained in Appendix A3, Figure A3.

## 3.7. **Experimental Procedures** *(Adapted from Rathilal, 2010)*

### 3.7.1. **Experimental Procedure for Hydrodynamic Experiments**

*The hydrodynamic experiments were conducted using a toluene-water test system, without the presence of acetone (solute).*

1. The conductivity probe used to measure the interface level was set at a fixed measured level below the raffinate overflow point.
2. Water was allowed to fill up to the level set by the probe.
3. Water flow rate was set by adjusting the speed of the water pump and the operation of the level controller was tested.
4. The agitation level was set to the required value. (NB. The amplitude was fixed and only the frequency was varied.)
5. The feed pump containing the toluene was started after ensuring that the feed valve was opened and thereafter the toluene flow rate was set by adjusting the speed of the feed pump.
6. A certain period of time was allocated in order to reach steady state (previous experimental studies from Rathilal, 2010, indicated that 45 minutes was sufficient).
7. The lights surrounding the Perspex box were switched on so that the droplets were illuminated and thereafter the droplets were photographed.
8. The interface level that was being maintained by the level controller, in the top settling tank was marked off.
9. The feed (toluene) and water pumps were stopped.
10. In order to obtain the dispersed phase holdup, the vibrating plate extraction column was allowed to run for 20 minutes with a frequency setting of 1.5 Hz, to allow the dispersed phase droplets to coalesce and accumulate in the top settling tank (Rathilal, 2010).
11. The amount of the dispersed phase (toluene) collected in the top settling tank, that was found to be below the marked off interface level was recorded.
12. The dispersed phase droplet photographs taken were then analysed using the Image Pro Plus software with the purpose of establishing the drop size distribution and the Sauter mean drop diameter.

3.7.2. **Experimental Procedure for Mass Transfer Experiments** *(Adapted from Rathilal, 2010)*

*The mass transfer experiments were conducted using a toluene-acetone-water standard test system.*

1. The feed solution consisting of 6 mass% acetone in toluene was prepared.
2. The conductivity probe used to measure the interface level was set at a fixed measured level below the raffinate overflow point.
3. Water was allowed to fill up to the level set by the probe.
4. Water flow rate was set by adjusting the speed of the water pump and the operation of the level controller was tested.
5. The agitation level was set to the required value (NB. the amplitude was fixed and only the frequency was varied).
6. The feed pump was started after ensuring that the feed valve was opened and thereafter the feed flow rate was set by adjusting the speed of the feed pump.
7. A certain period of time was allocated in order to reach steady state (previous experimental studies from Rathilal, 2010, indicated that 45 minutes was sufficient).
8. The lights surrounding the Perspex box were switched on so that the droplets were illuminated and thereafter the droplets were photographed.
9. The interface level that was being maintained by the level controller in the top settling tank was marked off.
10. Extract and raffinate samples as well as samples at different lengths along the extraction column were taken.
11. The feed and water pumps were stopped.
12. In order to obtain the dispersed phase holdup, the vibrating plate extraction column was allowed to run for 20 minutes with a frequency setting of 1.5 Hz, to allow the dispersed phase droplets to coalesce and accumulate in the top settling tank (Rathilal, 2010).
13. The amount of the dispersed phase collected in the top settling tank that was found to be below the marked off interface level, was recorded.
14. The dispersed phase droplet photographs taken were then analysed using the Image Pro Plus software with the purpose of establishing the drop size distribution and the Sauter mean drop diameter.
15. Thereafter all the samples obtained (raffinate, extract and along the length of the extraction column) were analysed using the Flame Ionization Detector Gas Chromatograph in order to establish the amount of acetone present.

### 3.7.3. __Dispersed Phase Holdup Procedure__

After the experiment was allowed 45 minutes in order to reach stability and the photographs and samples were obtained, the aqueous-organic interface level was marked off in the top settling tank. Thereafter the pumps were stopped and the perforated plates were vibrated at a frequency setting of 1.5 Hz, which was found from previous investigations to be the frequency at which a minimum dispersed phase holdup is obtained (Rathilal, 2010). The system was thereafter allowed to vibrate for 20 minutes in order for the dispersed phase droplets to coalesce and accumulate in the top settling tank. The height of dispersed phase that was found to be below the marked off aqueous-organic interface level was then measured.

The dispersed phase holdup was determined by firstly calculating the volume of the raffinate, by multiplying the measured height of the dispersed phase by the cross sectional area of the top settling tank. Thereafter the dispersed phase fractional holdup was established by dividing the volume of raffinate by the active volume in the column, which was then represented as a percentage.

The active volume represents the volume of the continuous phase, without the presence of the dispersed phase, which occupies the active region of the extraction column. The active volume is measured by collecting the continuous phase (water) during the draining process from the active part of the column. This active region starts from the first perforated plate at the top of the column to the last perforated plate at the bottom of the column. The active volume's measured at different tray spacing are contained in the following Table 3.11.

*Table 3.12: Active Volume Data.*

| Tray Spacing, h, (mm) | Active Volume (L) |
| --- | --- |
| h = 100 | 7.8 |
| h = 150 | 7.9 |
| h = 200 | 8.0 |

For detailed sample calculations for the dispersed phase holdup please refer to Appendix C1.

### 3.7.4. <u>**Drop Size Distribution Procedure**</u>

Three to five photographs were taken of the droplets through the Perspex box after the experiment was allowed to run for 45 minutes (for the system to reach stability). The Perspex box was filled with water in order to eliminate refractive distortions due to the curvature of the extraction column. The Perspex box was illuminated from either side by floodlights to allow high contrast photographs of the droplets to be taken, as depicted in Photograph 3.2. Thereafter the drop sizes and number of droplets were analysed using the Image Pro Plus software.

The Image Pro Plus software requires a reference point as an input, thus the ruler in the photograph was used. For the droplet sizes 15 to 20 random droplets of different sizes were selected by drawing a circle around each droplet. The software highlights the droplets selected and establishes the size of the selected droplets and the number of these droplets contained in the image. This information was used in order to obtain the drop size distribution which in turn was used to determine the Sauter mean drop diameter. The Sauter mean drop diameter was calculated using Equation (2.13) which uses the average drop size and the number of droplets for that particular droplet size.

For detailed sample calculations for the drop size distribution and the Sauter mean drop diameter please refer to Appendix C2 and Appendix C3.

### 3.7.5. <u>**Sample Withdrawal Procedure**</u>

After the system was given 45 minutes to reach stability the raffinate, extract and samples along the length of the extraction column were taken. Two samplers were located at each of the three different locations along the column with the exact location details for the samplers for the different tray spacing evaluated shown in Table 3.9. At each of the three locations along the length of the extraction column samples of the continuous and the dispersed phases were taken.

Firstly the screw valve on the sampler was slightly opened and the liquid contained in the sampler was collected in a waste beaker. The sample was withdrawn once the sought after phase was noticed to be removed from the sampler, this phase was then collected in the sample vial. The samples were then analysed using the gas chromatograph in order to establish the mass percentage of acetone contained in the samples.

### 3.7.6. <u>Gas Chromatograph Analysis Procedure</u>

For the mass transfer experiments performed the raffinate sample, extract sample and samples along the length of the extraction column were collected after the system established stability. A sample volume of 0.5 $\mu$L was injected through the septum of the injector into the packed column in the gas chromatograph. Each sample was analysed three times and the average result was taken, in order to achieve acceptable results. A percentage error of 2% was attained among the analysed samples.

From the gas chromatograph analysis the mass percentage of acetone in each phase was obtained and was then used in order to establish the percent acetone extracted for each experimental run performed. The operating line for the establishment of the number of real and ideal equilibrium stages was plotted from the gas chromatograph results as well.

### 3.8. <u>Outline of the Experimental Work Layout</u>

The following figures indicate the experimental work layout for the hydrodynamic and mass transfer experiments that were performed, for varied process and equipment parameters.

### 3.8.1. <u>Experimental Layout for Hydrodynamics Experiments</u>

For a constant amplitude of vibration of 2.5 mm, the dispersed phase holdup, drop size distribution and Sauter mean diameter at each frequency was measured. The water and toluene flow rates as well as the frequencies that will be used for the hydrodynamics experimental work is illustrated in Figure 3.7.
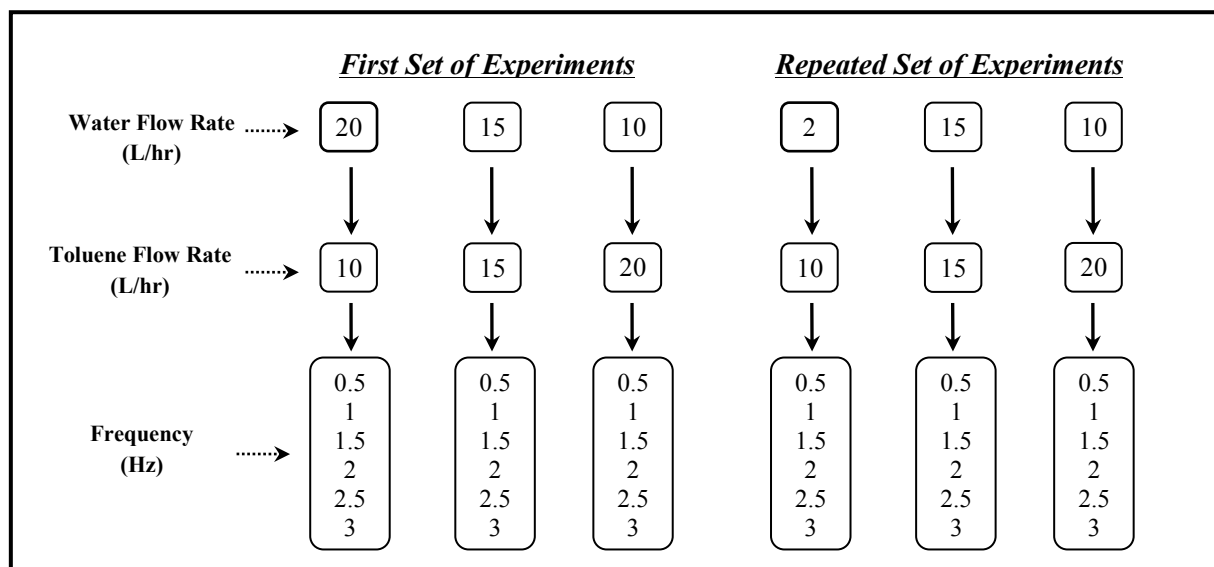


*Figure 3.7: Hydrodynamics Experimental Layout*

3.8.2. **Experimental Layout for Mass Transfer Experiments**

For three different plate spacings, at a constant amplitude of vibration of 2.5 mm, the extract, raffinate and concentrations along the length of the extraction column are obtained as well as the dispersed phase holdup. Thereafter the drop size distribution and Sauter mean diameter at each frequency will be established as well as the percentage acetone extracted, the number of real and ideal equilibrium stages, the mass transfer coefficient and the overall efficiency. The mass transfer experimental layout is illustrated in Figure 3.8.
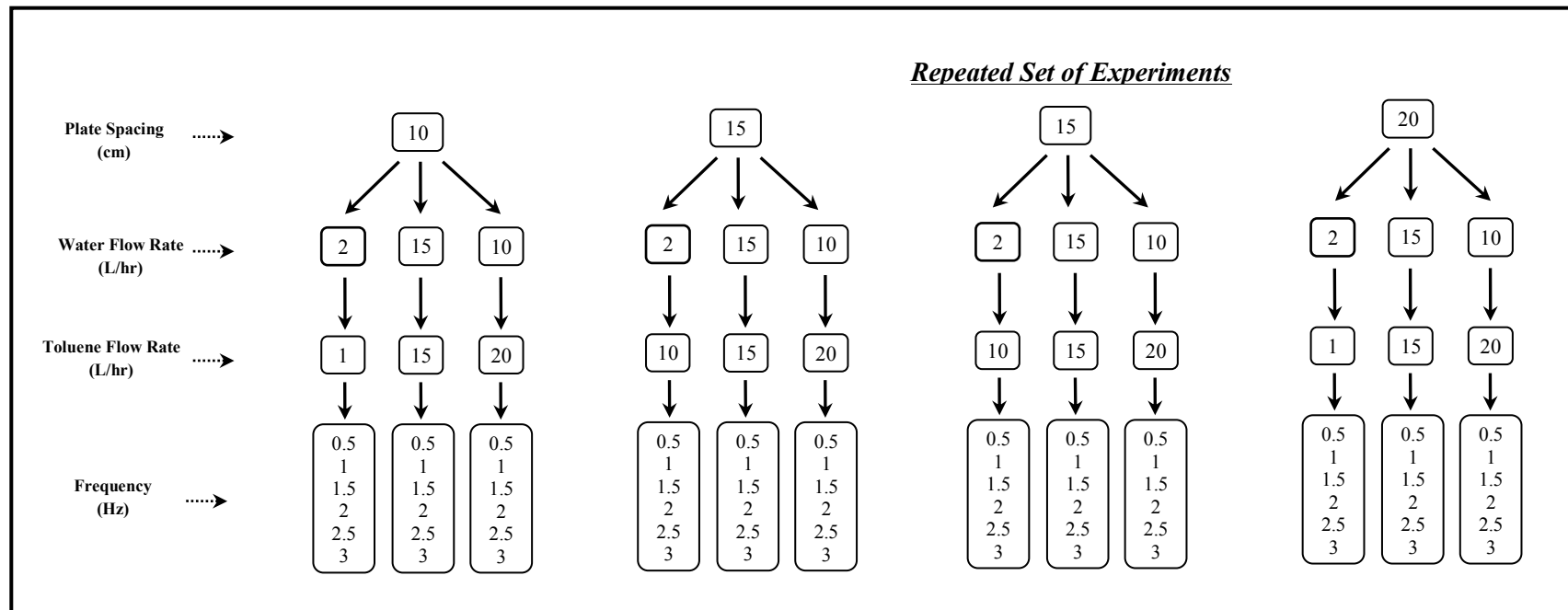


*Figure 3.8: Mass Transfer Experimental Layout*

# CHAPTER 4: RESULTS AND DISCUSSION

## 4.1. Hydrodynamic Experimental Results

The hydrodynamic experiments were performed using a water-toluene test system, with no solute (acetone) present. The solvent to feed ratio (S/F) and the agitation level (*af*), which is the product of the amplitude and frequency of vibration, were varied in order to establish the effect on the hydrodynamics of the system. Three different solvent to feed ratios (1:1, 1:2 and 2:1) were tested for varied agitation levels between 1.25 mm/s and 7.5 mm/s, in increments of 1.25 mm/s, up until flooding took place in the extraction column. The hydrodynamic experiments were conducted for a tray spacing of 100 mm.

The results obtained for the hydrodynamic experiments include the dispersed phase holdup, the drop size distribution, the Sauter mean drop diameter and a repeatability analysis, were the hydrodynamic experiments were repeated in order to test the repeatability of the experiments.

## 4.1.1. Dispersed Phase Holdup Results

For the hydrodynamic experiments performed on the system the dispersed phase holdup was calculated for different solvent to feed ratios (S/F = 1:2, S/F = 1:1 and S/F = 2:1) as well as for different agitation levels, these results are indicated in Figure 4.1. Solvent and feed flow rates of 10 l/h, 15 l/h and 20 l/h were set (please refer to Appendix C1 for detailed dispersed phase holdup calculations)
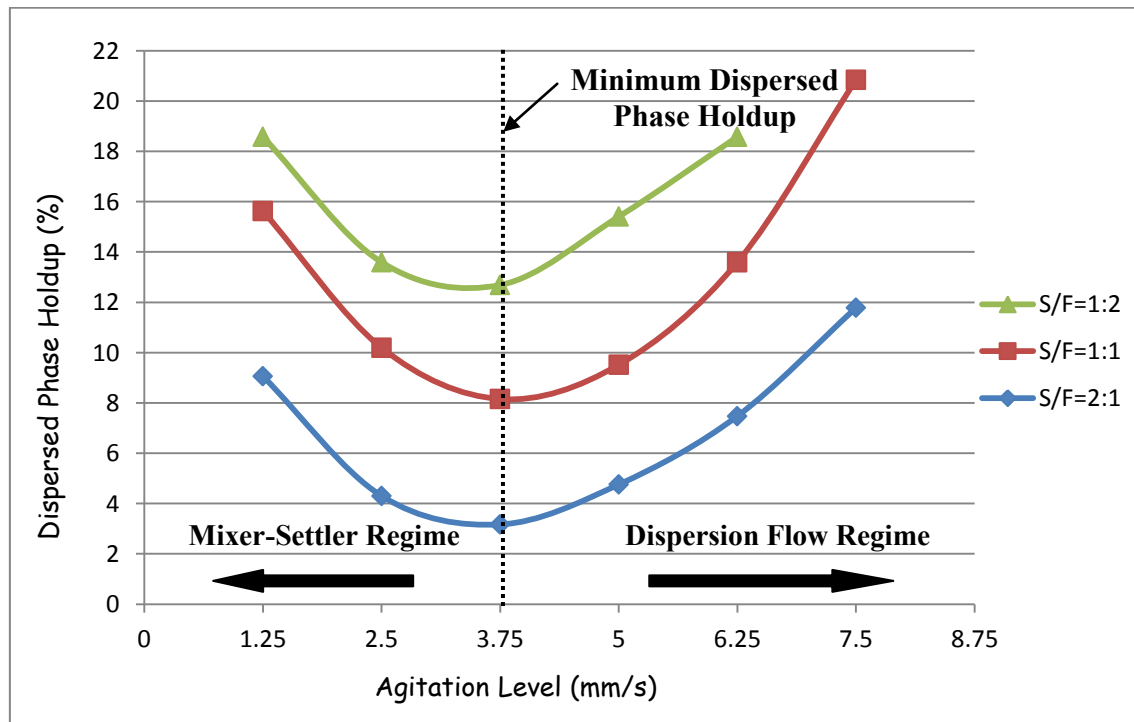


*Figure 4.1: Dispersed phase holdup results for hydrodynamic experiments.*

The dispersed phase holdup at varied agitation levels indicate similar trends for each solvent to feed ratio tested, the trend is also found to be in agreement with previous investigations conducted by Rama Rao et al., (1991) and Rathilal, (2010).

Figure 4.1 displays two distinct hydrodynamic regime flows which have resulted from the hydrodynamic experiments. The first regime flow is the mixer-settler regime where a high initial dispersed phase percentage holdup is obtained. This high initial holdup is as a result of an accumulation of the dispersed phase (toluene) under each tray in the vibrating plate extraction column. Thereafter, results show that as the agitation level is increased, the layer accumulated under each tray decreases, which thus corresponds to a reduction in the dispersed phase holdup.

For all three solvent to feed ratios tested, at an agitation level of 3.75 mm/s, experimental results indicate a minimum dispersed phase holdup. This minimum holdup depicts the change in the hydrodynamic flow regime from a mixer-settler regime to the dispersed phase regime.

After the minimum holdup was reached, a rise in the dispersed phase holdup is noticed upon an increase in the agitation level. The increase in the agitation level causes the formation of smaller droplet sizes and an increase in the number of droplets. In turn these smaller droplets (instead of passing through the plates to accumulate in the top settling tank) remain between the plates, resulting in a higher residence time of the droplets in the extraction column and therefore results in an increase in the dispersed phase holdup (Rathilal, 2010).

A further increase in the agitation level causes a substantial increase in the dispersed phase holdup, which drives the system to the emulsion regime and thereafter flooding is deemed to take place. Thus the dispersed phase holdup is a key factor, since it does not only determine mass transfer but also indicates the onset of flooding, (Aravamudan & Baird, 1999).

Previous investigations conducted by Nemecek & Prochazka (1974), Kim & Baird, (1976) and Ju et al., (1990) have deduced that the dispersed phase holdup is dependent on both the agitation level and the throughput rate for different reciprocating extraction columns. Investigative research by Rama Rao et al. (1991) also discovered that an increase in the dispersed phase flow results in a considerable growth in the holdup, which is expected.

Figure 4.1 illustrates a higher dispersed phase holdup for the solvent to feed ratio of 1:2 at the different agitation levels tested as compared to the other higher solvent to feed ratios. Thus confirming deductions made by Rama Rao et al. (1991) that as the dispersed phase (toluene) increases, the holdup increases. Experimental worked conducted by Rathilal (2010) also indicates that the holdup may be considered independent of the continuous phase flow. For the solvent to feed ratio of 1:2, experiments could not be performed at higher agitation levels since flooding of the column occurred.

### 4.1.2. **Drop Size Distribution Results**

The drop size distribution of the dispersed phase was established for different solvent to feed ratios and varied agitation levels, using Image Pro Plus software. For each hydrodynamic experiment performed several photographs of the droplets were taken and the software was utilised to analyse the drop size distribution.

Photograph 4.1 illustrate the droplet size differences for the different agitation levels tested for the solvent to feed ratio of 1:1, using a solvent and feed flow rate of 15 l/h.



*(a) Agitation Level = 1.25 mm/s*    *(b) Agitation Level = 2.5 mm/s*

*(c) Agitation Level = 3.75 mm/s*    *(d) Agitation Level = 5 mm/s*

*(e) Agitation Level = 6.25 mm/s*    *(f) Agitation Level = 7.5 mm/s*
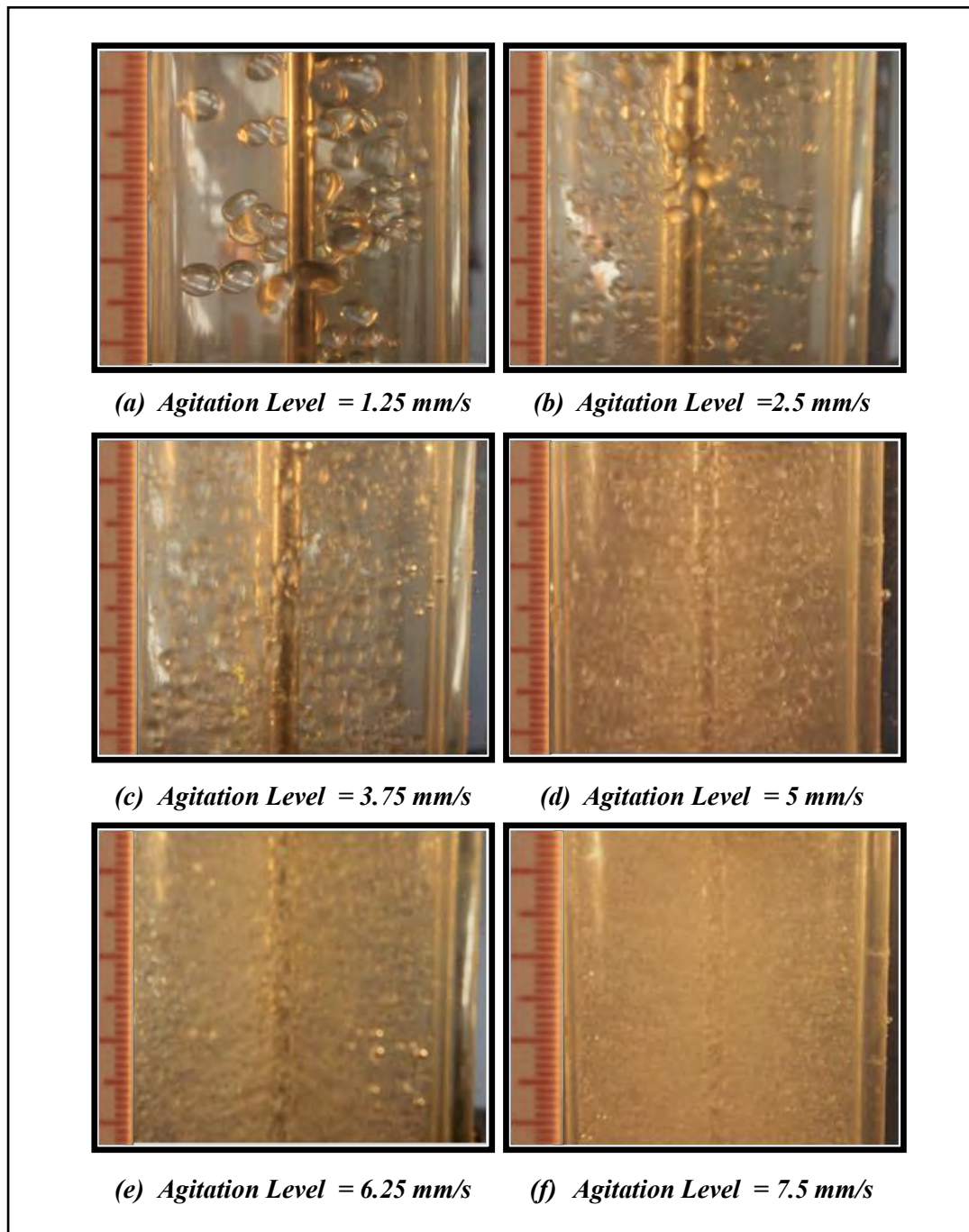
***Photograph 4.1: Photographs of droplets analysed to determine drop size distribution.***
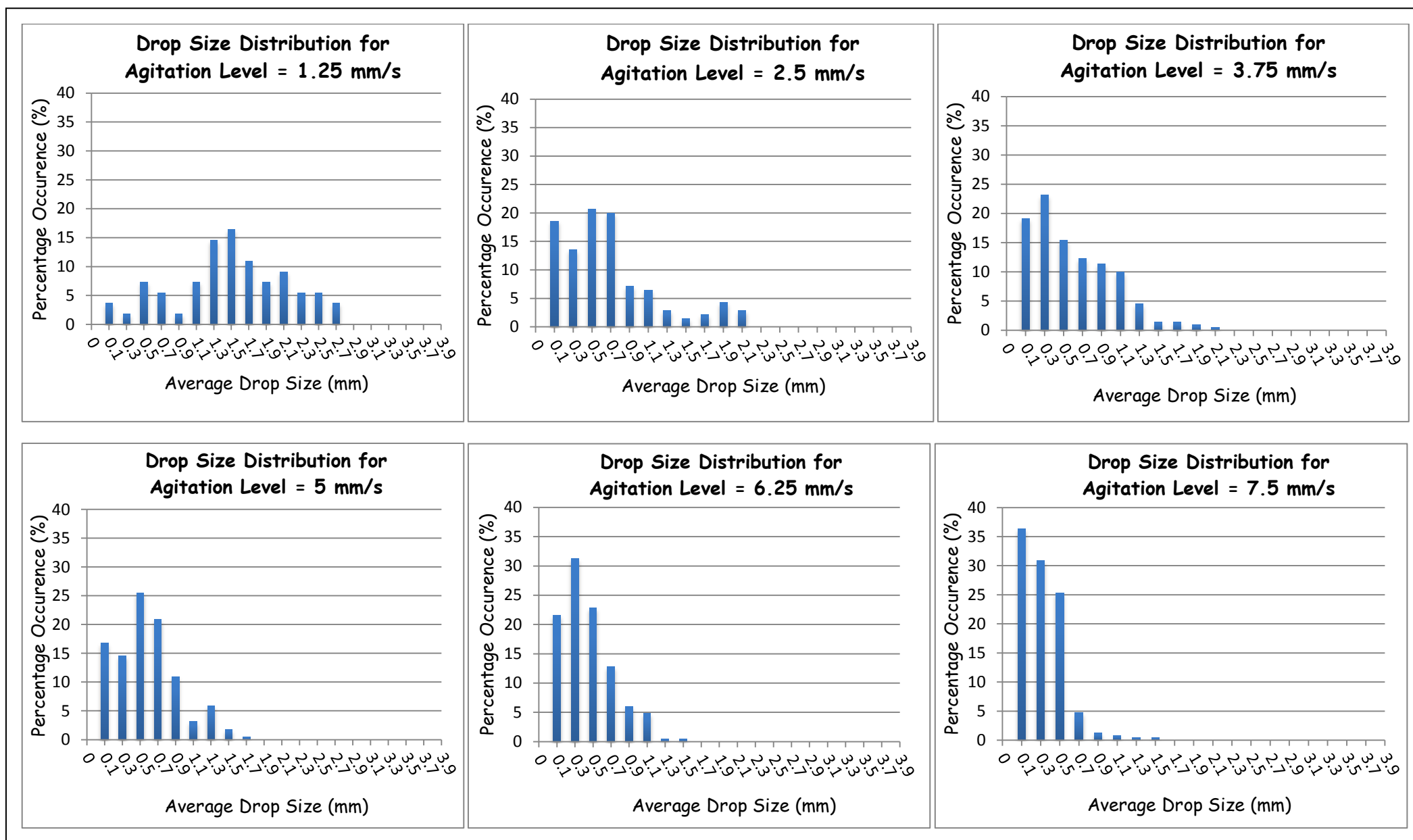
*Figure 4.2: Drop size distribution graphs at different agitation levels for hydrodynamic experiments (S/F =1:1 and h = 100 mm).*
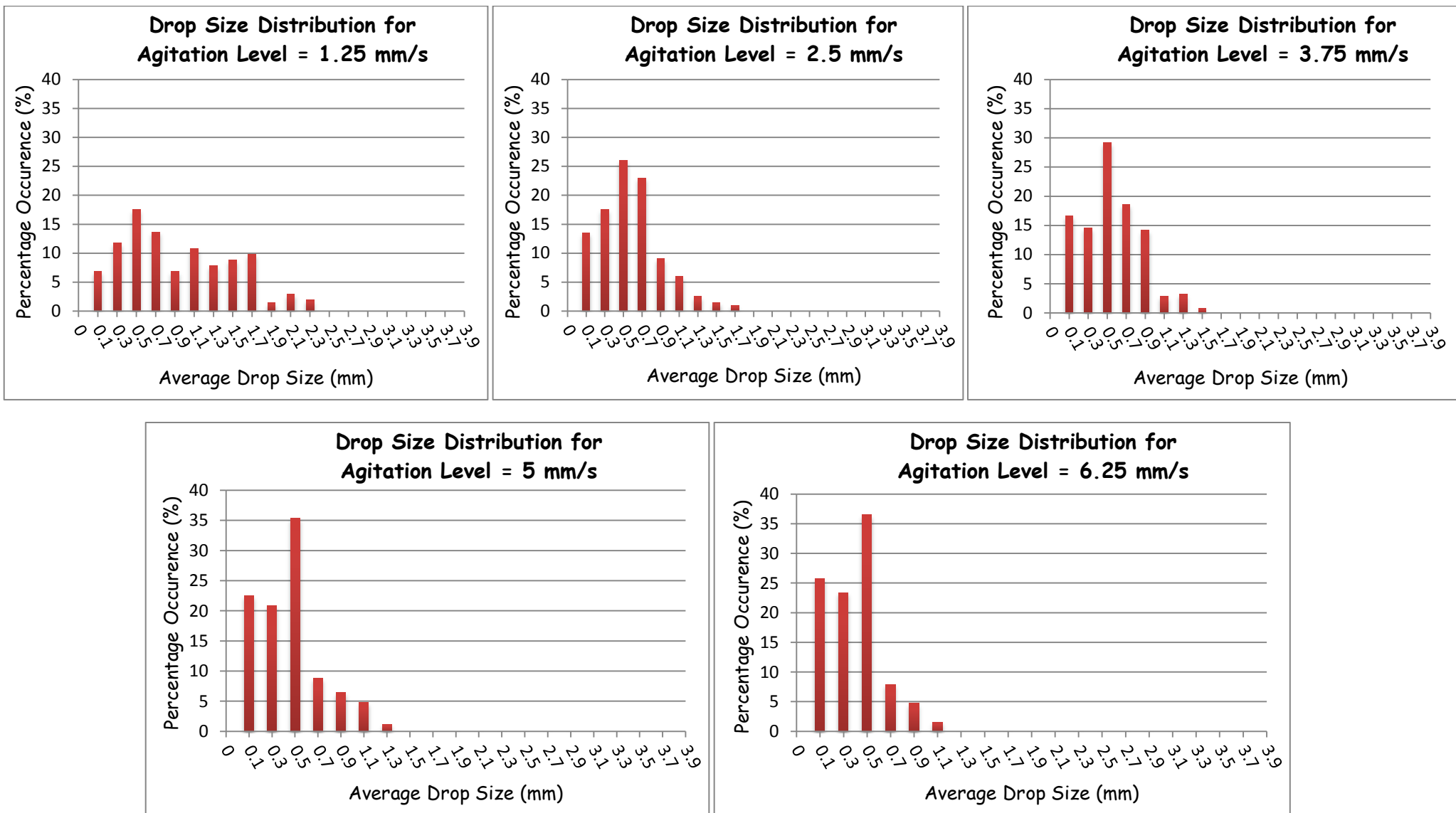
*Figure 4.3: Drop size distribution graphs at different agitation levels for hydrodynamic experiments (S/F =1:2 and h = 100 mm).*

71
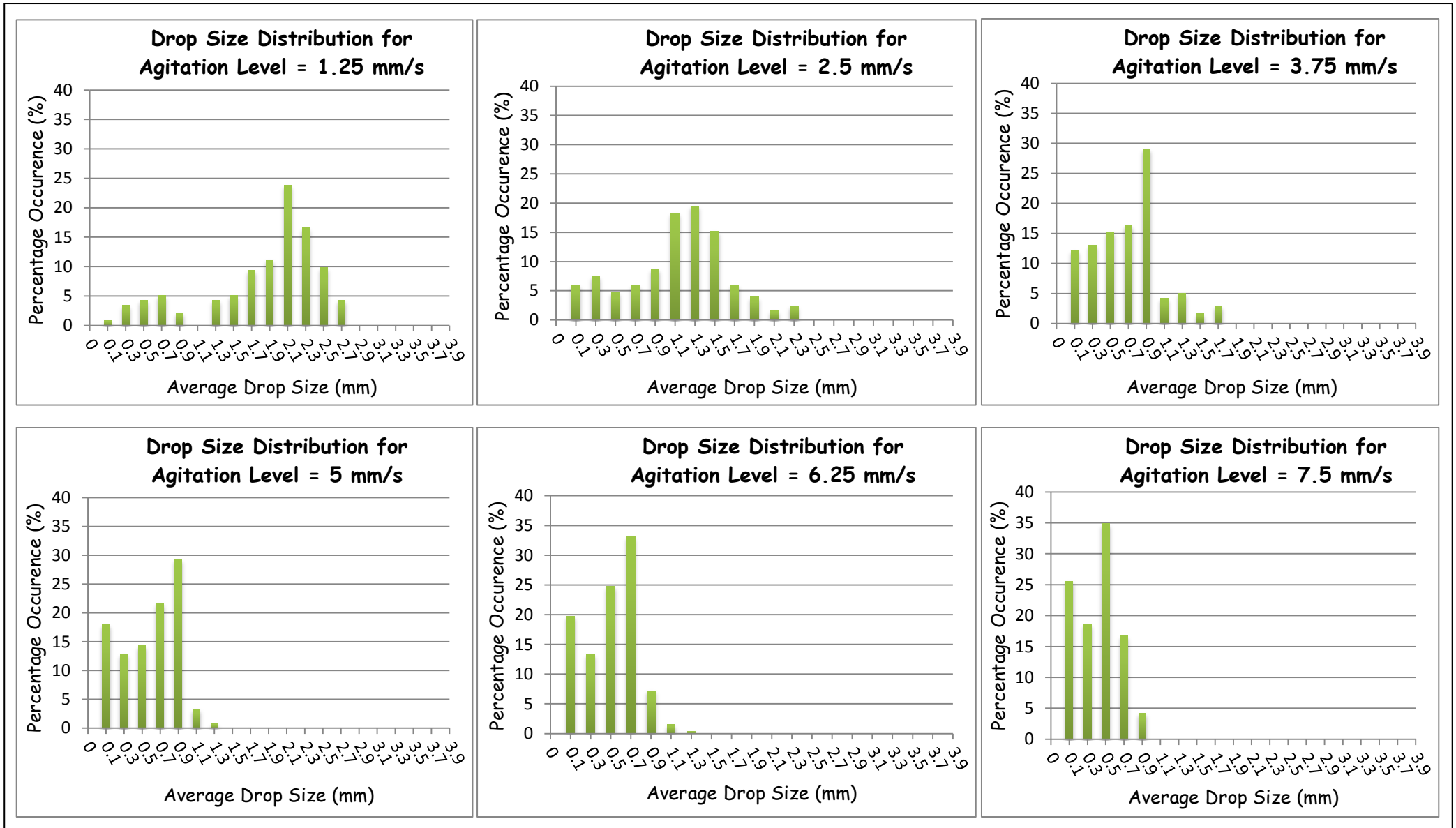
*Figure 4.4: Drop size distribution graphs at different agitation levels for hydrodynamic experiments (S/F =2:1 and h = 100 mm)*

The drop size distribution results illustrated in Figure 4.2 for S/F = 1:1, Figure 4.3 for S/F = 2:1 and Figure 4.4 for S/F = 1:2, at a tray spacing of 100 mm, clearly indicates that at lower agitation levels there exists a greater size distribution whereas for higher agitation levels a smaller size distribution is noticed. The drop size distribution displays such results since with a higher agitation level the plates vibrate much faster thus resulting in the production of smaller and more uniform droplets (please refer to Appendix C2 for detailed calculation of the drop size distribution).

The results obtained from the drop size distribution are then used to establish the Sauter mean drop diameter.

### 4.1.3. Sauter Mean Diameter Results

The Sauter mean drop diameter at different agitation levels for each solvent to feed ratio was calculated for a tray spacing of 100 mm using the drop size distribution results. Equation (2.13) was used in order to determine the Sauter mean drop diameter (please refer to Appendix C3 for detailed calculation of the Sauter mean diameter). Figure 4.5 below contains the Sauter mean diameter results.
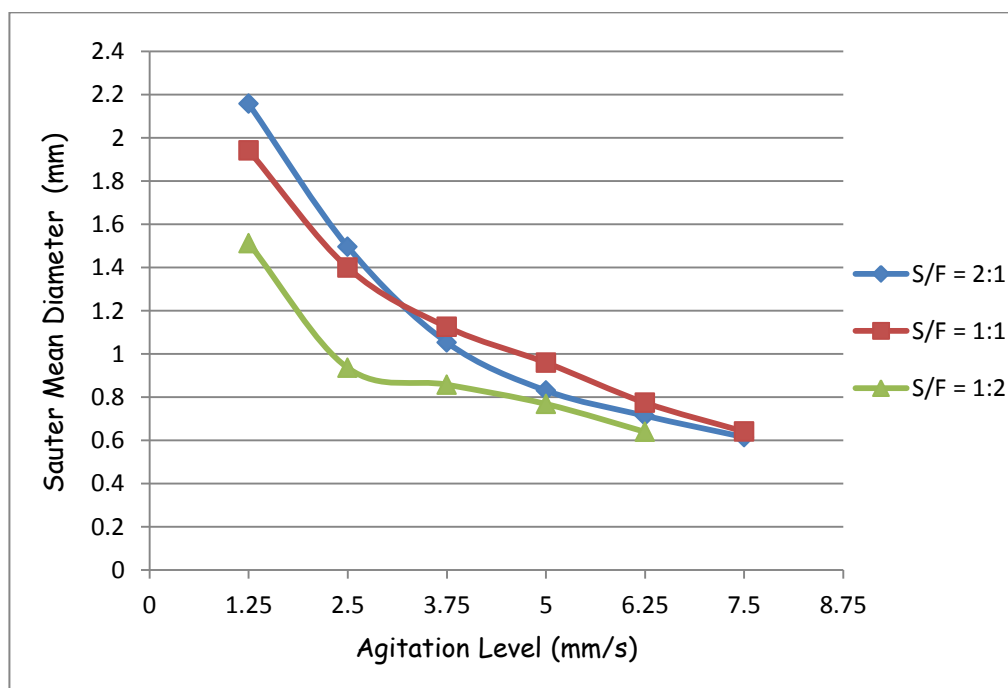


*Figure 4.5: Sauter mean drop diameter results for hydrodynamic experiments*

The result displayed in Figure 4.5 indicates that with an increase in the agitation level from 1.25 mm/s to 7.5 mm/s, there is a reduction in the Sauter mean drop diameter. This result is obtained since at higher agitation levels the perforated plates are vibrating much faster, thus more energy is dissipated to the fluid producing much smaller size droplets.

### 4.1.4. **Repeatability Analysis for Hydrodynamic Experiments**

Each hydrodynamic experimental run was repeated for each of the varied solvent to feed ratios and agitation levels and the raw data for the repeated runs are contained in Appendix B, Table B1.2. Dispersed phase holdup data gathered for the repeated hydrodynamic experiments indicate fairly similar measurements to the data obtained from the first set of hydrodynamic experiments. This thus indicates a good reproducibility of the results upon repetition of experiments.

For the drop size distribution results, three to five photographs of the droplets taken during the experiments were analysed using the Image Pro Plus software in order to achieve suitable results for the size distribution of the droplets and the Sauter mean drop diameter. An uncertainty of $\pm$ 0.3 mm was obtained for the Sauter mean drop diameter.

## 4.2. **Mass Transfer Experimental Results**

The mass transfer experiments were performed using the selected standard test system, toluene-acetone-water test system, with the feed mixture containing 6 mass % acetone in toluene. The mass transfer experiments were conducted for different tray spacing at varied solvent to feed ratio (S/F) and agitation levels (*af*) in order to establish the effect of these process and equipment parameters on the mass transfer of the system.

Three different tray spacings were investigated, 100 mm, 150 mm and 200 mm at solvent to feed ratios of 1:1, 1:2 and 2:1 and at agitation levels between 1.25 mm/s and 7.5 mm/s (in increments of 1.25 mm/s) until flooding occurred in the column. Solvent and feed flow rates of 10, 15 and 20 l/h were used.

Hydrodynamic experiments were conducted for a tray spacing of 100 mm and the hydrodynamic experiments were repeated in order to test the repeatability of the experiments.

## 4.2.1. **Dispersed Phase Holdup Results**

The dispersed phase holdup results for the mass transfer experiments at differing tray spacings, solvent to feed ratios and agitation levels is indicated in Figure 4.6. (Please refer to Appendix C1 for detailed dispersed phase holdup calculations).
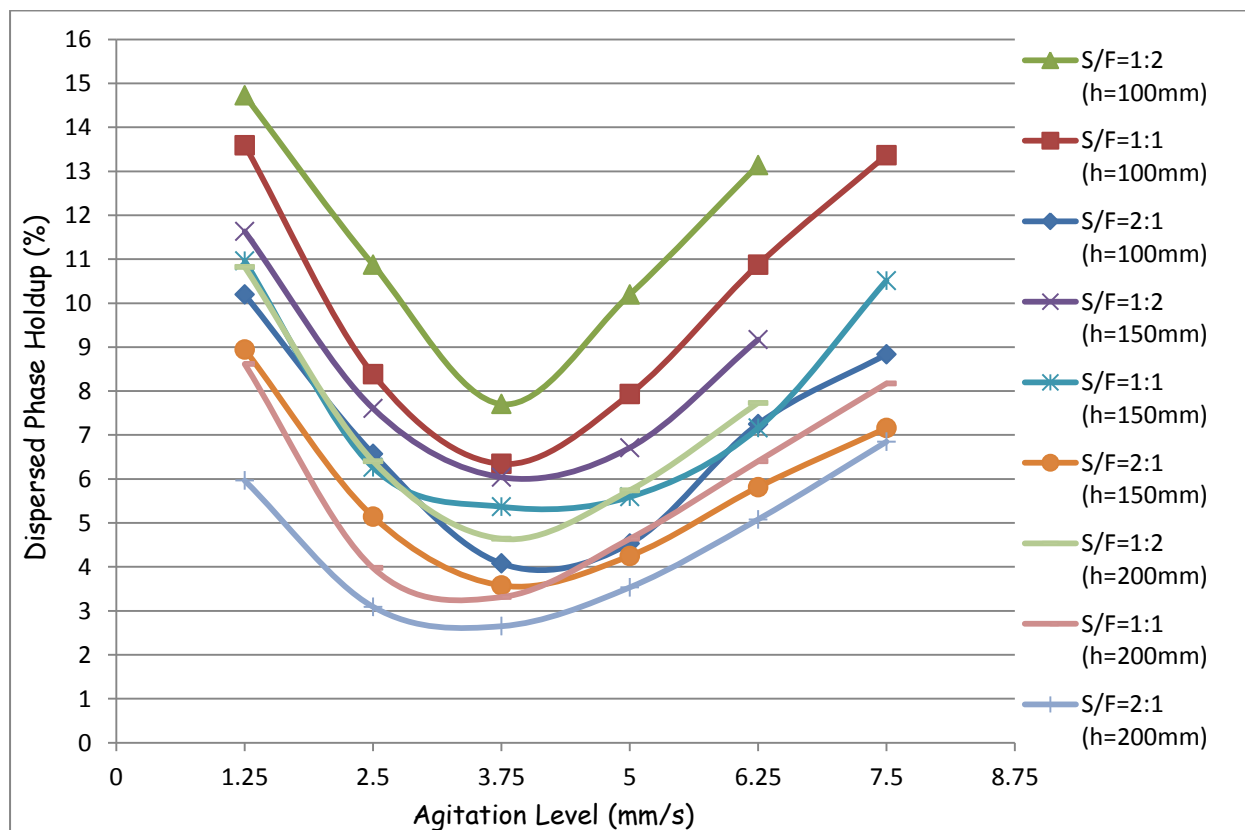


***Figure 4.6: Dispersed phase holdup results for mass transfer experiments***

Figure 4.6 which contains the dispersed phase holdup results for the mass transfer experiments also depicts a similar trend to the holdup results for the hydrodynamic experiments, this trend is also found to be in agreement with previous mass transfer investigations conducted by Rathilal (2010).

Mass transfer experiments also indicate the presence of two distinct hydrodynamic regime flows. The mixer-settler regime and the dispersion flow regime. A high initial dispersed phase holdup is also noticed for mass transfer experiments since the system operates in the mixer-settler regime. Figure 4.6 also indicates that as the agitation level rises a minimum value is reached at $af = 3.25$ mm/s. This is the point where there is a transition from the mixer-settler flow regime to the dispersion flow regime. Further increase from this agitation level shows an increase in the dispersed phase holdup while the system operates in the dispersion flow regime.

The dispersed phase holdup for the mass transfer experimental runs illustrates that as the solvent to feed ratio decreases the dispersed phase holdup increases, thus higher holdups are obtained for S/F = 1:2, as a result of there being more of the dispersed phase in the system. This result reconfirms the research work of Rama Rao et al. (1991), indicating that as the dispersed phase flow increases the holdup increases.

Figure 4.6 also depicts that with an increase in the tray spacing there is a reduction in the dispersed phase holdup. This result is displayed because as the tray spacing increases there is a lower accumulation of the dispersed phase under the perforated plate, thus contributing to a lower dispersed phase holdup.

For each of the tray spacings investigated at a solvent to feed ratio of 1:2, flooding of the extraction column was noticed for an agitation level of 7.5 mm/s. Therefore it can be deduced that for experiments conducted at higher solvent to feed ratios above an agitation level of 6.25 mm/s results in the onset of flooding in the extraction column irrespective of the tray spacing in the column.

### 4.2.2. __Comparison between Dispersed Phase Holdup for Hydrodynamic and Mass Transfer Experiments__

Figure 4.7 displays the comparison between the hydrodynamic and mass transfer dispersed phase holdup for a tray spacing of 100 mm and a solvent to feed ratio of 1:1.
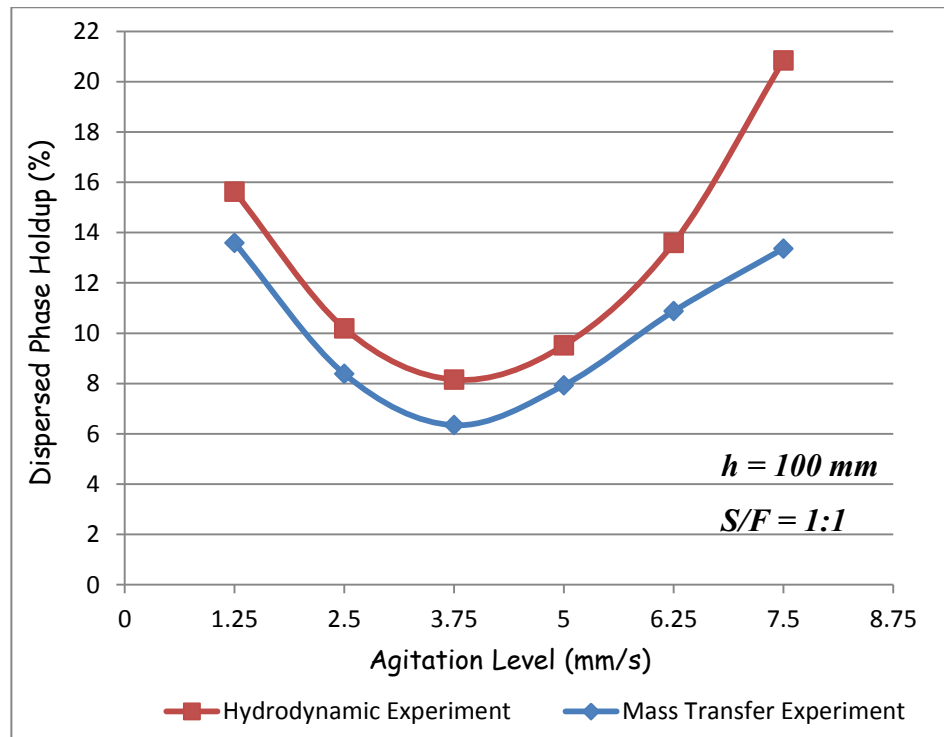


***Figure 4.7: Dispersed phase holdup comparison.***

The result in Figure 4.7 clearly indicates that for the hydrodynamic experiments, in the absence of the solute, the dispersed phase holdup is higher as compared to the holdup for the mass transfer experiments. Figure 4.7 only depicts the comparison for a tray spacing of 100 mm at a solvent to feed ratio of 1:1, but the other solvent to feed ratios at the same tray spacing also illustrates a similar outcome.

This outcome of a lower dispersed phase holdup for the mass transfer experiments can be attributed to the continuous extraction of the solute in the dispersed phase into the continuous phase during mass transfer, which results in a reduction of the dispersed phase during mass transfer. Since there is less dispersed phase present this contributes to the lower dispersed phase holdup for the mass transfer experiments.

Previous investigations conducted by Rathilal (2010) on vibrating plate extractions display a similar result of a higher dispersed phase holdup for the hydrodynamic experiments, except a similar minimum holdup was approached for both the hydrodynamic and mass transfer experiments, which does not seem to be the case in Figure 4.7.

The comparison between the hydrodynamic and mass transfer experiments dispersed phase holdup reveals that predictions for mass transfer may not be carried out using hydrodynamic dispersed phase data since mass transfer experiments affect the dispersed phase holdup. A similar deduction was also made from results obtained by Rathilal (2010).

### 4.2.3. **Drop Size Distribution Results**

The Image Pro Plus software was also utilised for the mass transfer experiments to analyse the drop sizes and number of droplets in each drop size range.

The drop size distribution results for the mass transfer experiments illustrated in Figure 4.8 for S/F = 1:1, Figure 4.9 for S/F = 2:1 and Figure 4.10 for S/F = 1:2, at a tray spacing of 100 mm, indicates a similar result as compared to the hydrodynamic experiments. This result means that at lower agitation levels there exists a greater size distribution whereas for higher agitation levels a smaller size distribution is noticed. Such results are displayed since at higher agitation level the plates vibrate much faster thus resulting in the production of smaller and more uniform droplets (please refer to Appendix C2 for detailed drop size distribution calculations).

Refer to Appendix D1 for the additional drop size distribution results for tray spacings of 150 mm and 200 mm at varied solvent to feed ratios for the mass transfer experiments. The same deduction of a smaller size distribution at higher agitation level can be made for the other tray spacings investigated. Larger drop sizes are noticed, with an increase in the tray spacing, this is as a result of a reduction in the breakup of the droplets due to the plates being further apart, thus not allowing for the dispersion of smaller sized droplets.

A more conclusive analysis of the effect of the tray spacing on the droplet sizes can be drawn from the Sauter mean diameter results, since the drop size distribution results were used to establish the Sauter mean drop diameter.
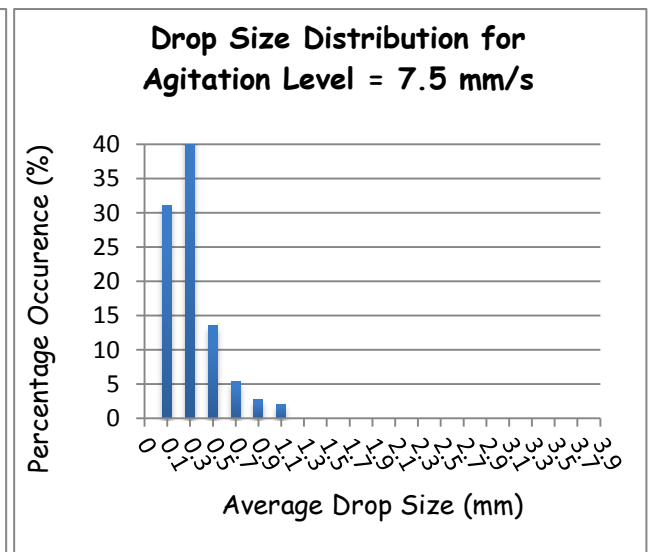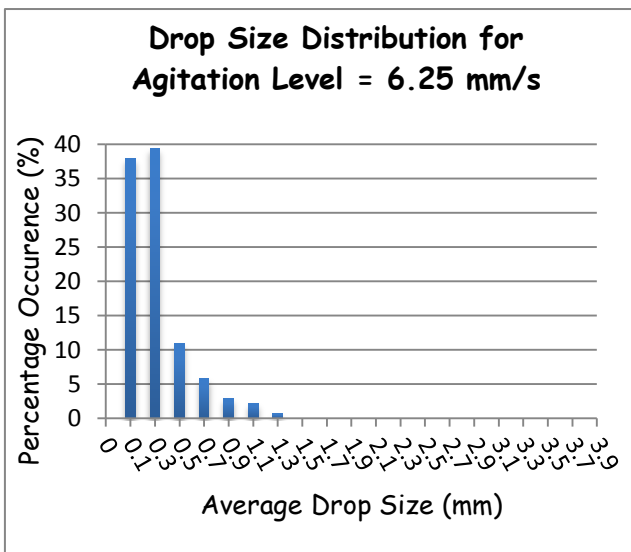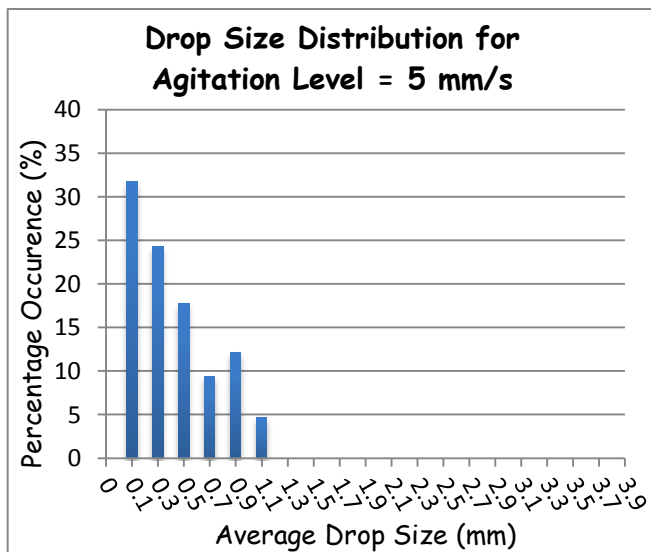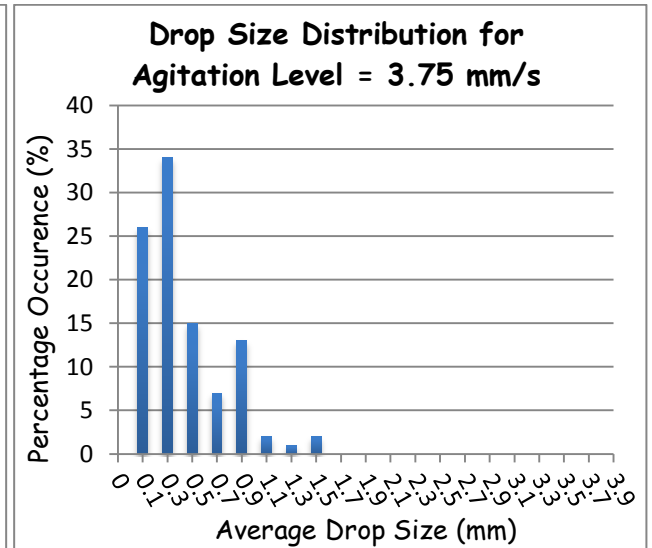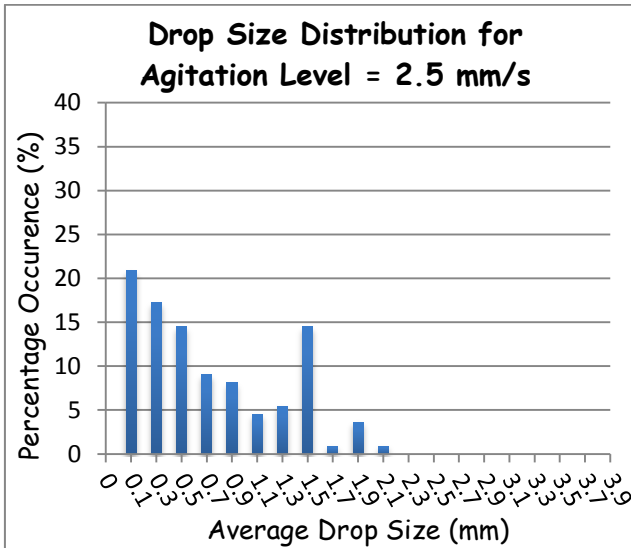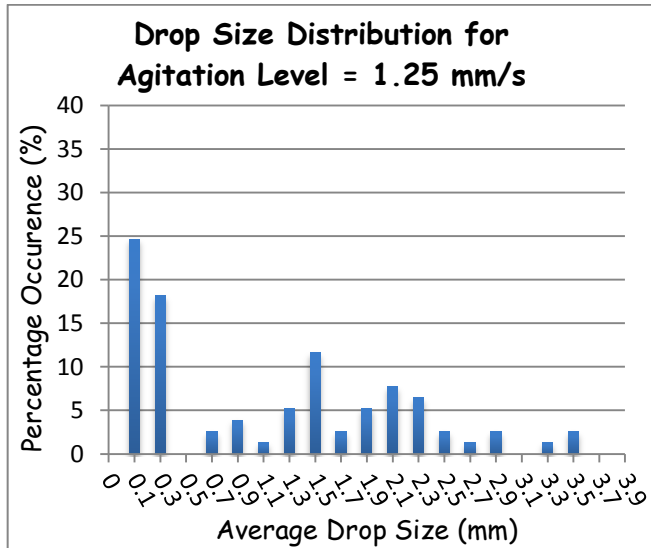
*Figure 4.8: Drop size distribution graphs at different agitation levels for mass transfer experiments (S/F =1:1 and h = 100mm).*
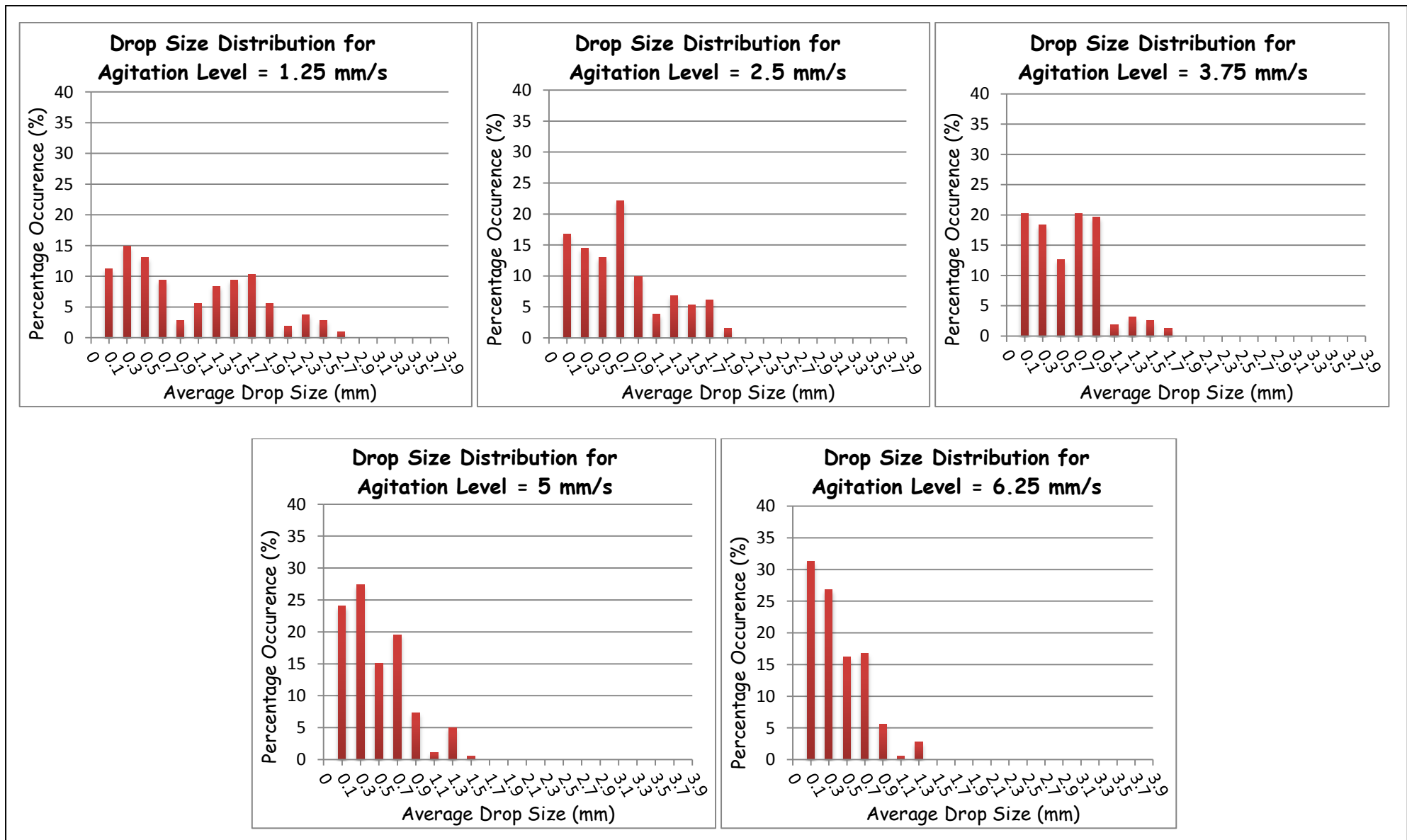
*Figure 4.9: Drop size distribution graphs at different agitation levels for mass transfer experiments (S/F =1:2 and h = 100mm).*
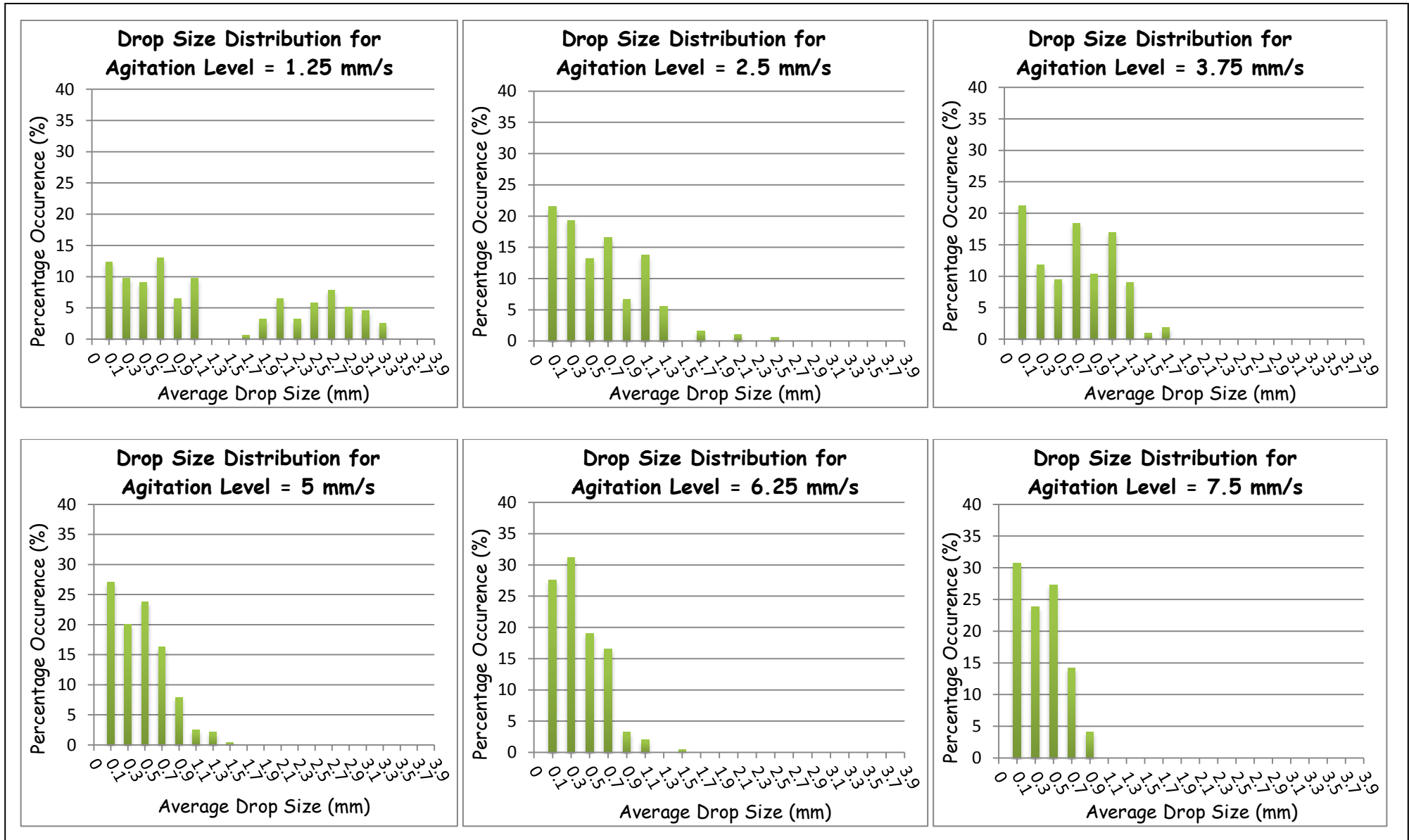
*Figure 4.10: Drop size distribution graphs at different agitation levels for mass transfer experiments (S/F =2:1 and h = 100mm).*

## 2.4. **Sauter Mean Diameter Results**

Figure 4.11 below indicates the Sauter mean drop diameter results investigated at three different tray spacings, for varied agitation levels and solvent to feed ratios, with the use of Equation (2.13) (please refer to Appendix C3 for detailed calculation of the Sauter mean diameter).
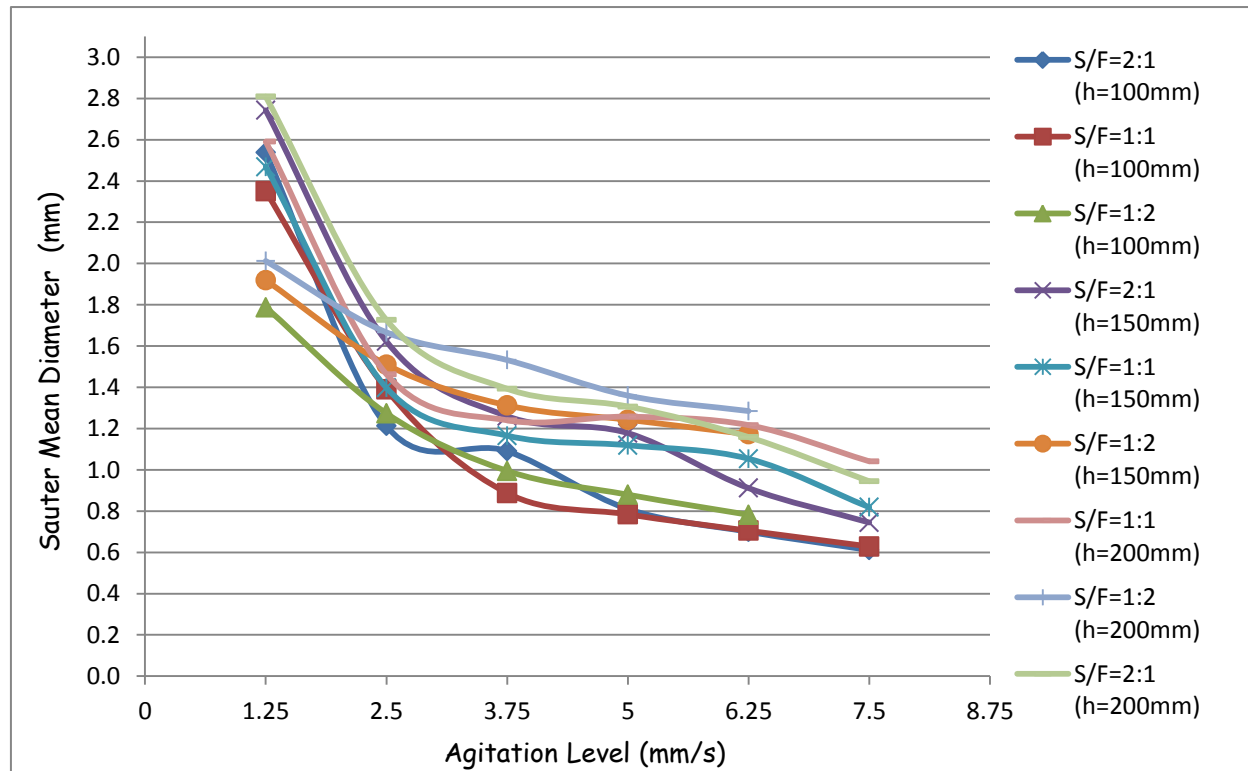


*Figure 4.11: Sauter mean drop diameter results for mass transfer experiments.*

Similarly to the hydrodynamic experiments a reduction in the Sauter mean diameter is depicted with increasing agitation levels from 1.25 mm/s to 7.5 mm/s for the mass transfer experiments. This result occurs due to the perforated plates vibrating faster at higher agitation levels, thus dissipating more energy to the fluid resulting in the production of much smaller size droplets, thus contributing to a smaller Sauter mean diameter.

In the mixer-settler regime (between agitation levels 1.25 mm/s and 3.75 mm/s), for solvent to feed ratios 2:1 and 1:1, the Sauter mean diameter results seem to display fairly similar values for a varied tray spacing, but for a solvent to feed ratio of 1:2, with an increased presence of the dispersed phase, Figure 4.11 illustrates a wider Sauter mean diameter range. In the dispersion flow regime the Sauter mean diameter for the different solvent to feed ratios investigated seem to display fairly similar values for the different tray spacings.

The Sauter mean diameter results depict that with an increase in the tray spacing, there is a consequent increase in the Sauter mean diameter. Since the perforated plates are placed further apart, there is a decline in the breakup of the dispersed phase droplets. With the presence of fewer perforated plates at higher tray spacings, less energy is actually dissipated to the fluid resulting in the production of larger sized dispersed phase droplets.

### 4.2.5. **Comparison between Sauter Mean Diameter for Hydrodynamic and Mass Transfer Experiments**

The following Figure 4.12 displays the comparison between the hydrodynamic and mass transfer Sauter mean drop diameter, for a tray spacing of 100 mm and a solvent to feed ratio of 1:1.
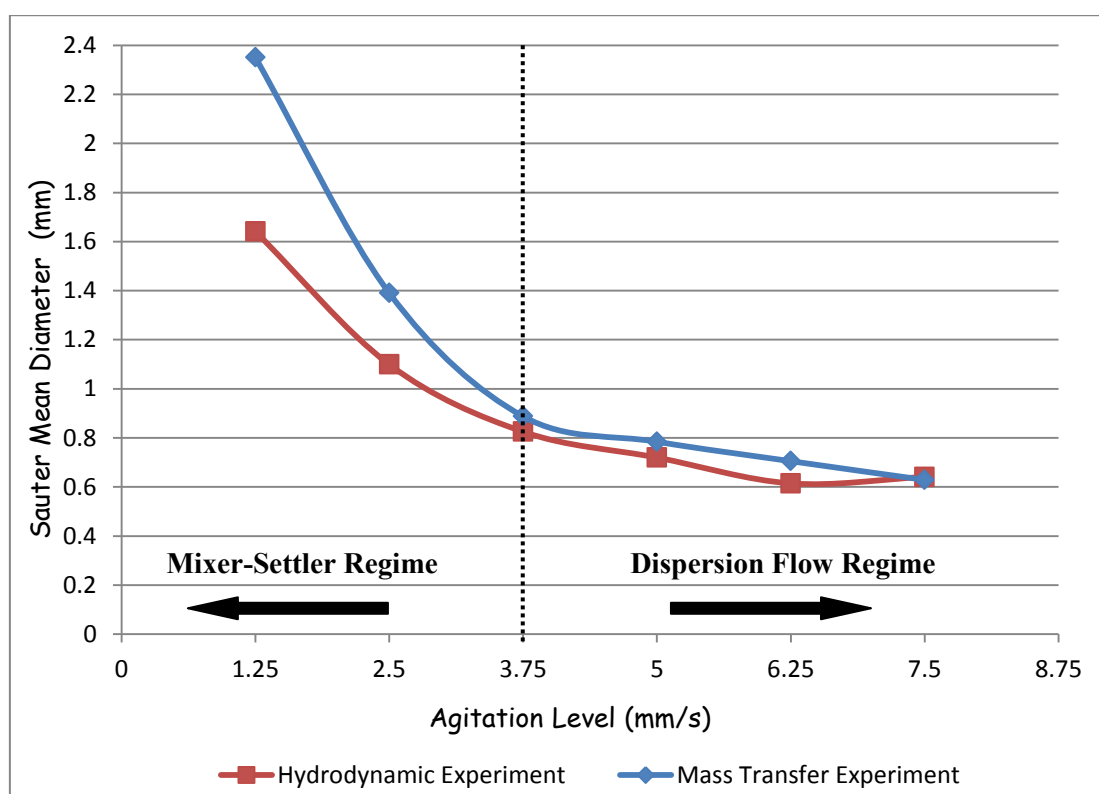


*Figure 4.12: Sauter mean drop diameter comparison.*

Figure 4.13 clearly indicates that for the hydrodynamic experiments, in the absence of the solute, the Sauter mean drop diameter is lower as compared to the Sauter mean drop diameter for the mass transfer experiments. A larger difference in the Sauter mean diameter is distinguished between the hydrodynamic and mass transfer experiments in the mixer-settler flow regime as compared to the dispersion flow regime.

Figure 4.12 only depicts the comparison for a tray spacing of 100 mm at a solvent to feed ratio of 1:1, but the other solvent to feed ratios at the same tray spacing also illustrates a similar outcome.

Shen et al. (1985) as well as Aravamudan and Baird (1999) explain that this result of a lower Sauter mean drop diameter for hydrodynamic experiments as compared to the mass transfer experiments is due to the enhanced coalescence effects during the mass transfer operation. The surface tension is found to be reduced as two dispersed phase droplets approach each other, due to the transfer of the solute from the dispersed phase to the continuous phase. Thus the continuous phase present between the droplets is drained and the droplets coalesce leading to the development of larger drops during the mass transfer experiments.

The comparison between the hydrodynamic and mass transfer experiments Sauter mean diameter also reveals that predictions for mass transfer may not be carried out using hydrodynamic Sauter mean diameter data since mass transfer experiments also affects the Sauter mean drop diameter. Research conducted by Rathilal (2010) resulted in similar deductions.

### 4.2.6. **Percentage Acetone Extracted**

The following Figure 4.13 depicts the percentage acetone extracted from the dispersed phase for the three different tray spacings investigated at varied agitation levels and solvent to feed ratios.
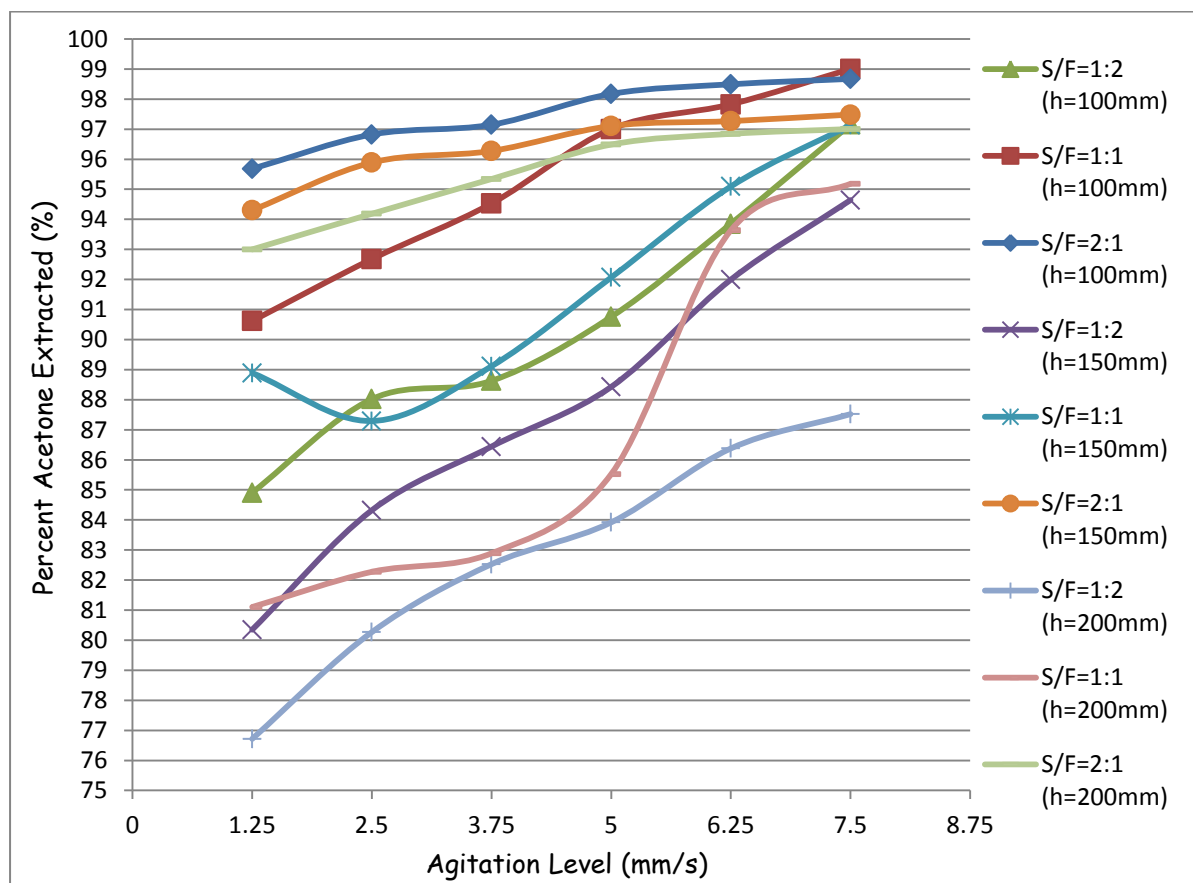


*Figure 4.13: Percentage acetone extracted for different tray spacings at varied agitation levels and solvent to feed ratios.*

The percentage acetone extracted from the dispersed phase was determined using the feed and raffinate acetone concentrations obtained from the gas chromatograph analysis. Refer to Appendix C4 for detailed sample calculations regarding the determination of the percentage acetone extracted. Please note it was assumed that there is no solvent present in the raffinate and no carrier present in the extract.

Figure 4.13 indicates that there is an increase in the amount of acetone extracted from the dispersed phase as the agitation level is increased. It can be deduced that as the solvent to feed ratio increases there is a subsequent increase in the amount of acetone extracted. This effect of an increase in the amount of acetone extracted with an increase in the solvent to feed ratio is as a result of more solvent being available in order to remove acetone from the dispersed phase. This result is also in agreement with Rathilal (2010) where there was an improvement in the extraction effectiveness with an increase in the solvent to feed ratio.

The tray spacing seems to have a distinct influence on the amount of acetone being extracted using a vibrating plate extraction column. As the tray spacing is increased there is a reduction in the extraction effectiveness of acetone, which could be attributed to there being fewer plates required for mass transfer. Figure 4.13 also displays the lowest extraction effectiveness for a tray spacing of 200 mm investigated at a solvent to feed ratio of 1:2.

Rathilal (2010) also indicated that a greater extraction of acetone could be achieved for larger tray spacings, at agitation levels above 7.5 mm/s. This was as a result of the vibrating plate extraction column not operating near flooding conditions for tray spacings of 150 mm and 200 mm at an agitation level of 7.5 mm/s for solvent to feed ratios 1:2 and 1:1, since it did flood for a tray spacing of 100 mm.

The interfacial area available for mass transfer plays an integral role as well in the extraction effectiveness of a vibrating plate extraction column. Aravamudan and Baird (1999) indicates that the interfacial area depends on the dispersed phase holdup and the Sauter mean diameter. Thus a higher amount of acetone is extracted when the extraction column is operated in the dispersion flow regime, since a higher dispersed phase holdup and a lower Sauter mean diameter is achieved in this regime as compared to the mixer-settler regime. Therefore with a larger dispersed phase holdup and a lower Sauter mean diameter a larger interfacial area is available for mass transfer and consequently there is a larger extent of extraction of acetone.

### 4.2.7. **Mass Transfer Coefficient**

The measured mass transfer coefficient was calculated by using the true NTU, (which is $N_{ox}$), the dispersed phase velocity (m/s), the Sauter mean diameter (m), the dispersed phase holdup and the effective height of the extraction column, as depicted in Equation (4.1), which is a combination of Equation (2.24) and Equation (2.52) (Rathilal, 2010). The effective height of the extraction column was 4.76 m and the true NTU for the different tray spacing is indicated in Table 4.1 below.

$$k_{oxm} = \frac{N_{ox} U_d d_{32}}{6 \emptyset H} \qquad \dots (4.1)$$

*Table 4.1: $N_{ox}$ values for the different tray spacings investigated.*

| *Tray Spacing (mm)* | 100 | 150 | 200 |
|---|---|---|---|
| $N_{ox}$ | 45 | 30 | 23 |

The results for the measured mass transfer coefficients can be found in Table 4.2, which also contains the values for the predicted mass transfer coefficients. Refer to Appendix C5 for detailed sample calculations regarding the determination of the measured mass transfer coefficient. The predicted mass transfer coefficients were calculated using the correlation developed by Rathilal (2010) which relates the mass transfer coefficient to the agitation levels and the tray spacing.

Equation (4.2) below established by Rathilal (2010) illustrates the mass transfer coefficient correlation in units of mm/s, where the agitation level is in mm/s and the tray spacing in mm. The following correlation applies to the dispersion flow regime and emulsion flow regimes, as a result of using Equation (2.24) to determine the interfacial area, which utilises the drop dispersion holdup. The dispersed phase holdup in the mixer-settler regime includes the coalesced dispersed phase layer collected under the perforated plates.

$$k_{ox} = -0.007(af) + 0.06 + \frac{h}{10000} \qquad \dots (4.2)$$

Table 4.2 contains the values calculated for the measured mass transfer coefficient ($k_{oxm}$) using Equation (4.1) and the predicted mass transfer coefficient ($k_{oxp}$) using the correlation developed in Equation (4.2) by Rathilal (2010) for the different tray spacings, solvent to feed ratios and agitation levels investigated. It should be noted that Equation (4.2) is only valid in the dispersed regime, therefore comparison could only be made for agitation levels greater than or equal to 3.75 mm/s.

***Table 4.2: Comparison between measured and predicted mass transfer coefficients.***

| af (mm/s) | h = 100 mm | | | | | | h = 150 mm | | | | | | h = 200 mm | | | | | |
|---|---|---|---|---|---|---|---|---|---|---|---|---|---|---|---|---|---|---|
| | S/F = 1:1 | | S/F = 2:1 | | S/F = 1:2 | | S/F = 1:1 | | S/F = 2:1 | | S/F = 1:2 | | S/F = 1:1 | | S/F = 2:1 | | S/F = 1:2 | |
| | $k_{oxm}$ | $k_{oxp}$ | $k_{oxm}$ | $k_{oxp}$ | $k_{oxm}$ | $k_{oxp}$ | $k_{oxm}$ | $k_{oxp}$ | $k_{oxm}$ | $k_{oxp}$ | $k_{oxm}$ | $k_{oxp}$ | $k_{oxm}$ | $k_{oxp}$ | $k_{oxm}$ | $k_{oxp}$ | $k_{oxm}$ | $k_{oxp}$ |
| 1.25 | 0.0635 | 0.0613 | 0.0610 | 0.0613 | 0.0595 | 0.0613 | 0.0552 | 0.0663 | 0.0500 | 0.0663 | 0.0539 | 0.0663 | 0.0565 | 0.0713 | 0.0590 | 0.0713 | 0.0465 | 0.0713 |
| 2.5 | 0.0609 | 0.0525 | 0.0452 | 0.0525 | 0.0574 | 0.0525 | 0.0547 | 0.0575 | 0.0515 | 0.0575 | 0.0648 | 0.0575 | 0.0691 | 0.0625 | 0.0699 | 0.0625 | 0.0651 | 0.0625 |
| 3.75 | 0.0514 | 0.0438 | 0.0655 | 0.0438 | 0.0633 | 0.0438 | 0.0532 | 0.0488 | 0.0575 | 0.0488 | 0.0710 | 0.0488 | 0.0703 | 0.0538 | 0.0658 | 0.0538 | 0.0827 | 0.0538 |
| 5 | 0.0363 | 0.0350 | 0.0438 | 0.0350 | 0.0423 | 0.0350 | 0.0490 | 0.0400 | 0.0453 | 0.0400 | 0.0605 | 0.0400 | 0.0509 | 0.0450 | 0.0463 | 0.0450 | 0.0593 | 0.0450 |
| 6.25 | 0.0238 | 0.0263 | 0.0236 | 0.0263 | 0.0292 | 0.0263 | 0.0361 | 0.0313 | 0.0256 | 0.0313 | 0.0417 | 0.0313 | 0.0357 | 0.0363 | 0.0286 | 0.0363 | 0.0416 | 0.0363 |
| 7.5 | 0.0173 | 0.0175 | 0.0169 | 0.0175 | - | 0.0175 | 0.0191 | 0.0225 | 0.0170 | 0.0225 | - | 0.0225 | 0.0239 | 0.0275 | 0.0173 | 0.0275 | - | 0.0275 |

A fairly close approximation exists between the predicted mass transfer coefficient values and the measured mass transfer coefficient values for the different tray spacings, solvent to feed ratios and agitation levels greater than or equal to 3.75 mm/s investigated. Thus the correlation developed by Rathilal (2010) seems to predict the mass transfer coefficient utilising the agitation level and the solvent to feed ratio appropriately for the data gathered, with a maximum error of approximately 15%.

## 4.2.8. <u>**Number of Equilibrium Stages With and Without Forward Mixing and Backmixing**</u>

In order to determine the number of equilibrium stages with and without backmixing and forward mixing, the McCabe Thiele method was used for the stepping off of the stages. The equilibrium line was plotted using equilibrium data for the acetone-toluene-water system and linear relation was established with a gradient of 0.832 (Lisa, et al., 2003 and Saien, et al., 2006). The actual operating line was plotted using the acetone concentrations from the gas chromatograph analysis for the extract binary sample (assuming no carrier present), raffinate binary sample (assuming no solvent present) and binary samples along the length of the extraction column. An uncertainty of ± 2 % was established in the compositions using the gas chromatograph detector. The measured number of equilibrium stages with backmixing was then determined by stepping off between the actual operating line and the equilibrium line, while the number of equilibrium stages without backmixing was established by stepping off between the ideal operating line and the equilibrium line and using Equation (2.45). Refer to Appendix C6 for detailed sample calculations regarding the determination of the ideal number of equilibrium stages.

The stepping off of the equilibrium stages using the McCabe Thiele technique is depicted in Figure 4.14 below, which is for a tray spacing of 100 mm at a solvent to feed ratio of 1:2, for the lowest agitation level of 1.25 mm/s investigated.
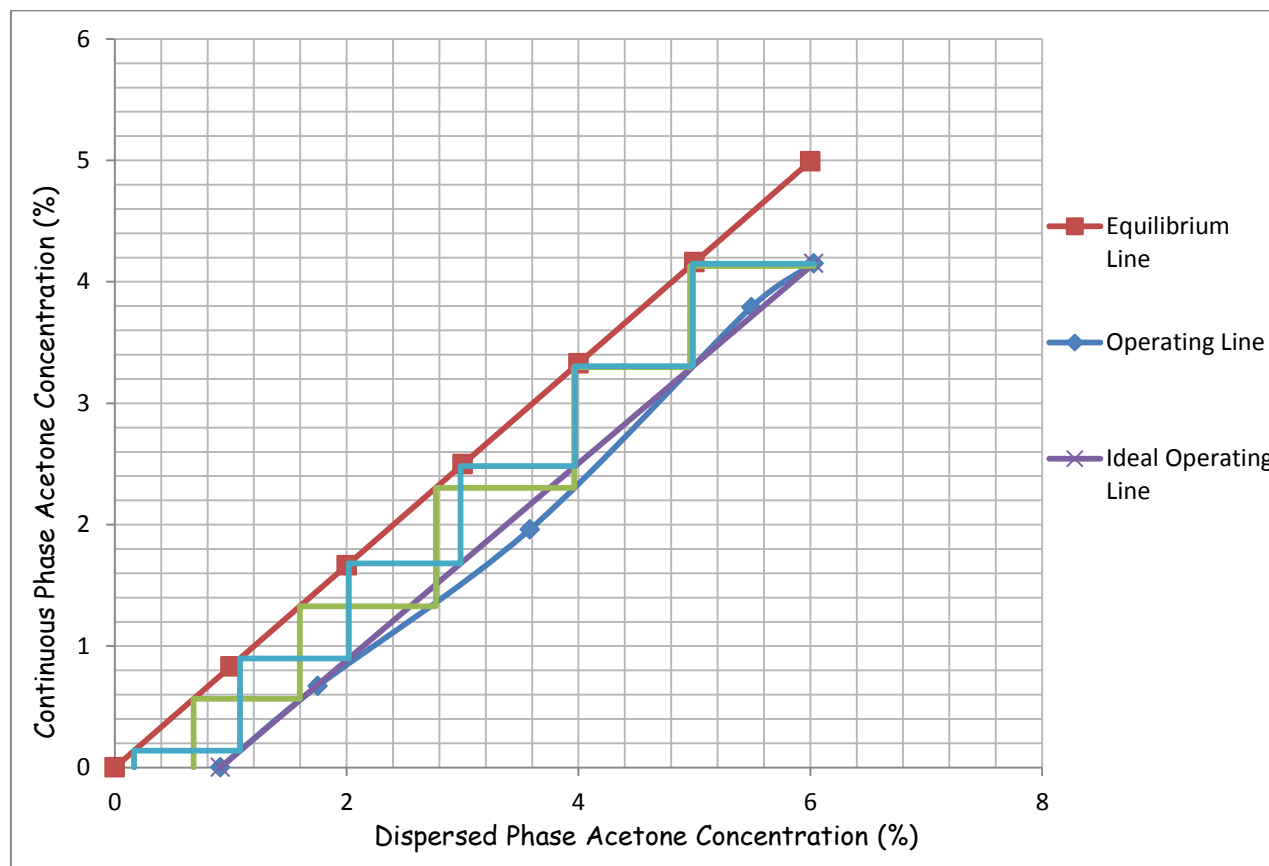


***Figure 4.14: Stepping off stages by the McCabe Thiele method for the acetone-toluene-water system,***

***for  h = 100 mm, S/F =1:2 and af = 1.25 mm/s.***

Figure 4.14 indicates a fairly linear operating line for the lowest agitation level investigated, thus indicating negligible backmixing occurring in the dispersed phase, as compared to Figure 4.15 which illustrates a nonlinear operating line for the highest agitation level investigated, indicating the occurrence of backmixing as well as forward mixing in the dispersed phase. This result was also deduced by Rathilal (2010) through his investigations on vibrating plate extraction columns.

Backmixing in the dispersed phase is due to a decrease in the accumulation of the dispersed phase under each perforated plate as the agitation level is increased, therefore the dispersed phase droplets re-enters the previous stage it came from. Forward mixing is the case where the dispersed phase droplets move through the downcomers fixed on the perforated plates above, thus allowing the droplets to pass a stage and circulate within the next stage. Rathilal (2010), also explains that forward mixing is also experienced by very fine dispersed phase droplets which bypass stages and thus have no residence time in that stage.

The stepping off of the equilibrium stages using the McCabe Thiele technique is depicted in Figure 4.15 below, which is for a tray spacing of 100 mm at a solvent to feed ratio of 1:2, for the highest agitation level of 7.5 mm/s investigated.
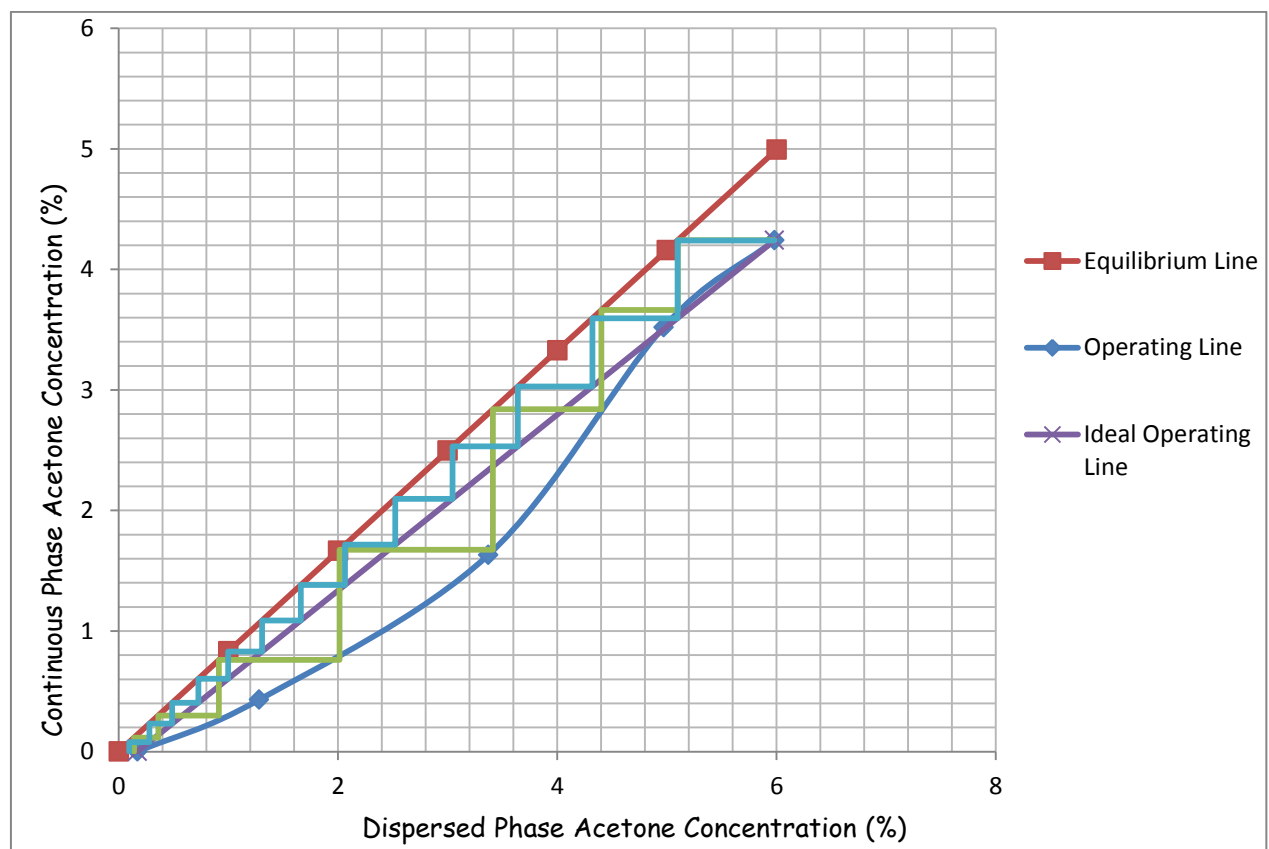


***Figure 4.15: Stepping off stages by the McCabe Thiele method for the acetone-toluene-water system, for h = 100 mm, S/F = 1:2 and af = 7.5 mm/s.***

Thus from a comparison between Figure 4.14 and Figure 4.15 it can be gathered that the backmixing in the dispersed phase increases as the agitation level increases, consequently a higher number of equilibrium stages without backmixing is obtained, as shown in Table 4.3 below. Please refer to Appendix D 2 for the stepping of stages using the McCabe Thiele method for the other tray spacings, solvent to feed ratios and agitation levels investigated, where Appendix D 2.1 contains the stepping off plots for h = 100 mm, Appendix D 2.2 for h = 150 mm and Appendix D 2.3 for h = 200 mm.

Table 4.3 below contains the number of equilibrium stages with and without backmixing obtained from stepping off using the McCabe Thiele method, for the different tray spacings, solvent to feed ratios and agitation levels investigated. These results indicate fairly similar real and ideal values for the number of equilibrium stages, but in some cases the number of stages without backmixing is higher than the number of stages with backmixing and this is attributed to backmixing occurring in the dispersed phase.

**Table 4.3: Number of equilibrium stages with and without backmixing from stepping off.**

| $af$ (mm/s) | h = 100 mm | | | | | | h = 150 mm | | | | | | h = 200 mm | | | | | |
|---|---|---|---|---|---|---|---|---|---|---|---|---|---|---|---|---|---|---|
| | S/F = 1:1 | | S/F = 2:1 | | S/F = 1:2 | | S/F = 1:1 | | S/F = 2:1 | | S/F = 1:2 | | S/F = 1:1 | | S/F = 2:1 | | S/F = 1:2 | |
| | $N_{ox}$ With Backmixing | $N_{ox}$ Without Backmixing | $N_{ox}$ With Backmixing | $N_{ox}$ Without Backmixing | $N_{ox}$ With Backmixing | $N_{ox}$ Without Backmixing | $N_{ox}$ With Backmixing | $N_{ox}$ Without Backmixing | $N_{ox}$ With Backmixing | $N_{ox}$ Without Backmixing | $N_{ox}$ With Backmixing | $N_{ox}$ Without Backmixing | $N_{ox}$ With Backmixing | $N_{ox}$ Without Backmixing | $N_{ox}$ With Backmixing | $N_{ox}$ Without Backmixing | $N_{ox}$ With Backmixing | $N_{ox}$ Without Backmixing |
| 1.25 | 4 | 4 | 3 | 3 | 7 | 6 | 4 | 3 | 4 | 2 | 7 | 5 | 3 | 2 | 3 | 2 | 7 | 5 |
| 2.5 | 4 | 4 | 3 | 3 | 7 | 7 | 3 | 3 | 6 | 3 | 7 | 7 | 3 | 3 | 3 | 2 | 6 | 5 |
| 3.75 | 5 | 5 | 3 | 4 | 8 | 7 | 4 | 3 | 3 | 3 | 8 | 8 | 3 | 3 | 3 | 2 | 7 | 6 |
| 5 | 6 | 6 | 2 | 4 | 7 | 8 | 4 | 4 | 3 | 3 | 7 | 9 | 4 | 3 | 2 | 3 | 7 | 6 |
| 6.25 | 7 | 7 | 2 | 4 | 9 | 10 | 5 | 5 | 6 | 3 | 8 | 12 | 4 | 4 | 5 | 3 | 6 | 6 |
| 7.5 | 6 | 7 | 4 | 4 | 7 | 13 | 6 | 6 | 9 | 6 | 9 | 13 | 5 | 4 | 5 | 3 | 6 | 6 |

As indicated by Rathilal (2010) the agitation level affects the occurrence of backmixing in the dispersed phase as a result of a decline in the accumulation of the dispersed phase beneath each perforated plate as the agitation level is increased. At lower agitation levels, the layer of dispersed phase accumulated beneath the perforated plate acts as a barrier preventing the dispersed phase droplets from returning to the previous stage it came from. In this way backmixing is prevented from occurring.

The solvent to feed ratios investigated also has an effect on the backmixing in the dispersed phase taking place, for higher solvent to feed ratios of 2:1 it was noticed that minimal backmixing occurred since there was always the presence of a dispersed phase layer accumulated under each perforated plate, thus not allowing the dispersed phase droplets from re-entering into the previous stage. Whereas for the lowest solvent to feed ratio of 1:2, a substantial amount of backmixing occurred as a result of there being larger dispersed phase droplets present leading to re-circulation within the stages and the re-entering of the dispersed phase droplets into the previous stage.

The Table 4.4 shows the results for comparison between the measured number of equilibrium stages (with backmixing) from stepping off and the predicted number of stages using the correlation in Equation (2.56) developed by Rathilal (2010). The model developed to predict the number of equilibrium stages for a vibrating plate extraction column utilises the different parameters investigated, which include the agitation level, the solvent to feed ratio and the tray spacing.

*Table 4.4: Comparison between measured and predicted number of equilibrium stages.*

| af (mm/s) | h = 100 mm | | | | | | h = 150 mm | | | | | | h = 200 mm | | | | | |
|---|---|---|---|---|---|---|---|---|---|---|---|---|---|---|---|---|---|---|
| | S/F = 1:1 | | S/F = 2:1 | | S/F = 1:2 | | S/F = 1:1 | | S/F = 2:1 | | S/F = 1:2 | | S/F = 1:1 | | S/F = 2:1 | | S/F = 1:2 | |
| | $N_{oxm}$ | $N_{oxp}$ | $N_{oxm}$ | $N_{oxp}$ | $N_{oxm}$ | $N_{oxp}$ | $N_{oxm}$ | $N_{oxp}$ | $N_{oxm}$ | $N_{oxp}$ | $N_{oxm}$ | $N_{oxp}$ | $N_{oxm}$ | $N_{oxp}$ | $N_{oxm}$ | $N_{oxp}$ | $N_{oxm}$ | $N_{oxp}$ |
| 1.25 | 6 | 4 | 3 | 3 | 11 | 7 | 4 | 4 | 4 | 4 | 7 | 7 | 3 | 3 | 3 | 3 | 6 | 7 |
| 2.5 | 6 | 4 | 3 | 3 | 11 | 7 | 4 | 3 | 4 | 6 | 7 | 7 | 3 | 3 | 3 | 3 | 6 | 6 |
| 3.75 | 5 | 5 | 3 | 3 | 10 | 8 | 3 | 4 | 2 | 3 | 7 | 8 | 3 | 3 | 3 | 3 | 5 | 7 |
| 5 | 7 | 6 | 4 | 2 | 15 | 7 | 5 | 4 | 2 | 3 | 10 | 7 | 4 | 4 | 3 | 2 | 7 | 7 |
| 6.25 | 10 | 7 | 5 | 2 | 21 | 9 | 7 | 5 | 5 | 6 | 14 | 8 | 5 | 4 | 3 | 5 | 10 | 6 |
| 7.5 | 15 | 6 | 7 | 4 | 29 | 7 | 10 | 6 | 7 | 9 | 20 | 9 | 7 | 5 | 4 | 5 | 15 | 6 |

A fairly close approximation exists for S/F = 2:1 at each tray spacing investigated between the predicted number of stages and the measured number of equilibrium stages , as compared to the other solvent to feed ratios investigated. Thus indicating that the correlation developed by Rathilal (2010) predicts the number of stages fairly accurately for all tray spacings investigated, for higher solvent to feed ratios as well as for agitation levels between 1.25 mm/s and 5 mm/s. The model established by Rathilal (2010) seems to over predict the number of stages for experiments conducted at lower solvent to feed ratios of 1:2 and for higher agitation levels investigated.

## 4.2.9. <u>**Repeatability Analysis for Mass Transfer Experiments**</u>

Each mass transfer experimental run for a tray spacing of 150 mm was repeated for each of the varied solvent to feed ratios and agitation levels and the raw data for the repeated mass transfer experimental runs are contained in Appendix B, Table B2.3.

The dispersed phase holdup data gathered for the repeated mass transfer experiments indicate fairly similar measurements to the data obtained from the first set of mass transfer experiments at a tray spacing of 150 mm. The gas chromatograph analysis results for the extract and raffinate samples as well as for the samples collected along the length of the column for mass transfer experiments investigated for a tray spacing of 150 mm also displays fairly similar values to the results obtained from the first set of mass transfer experiments at a tray spacing of 150 mm. Refer to Appendix B, Table B2.2 and Table B2.3 which depicts the similarity in the first set of mass transfer experiments and the repeated runs respectively, performed for a tray spacing of 150 mm.  This thus indicates a good reproducibility of the dispersed phase holdup results and the gas chromatograph analysis results upon repetition of experiments. An uncertainty of ± 2% was established for the dispersed phase holdup and ± 3% for the samples analysed using the gas chromatograph detector.

For the drop size distribution results, three to five photographs of the droplets taken during the mass transfer experiments were analysed using the Image Pro Plus software in order to achieve suitable results for the size distribution of the droplets and the Sauter mean drop diameter, with an uncertainty of ± 3 mm established for the Sauter mean drop diameter.

# CHAPTER 5: CONCLUSIONS

## 5.1. *Dispersed Phase Holdup*

- The dispersed phase holdup graphs for both the hydrodynamic experiments and the mass transfer experiments displayed two distinct hydrodynamic regime flows; the mixer-settler regime and the dispersion flow regime.

- As the agitation level was varied from 1.25 mm/s to 3.75 mm/s a reduction in the dispersed phase holdup was noticed, with the system operating in the mixer-settler regime. At 3.75 mm/s, there was a changeover from the mixer-settler regime to the dispersion flow regime where upon further increase in the agitation level resulted in an increase in the dispersed phase holdup.

- Both the mass transfer and hydrodynamic experimental results indicated that decrease in the solvent to feed ratio implies an increase in the dispersed phase holdup, thus the holdup may be considered to be independent of the continuous phase.

- The effects of the tray spacing on the dispersed phase holdup can be drawn from the mass transfer experimental results which show that an increase in the tray spacing results in a reduction in the dispersed phase holdup. This effect is due to there being a lower accumulation of the dispersed phase under the perforated plate with an increase in the tray spacing, hence contributing to a lower dispersed phase holdup.

- A comparison between the hydrodynamic and mass transfer experiments dispersed phase holdup clearly indicated that in the absence of the solute (hydrodynamic experiments), a higher dispersed phase holdup is attained. This outcome is attributed to the continuous extraction of the solute in the dispersed phase into the continuous phase during mass transfer, which results in a reduction of the dispersed phase during mass transfer, contributing to a lower holdup.

- The comparison between the hydrodynamic and mass transfer experiments dispersed phase holdup reveals that predictions for mass transfer may not be carried out using hydrodynamic dispersed phase data since mass transfer affects the dispersed phase holdup.

5.2. *__Drop Size Distribution__*

- Both the mass transfer and hydrodynamic experimental results for the drop size distribution indicated that at lower agitation levels there exists a larger size distribution whereas for higher agitation levels a smaller size distribution is noticed.

- This result is attributed to the formation of smaller and more uniform droplets, at higher agitation levels since the perforated plates vibrate faster.

5.3. *__Sauter Mean Diameter__*

- The mass transfer and hydrodynamic experimental results for the Sauter mean diameter illustrate that with an increase in the agitation level there is a consequent reduction in the Sauter mean drop diameter.

- At higher agitation levels the perforated plates vibrate much faster, therefore more energy is dissipated to the fluid resulting in the production of much smaller size droplets.

- The effect of the tray spacing on the Sauter mean diameter was reflected by the mass transfer experiments which indicate that with an increase in the tray spacing there is an increase in the Sauter mean diameter.

- A comparison between the hydrodynamic and mass transfer experiments clearly indicated that in the absence of the solute (hydrodynamic experiments), a lower Sauter mean diameter is attained. The mixer-settler regime indicated a larger difference in the Sauter mean diameter between the hydrodynamic and mass transfer experiments as compared to the dispersion flow regime.

- The comparison between the hydrodynamic and mass transfer experiments Sauter mean diameter also reveals a similar finding to the dispersed phase holdup results. It was found that predictions for mass transfer may not be carried out using hydrodynamic Sauter mean diameter data since mass transfer affects the Sauter mean diameter.

## 5.4. *Repeatability Analysis*

- The mass transfer and hydrodynamic experiments were repeated for a tray spacing of 100 mm and 150 mm respectively, at various solvent to feed ratios and agitation levels. A good reproducibility of the dispersed phase holdup and the gas chromatograph analysis results were found upon repetition of experiments. An uncertainty of $\pm$ 2% was established for the dispersed phase holdup and $\pm$ 3% for the samples analysed using the gas chromatograph detector.

## 5.5. *Percentage Acetone Extracted*

- Mass transfer experiments show an increase in the amount of acetone extracted from the dispersed phase as the agitation level is increased.

- The results also indicate that with an increase in the solvent to feed ratio there is a subsequent increase in the amount of acetone extracted. This effect is as a result of the presence of more solvent in order to remove acetone from the dispersed phase.

- A distinct result is noticed for the effect of the tray spacing on the amount of acetone extracted, which shows that there is a decrease in the extraction effectiveness with an increase in the tray spacing.

- A further deduction that can be made is that with a larger dispersed phase holdup and a lower Sauter mean diameter, a larger interfacial area is available for mass transfer and consequently a larger extent of extraction of acetone can be achieved.

## 5.6. *Mass Transfer Coefficient*

- A comparison of the measured mass transfer coefficient with the model developed by Rathilal (2010) for the predicted mass transfer coefficient indicates a fairly close approximation with the measured values. Thus the correlation seems to predict the mass transfer coefficients for the experimental data appropriately.

## 5.7. _Number of Equilibrium Stages With and Without Backmixing_

- As a result of backmixing and forward mixing in the dispersed phase, a higher number of equilibrium stages without backmixing were obtained as compared to the number of equilibrium stages with backmixing.

- The agitation level was found to contribute to the occurrence of backmixing in the dispersed phase which has an effect on the number of equilibrium stages, therefore an increase in the agitation level resulted in an increase in backmixing in the dispersed phase.

- The solvent to feed ratios were also found to have an effect on the backmixing in the dispersed phase such that a decrease in the solvent to feed ratio causes an increase in the backmixing in the dispersed phase.

- A comparison of the measured number of equilibrium stages with the model developed by Rathilal (2010) for the predicted number of stages indicates a fairly accurate prediction for all tray spacings investigated at higher solvent to feed ratios and for agitation levels between 1.25 mm/s and 5 mm/s.

- The model was found to over predict the number of stages for experiments conducted at lower solvent to feed ratios and higher agitation levels for all tray spacings investigated.

# CHAPTER 6: RECOMMENDATIONS

- Another feed rotameter as well as a flow controller should be installed for the experimental setup in order to reduce the fluctuations in the feed flow rate and achieve a stable flow rate.

- Further experimental work should be conducted for the system operating in the emulsion flow regime in order to determine the operating parameters that lead to the onset of flooding of the extraction column. Therefore it would be beneficial to perform experiments at agitation levels above 7.5 mm/s.

- Since the research conducted varied the agitation level by only varying the frequency of vibration and keeping the amplitude of vibration constant, additional experiments should be carried out to investigate the effect of varying the amplitude of vibration as well.

- Thermal Conductivity Detector should be utilized for any aqueous system studied and the Gas Chromatograph detector calibration should be carefully carried out to include mass balancing of the ternary system studied.

# REFERENCES

**Aravamudan, K. and Baird, M. H. I., (**1999), "Effects on Mass Transfer on the Hydrodynamic Behavior of a Karr Reciprocating Plate Column", *Industrial and Engineering Chemistry Research*, Vol: 38, pg: 1596 - 1604.

**Bahmanyar, H., Nazari, L. and Sadr, A.,** (2008), "Prediction of effective diffusivity and using of it in designing pulsed sieve plate extraction columns", *Chemical Engineering and Processing*, Vol: 47, pg: 57-65.

**Baird, M.H.I.,** (1974), "Axial Dispersion in a Pulsed Plate Column", *The Canadian Journal of Chemical Engineering*, Vol: 52, pg: 750-757.

**Baird, M. H. I. and Lane, S. J.,** (1973), "Drop size and holdup in a reciprocating plate extraction column", *Chemical Engineering Science*, Vol: 28(3), pg: 947-957.

**Baird, M. H. I. and Shen, Z. J.,** (1984), "Holdup and flooding in reciprocating plate extraction columns", *The Canadian Journal of Chemical Engineering*, Vol: 62(2), pg: 218-227.

**Baird, M. H. I., McGinnis, G. C. and Tan, G. C.,** (1971), "Flooding Conditions in a Reciprocating Plate Extraction Column", *Proceedings of ISEC 1971 International Solvent Conference*, Society of Chemical Industry, The Hague, pg: 252-259.

**Baird, M. H. I., Vijayan, S., Rama Rao, N. V. and Rohatgi, A.,** (1989), "Extraction and Absorption with a Vibrating Perforated Plate", *The Canadian Journal of Chemical Engineering*, Vol: 67, pg: 787-800.

**Bensalem, A. K.,** (1985), "Hydrodynamics and Mass Transfer in a Reciprocating-Plate Extraction Column". Ph.D.Thesis, Swiss Federal Institute of Technology, Zurich, Switzerland.

**Boyadzhiev, L. and Spassov, M.,** (1982), "On the Size of Drops in Pulsed and Vibrating Plate Extraction Columns", *Chemical Engineering Science*, Vol: 37(2), pg: 337-340.

**Brodkorb, M.J., Bosse, D., von Reden, C., Gorak, A. and Slater, M.J.,** (2003), "Single drop mass transfer in ternary and quaternary liquid-liquid extraction systems", *Chemical Engineering and Processing*, Vol: 42, pg: 825-840.

**Camurdan, M. C., Baird, M. H. I. and Taylor, P. A.,** (1989), "Steady State hydrodynamics and Mass Transfer Characteristics of a Karr Extraction Column", *The Canadian Journal of Chemical Engineering*, Vol: 67(4), pg: 554-559.

**Camurdan, M.C., (**1986), "Application of Adaptive Control to a Reciprocating Plate Liquid-Liquid Solvent Extraction Column", Open Access Dissertations and Theses, Paper 1068, Canada.

**Chilton, T. H. and Colburn, A. P.,** (1935), "Distillation and absorption in packed columns", *Industrial and Engineering Chemistry Research*, Vol: 27, pg: 255-260.

**Collectioncare.org,** (2011), "Material Safety Data Sheet Acetone MSDS", (Updated: 07/07/2011), Available at: http://www.collectioncare.org/MSDS/Acetonemsds.pdf, [Date Accessed: 08/05/2012].

**Dongaonkar, K. R., Stevens, G. W. and Pratt, H. R. C., (**1991), "Mass Transfer and Axial Dispersion in a Kühni Column", *Amercian Institute of Chemical Engineers Journal*, Vol: 5, pg: 37.

**Dongaonkar, K. R., Stevens, G. W. and Pratt, H. R. C., (**1993), "Generalised Solution of the Transient Backflow Model Equations for Tracer Concentration in Stagewise Liquid Extraction Columns", *Industrial and Engineering Chemistry Research*, Vol: 32, pg: 1169-1173.

**Enders, S., Kahl, H. and Winkelmann, J.,** (2007), "Surface Tension of the Ternary System Water + Acetone + Toluene", *Journal of Chemical and Engineering Data*, Vol: 52, pg: 1072-1079.

**European Federation of Chemical Engineering,** (1985), "Standard Test System for Liquid Extraction", 2nd Edition, E Publications Series, Vol: 46.

**Fair, J.R. and Humphrey, J.L.,** (1983), "Liquid-Liquid Extraction Processes", *5th Industrial Energy Technology Conference*, Vol: II, pg: 846-856.

**Gayler, R., Roberts, N. W. and Pratt, H. R. C., (**1953), "Liquid–liquid extraction. A further study of hold-up in packed columns", *Transactions of the Institute of Chemical Engineering*, Vol: 31, pg: 57-58.

**Google SketchUp8**, (2010), Google – Google SketchUp8 created by Ulrich von Zadow, Version 8.0.4811.

**Graham, D.J. and Midgley, N.G.,** (2000), "Graphical representation of particle shape using triangular diagrams: an Excel Spreadsheet method", *Earth Surface Processes and Landforms*, Vol: 25(13), pg: 1473-1477.

**Hafez, M. M. and Baird, M. H. I.,** (1978), "Power Consumption in a Reciprocating Plate Extraction Column", *Transactions of the Institute of Chemical Engineering*, Vol: 56, pg: 229-238.

**Hafez, M. M., Baird, M. H. I. and Nirdosh, I.,** (1979), "Flooding and Axial Dispersion in Reciprocating Plate Extraction Columns", *The Canadian Journal of Chemical Engineering*, Vol: 57, pg: 150-158.

**Holmes, T. L., Karr, A. E. and Cusack, R.,** (1987), "Performance Characteristics of Packed and Agitated Extraction Columns", Amercian Institute of Chemical Engineers Summer National Meeting.

**Humphrey, J. L. and Keller II, G. E.,** (1997), "Separation Process Technology", McGraw-Hill, Chapter 3, pg: 113-151.

**Ju, J. D., Yu, Y. H. and Kim, S. D.,** (1990), "Axial Dispersion and Phase Holdup Characteristics in Reciprocating Plate Extraction Columns", *Separation Science and Technology*, Vol: 25, pg: 921-940.

**Karr, A. E. and Ramanujam, S.,** (1987), "Scale-up and Performance of 5Ft. Diameter Reciprocating Plate Extraction Column", Amercian Institute of Chemical Engineers Symposium.

**Kim, S. D. and Baird, M. H. I.,** (1976), "Effect of hole size on the hydrodynamics of a reciprocating perforated plate extraction column", *The Canadian Journal of Chemical Engineering*, Vol: 54, pg: 235-237.

**Kolmogorov, A. N.,** (1941), "The local structure of the turbulence in incompressible viscous fluid for very large Reynolds numbers", *Dokl. Akad.NaukSSSR*, Vol: 30, pg: 301-306.

**Kostanyan, A. E., Pabalk, V. L. and Pelevina, Y. K.,** (1980), "Investigation of the operating characteristics of column extractors with vibrating plates", *Theoretical Foundations of Chemical Engineering*, Vol: 14(2), pg: 115-118.

**Kumar, A. and Hartland, S.,** (1985), "Gravity settling in liquid/liquid dispersions", *The Canadian Journal of Chemical Engineering*, Vol: 63(3), pg: 368-376.

**Kumar, A. and Hartland, S.,** (1988), "Prediction of Dispersed-Phase Holdup and Flooding Velocities in Karr Reciprocating-Plate Extraction Columns", *Industrial and Engineering Chemistry Research*, Vol: 27, pg: 131-138.

**Kumar, A. and Hartland, S.,** (1989), "Prediction of Continuous-Phase Axial Mixing Coefficients in Pulsed Perforated-Plate Extraction Columns", *Industrial and Engineering Chemistry Research*, Vol: 28, pg: 1507-1513.

**Kumar, A. and Hartland, S.,** (1996), "Unified Correlations for the Prediction of Drop Size in Liquid-Liquid Extraction Columns", *Industrial and Engineering Chemistry Research*, Vol: 35(8), pg: 2682-2695.

**Kumar, A. and Hartland, S.,** (1999), "Computational Strategies for Sizing Liquid-Liquid Extractors", *Industrial and Engineering Chemistry Research*, Vol: 38, pg: 1040-1056.

**Kumar, A., Vohra, D. K. and Hartland, S.,** (1980), "Sedimentation of droplet dispersions in counter—current spray columns", *The Canadian Journal of Chemical Engineering*, Vol: 58, pg: 154-159.

**Laddha, G. S. and Degaleesan, T. E.,** (1983), "Dispersion and Coalescence". In: T. C. Lo, M. H. I. Baird, C. Hanson, ed. 1983., Handbook of Solvent Extraction, John Wiley & Sons, Chapter 4.

**Lisa, G. A., Tudose, R. Z. and Kadi, H.,** (2003), "Mass transfer resistance in liquid-liquid extraction with individual phase mixing", *Chemical Engineering and Processing*, Vol: 42, pg: 909-916.

**Lo, T. C. and Prochazka, J.,** (1983), "Reciprocating-plate extraction columns", In: Lo, T. C., Baird, M. H. I. and Hanson, C., ed., 1983, Handbook of Solvent Extraction, Chapter 12, John Wiley & Sons.

**Lo, T. C.,** (1975), "Recent Developments in Commercial Extractors", *Engineering Foundation Conference on Mixing Research*, Rindge, N. H, The Engineering Foundation, New York.

**Lo, T. C., and Baird, M. H. I.,** (1994), "Extraction, Liquid-Liquid Extraction", 4[th]Edition, Kirk-Othmer Encyclopedia of Chemical Technology, Vol: 10, John Wiley& Sons, New York.

**Lo, T.C., Baird, M.H.I. and Rama Rao, N.V.,** (1992), "The Reciprocating Plate Column – Development and Applications", *Chemical Engineering Communications*, Vol: 116, pg: 67-88.

**Misek, T., Berger, R. and Schröter, J.,** (1985), "Standard Test Systems for Liquid Extraction", Rugby, England.

**Miyauchi, T. and Oya, H.,** (1965), "Longitudinal Dispersion in Pulsed-Perforated Plate Columns", *Amercian Institute of Chemical Engineers Journal*, Vol: 11, pg: 395-402.

**Nemecek, M. and Prochazka, J.,** (1974), "Longitudinal Mixing in a Vibrating-Sieve-Plate Column Two Phase Flow", *The Canadian Journal of Chemical Engineering*, Vol: 52, pg: 739-749.

**Novak, I. P., Matons, J. and Pick, J**, (1987),"Liquid-liquid equilibria", Elsevier, Amsterdam

**Novotny, P., Prochazka, J. and Landau, J.,** (1970), "Longitudinal mixing in a reciprocating and pulsed sieve-plate column – single phase flow", *The Canadian Journal of Chemical Engineering*, Vol: 48, pg: 405-410.

**Obukhov, A. M.,** (1941), "Spectral energy distribution in turbulent flow", *Izv. Akad. Nauk. SSSR*, Vol: 5, pg: 453-566.

**Parthasarathy, P., Sriniketan, G., Srinivas, N. S. and Varma, Y. B. G.,** (1984), "Axial mixing of continuous phase in reciprocating plate columns", *Chemical Engineering Science*, Vol: 39(6), pg: 987-995.

**Pratt, H. R. C.,** (1983a), "Interface Mass Transfer". In: T. C. Lo, M. H. I. Baird, C. Hanson, ed. 1983., Handbook of Solvent Extraction, John Wiley & Sons, Chapter 3.

**Pratt, H. R. C.,** (1983b), *"Computation of Stagewise and Differential Contactors: Plug Flow"*. In: T. C. Lo, M. H. I. Baird, C. Hanson, ed. 1983., Handbook of Solvent Extraction, John Wiley & Sons, Chapter 5.

**Prochazka, J., Landau, J., Souhrada, F. and Heyberger, A.,** (1971), "Reciprocating-plate extraction column", *British Chemical Engineering*, Vol: 16(1), pg: 42-44.

**Rama Rao, N. V, Vijayan, S. and Baird, M. H. I., (**1991), "Hydrodynamics of a Vibrating Perforated Plate Extraction Column", *The Canadian Journal of Chemical Engineering,* Vol: 69(1), pg: 212-221.

**Rathilal, S.,** (2010), "Modelling of a Vibrating-Plate Extraction Column"*, Ph.D. Thesis, University of KwaZulu-Natal, Durban, pg: 3-157.

**Rocha, J. A., Humphrey, J. L. & Fair, J. R.,** (1986), "Mass-Transfer Efficiency of Sieve Tray Extractors"*, Industrial & Engineering Chemistry Process Design & Development*, Vol: 25, pg: 862-871.

**Rosen, A. M. and Krylov, V. S.,** (1974), "Theory of scaling up and hydrodynamic modelling of industrial mass transfer equipment", *The Chemical Engineering Journal*,Vol: 7,Pg: 85-97.

**Rousseau, R. W.,** (1987), "Handbook of Separation Process Technology", John Wiley & Sons, New York, Chapters 7 and 22.

**Saien, J., Riazikhah, M. and Ashrafizadeh, S. N.,** (2006), "Comparative Investigations on the Effects of Contamination and Mass Transfer Direction in Liquid-Liquid Extraction", *Industrial and Engineering Chemistry Research*, Vol: 45, pg: 1434-1440.

**Schulz partner verfahrenstechnik GmbH**, (2009), "Liquid-Liquid Extraction: Agitated Columns, Mixer Settlers, Multi Compartment Reactors"*, Thermal process Engineering.*

**Schweitzer, P. A.,** (1997), "Handbook of Separation Techniques for Chemical Engineers", 3$^{rd}$ Edition, McGraw-Hill, New York.

**Sciencelab.com,** (2011), "Material Safety Data Sheet Toluene MSDS," (Updated: 07/07/2011), Available at: http://www.sciencelab.com/msds.php?msdsId=9927301, [Date Accessed: 08/05/2012].

**Seader, J. D. and Henley, E. J.,** (2006), "Separation Process Principles", 2$^{nd}$ Edition, John Wiley & Sons, Inc., United States of America, Chapters 4 and 8.

**Shen, Z. J., Rama Rao, N. V. and Baird, M. H. I.,** (1985), "Mass Transfer in a Reciprocating Plate Extraction Column – Effects of Mass Transfer Direction and Plate Material", *The Canadian Journal of Chemical Engineering*, Vol: 63(1), pg: 29-36.

**Slater, M. J.,** (1985), "Liquid-liquid extraction column design", *The Canadian Journal of Chemical Engineering*, Vol: 63(6), pg: 1004-1005.

**Sleicher, C. A.,** (1959), "Axial Mixing and Extraction Efficiency", *Amercian Institute of Chemical Engineers Journal*, Vol: 5(2), pg: 145-149.

**Smoot, L. D. and Babb, A. L., (**1962), "Mass transfer studies in a pulsed extraction column-longitudinal concentration profiles", *Industrial and Engineering Chemistry Fundamentals*, Vol: 1, pg: 93-103.

**Steiner, L., Oezdemir, G. & Hartland, S.,** (1990), "Single-Drop Mass Transfer in the Water-Toulene-Acetone System"*, Industrial & Engineering Chemistry Research*, Vol: 29, pg: 1313-1318.

**Stella, A. and Pratt, H. R. C., (**2006), "Backmixing in Karr Reciprocating-Plate Extraction Columns", *Industrial & Engineering Chemistry Research*, Vol: 45, pg: 6555-6562.

**Stichlmair, J.,** (1980), "Performance and Cost Comparison of Various Equipment Designs for Liquid-Liquid Extraction"*, Chemie- Ingenieur-Technik*, Vol: 52(3),pg: 253-255.

**Takacs, I., Beszedics, G., Fabry, G. and Rudolf, P.,** (1993), "Apparatus to contact liquids of different density", *United States Patent*, Patent No: 5194152.

**Taylor, P. A., Baird, M. H. I. and Kusuma, I.,** (1982), "Computer Control of Holdup in a Reciprocating Plate Extraction Column", *The Canadian Journal of Chemical Engineering*, Vol: 60, pg: 556-565.

**Thornton, J. D.,** (1956), "Spray liquid-liquid extraction columns: Prediction of limiting holdup and flooding rates", *Chemical Engineering Science*, Vol: 5(5), pg: 201-208.

**Thornton, J. D.,** (1992), "Science and Practice of Liquid-Liquid Extraction", Oxford Engineering Science Series 27, Volume 1, Oxford.

**Treybal, R. E.,** (1963), "Liquid Extraction", 2nd Edition, McGraw-Hill, New York, pg: 1-55, 150-195.

**Tsouris, C., Kirou, V.I. and Tavlarides, L.L.,** (1994), "Drop Size Distribution and Holdup Profiles in Multistage Extraction Column"*, Amercian Institute of Chemical Engineers Journal*, Vol: 40, pg: 407-418.

**U.S.Geological Survey's (USGS)**, (2012), "Water Properties", USGS Water Resources of the United States, ga.**water**.usgs.gov/edu/**waterproperties**.html, [Accessed Date: 22/03/2012].

**Usman, M.R., Rehman, L. & Bashir, M.,** (2008), "Drop Size and Drop Size Distribution in a Pulsed Sieve-Plate Extraction Column", *The Proceedings of the Pakistan Academy of Sciences*, Vol: 45(1), pg: 41- 46.

**Van Dijck, W. J. D.,** (1935), "Process and Apparatus for Intimately Contacting Fluids", *United States Patent*, Patent No: 2,011,186, The Hague, Netherlands.

**Walton, J.H. and Jenkins, J.D.,** (1923), "A Study of the Ternary System, Toluene-Acetone-Water", *Journal of the American Chemical Society*, Vol: 45(11), pg 2555-2559.

**Wikipedia**, (2013), "Acetone and Toluene", (Updated:08/09/2012), Available at: http://en.wikipedia.org/wiki/Acetone and http://en.wikipedia.org/wiki/Toluene, [Date Accessed: 19/03/2013].

# APPENDICES

# APPENDIX A: EQUIPMENT CALIBRATION GRAPHS

## Appendix A1: Vibration Motor Calibration Graph

The sieve plates inside the vibrating plate extraction column are connected to a central shaft, which is attached to a yoke at the top of the extraction column and is driven by a variable speed motor. The calibration of the vibration motor carried out in order to establish the relation between the frequency and the variable speed motor's controller readings.

Figure A1 depicts the relation between the vibration motor speed in units of number of revolutions per minute and the motor's controller settings. It can be seen that an almost linear relation is exhibited. An uncertainty of ± 30 RPM was established.
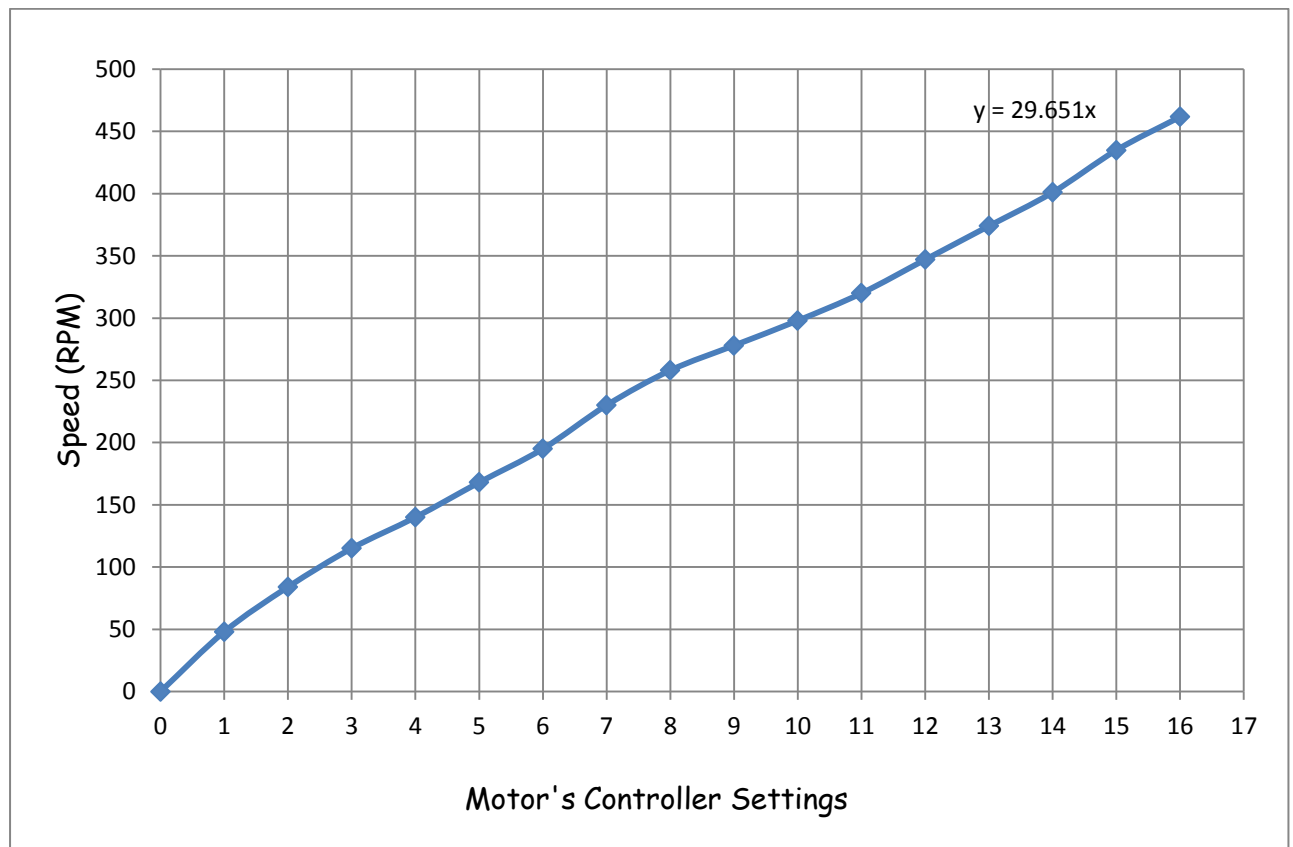


*Figure A 1.1: Graph of Speed (RPM) versus Motor's Controller Settings*
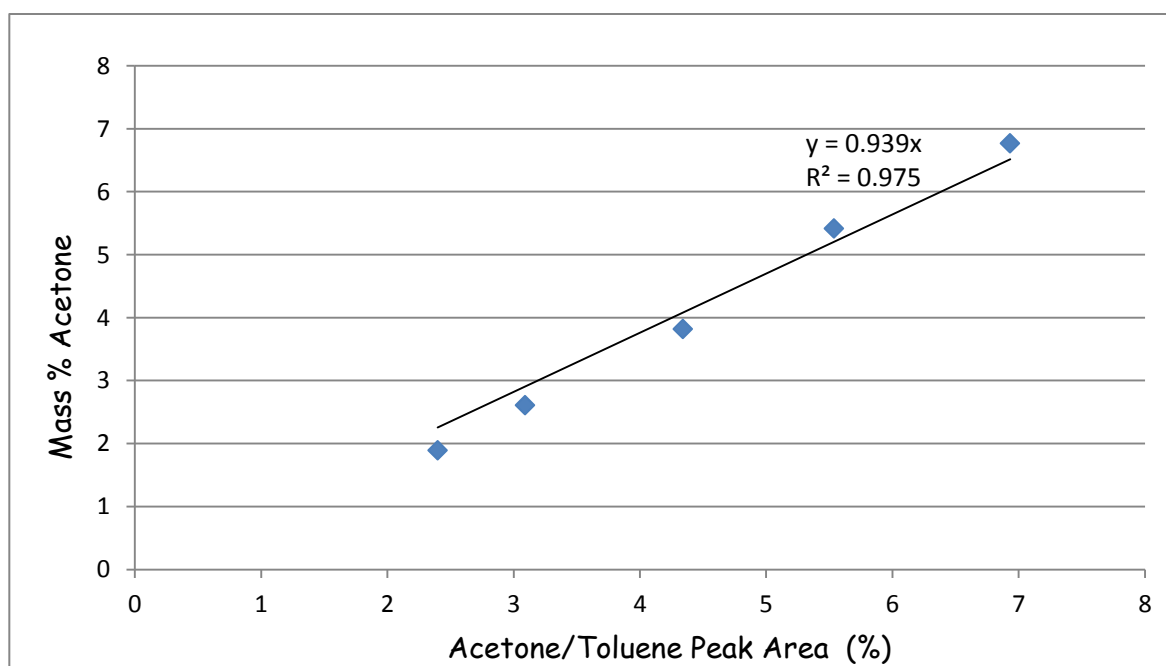
## Appendix A2: GC Calibration for Acetone in Toluene

Several different standards of acetone in toluene were prepared in order to calibrate the gas chromatograph. Two different peaks were identified by the GC, thus the ratio of acetone and toluene peak areas were taken and plotted against the acetone mass percentage data below indicated in Table A2.

*Table A2.1: Data used for GC Calibration for Acetone in Toluene.*

| Sample no. | Mass Toluene (g) | Mass Toluene + Acetone (g) | Mass Acetone (g) | Mass % Acetone | (Acetone/Toluene ) Area (%) |
|---|---|---|---|---|---|
| 1 | 1.8789 | 1.9151 | 0.0362 | 1.89 | 2.40 |
| 2 | 2.5500 | 2.6183 | 0.0683 | 2.61 | 3.09 |
| 3 | 2.3157 | 2.4076 | 0.0919 | 3.82 | 4.34 |
| 4 | 2.5367 | 2.6819 | 0.1452 | 5.41 | 5.54 |
| 5 | 2.6001 | 2.7888 | 0.1887 | 6.77 | 6.93 |

Figure A2 below depicts the relation between the mass percentage of acetone and the acetone to toluene peak area ratio for different standards of acetone in toluene. From the calibration plot the trendline equation was used in order to establish the mass % of acetone present in samples along the length of the column and in the raffinate phase. An uncertainty of ± 2% was established for the compositions using the gas chromatograph.



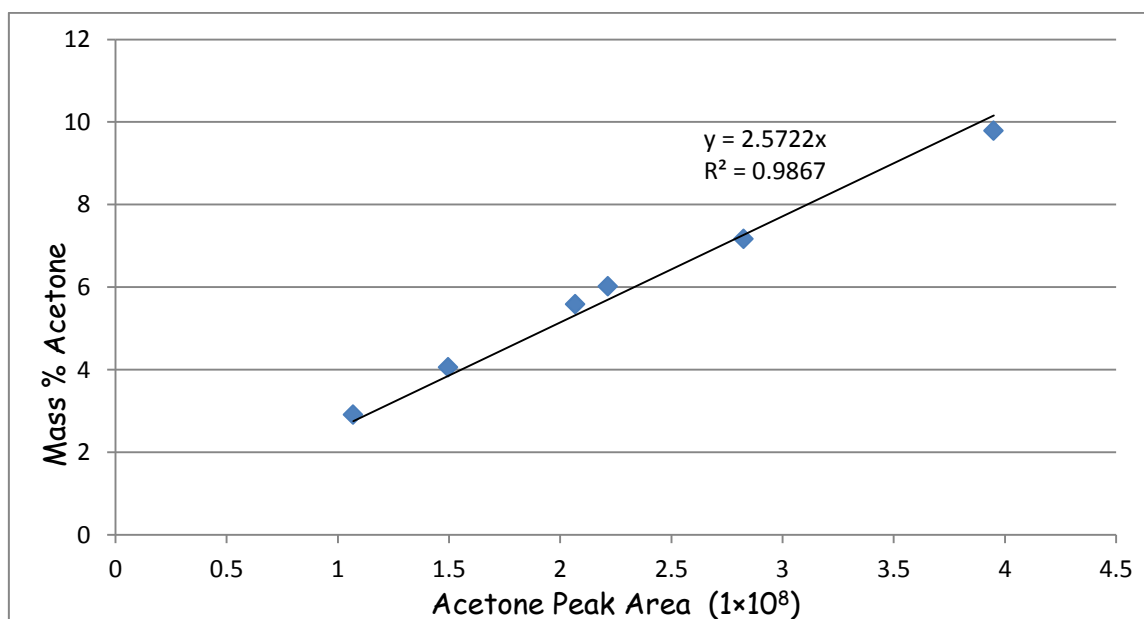*Figure A 2.1: GC Detector Calibration for Acetone in Toluene*

## Appendix A3: GC Calibration for Acetone in Water

Several different standards of acetone in water were prepared in order to calibrate the gas chromatograph detector. Since the flame ionisation detector detects only the presence of hydrocarbons, water was not detected by the GC, thus the peak area of the acetone was obtained. Using the mass % acetone data from the prepared standards and the acetone peak areas obtained from the GC from Table A3 below, the GC calibration for acetone in water was plotted as illustrated in Figure A3. Please note that the following method for the calibration assumes no toluene was present in the samples analysed.

*Table A3.1: Data used for GC Calibration for Acetone in Water*

| Sample No. | Mass Water (g) | Mass Water + Acetone (g) | Mass Acetone (g) | Mass % Acetone | Acetone Peak Area $(1\times10^8)$ |
|---|---|---|---|---|---|
| 1 | 5.2453 | 5.4024 | 0.1571 | 2.91 | 1.07 |
| 2 | 4.9005 | 5.1076 | 0.2071 | 4.05 | 1.50 |
| 3 | 4.7011 | 4.9792 | 0.2781 | 5.59 | 2.07 |
| 4 | 4.4533 | 4.7385 | 0.2852 | 6.02 | 2.22 |
| 5 | 5.1832 | 5.5832 | 0.4000 | 7.16 | 2.82 |
| 6 | 4.2308 | 4.6900 | 0.4592 | 9.79 | 3.95 |

Figure A3 below depicts the relation between the mass percentage of acetone and the acetone peak area for different standards of acetone in water. From the calibration plot the trendline equation was used in order to establish the mass % of acetone present in samples along the length of the column and in the extract phase. An uncertainty of $\pm$ 1% was established for the compositions using the gas chromatograph.



*Figure A 3.1: GC Detector Calibration for Acetone in Water*

# APPENDIX B: RAW DATA

## Appendix B1: Hydrodynamic Experimental Raw Data

Appendix B1 contains the hydrodynamic experimental raw data gathered for experiments conducted for varied solvent to feed ratios and different agitation levels at a tray spacing of 100 mm. The raw data collected for the first set of hydrodynamic experiments can be found in Table B1.1. From the data it can be seen that flooding occurred for S/F = 1:2 at an agitation level of 7.5 mm/s, therefore no dispersed phase holdup could be calculated.

*Table B1.1: Hydrodynamic Experimental Data for h = 100mm (First set of experiments).*

| Water Flow Rate | Feed Flow Rate | S/F | Frequency (f) | *af | Dispersed Phase Holdup | | |
|---|---|---|---|---|---|---|---|
| (l/hr) | (l/hr) | Ratio | (Hz) | mm/s | mm | m³ | % |
| 20 | 10 | 2:1 | 0.5 | 1.25 | 40 | 0.00071 | 9.06 |
| 20 | 10 | 2:1 | 1 | 2.5 | 19 | 0.00034 | 4.30 |
| 20 | 10 | 2:1 | 1.5 | 3.75 | 14 | 0.00025 | 3.17 |
| 20 | 10 | 2:1 | 2 | 5 | 21 | 0.00037 | 4.76 |
| 20 | 10 | 2:1 | 2.5 | 6.25 | 33 | 0.00058 | 7.48 |
| 20 | 10 | 2:1 | 3 | 7.5 | 52 | 0.00092 | 11.78 |
|  |  |  |  |  |  |  |  |
| 15 | 15 | 1:1 | 0.5 | 1.25 | 69 | 0.00122 | 15.63 |
| 15 | 15 | 1:1 | 1 | 2.5 | 45 | 0.00080 | 10.19 |
| 15 | 15 | 1:1 | 1.5 | 3.75 | 36 | 0.00064 | 8.16 |
| 15 | 15 | 1:1 | 2 | 5 | 42 | 0.00074 | 9.52 |
| 15 | 15 | 1:1 | 2.5 | 6.25 | 60 | 0.00106 | 13.59 |
| 15 | 15 | 1:1 | 3 | 7.5 | 92 | 0.00163 | 20.84 |
|  |  |  |  |  |  |  |  |
| 10 | 20 | 1:2 | 0.5 | 1.25 | 82 | 0.00145 | 18.58 |
| 10 | 20 | 1:2 | 1 | 2.5 | 60 | 0.00106 | 13.59 |
| 10 | 20 | 1:2 | 1.5 | 3.75 | 56 | 0.00099 | 12.69 |
| 10 | 20 | 1:2 | 2 | 5 | 68 | 0.00120 | 15.41 |
| 10 | 20 | 1:2 | 2.5 | 6.25 | 82 | 0.00145 | 18.58 |
| 10 | 20 | 1:2 | 3 | 7.5 | Flooding | 0.00000 | 0.00 |

*For the Agitation Level (af), the amplitude of vibration was kept constant at 2.5 mm while the frequency was varied.*

The repeatability of the system was tested for the hydrodynamic experiments performed. Therefore Table B1.2 contains the raw data for the repeated set of hydrodynamics experiments. From the data collected for the repeated experiments it can be deduced the system depicts a good repeatability with the repeated experiments dispersed phase holdup values being fairly similar to that of the first set of experiments.

**Table B1.2:** *Hydrodynamic Experimental Data for h = 100mm (Repeated set of experiments).*

| Water Flow Rate | Feed Flow Rate | S/F | Frequency (f) | *af | Dispersed Phase Holdup | | |
|---|---|---|---|---|---|---|---|
| (l/hr) | (l/hr) | Ratio | (Hz) | mm/s | mm | m$^3$ | % |
| 20 | 10 | 2:1 | 0.5 | 1.25 | 44 | 0.00078 | 9.97 |
| 20 | 10 | 2:1 | 1 | 2.5 | 22 | 0.00039 | 4.98 |
| 20 | 10 | 2:1 | 1.5 | 3.75 | 15 | 0.00027 | 3.40 |
| 20 | 10 | 2:1 | 2 | 5 | 26 | 0.00046 | 5.89 |
| 20 | 10 | 2:1 | 2.5 | 6.25 | 38 | 0.00067 | 8.61 |
| 20 | 10 | 2:1 | 3 | 7.5 | 52 | 0.00092 | 11.78 |
| | | | | | | | |
| 15 | 15 | 1:1 | 0.5 | 1.25 | 62 | 0.00110 | 14.05 |
| 15 | 15 | 1:1 | 1 | 2.5 | 42 | 0.00074 | 9.52 |
| 15 | 15 | 1:1 | 1.5 | 3.75 | 30 | 0.00053 | 6.80 |
| 15 | 15 | 1:1 | 2 | 5 | 47 | 0.00083 | 10.65 |
| 15 | 15 | 1:1 | 2.5 | 6.25 | 69 | 0.00122 | 15.63 |
| 15 | 15 | 1:1 | 3 | 7.5 | 88 | 0.00156 | 19.94 |
| | | | | | | | |
| 10 | 20 | 1:2 | 0.5 | 1.25 | 78 | 0.00138 | 17.67 |
| 10 | 20 | 1:2 | 1 | 2.5 | 64 | 0.00113 | 14.50 |
| 10 | 20 | 1:2 | 1.5 | 3.75 | 56 | 0.00099 | 12.69 |
| 10 | 20 | 1:2 | 2 | 5 | 72 | 0.00127 | 16.31 |
| 10 | 20 | 1:2 | 2.5 | 6.25 | 86 | 0.00152 | 19.48 |
| 10 | 20 | 1:2 | 3 | 7.5 | Flooding | 0.00000 | 0.00 |

*For the Agitation Level (af), the amplitude of vibration was kept constant at 2.5 mm while the frequency was varied.

# Appendix B2: Mass Transfer Experimental Raw Data

Appendix B2 contains the mass transfer experimental raw data gathered for experiments conducted at varied solvent to feed ratios and different agitation levels for three different tray spacings. The raw data collected for the first set of mass transfer experiments can be found in Table B 2.1 for h =100 mm, Table B 2.2 for h = 150 mm and Table B 2.4 for h =200 mm. Table B 2.3 contains data gathered for the repeated experimental runs conducted at a tray spacing of 150 mm.

The data obtained for the mass transfer experimental work include the dispersed phase holdup and the acetone concentrations from the gas chromatograph analysis for the feed, extract, raffinate and samples at different locations along the extraction column. With $d_1$-$d_3$ representing the acetone concentration in the dispersed phase for locations 1 to 3 along the column and $c_1$-$c_3$ representing the acetone concentration in the continuous phase for locations 1 to 3 along the column. From the raw data it can be seen that flooding occurred for all tray spacings investigated at a S/F = 1:2 at an agitation level of 7.5 mm/s, therefore no dispersed phase holdup could be calculated.

The repeatability of the system was tested for the mass transfer experiments performed. Therefore Table B 2.3 contains the raw data for the repeated set of mass transfer experiments. From the data collected for the repeated experiments it can be deduced that the system depicts good repeatability. This is due to the repeated experiments dispersed phase holdup values as well as the acetone concentrations for the extract, raffinate and samples along the length of the column from the gas chromatograph analysis being fairly similar to that of the first set of mass transfer experiments performed for a tray spacing of 150 mm. An uncertainty of ± 2% was established for the dispersed phase holdup and ± 3% for the samples analysed using the gas chromatograph detector.

### Table B2.1: Mass Transfer Experimental Data for h = 100mm.

| Water Flow Rate | Feed Flow Rate | S/F | Frequency | af | Dispersed Phase Holdup | | | Percentage Acetone (%) | | | | | | | | |
|---|---|---|---|---|---|---|---|---|---|---|---|---|---|---|---|---|
| (l/hr) | (l/hr) | Ratio | (Hz) | mm/s | mm | $m^3$ | % | $x_f$ | $x_r$ | $x_e$ | $d_1$ | $d_2$ | $d_3$ | $c_1$ | $c_2$ | $c_3$ |
| 20 | 10 | 2:1 | 0.5 | 1.25 | 45 | 0.00080 | 10.19 | 6.02 | 0.26 | 1.72 | 3.41 | 2.66 | 1.31 | 1.54 | 0.32 | 0.13 |
| 20 | 10 | 2:1 | 1 | 2.5 | 29 | 0.00051 | 6.57 | 5.98 | 0.19 | 1.74 | 3.52 | 2.72 | 1.08 | 1.46 | 0.32 | 0.14 |
| 20 | 10 | 2:1 | 1.5 | 3.75 | 18 | 0.00032 | 4.08 | 5.96 | 0.17 | 1.75 | 3.7 | 3.05 | 1.42 | 1.32 | 0.33 | 0.16 |
| 20 | 10 | 2:1 | 2 | 5 | 20 | 0.00035 | 4.53 | 6.02 | 0.11 | 1.6 | 3.42 | 3.24 | 1.3 | 1.33 | 0.27 | 0.13 |
| 20 | 10 | 2:1 | 2.5 | 6.25 | 32 | 0.00057 | 7.25 | 5.97 | 0.09 | 1.62 | 3.31 | 2.94 | 1.19 | 1.12 | 0.21 | 0.11 |
| 20 | 10 | 2:1 | 3 | 7.5 | 39 | 0.00069 | 8.84 | 6.03 | 0.08 | 1.78 | 3.3 | 2.36 | 0.46 | 1.01 | 0.17 | 0.1 |
|  |  |  |  |  |  |  |  |  |  |  |  |  |  |  |  |  |
| 15 | 15 | 1:1 | 0.5 | 1.25 | 60 | 0.00106 | 13.59 | 5.97 | 0.56 | 2.75 | 4.16 | 2.19 | 0.92 | 1.76 | 0.82 | 0.38 |
| 15 | 15 | 1:1 | 1 | 2.5 | 37 | 0.00065 | 8.38 | 6.01 | 0.44 | 2.98 | 4.28 | 2.27 | 0.96 | 1.89 | 0.89 | 0.38 |
| 15 | 15 | 1:1 | 1.5 | 3.75 | 28 | 0.00049 | 6.34 | 6.03 | 0.33 | 3.05 | 4.41 | 2.53 | 0.97 | 1.92 | 0.93 | 0.4 |
| 15 | 15 | 1:1 | 2 | 5 | 35 | 0.00062 | 7.93 | 6.01 | 0.18 | 3.16 | 4.45 | 2.48 | 0.72 | 1.99 | 0.87 | 0.34 |
| 15 | 15 | 1:1 | 2.5 | 6.25 | 48 | 0.00085 | 10.87 | 5.98 | 0.13 | 3.22 | 4.31 | 2.24 | 0.52 | 2.11 | 0.79 | 0.27 |
| 15 | 15 | 1:1 | 3 | 7.5 | 59 | 0.00104 | 13.37 | 6.02 | 0.06 | 3.28 | 4.06 | 2.06 | 0.41 | 1.97 | 0.71 | 0.13 |
|  |  |  |  |  |  |  |  |  |  |  |  |  |  |  |  |  |
| 10 | 20 | 1:2 | 0.5 | 1.25 | 65 | 0.00115 | 14.73 | 6.03 | 0.91 | 3.75 | 4.89 | 3.58 | 1.75 | 3.79 | 1.96 | 0.67 |
| 10 | 20 | 1:2 | 1 | 2.5 | 48 | 0.00085 | 10.87 | 6.01 | 0.72 | 4.02 | 4.92 | 3.49 | 1.59 | 3.85 | 1.82 | 0.59 |
| 10 | 20 | 1:2 | 1.5 | 3.75 | 34 | 0.00060 | 7.70 | 5.98 | 0.68 | 4.13 | 5.02 | 3.63 | 1.84 | 3.97 | 2.16 | 0.76 |
| 10 | 20 | 1:2 | 2 | 5 | 45 | 0.00080 | 10.19 | 5.95 | 0.55 | 4.26 | 5.09 | 3.82 | 1.79 | 3.86 | 2.19 | 0.78 |
| 10 | 20 | 1:2 | 2.5 | 6.25 | 58 | 0.00102 | 13.14 | 6.02 | 0.37 | 4.28 | 4.98 | 3.7 | 1.68 | 3.84 | 2.22 | 0.77 |
| 10 | 20 | 1:2 | 3 | 7.5 | Flooding | 0.00000 | 0.00 | 5.98 | 0.17 | 4.24 | 4.97 | 3.37 | 1.28 | 3.52 | 1.63 | 0.43 |

**_Table B2.2: Mass Transfer Experimental Data for h = 150mm._**

| Water Flow Rate (l/hr) | Feed Flow Rate (l/hr) | S/F Ratio | Frequency (Hz) | af mm/s | Dispersed Phase Holdup | | | Percentage Acetone (%) | | | | | | | | |
|---|---|---|---|---|---|---|---|---|---|---|---|---|---|---|---|---|
| | | | | | mm | $m^3$ | % | $x_f$ | $x_r$ | $x_e$ | $d_1$ | $d_2$ | $d_3$ | $c_1$ | $c_2$ | $c_3$ |
| 20 | 10 | 2:1 | 0.5 | 1.25 | 40 | 0.00071 | 8.95 | 5.97 | 0.34 | 1.27 | 3.05 | 1.35 | 0.59 | 1.03 | 0.31 | 0.13 |
| 20 | 10 | 2:1 | 1 | 2.5 | 23 | 0.00041 | 5.14 | 6.01 | 0.25 | 1.19 | 3.14 | 1.49 | 0.64 | 0.97 | 0.32 | 0.15 |
| 20 | 10 | 2:1 | 1.5 | 3.75 | 16 | 0.00028 | 3.58 | 6.03 | 0.22 | 1.22 | 3.37 | 1.68 | 0.79 | 0.94 | 0.51 | 0.19 |
| 20 | 10 | 2:1 | 2 | 5 | 19 | 0.00034 | 4.25 | 6.08 | 0.18 | 1.29 | 3.21 | 1.35 | 0.42 | 0.94 | 0.28 | 0.10 |
| 20 | 10 | 2:1 | 2.5 | 6.25 | 26 | 0.00046 | 5.82 | 6.01 | 0.16 | 1.34 | 2.85 | 1.28 | 0.35 | 0.86 | 0.20 | 0.09 |
| 20 | 10 | 2:1 | 3 | 7.5 | 32 | 0.00057 | 7.16 | 6.02 | 0.15 | 1.42 | 2.74 | 1.15 | 0.35 | 0.83 | 0.12 | 0.09 |
| | | | | | | | | | | | | | | | | |
| 15 | 15 | 1:1 | 0.5 | 1.25 | 49 | 0.00087 | 10.96 | 5.95 | 0.66 | 2.66 | 4.22 | 2.42 | 1.13 | 1.89 | 0.91 | 0.32 |
| 15 | 15 | 1:1 | 1 | 2.5 | 28 | 0.00049 | 6.26 | 5.98 | 0.76 | 2.70 | 4.23 | 2.53 | 1.14 | 1.94 | 0.92 | 0.32 |
| 15 | 15 | 1:1 | 1.5 | 3.75 | 24 | 0.00042 | 5.37 | 6.07 | 0.66 | 2.81 | 4.17 | 2.61 | 1.19 | 2.06 | 1.03 | 0.36 |
| 15 | 15 | 1:1 | 2 | 5 | 25 | 0.00044 | 5.59 | 6.05 | 0.48 | 2.88 | 4.22 | 2.47 | 0.97 | 2.12 | 1.05 | 0.31 |
| 15 | 15 | 1:1 | 2.5 | 6.25 | 32 | 0.00057 | 7.16 | 5.98 | 0.29 | 2.93 | 4.34 | 2.27 | 0.75 | 2.20 | 1.09 | 0.25 |
| 15 | 15 | 1:1 | 3 | 7.5 | 47 | 0.00083 | 10.51 | 6.03 | 0.17 | 2.97 | 4.41 | 2.11 | 0.58 | 2.25 | 1.13 | 0.17 |
| | | | | | | | | | | | | | | | | |
| 10 | 20 | 1:2 | 0.5 | 1.25 | 52 | 0.00092 | 11.63 | 6.03 | 1.18 | 3.53 | 4.97 | 3.71 | 1.98 | 3.93 | 2.11 | 0.52 |
| 10 | 20 | 1:2 | 1 | 2.5 | 34 | 0.00060 | 7.61 | 5.95 | 0.93 | 3.82 | 5.04 | 3.62 | 1.82 | 3.89 | 2.02 | 0.46 |
| 10 | 20 | 1:2 | 1.5 | 3.75 | 27 | 0.00048 | 6.04 | 5.98 | 0.81 | 3.89 | 5.07 | 3.67 | 2.05 | 3.95 | 1.98 | 0.67 |
| 10 | 20 | 1:2 | 2 | 5 | 30 | 0.00053 | 6.71 | 5.98 | 0.69 | 3.94 | 5.18 | 3.98 | 2.01 | 3.92 | 2.13 | 0.68 |
| 10 | 20 | 1:2 | 2.5 | 6.25 | 41 | 0.00072 | 9.17 | 6.01 | 0.48 | 3.97 | 5.09 | 3.83 | 1.87 | 3.90 | 2.29 | 0.65 |
| 10 | 20 | 1:2 | 3 | 7.5 | Flooding | 0.00000 | 0.00 | 5.97 | 0.32 | 3.92 | 5.08 | 3.51 | 1.73 | 3.71 | 2.03 | 0.41 |

**Table B2.3: Mass Transfer Experimental Data for h = 150mm (Repeated set of experiments).**

| Water Flow Rate (l/hr) | Feed Flow Rate (l/hr) | S/F Ratio | Frequency (Hz) | af mm/s | Dispersed Phase Holdup mm | m³ | % | Percentage Acetone (%) $x_f$ | $x_r$ | $x_e$ | $d_1$ | $d_2$ | $d_3$ | $c_1$ | $c_2$ | $c_3$ |
|---|---|---|---|---|---|---|---|---|---|---|---|---|---|---|---|---|
| 20 | 10 | 2:1 | 0.5 | 1.25 | 45 | 0.00080 | 10.07 | 6.01 | 0.35 | 1.29 | 2.97 | 1.32 | 0.61 | 1.05 | 0.30 | 0.14 |
| 20 | 10 | 2:1 | 1 | 2.5 | 31 | 0.00055 | 6.93 | 6.02 | 0.21 | 1.24 | 3.07 | 1.41 | 0.67 | 0.94 | 0.29 | 0.17 |
| 20 | 10 | 2:1 | 1.5 | 3.75 | 26 | 0.00046 | 5.82 | 6.02 | 0.19 | 1.17 | 3.27 | 1.59 | 0.74 | 0.92 | 0.47 | 0.21 |
| 20 | 10 | 2:1 | 2 | 5 | 24 | 0.00042 | 5.37 | 5.98 | 0.14 | 1.31 | 3.18 | 1.41 | 0.40 | 0.91 | 0.32 | 0.14 |
| 20 | 10 | 2:1 | 2.5 | 6.25 | 29 | 0.00051 | 6.49 | 5.97 | 0.15 | 1.38 | 2.80 | 1.33 | 0.37 | 0.84 | 0.25 | 0.11 |
| 20 | 10 | 2:1 | 3 | 7.5 | 43 | 0.00076 | 9.62 | 5.97 | 0.11 | 1.40 | 2.68 | 1.19 | 0.36 | 0.81 | 0.18 | 0.07 |
| | | | | | | | | | | | | | | | | |
| 15 | 15 | 1:1 | 0.5 | 1.25 | 38 | 0.00067 | 8.50 | 6.02 | 0.70 | 2.71 | 4.15 | 2.40 | 1.12 | 1.84 | 0.94 | 0.30 |
| 15 | 15 | 1:1 | 1 | 2.5 | 25 | 0.00044 | 5.59 | 6.01 | 0.72 | 2.76 | 4.19 | 2.49 | 1.14 | 1.90 | 0.95 | 0.28 |
| 15 | 15 | 1:1 | 1.5 | 3.75 | 18 | 0.00032 | 4.03 | 6.01 | 0.69 | 2.81 | 4.11 | 2.57 | 1.21 | 2.01 | 1.06 | 0.34 |
| 15 | 15 | 1:1 | 2 | 5 | 21 | 0.00037 | 4.70 | 5.97 | 0.53 | 2.93 | 4.24 | 2.45 | 0.99 | 2.15 | 1.09 | 0.31 |
| 15 | 15 | 1:1 | 2.5 | 6.25 | 24 | 0.00042 | 5.37 | 5.98 | 0.31 | 2.97 | 4.31 | 2.21 | 0.81 | 2.23 | 1.11 | 0.22 |
| 15 | 15 | 1:1 | 3 | 7.5 | 37 | 0.00065 | 8.28 | 5.97 | 0.19 | 3.02 | 4.48 | 2.04 | 0.62 | 2.28 | 1.18 | 0.19 |
| | | | | | | | | | | | | | | | | |
| 10 | 20 | 1:2 | 0.5 | 1.25 | 54 | 0.00095 | 12.08 | 5.97 | 1.15 | 3.49 | 4.95 | 3.69 | 1.94 | 3.87 | 2.09 | 0.49 |
| 10 | 20 | 1:2 | 1 | 2.5 | 37 | 0.00065 | 8.28 | 6.03 | 0.96 | 3.75 | 5.08 | 3.58 | 1.79 | 3.82 | 2.04 | 0.43 |
| 10 | 20 | 1:2 | 1.5 | 3.75 | 30 | 0.00053 | 6.71 | 6.01 | 0.87 | 3.84 | 5.11 | 3.61 | 2.01 | 3.91 | 2.01 | 0.62 |
| 10 | 20 | 1:2 | 2 | 5 | 33 | 0.00058 | 7.38 | 5.98 | 0.74 | 3.91 | 5.16 | 3.87 | 1.97 | 3.89 | 2.11 | 0.67 |
| 10 | 20 | 1:2 | 2.5 | 6.25 | 41 | 0.00072 | 9.17 | 6.02 | 0.52 | 3.96 | 5.10 | 3.79 | 1.88 | 3.86 | 2.19 | 0.64 |
| 10 | 20 | 1:2 | 3 | 7.5 | Flooding | 0.00000 | 0.00 | 6.01 | 0.38 | 3.87 | 5.06 | 3.46 | 1.79 | 3.74 | 2.04 | 0.47 |

## Table B2.4: Mass Transfer Experimental Data for h = 200mm.

| Water Flow Rate (l/hr) | Feed Flow Rate (l/hr) | S/F Ratio | Frequency (Hz) | af mm/s | Dispersed Phase Holdup mm | Dispersed Phase Holdup $m^3$ | Dispersed Phase Holdup % | $x_f$ | $x_r$ | $x_e$ | $d_1$ | $d_2$ | $d_3$ | $c_1$ | $c_2$ | $c_3$ |
|---|---|---|---|---|---|---|---|---|---|---|---|---|---|---|---|---|
| 20 | 10 | 2:1 | 0.5 | 1.25 | 27 | 0.00048 | 5.96 | 6.00 | 0.42 | 1.22 | 2.98 | 1.12 | 0.58 | 0.98 | 0.29 | 0.15 |
| 20 | 10 | 2:1 | 1 | 2.5 | 14 | 0.00025 | 3.09 | 6.02 | 0.35 | 1.15 | 3.07 | 1.26 | 0.52 | 0.96 | 0.30 | 0.18 |
| 20 | 10 | 2:1 | 1.5 | 3.75 | 12 | 0.00021 | 2.65 | 6.01 | 0.28 | 1.19 | 3.25 | 1.37 | 0.61 | 0.92 | 0.46 | 0.21 |
| 20 | 10 | 2:1 | 2 | 5 | 16 | 0.00028 | 3.53 | 5.98 | 0.21 | 1.24 | 3.17 | 1.18 | 0.39 | 0.90 | 0.21 | 0.16 |
| 20 | 10 | 2:1 | 2.5 | 6.25 | 23 | 0.00041 | 5.08 | 6.02 | 0.19 | 1.3 | 2.82 | 1.06 | 0.33 | 0.88 | 0.18 | 0.11 |
| 20 | 10 | 2:1 | 3 | 7.5 | 31 | 0.00055 | 6.85 | 6.01 | 0.18 | 1.39 | 2.79 | 1.04 | 0.33 | 0.81 | 0.10 | 0.12 |
| | | | | | | | | | | | | | | | | |
| 15 | 15 | 1:1 | 0.5 | 1.25 | 39 | 0.00069 | 8.61 | 5.98 | 1.13 | 2.54 | 4.31 | 2.53 | 1.29 | 2.05 | 1.24 | 0.28 |
| 15 | 15 | 1:1 | 1 | 2.5 | 18 | 0.00032 | 3.98 | 5.98 | 1.06 | 2.40 | 4.29 | 2.62 | 1.32 | 2.01 | 1.26 | 0.26 |
| 15 | 15 | 1:1 | 1.5 | 3.75 | 15 | 0.00027 | 3.31 | 6.02 | 1.03 | 2.52 | 4.32 | 2.73 | 1.35 | 2.15 | 1.32 | 0.29 |
| 15 | 15 | 1:1 | 2 | 5 | 21 | 0.00037 | 4.64 | 6.01 | 0.87 | 2.58 | 4.35 | 2.60 | 1.21 | 2.28 | 1.48 | 0.21 |
| 15 | 15 | 1:1 | 2.5 | 6.25 | 29 | 0.00051 | 6.41 | 5.97 | 0.38 | 2.64 | 4.42 | 2.49 | 1.15 | 2.31 | 1.49 | 0.18 |
| 15 | 15 | 1:1 | 3 | 7.5 | 37 | 0.00065 | 8.17 | 6.02 | 0.29 | 2.69 | 4.56 | 2.42 | 1.08 | 2.35 | 1.52 | 0.13 |
| | | | | | | | | | | | | | | | | |
| 10 | 20 | 1:2 | 0.5 | 1.25 | 49 | 0.00087 | 10.82 | 5.97 | 1.39 | 4.27 | 5.10 | 3.92 | 2.06 | 4.09 | 2.56 | 0.48 |
| 10 | 20 | 1:2 | 1 | 2.5 | 29 | 0.00051 | 6.41 | 5.98 | 1.18 | 4.16 | 5.14 | 3.86 | 1.95 | 3.97 | 2.31 | 0.42 |
| 10 | 20 | 1:2 | 1.5 | 3.75 | 21 | 0.00037 | 4.64 | 6.01 | 1.05 | 4.29 | 5.16 | 3.90 | 2.11 | 4.14 | 2.25 | 0.51 |
| 10 | 20 | 1:2 | 2 | 5 | 26 | 0.00046 | 5.74 | 5.97 | 0.96 | 4.23 | 5.19 | 4.06 | 1.99 | 4.04 | 2.59 | 0.53 |
| 10 | 20 | 1:2 | 2.5 | 6.25 | 35 | 0.00062 | 7.73 | 6.02 | 0.82 | 4.18 | 5.15 | 3.98 | 1.96 | 3.99 | 2.62 | 0.57 |
| 10 | 20 | 1:2 | 3 | 7.5 | Flooding | 0.00000 | 0.00 | 6.01 | 0.75 | 4.09 | 5.08 | 3.75 | 1.84 | 3.87 | 2.29 | 0.45 |

# APPENDIX C: SAMPLE CALCULATIONS

## Appendix C1: Dispersed Phase Holdup

The dispersed phase holdup percentage results were calculated using the holdup, which is represented by the height of the raffinate below the interface level, and the active volume of the column.

Firstly the height of the raffinate was multiplied by the cross sectional area of the top settling tank in order to obtain the volume of the raffinate. Thereafter the dispersed phase fractional holdup was established by dividing the volume of raffinate by the active volume in the column, which was then represented as a percentage.

The following dispersed phase holdup sample calculation was performed for a tray spacing of 100 mm, at a solvent to feed ratio of 2:1 and at an agitation level of 1.25 mm/s, with the use of the following data.

*Data:*

Cross Sectional Area of Top Settling Tank = 0.01767 m$^2$

Active Volume (h = 100 mm) = $7.8 \times 10^{-3}$ m$^3$

$$Volume\ of\ raffinate = \left(\frac{40}{1000}\right) m \times 0.01767 m^2$$

$$= \underline{7.068 \times 10^{-4}\ \text{m}^3}$$

$$Dispersed\ Phase\ Holdup = \left(\frac{7.068 \times 10^{-4}}{7.8 \times 10^{-3}}\right) \times 100$$

$$= \underline{9.06\ \%}$$

**Appendix C2: Drop Size Distribution**

The droplet sizes and number of droplets for each tray spacing, solvent to feed ratio and agitation level were determined using the Image Pro Plus software. Table C2.1 below contains the number of droplets for different size ranges. The following drop size distribution table was determined for a tray spacing of 100 mm, S/F = 1:1 and an agitation level of 7.5 mm/s for the hydrodynamic experiment.

*Table C2.1: Drop size distribution table.*

| Size Range (mm) | No. Of Drops (n) | Fraction of Drops % | Average Size (d) (mm) | $nd^3$ | $nd^2$ |
|---|---|---|---|---|---|
| 0 - 0.2 | 92 | 36.36 | 0.1 | 0.092 | 0.92 |
| 0.2 - 0.4 | 78 | 30.83 | 0.3 | 2.106 | 7.02 |
| 0.4 - 0.6 | 64 | 25.30 | 0.5 | 8 | 16 |
| 0.6 -0.8 | 12 | 4.74 | 0.7 | 4.116 | 5.88 |
| 0.8 - 1.0 | 3 | 1.19 | 0.9 | 2.187 | 2.43 |
| 1.0 - 1.2 | 2 | 0.79 | 1.1 | 2.662 | 2.42 |
| 1.2 - 1.4 | 1 | 0.40 | 1.3 | 2.197 | 1.69 |
| 1.4 - 1.6 | 1 | 0.40 | 1.5 | 3.375 | 2.25 |
| 1.6 - 1.8 | | 0 | 1.7 | 0 | 0 |
| 1.8 - 2.0 | | 0 | 1.9 | 0 | 0 |
| 2.0 - 2.2 | | 0 | 2.1 | 0 | 0 |
| 2.2 - 2.4 | | 0 | 2.3 | 0 | 0 |
| 2.4 - 2.6 | | 0 | 2.5 | 0 | 0 |
| 2.6 - 2.8 | | 0 | 2.7 | 0 | 0 |
| 2.8 - 3.0 | | 0 | 2.9 | 0 | 0 |
| 3.0 - 3.2 | | 0 | 3.1 | 0 | 0 |
| 3.2 - 3.4 | | 0 | 3.3 | 0 | 0 |
| 3.4 - 3.6 | | 0 | 3.5 | 0 | 0 |
| 3.6 - 3.8 | | 0 | 3.7 | 0 | 0 |
| 3.8 - 4.0 | | 0 | 3.9 | 0 | 0 |
| Total | 253 | 100 | | 24.735 | 38.61 |

## Appendix C2.1: Fraction of Drops Sample Calculation

The following sample calculation depicts the calculation for the fraction of drops for a size range of 0mm - 0.2mm, using data obtained from Table C2.1 above.

$$Fraction\ of\ Drops = \left(\frac{Number\ of\ drops\ per\ size\ range}{Total\ number\ of\ drops}\right) \times 100$$

$$Fraction\ of\ Drops = \left(\frac{92}{253}\right) \times 100$$

$$= \underline{36.36\ \%}$$

The fraction of drops is represented as the percentage occurrence therefore the drop size distribution is displayed graphically by plotting the percentage occurrence versus agitation level.

## Appendix C3: Sauter Mean Diameter

The sample calculation for the Sauter Mean Diameter was calculated using all the data contained in Table C2.1.

The sample calculation below is shown for the size range of 0-0.2mm.

$$nd^2 = (92)(0.1)^2$$

$$= \underline{0.92\ mm^2}$$

$$nd^3 = (92)(0.1)^3$$

$$= \underline{0.092\ mm^3}$$

The sample calculation for the sum of $nd^2$ and $nd^3$ for the data contained in Table C2.1 above is shown as follows.

$$\sum_{i=1}^{N} n_i d_i^2 = 0.92 + 7.02 + 16 + 5.88 + 2.43 + 2.42 + 1.69 + 2.25$$

$$= \underline{38.61\ mm^2}$$

$$\sum_{i=1}^{N} n_i d_i^3 = 0.092 + 2.106 + 8 + 4.116 + 2.187 + 2.662 + 2.197 + 3.375$$

$$= \underline{24.735\ mm^3}$$

Using the sum of $nd^2$ and $nd^3$ the Sauter Mean Diameter, $d_{32}$, was calculated as follows:

$$d_{32} = \frac{\sum_{i=1}^{N} n_i d_i^2}{\sum_{i=1}^{N} n_i d_i^3}$$

$$= \frac{24.735 \; mm^3}{38.61 \; mm^2}$$

$$= \underline{0.64 \; mm}$$

## Appendix C4: Percentage Acetone Extracted

The sample calculation for the percentage acetone extracted was calculated using the feed and raffinate concentrations for a tray spacing of 100mm, at S/F = 2:1 and agitation level of 1.25 mm/s.

Data: $x_{feed}$ = 6.02 and $x_{raffinate}$ = 0.26

$$Percentage \; Acetone \; Extracted = \frac{x_{feed} - x_{raffinate}}{x_{feed}} \times 100$$

$$= \frac{6.02 - 0.26}{6.02} \times 100$$

$$= \underline{95.68\%}$$

The extent of mass transfer was displayed graphically by plotting the percentage acetone extracted versus the agitation level.

## Appendix C5: Measured Mass Transfer Coefficient

The following sample calculation shows how the measured mass transfer coefficient was calculated using the following equation which combines Equation (2.24) and $N_{ox} = \frac{k_{ox} \, a \, H}{U_d}$ (Aravamudan & Baird, 1999).

The following data was used from the mass transfer experiments for h = 100 mm, S/F = 2:1 and agitation level = 1.25 mm/s.

Data: $N_{ox} = 45$ (For a tray spacing of 100 mm)

$U_d = 0.0016$ m/s

$d_{32} = 2.54$ m

$\emptyset = 0.1$

$H = 4.76$ m

$$k_{ox} = \frac{N_{ox}\,U_d d_{32}}{6\emptyset H}$$

$$= \frac{45\times0.0016\times2.54}{6\times0.1\times4.76}$$

$$= \underline{0.061\text{m/s}}$$

## Appendix C6: Number of Equilibrium Stages Without Backmixing

The sample calculation indicates how the ideal number of equilibrium stages was calculated for mass transfer experiments conducted at h = 100 mm, S/F = 1:1 and agitation level = 1.25 mm/s, the slope of the equilibrium line (m) was 0.832. Equation (2.54) was used in order to calculate the ideal number of stages.

Data:  $y_i = 0$                                    $y_o = x_{extract} = 0.0275$

$x_i = x_{feed} = 0.0597$                       $x_o = x_{raffinate} = 0.0056$

$$N_{oxp} = \frac{1}{[(y_i-y_o)/m(x_o-x_i)]-1}\; ln\left(\frac{y_i-mx_o}{y_o-mx_i}\right)$$

$$= \frac{1}{[(0-0.0275)/0.832(0.0056-0.0597)]-1}\; ln\left(\frac{0-0.832(0.0056)}{0.0275-0.832(0.0597)}\right)$$

$$= \underline{4}$$

# APPENDIX D: ADDITIONAL RESULTS

## Appendix D1: Drop Size Distribution

Figures D1.1 to D1.6 display the drop size distribution for tray spacings of 150 mm and 200 mm at three varying solvent to feed ratios.

The Image Pro Plus software was utilised in order to establish the size of the droplets and the number of droplets for each droplet size, thus resulting in the establishment of the drop size distribution. All the figures in Appendix D1 indicate that with an increase in the agitation level there is a reduction in the size distribution. A detailed examination of the drop size distribution for the mass transfer experiments is contained in Chapter 4.

The results obtained from the drop size distribution are then used to establish the Sauter mean drop diameter.
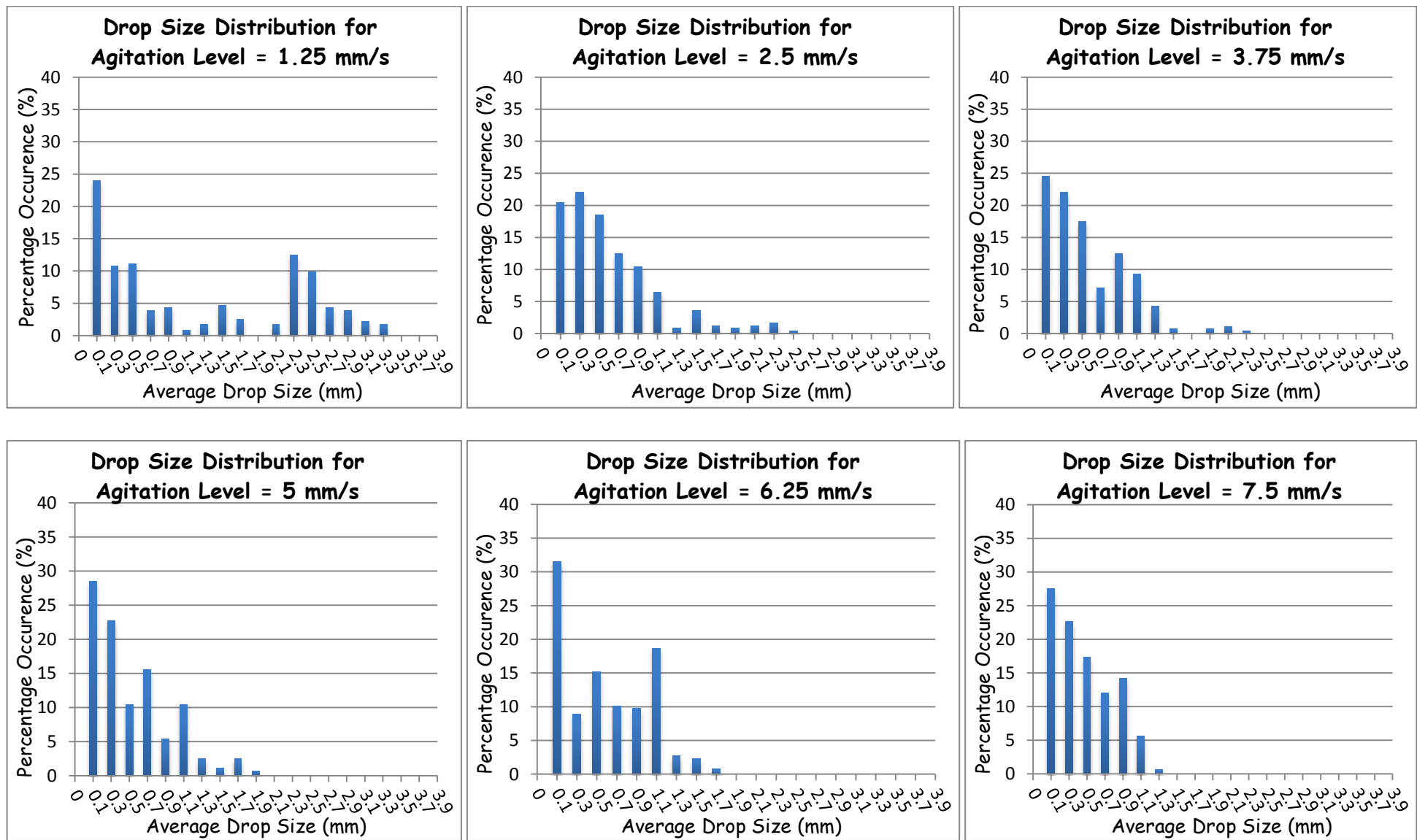
*Figure D 1.1: Drop size distribution graphs at different agitation levels for mass transfer experiments (S/F =1:1 and h = 150mm).*
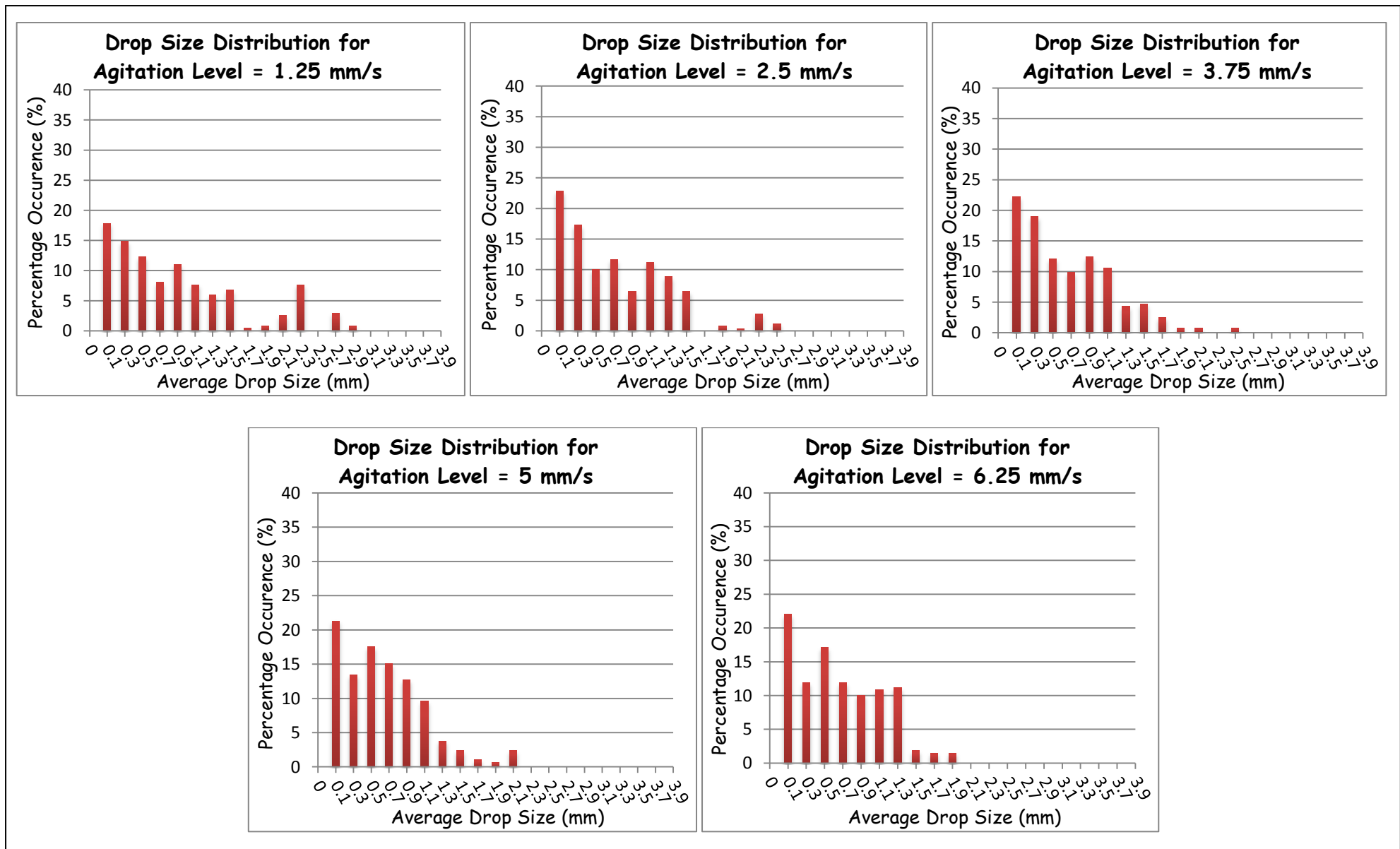
*Figure D 1.2: Drop size distribution graphs at different agitation levels for mass transfer experiments (S/F =1:2 and h = 150mm).*
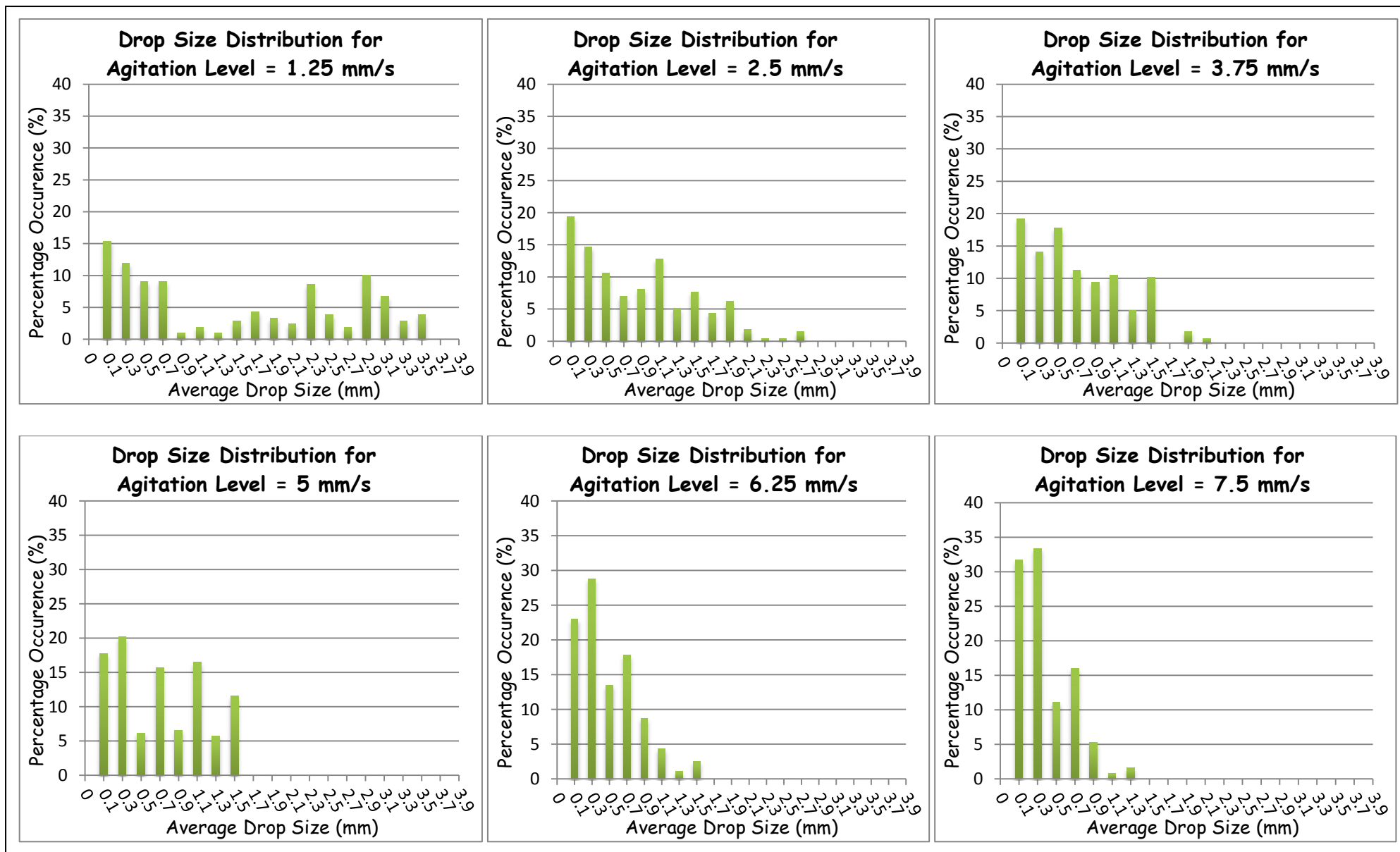
*Figure D 1.3: Drop size distribution graphs at different agitation levels for mass transfer experiments (S/F =2:1 and h = 150mm).*

124
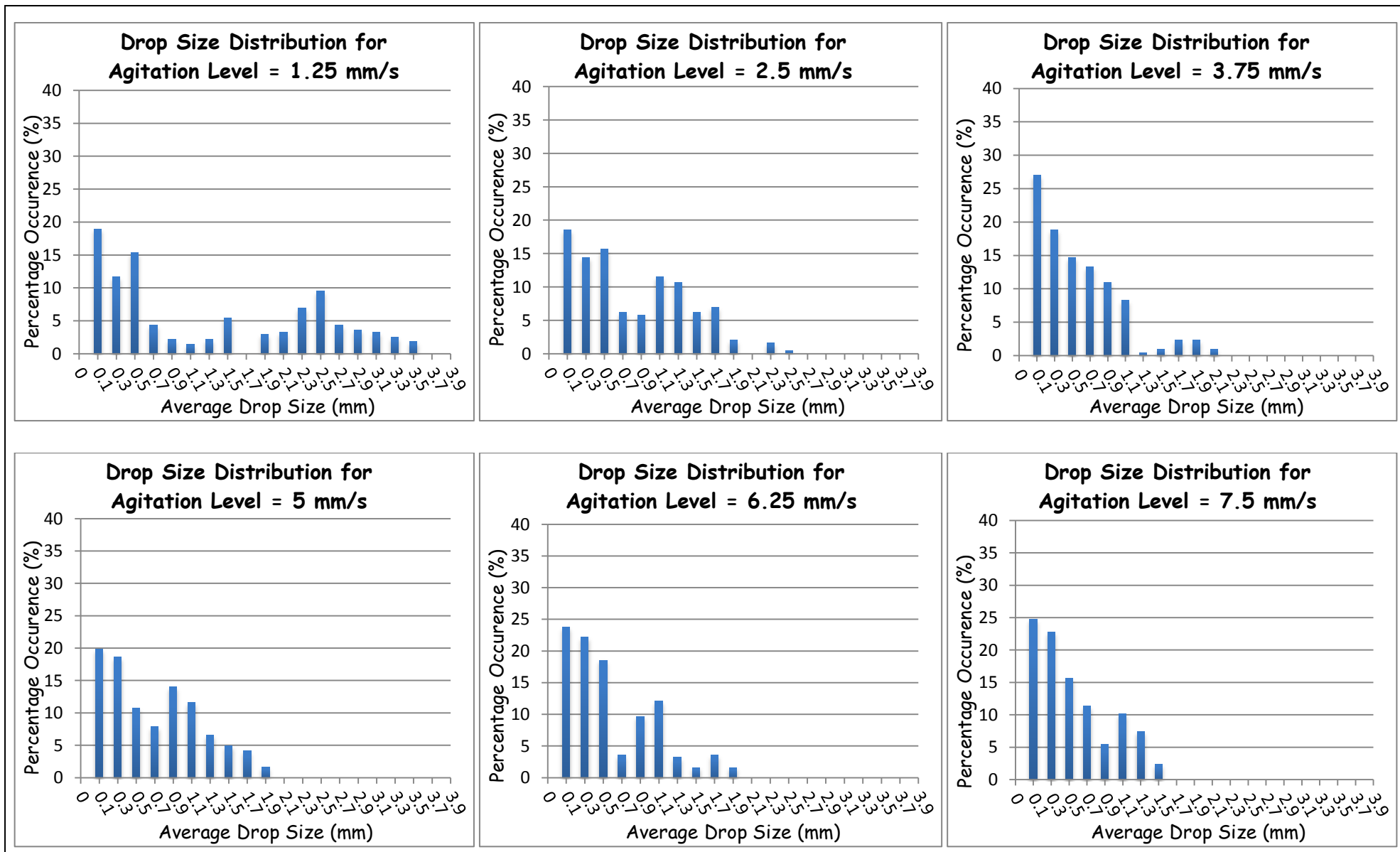
*Figure D 1.4: Drop size distribution graphs at different agitation levels for mass transfer experiments (S/F =1:1 and h = 200mm).*
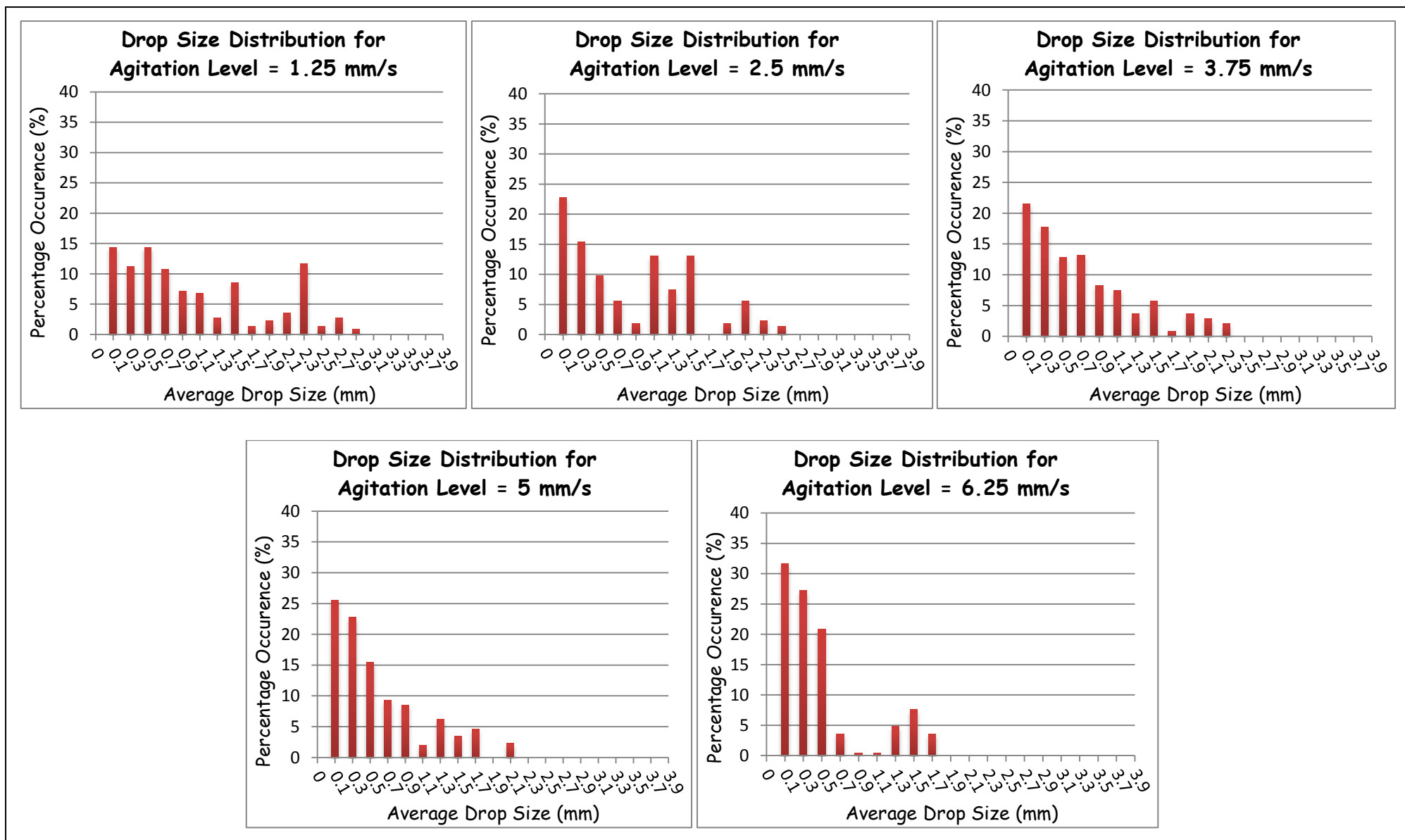
*Figure D 1.5: Drop size distribution graphs at different agitation levels for mass transfer experiments (S/F =1:2 and h = 200mm).*
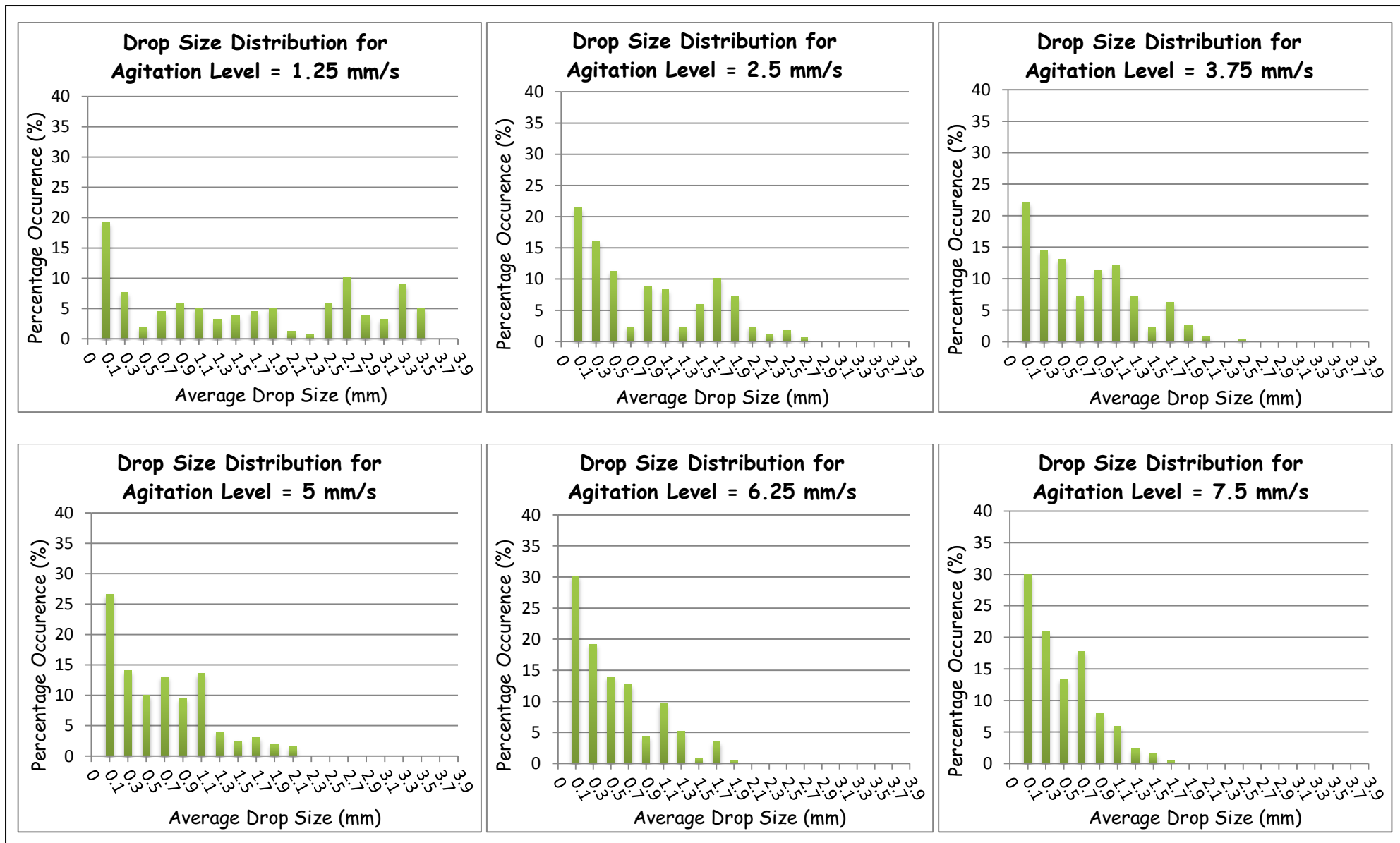
*Figure D 1.6: Drop size distribution graphs at different agitation levels for mass transfer experiments (S/F =2:1 and h = 200mm).*

## Appendix D2: Stepping-Off Stages by the McCabe Thiele Method

The following figures contained in Appendix D2 depict the stepping-off for the determination of the real and ideal number of stages for different tray spacings investigated at different solvent to feed ratios and agitation levels.

### Appendix D 2.1: Stepping-Off Stages for h = 100 mm
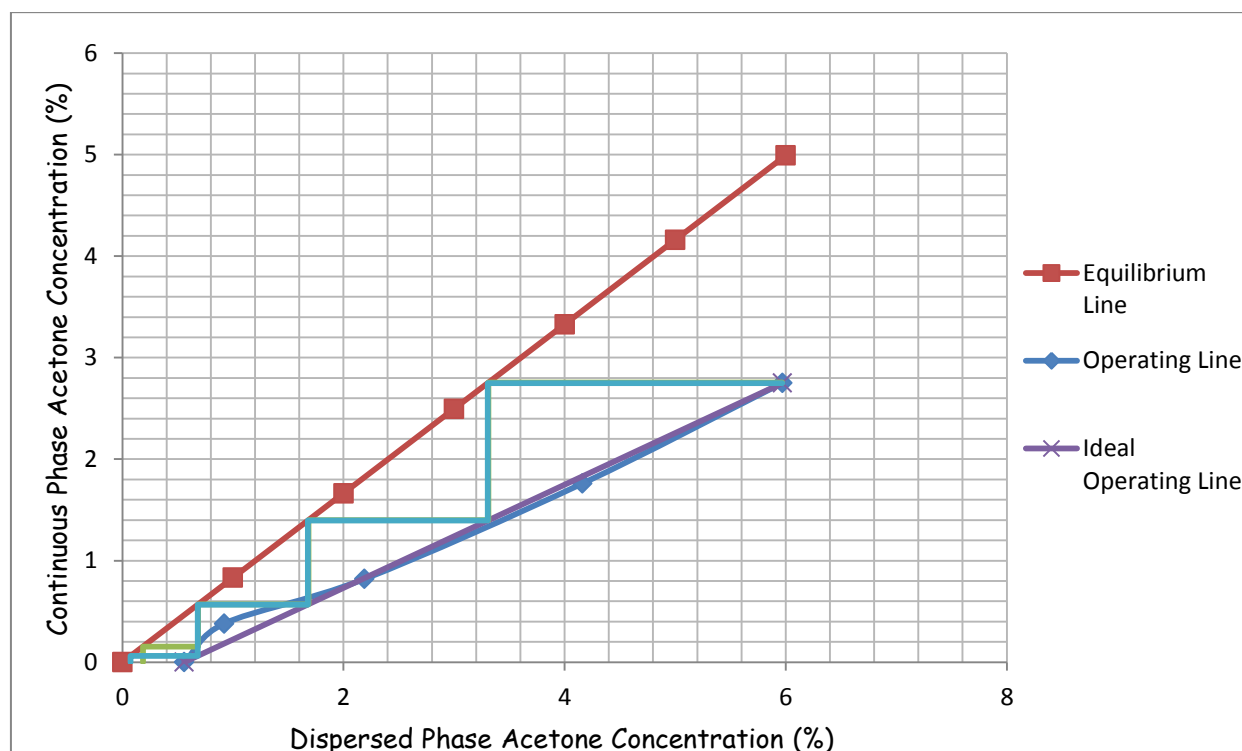


*Figure D 2.1.1: Equilibrium Stages With and Without Backmixing for h = 100 mm, S/F = 1:1 and af = 1.25 mm/s.*
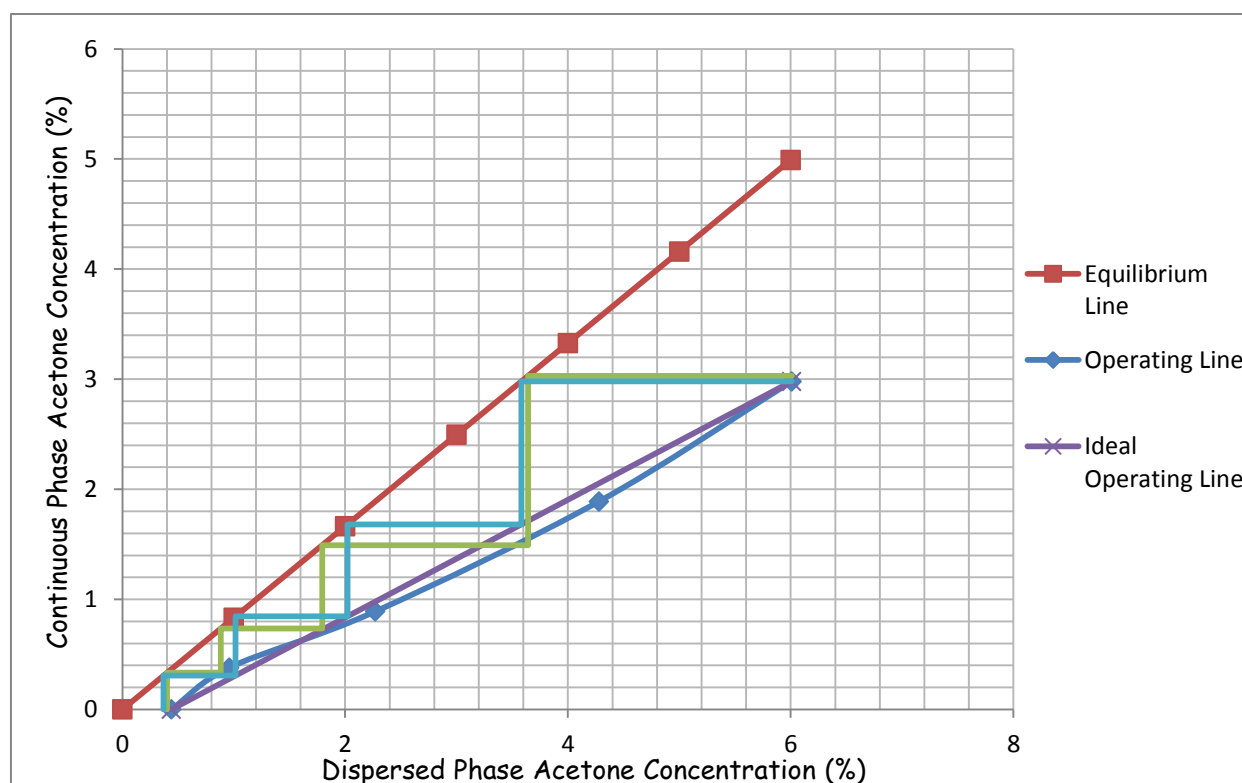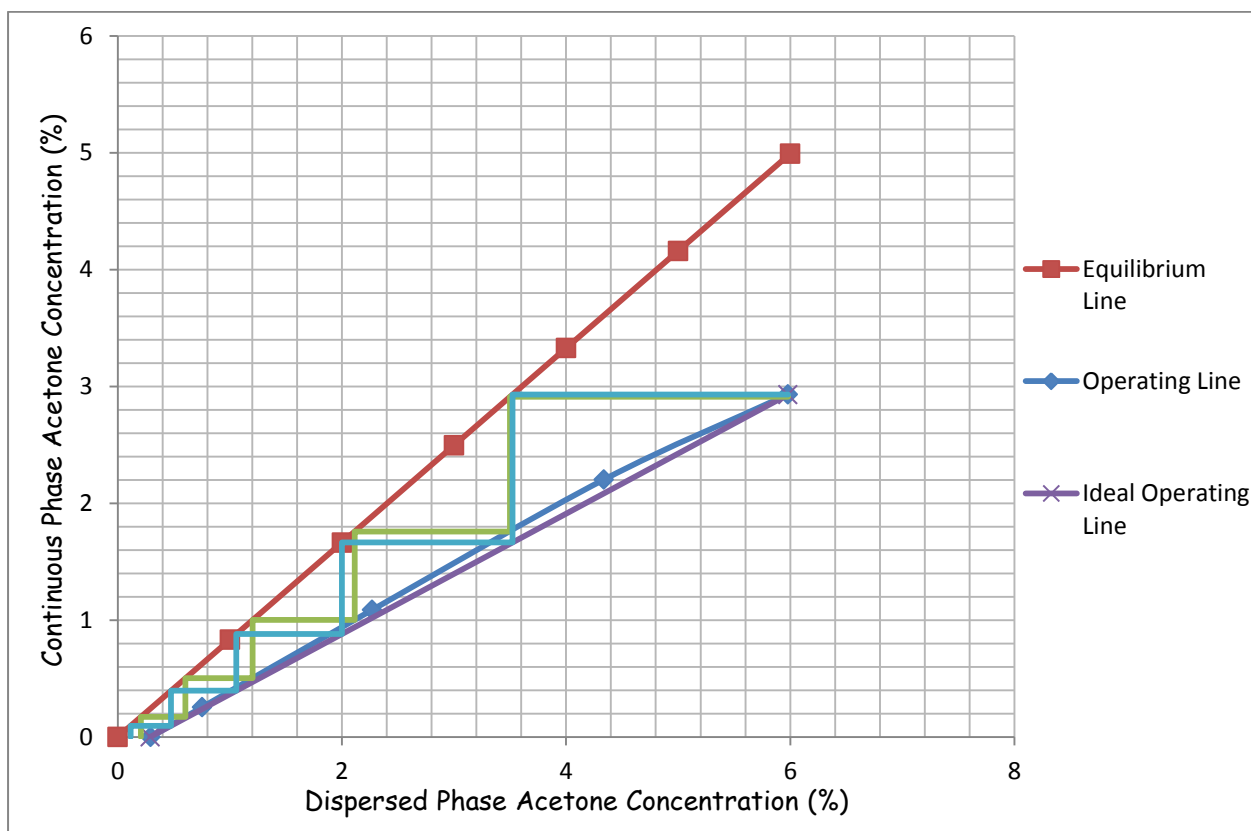


*Figure D 2.1.2: Equilibrium Stages With and Without Backmixing for h = 100 mm, S/F = 1:1 and af = 2.5 mm/s.*
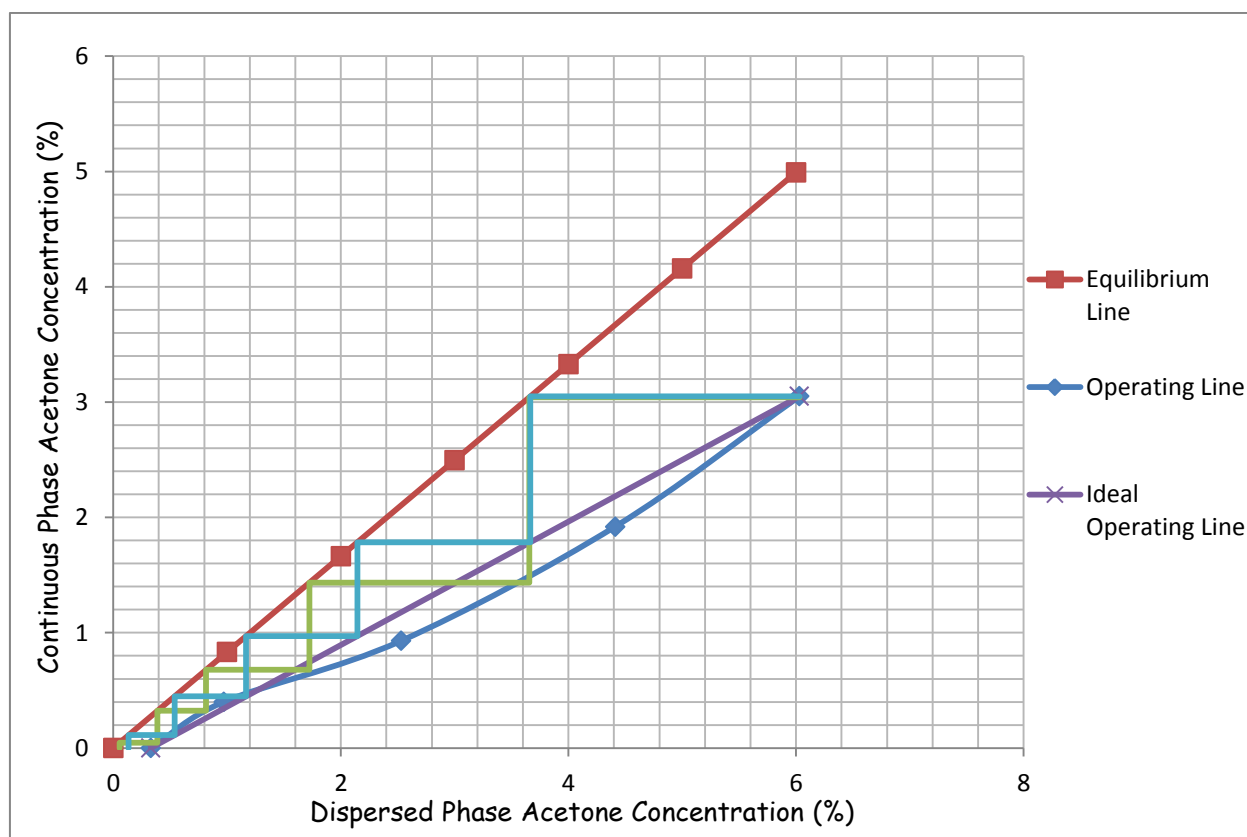
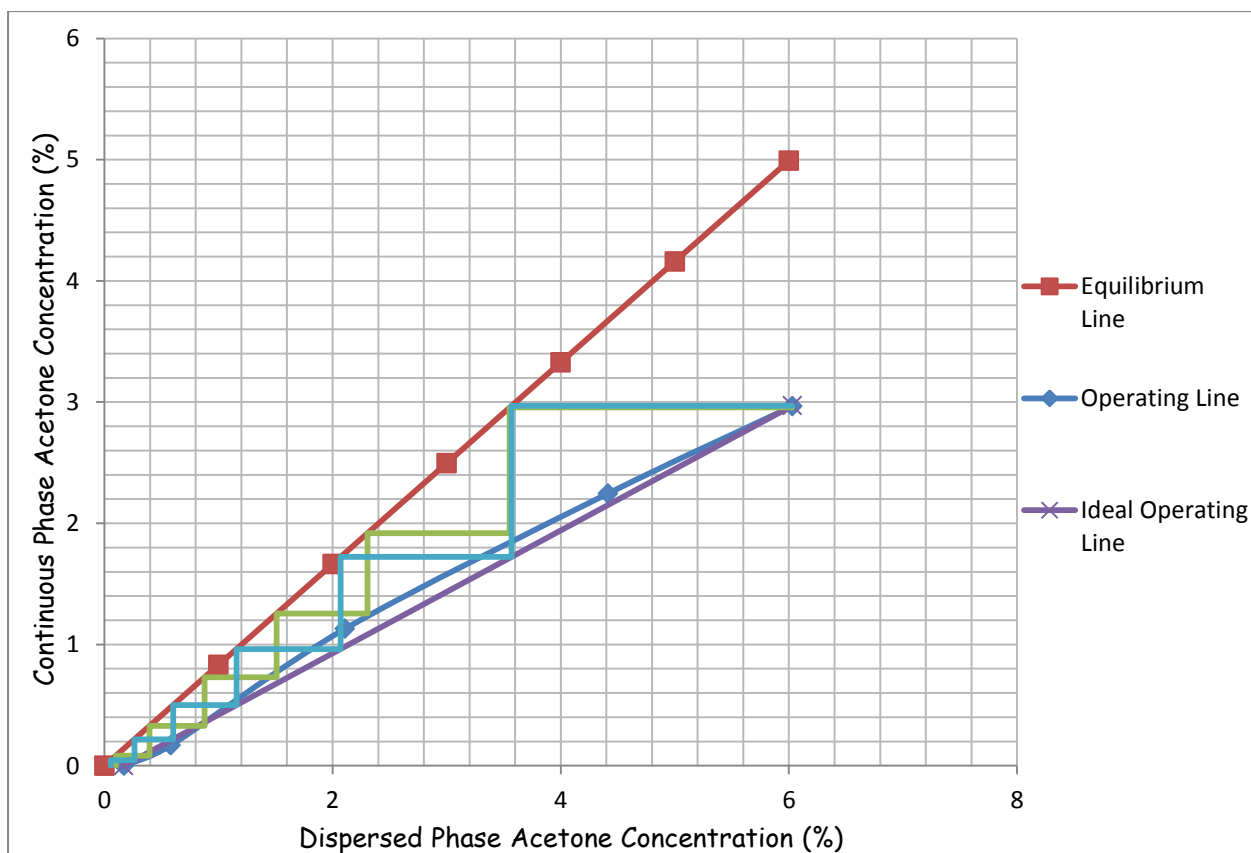*Figure D 2.1.3: Equilibrium Stages With and Without Backmixing for*
*h = 100 mm, S/F = 1:1 and af = 3.75 mm/s.*
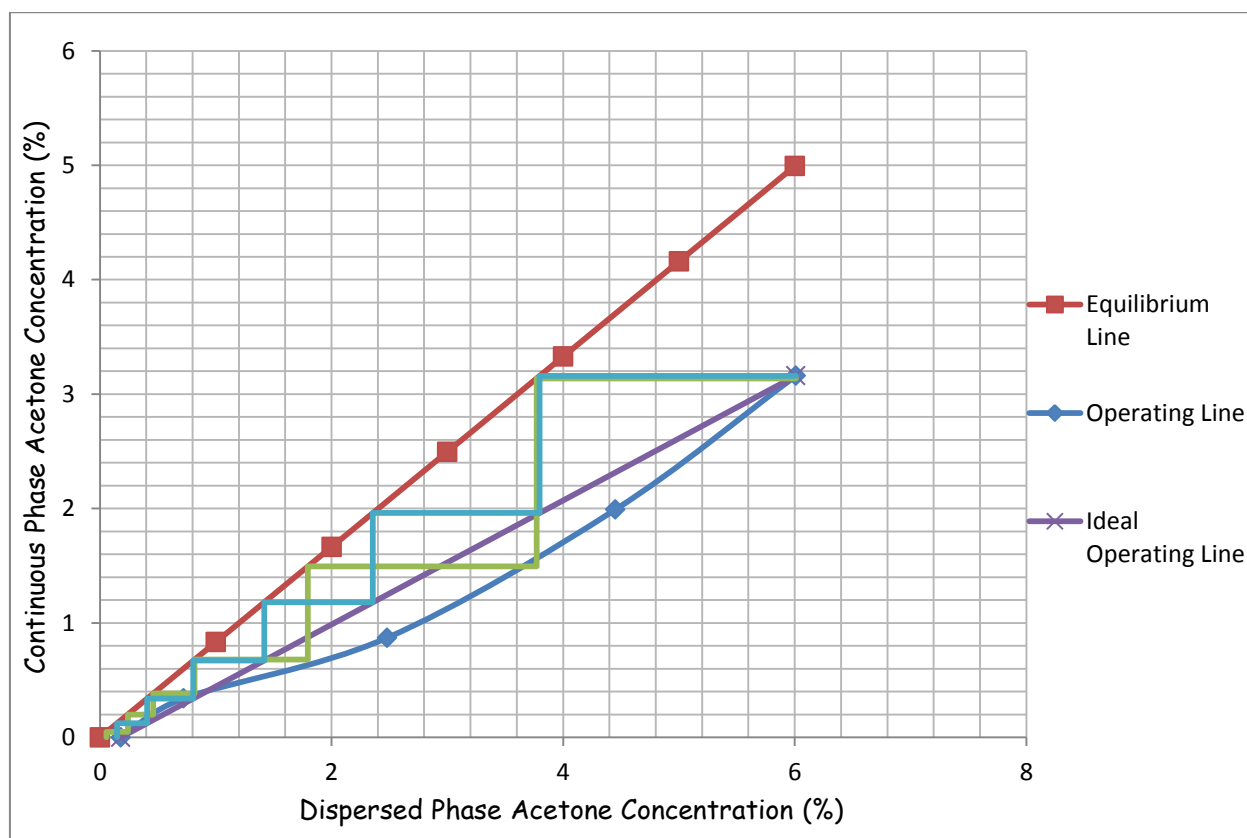


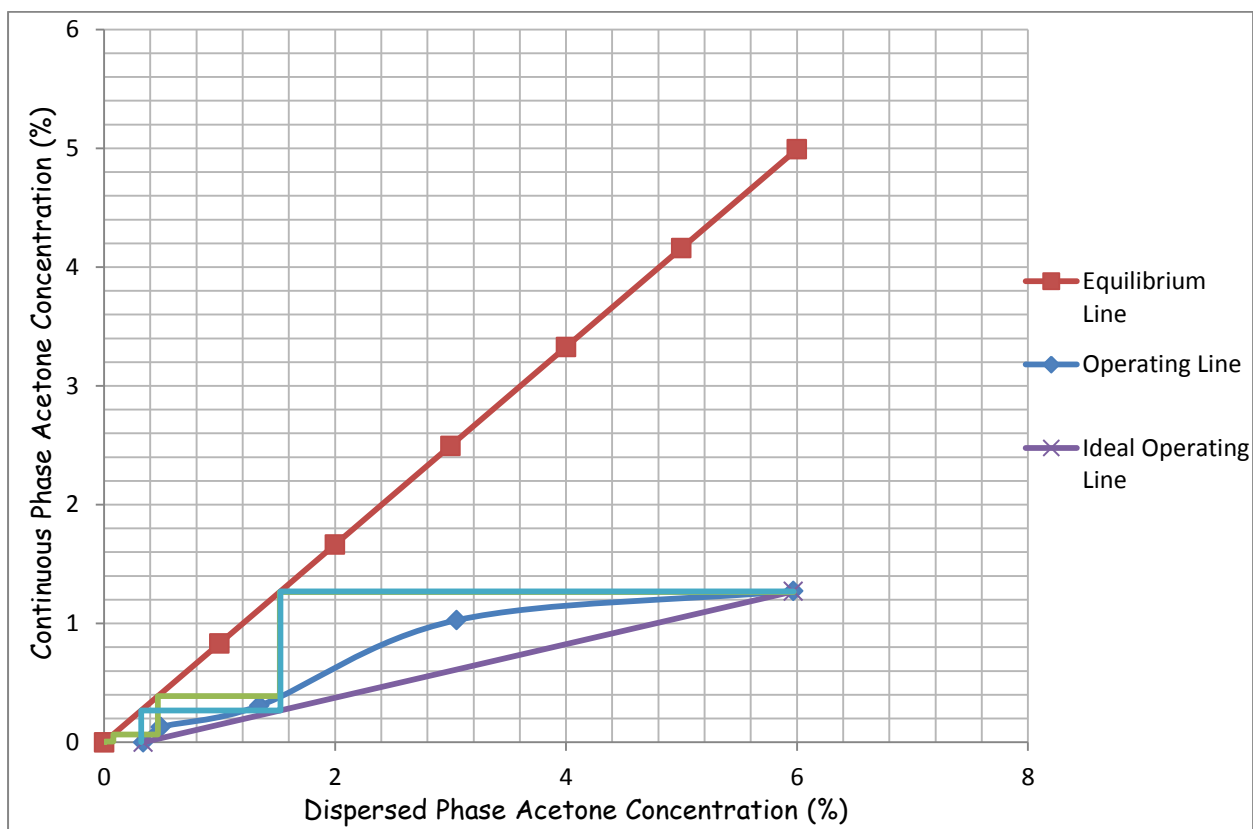*Figure D 2.1.4: Equilibrium Stages With and Without Backmixing for*
*h = 100 mm, S/F = 1:1 and af = 5 mm/s.*
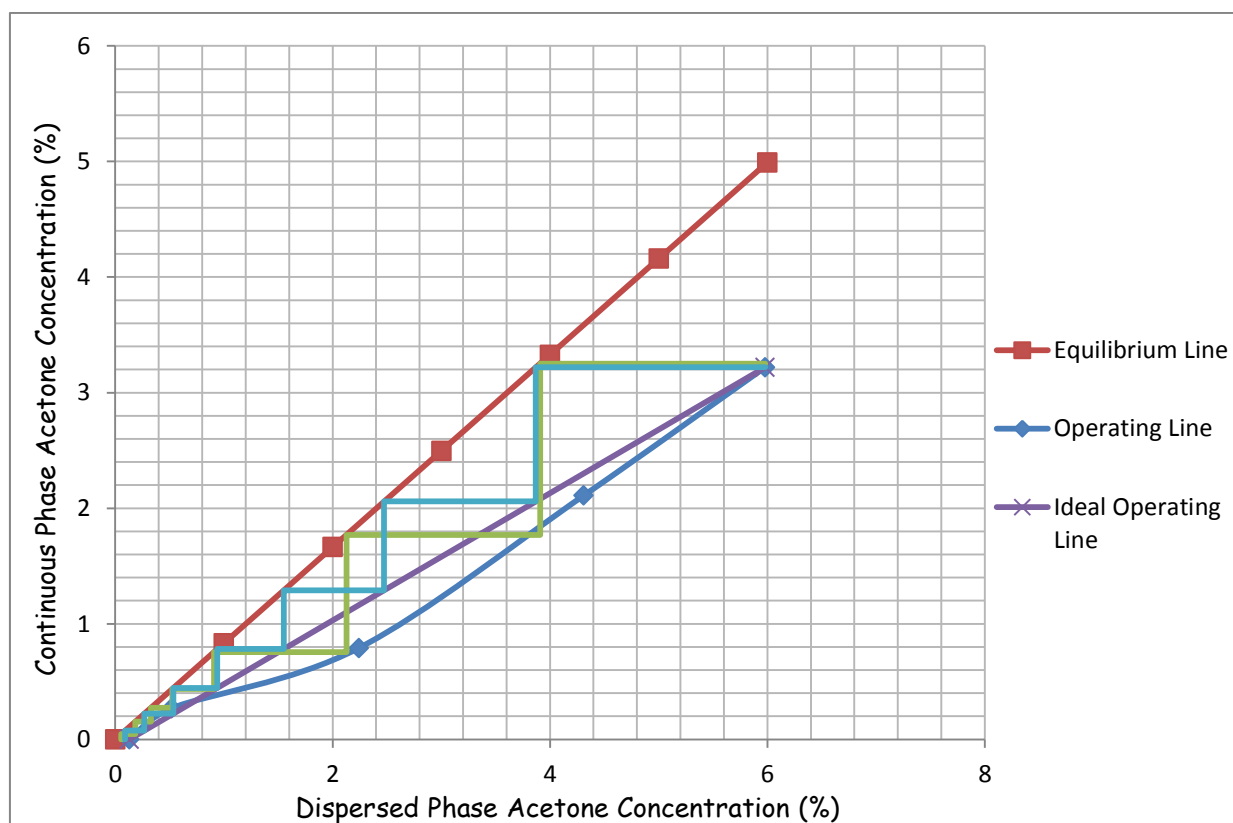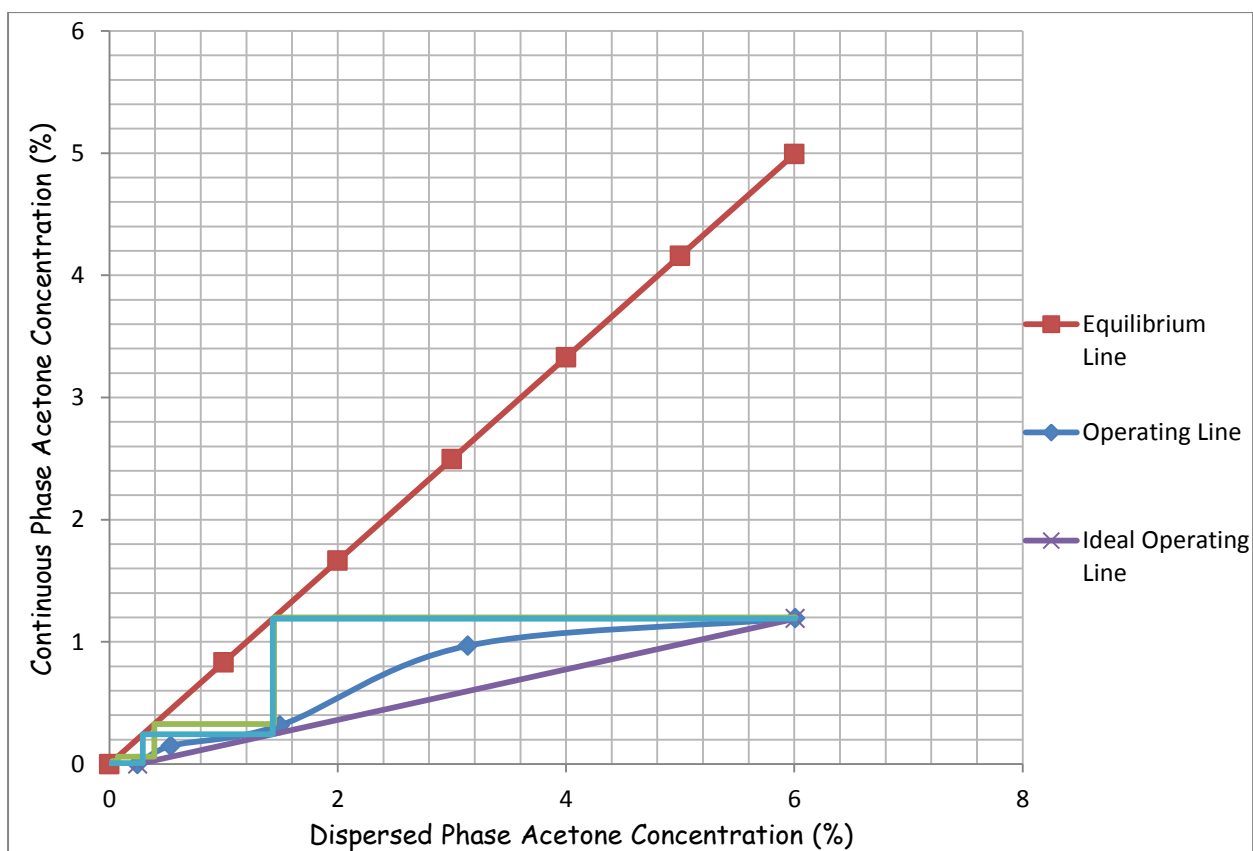
*Figure D 2.1.5: Equilibrium Stages With and Without Backmixing for*
*h = 100 mm, S/F = 1:1 and af = 6.25 mm/s.*
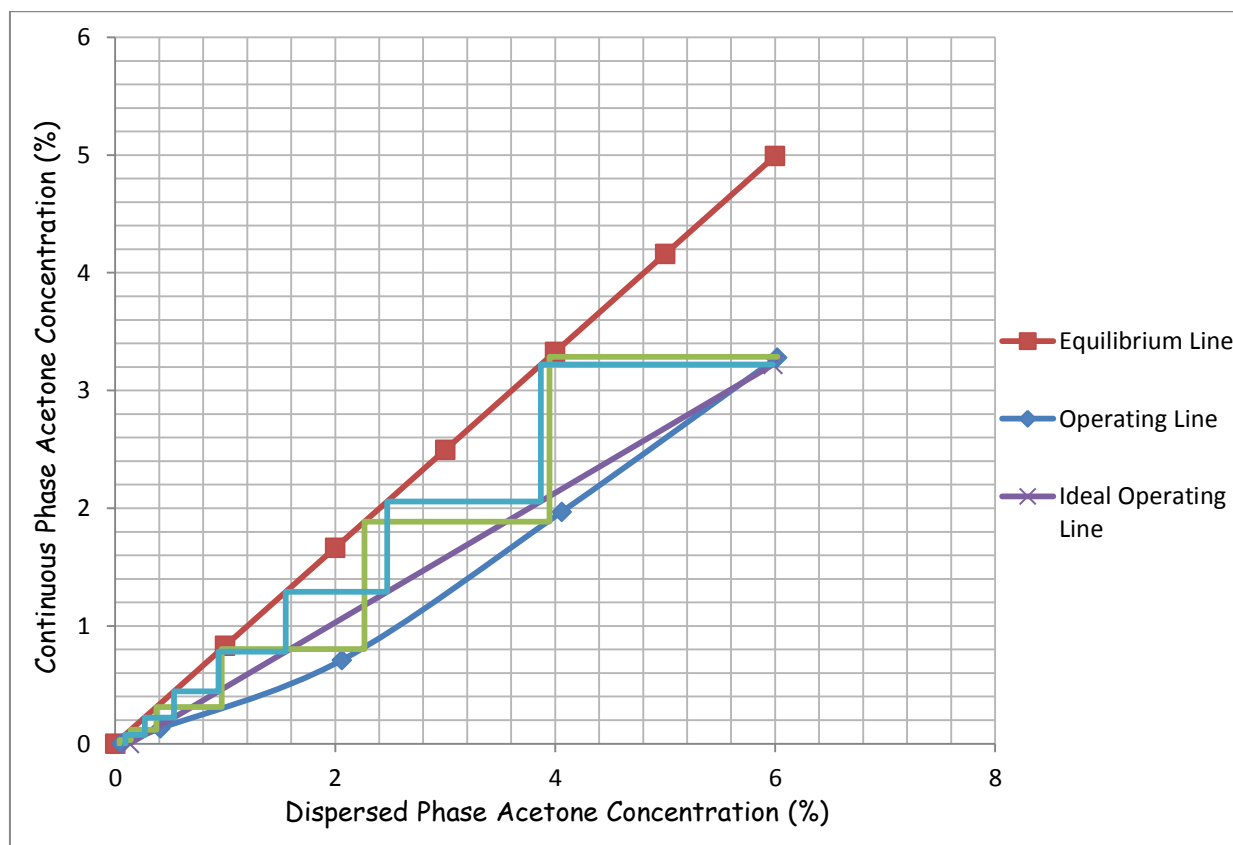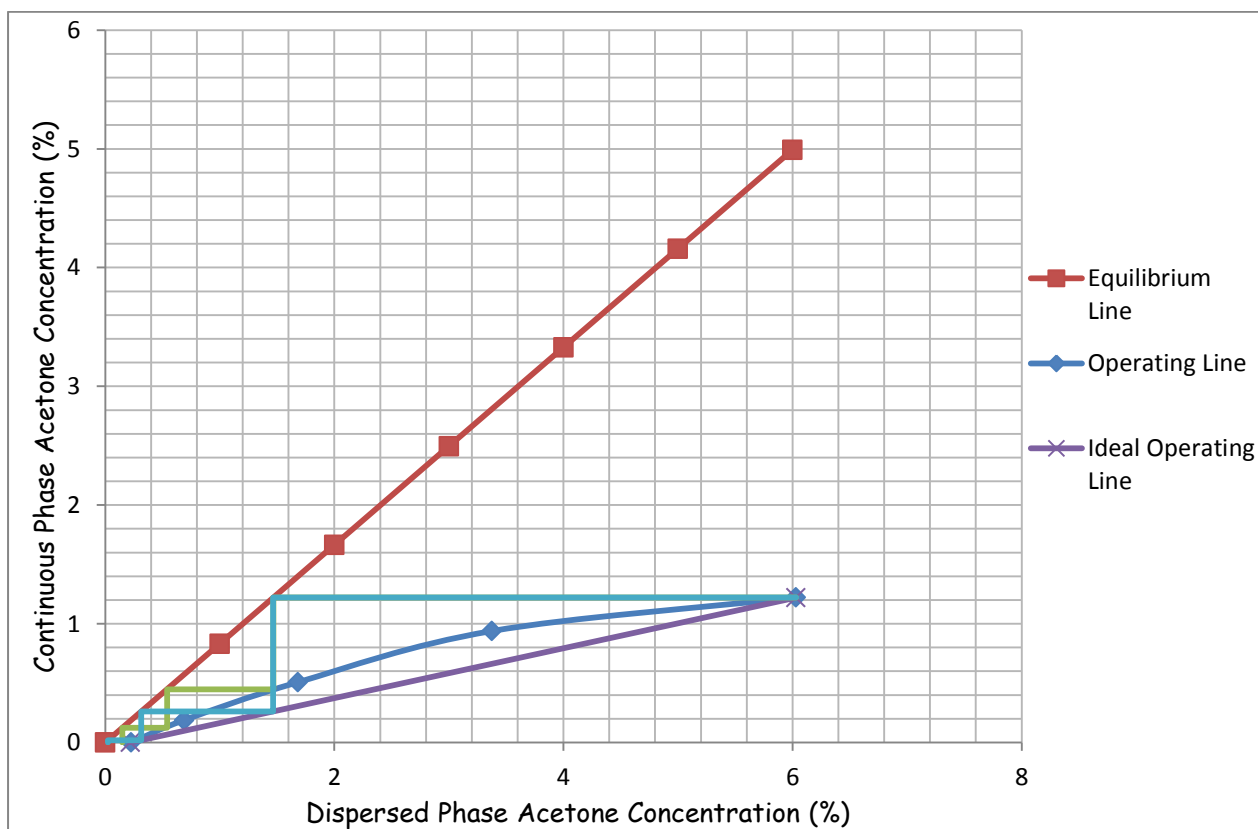


*Figure D 2.1.6: Equilibrium Stages With and Without Backmixing for*
*h = 100 mm, S/F = 1:1 and af = 7.5 mm/s.*
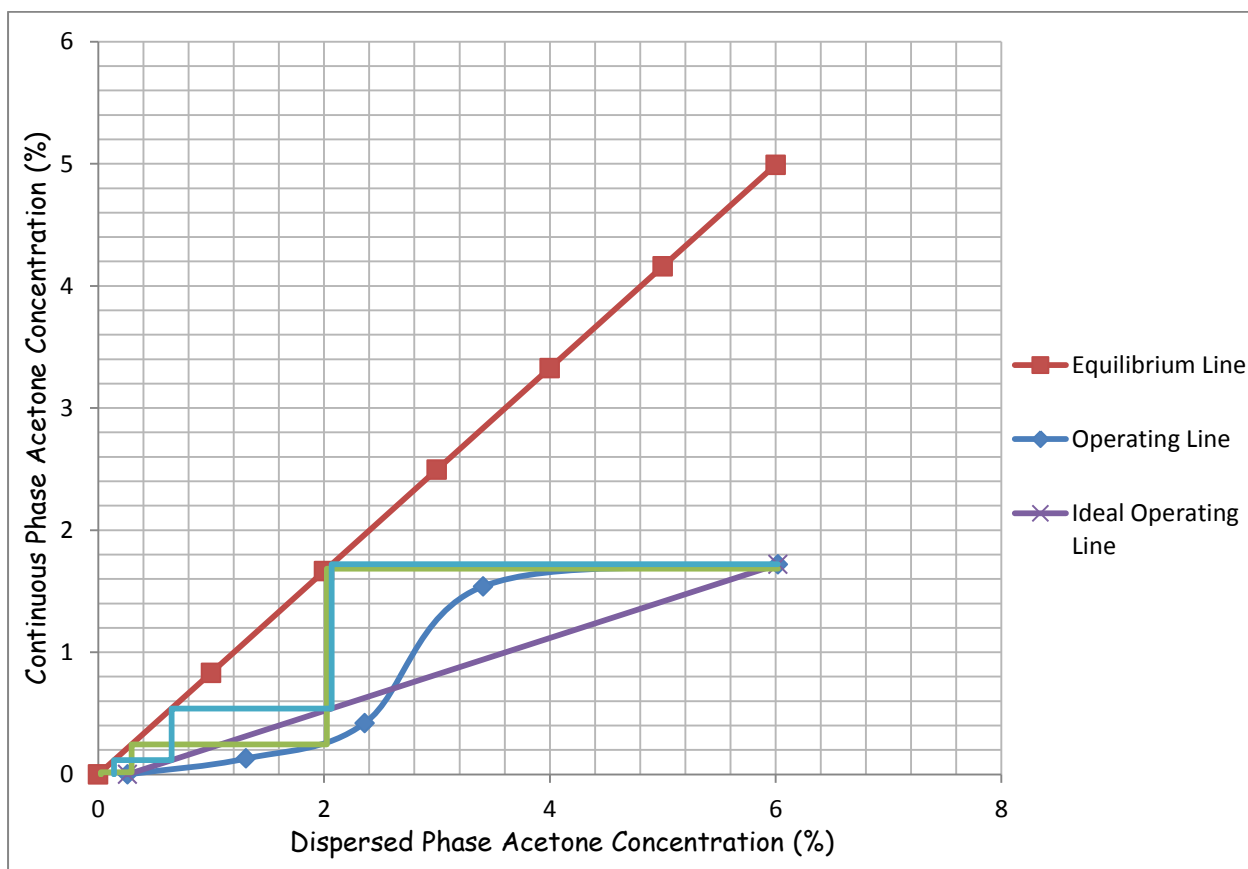
*Figure D 2.1.7: Equilibrium Stages With and Without Backmixing for*
*h = 100 mm, S/F = 2:1 and af = 1.25 mm/s.*
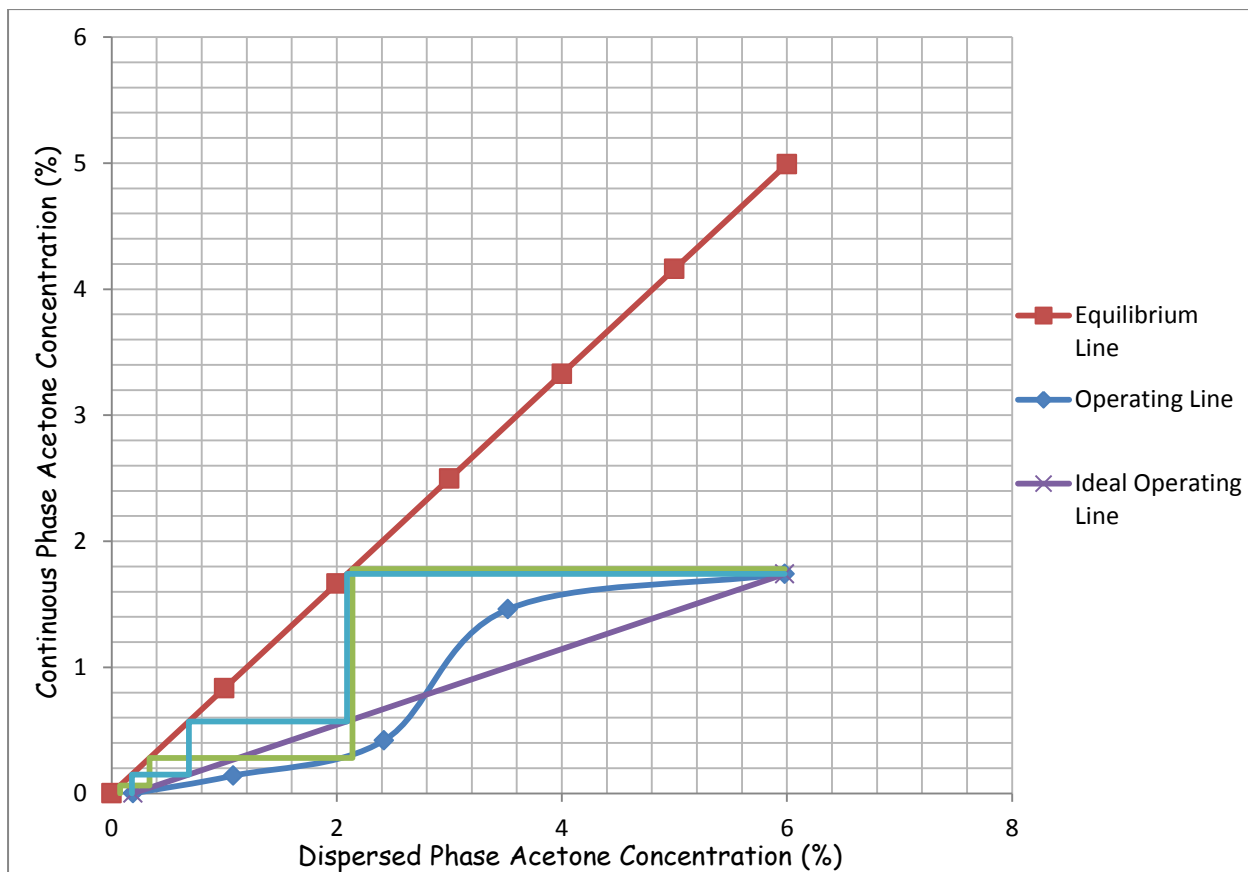


*Figure D 2.1.8: Equilibrium Stages With and Without Backmixing for*
*h = 100 mm, S/F = 2:1 and af = 2.5 mm/s.*
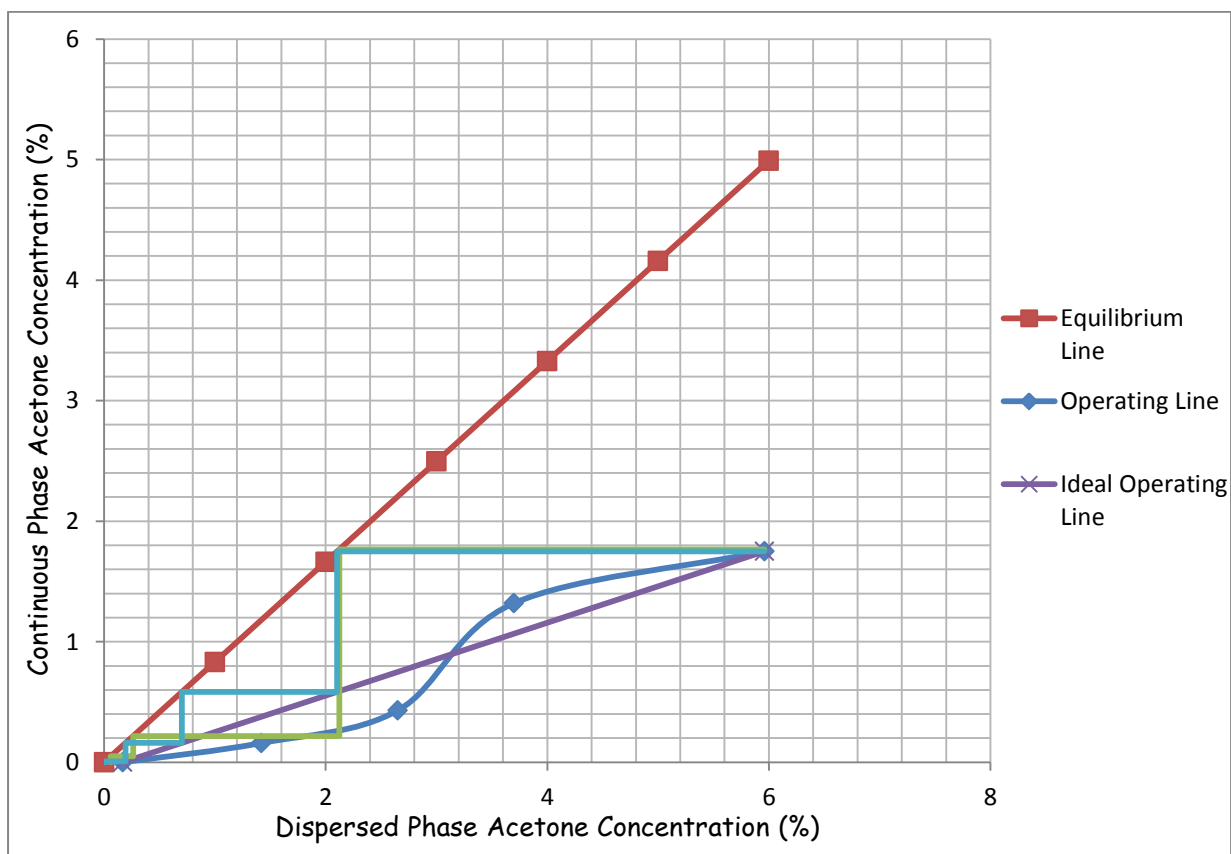
*Figure D 2.1.9: Equilibrium Stages With and Without Backmixing for h = 100 mm, S/F = 2:1 and af = 3.75 mm/s.*
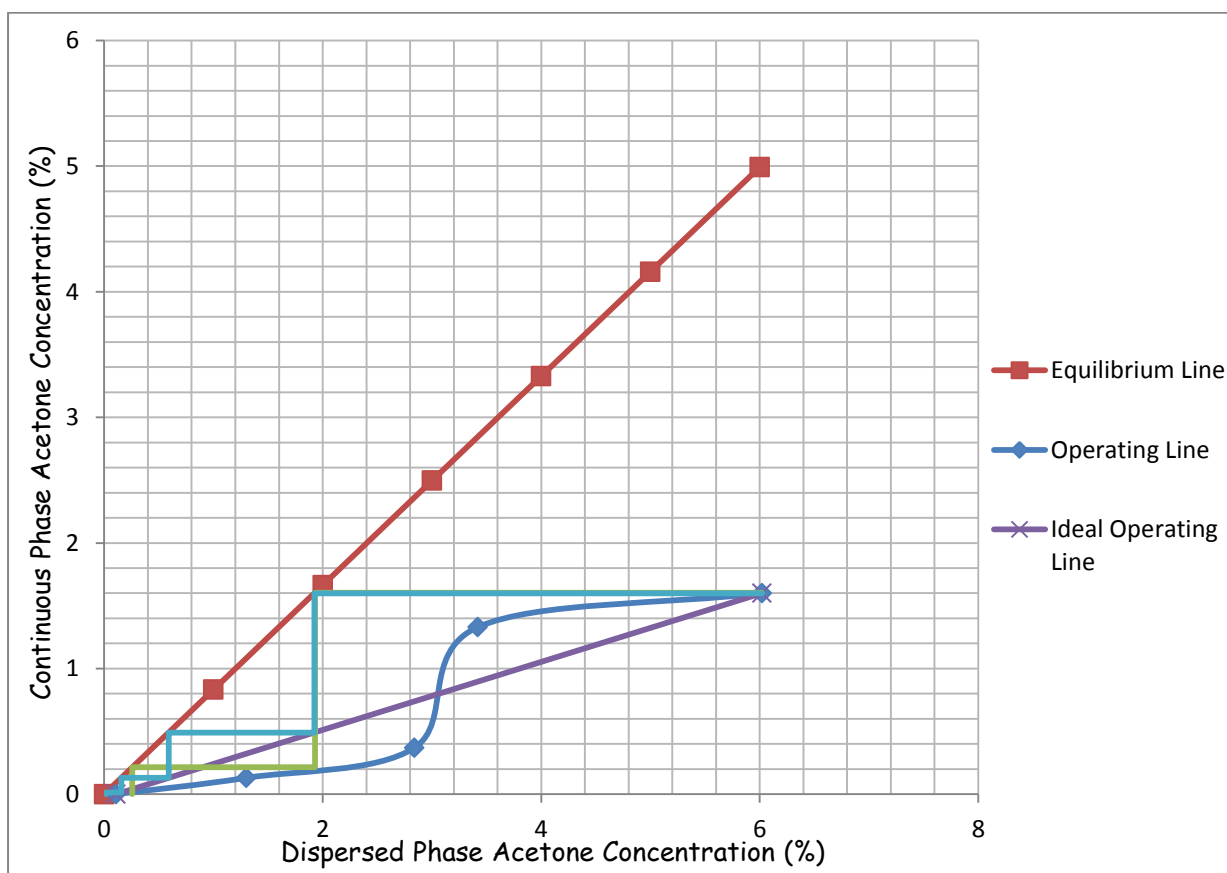


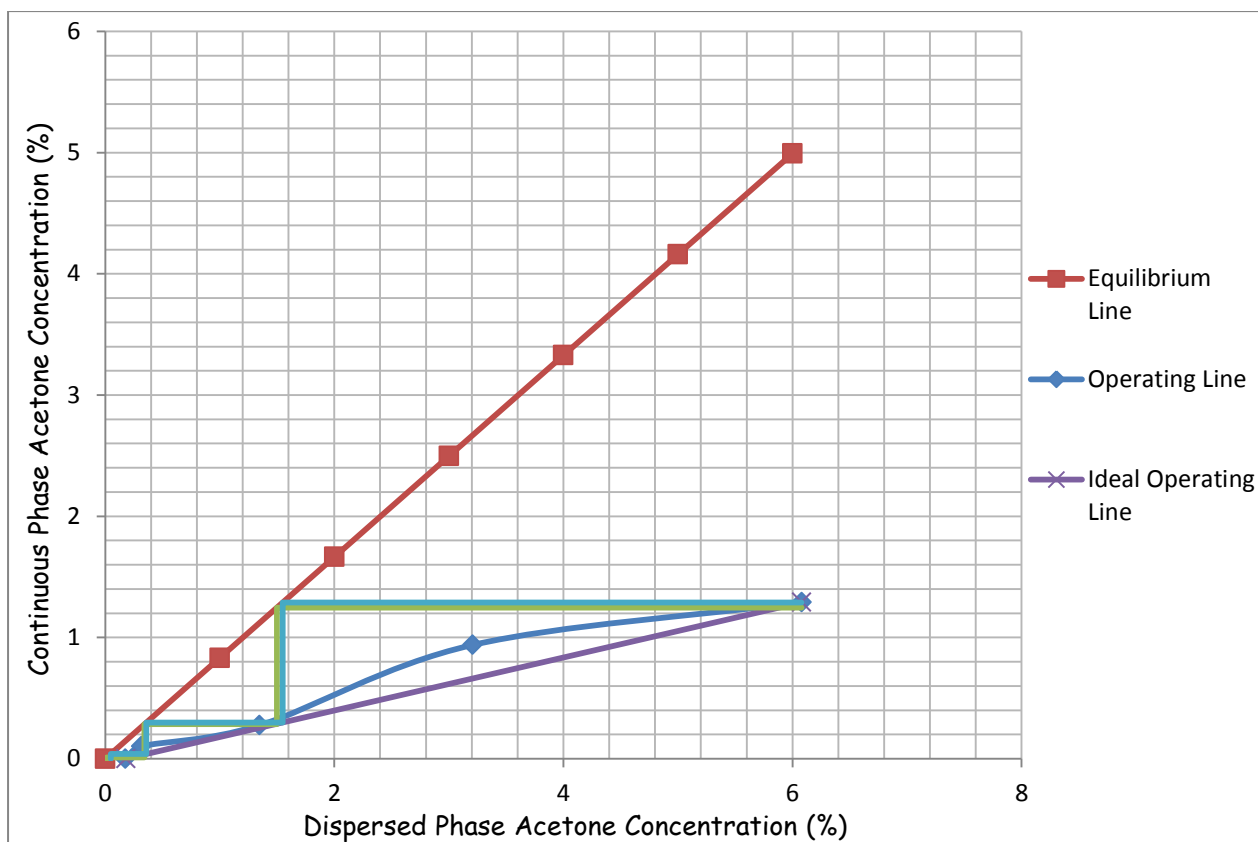*Figure D 2.1.10: Equilibrium Stages With and Without Backmixing for h = 100 mm, S/F = 2:1 and af = 5 mm/s.*
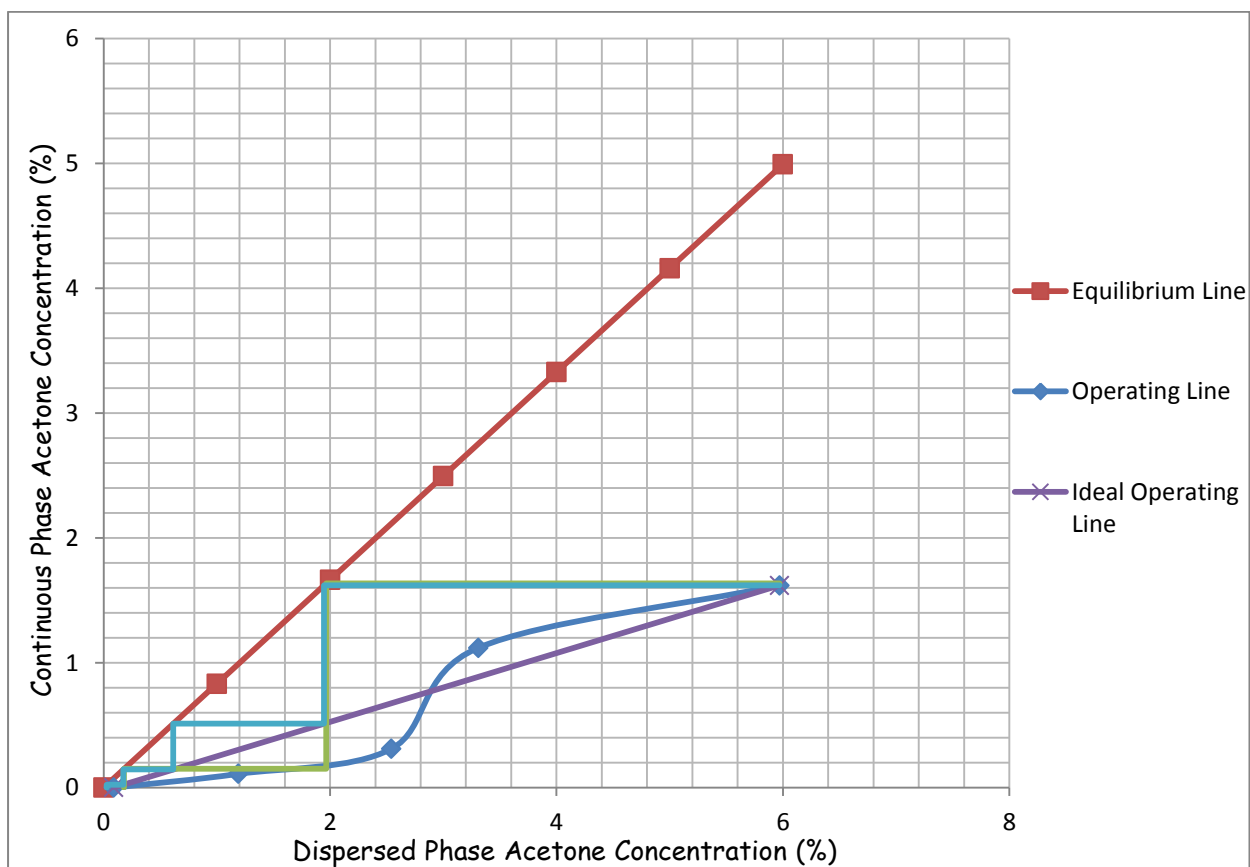
*Figure D 2.1.11: Equilibrium Stages With and Without Backmixing for*
*h = 100 mm, S/F = 2:1 and af = 6.25 mm/s.*
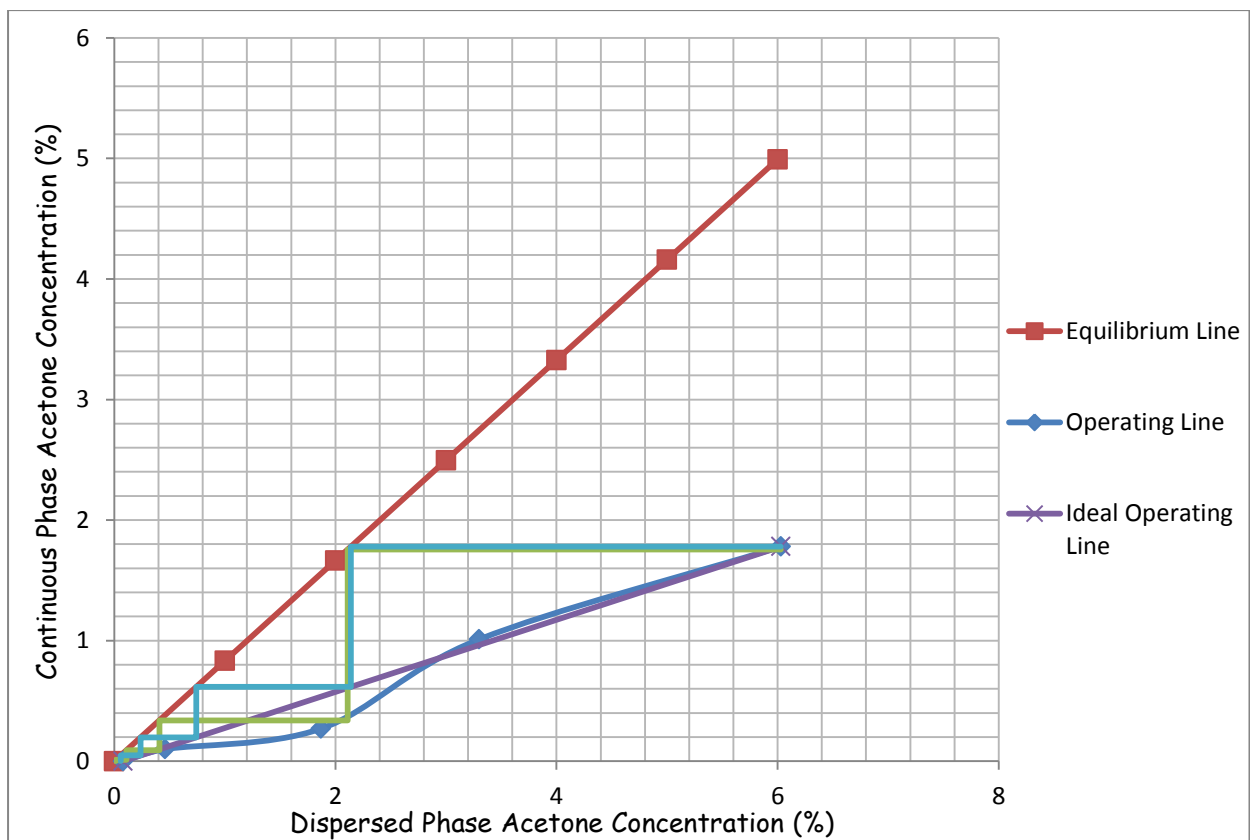


*Figure D 2.1.12: Equilibrium Stages With and Without Backmixing for*
*h = 100 mm, S/F = 2:1 and af = 7.5 mm/s.*
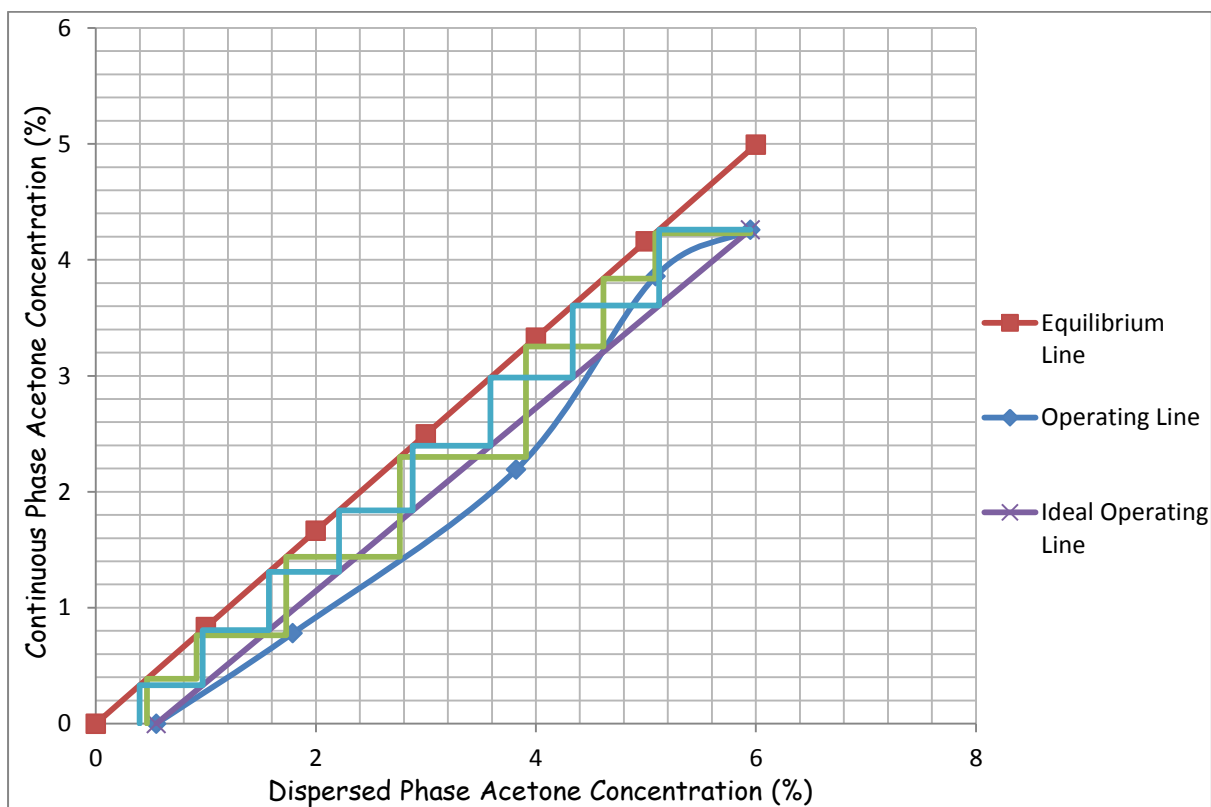
*Figure D 2.1.13: Equilibrium Stages With and Without Backmixing for*
*h = 100 mm, S/F = 1:2 and af = 2.5 mm/s.*
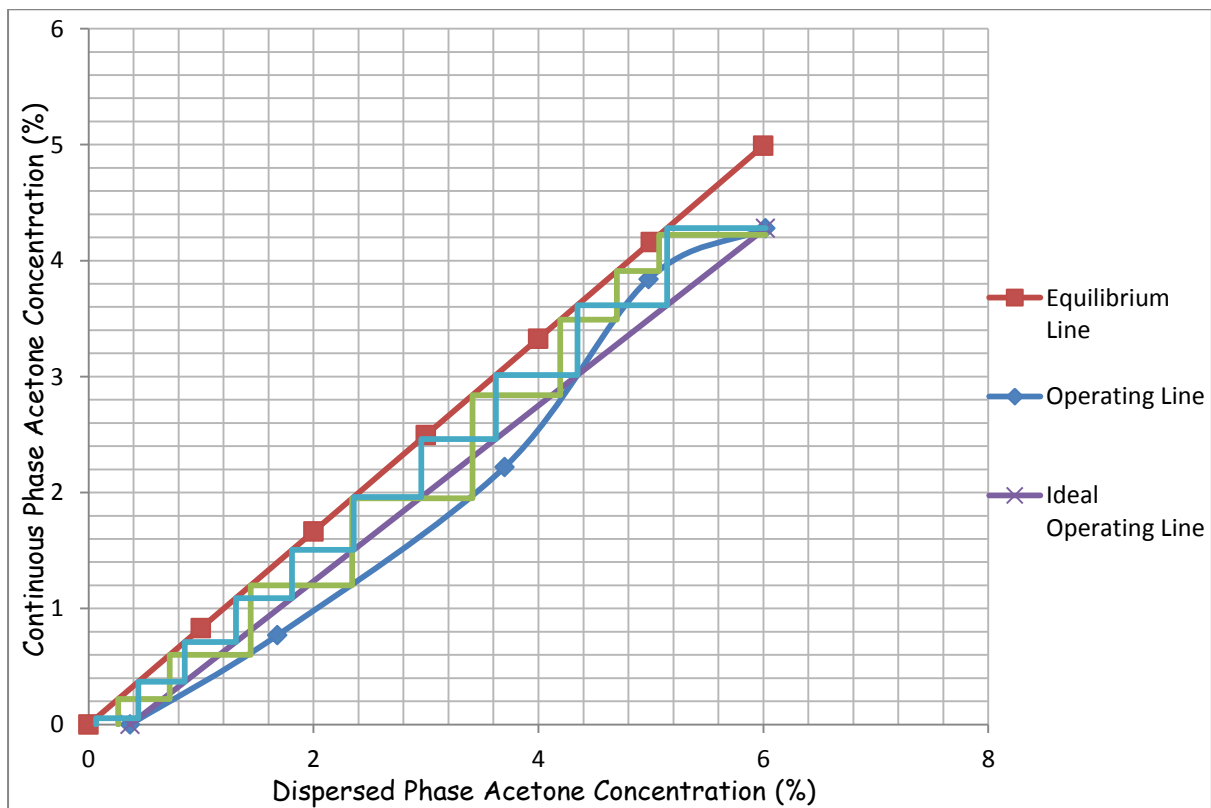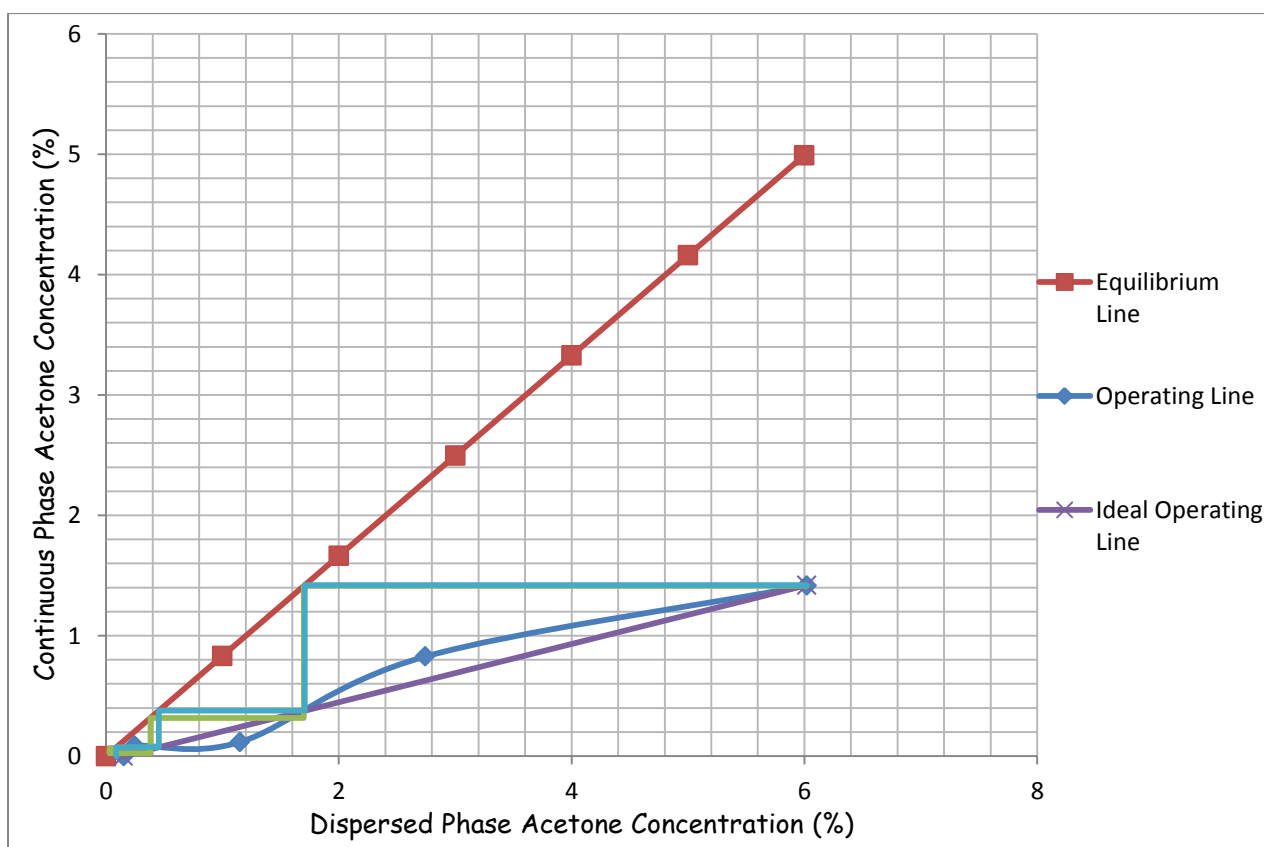


*Figure D 2.1.14: Equilibrium Stages With and Without Backmixing for*
*h = 100 mm, S/F = 1:2 and af = 3.75 mm/s.*
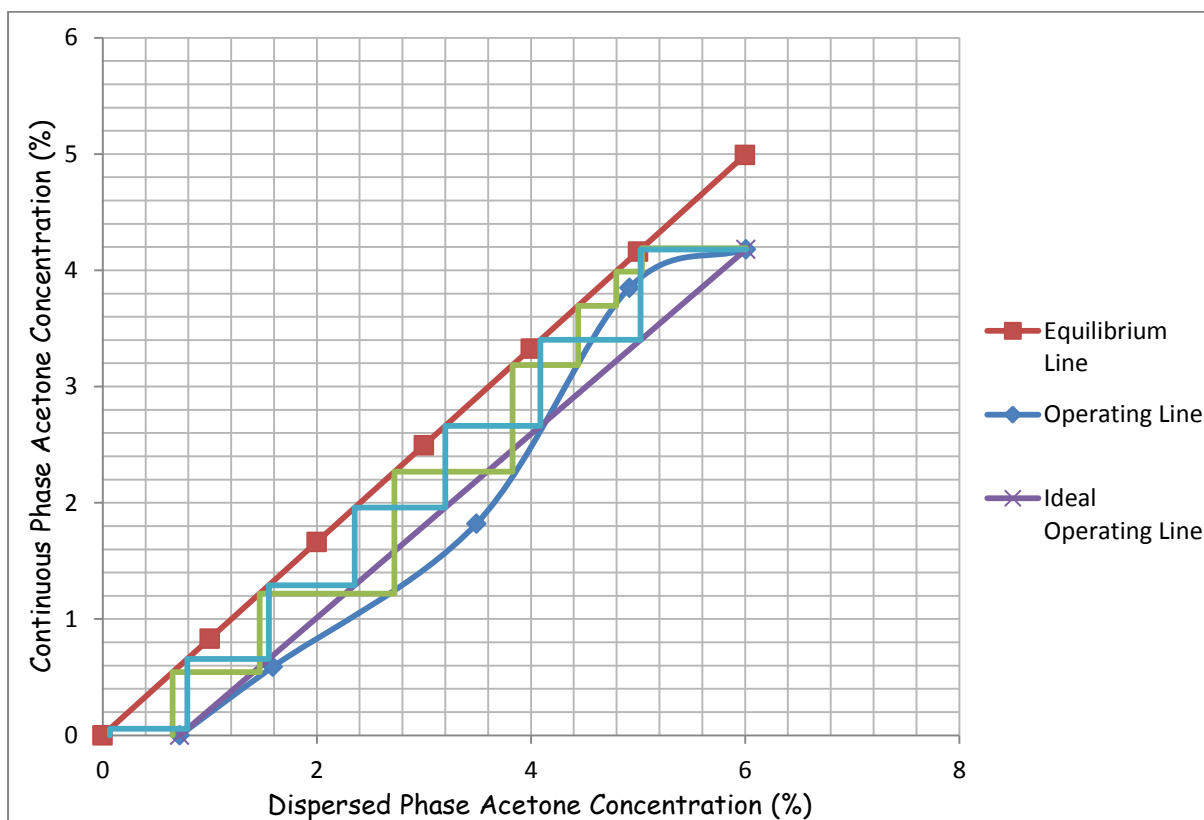
*Figure D 2.1.15: Equilibrium Stages With and Without Backmixing for*
*h = 100 mm, S/F = 1:2 and af = 5 mm/s.*
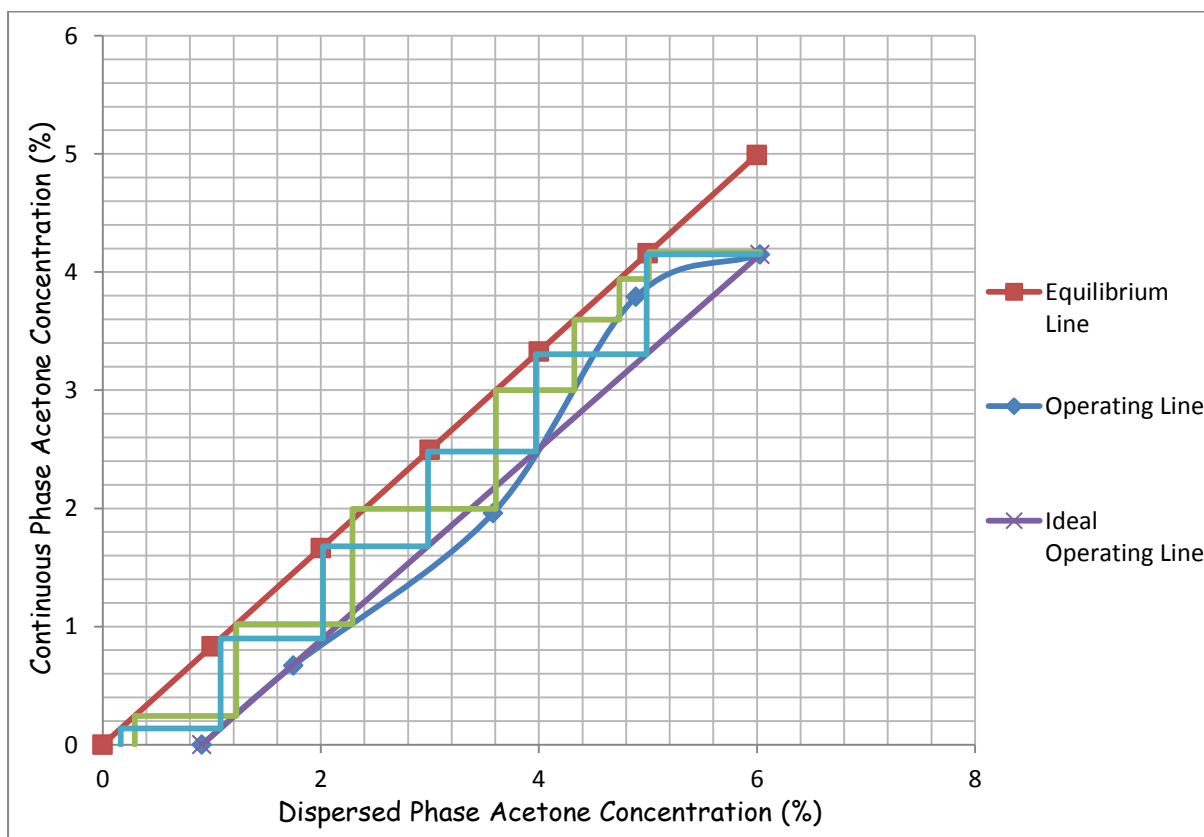


*Figure D 2.1.16: Equilibrium Stages With and Without Backmixing for*
*h = 100 mm, S/F = 1:2 and af = 6.25 mm/s.*
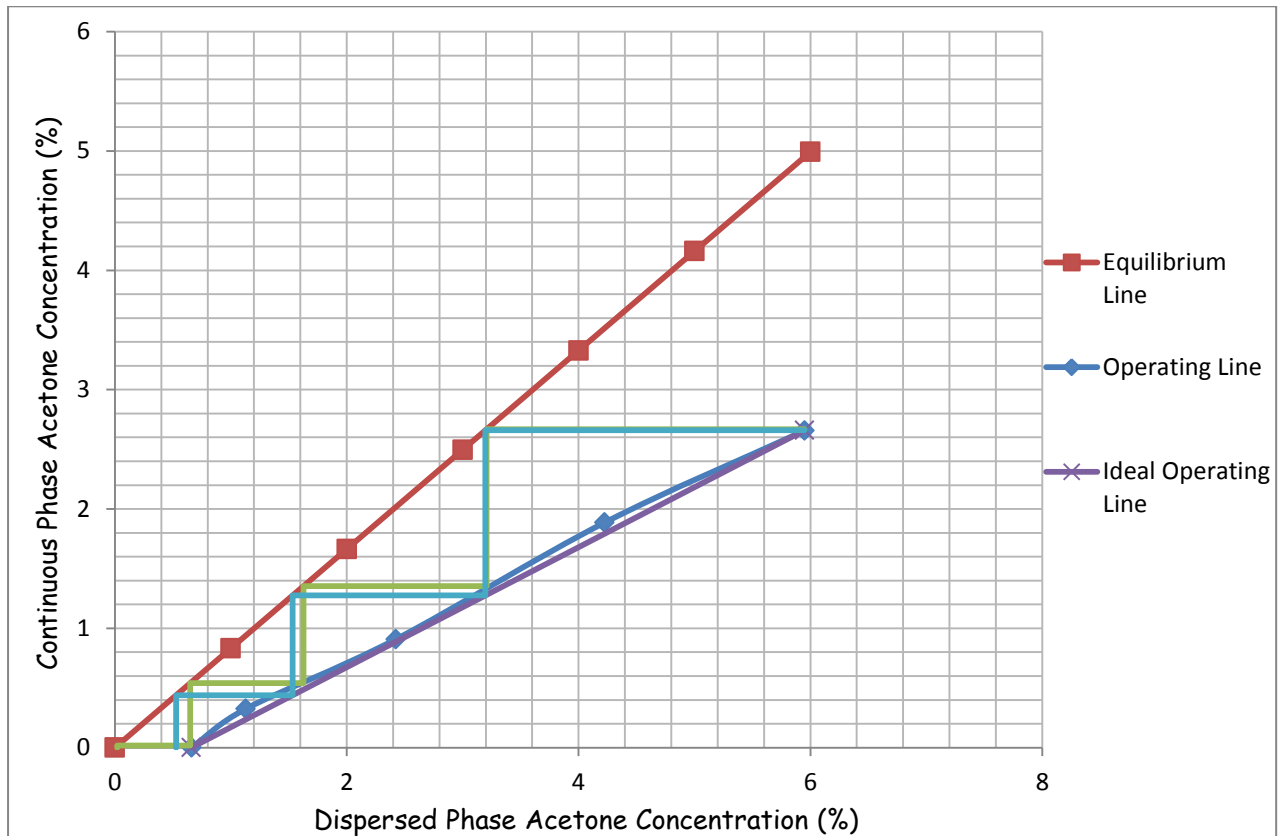
*Figure D 2.2.1: Equilibrium Stages With and Without Backmixing for*
*h = 150 mm, S/F = 1:1 and af = 1.25 mm/s.*
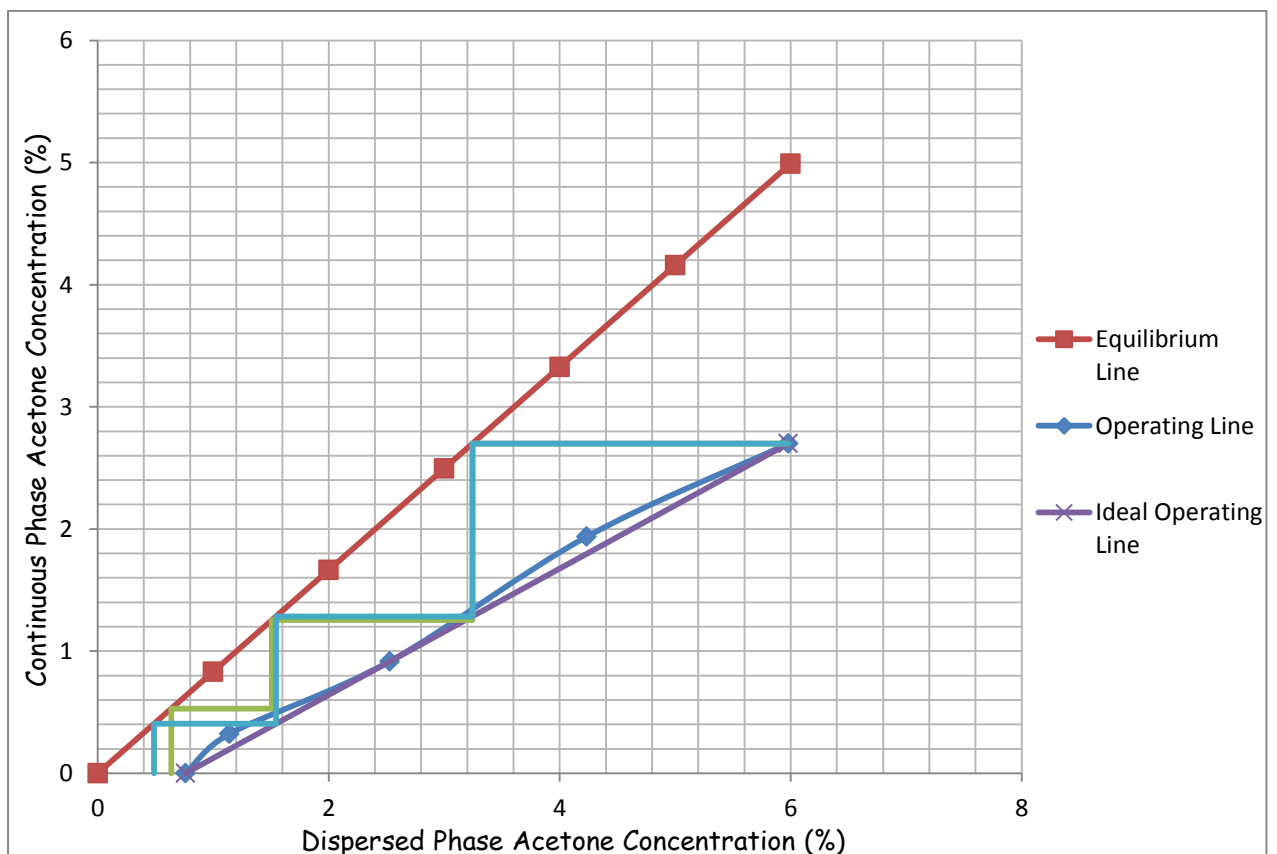


*Figure D 2.2.2: Equilibrium Stages With and Without Backmixing for*
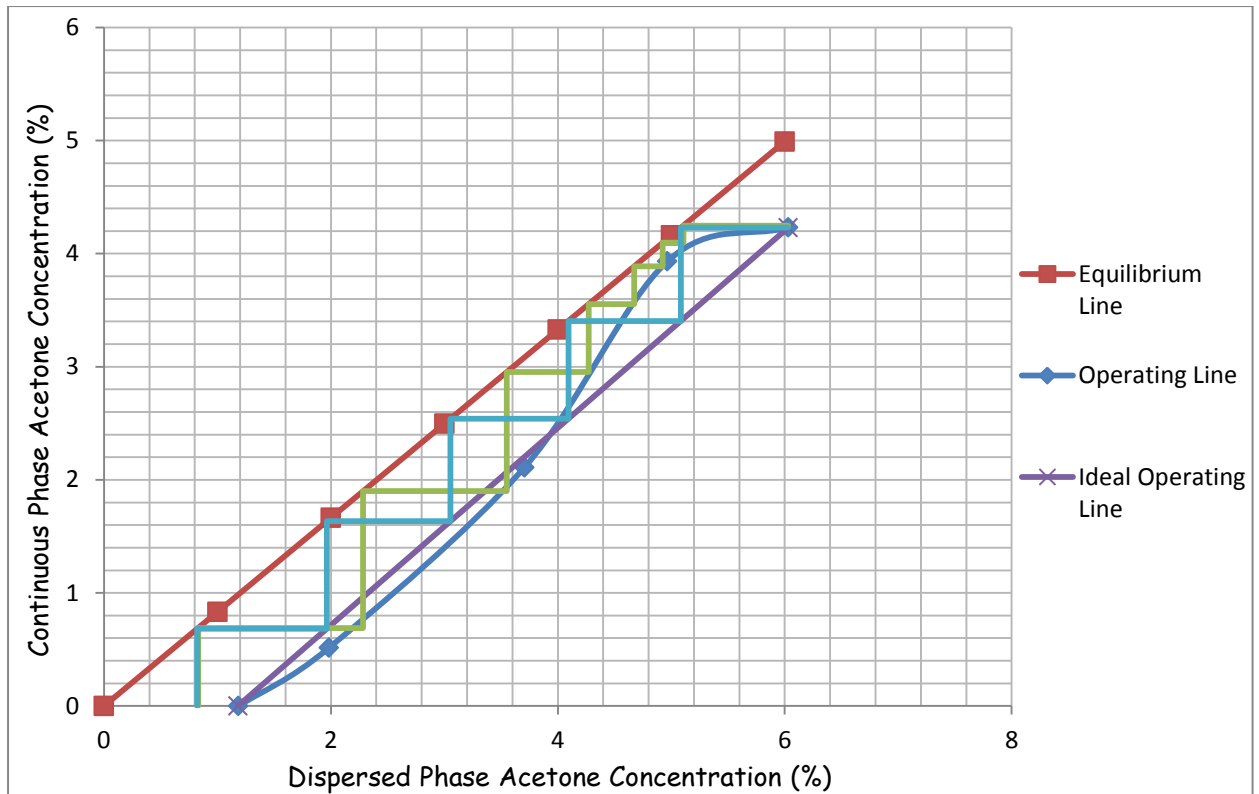*h = 150 mm, S/F = 1:1 and af = 2.5 mm/s.*
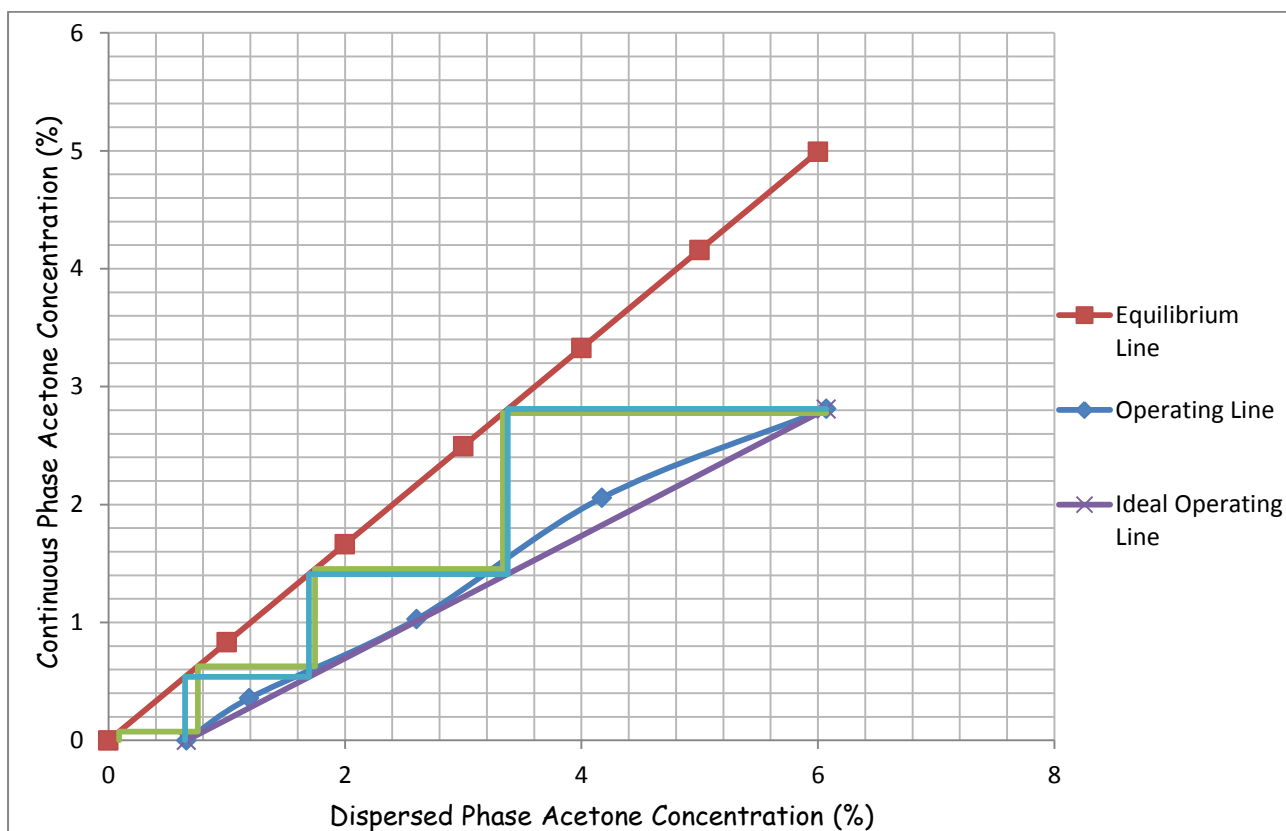
*Figure D 2.2.3: Equilibrium Stages With and Without Backmixing for
h = 150 mm, S/F = 1:1 and af = 3.75 mm/s.*
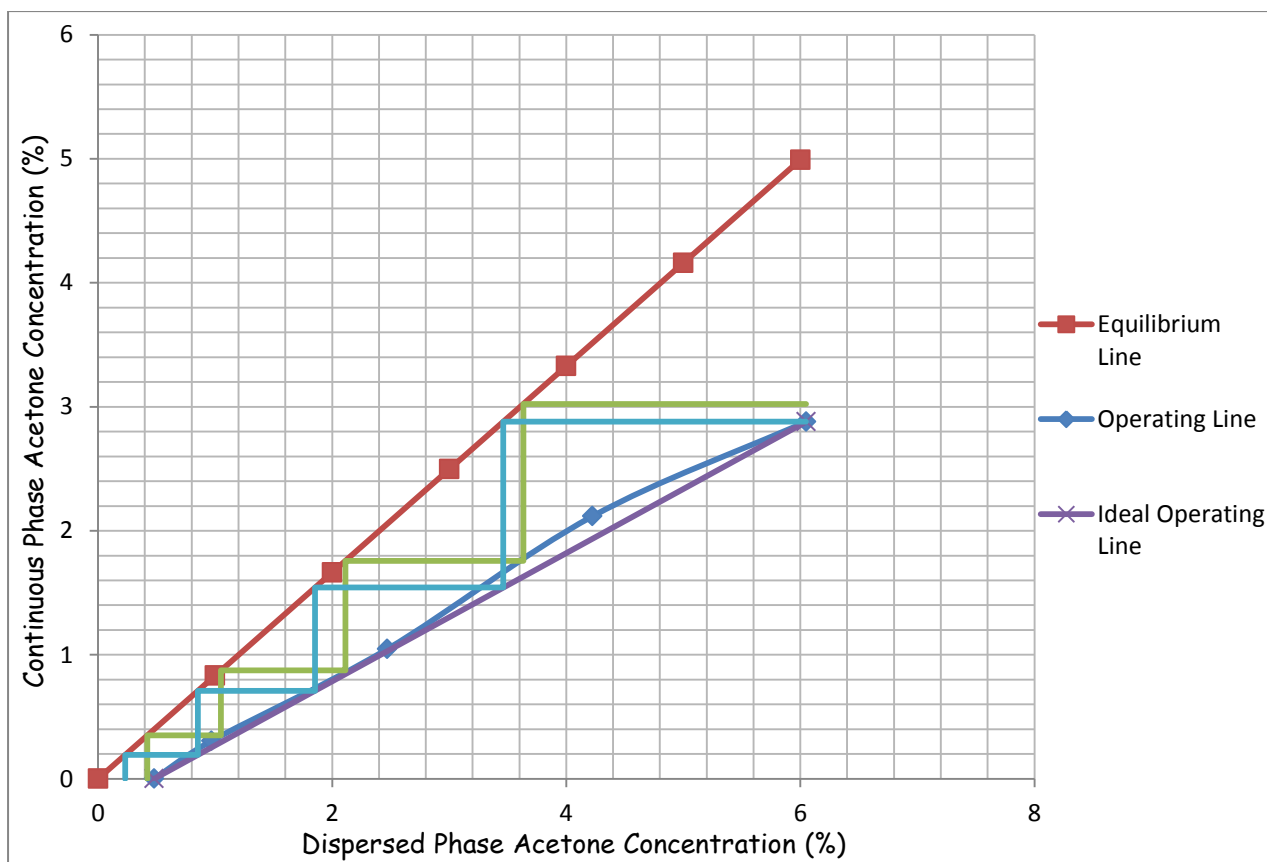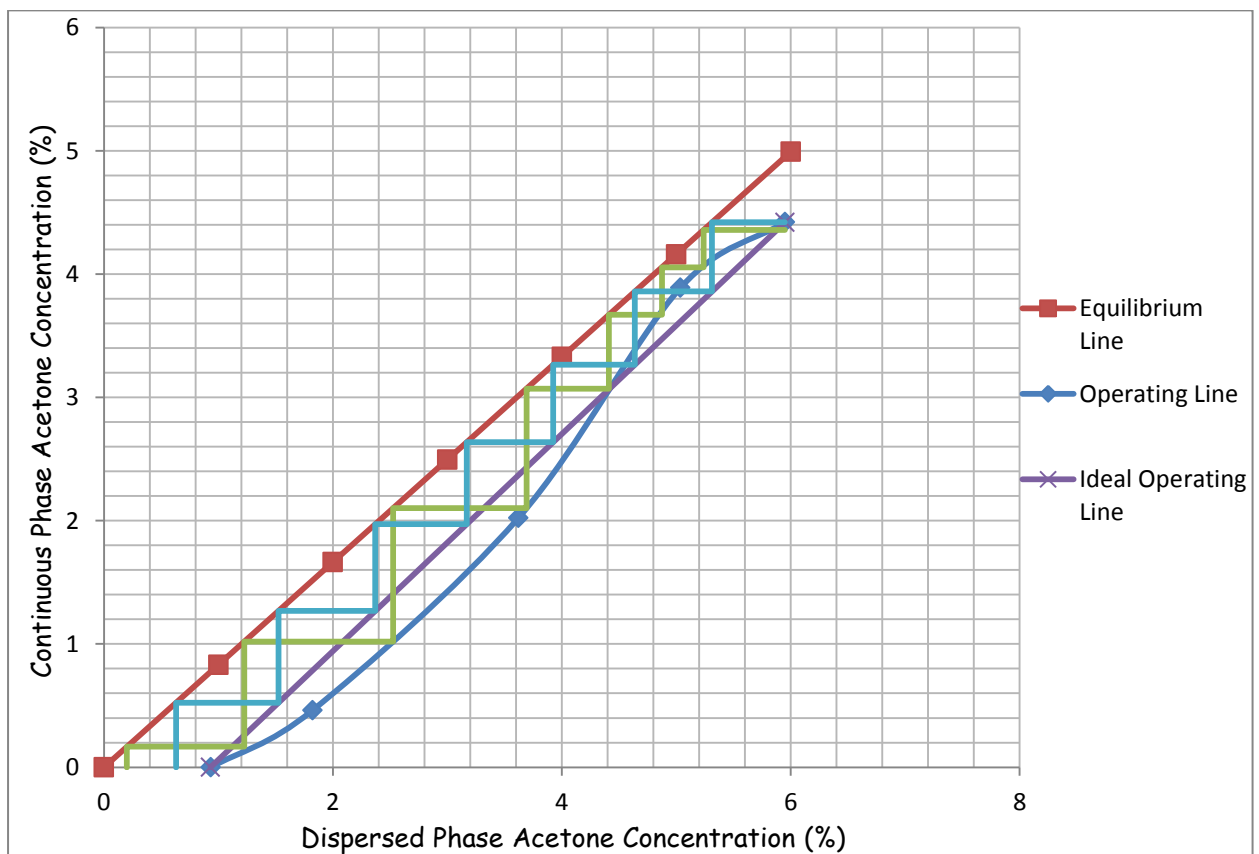


*Figure D 2.2.4: Equilibrium Stages With and Without Backmixing for
h = 150 mm, S/F = 1:1 and af = 5 mm/s.*

*Figure D 2.2.5: Equilibrium Stages With and Without Backmixing for*
*h = 150 mm, S/F = 1:1 and af = 6.25 mm/s.*



*Figure D 2.2.6: Equilibrium Stages With and Without Backmixing for*
*h = 150 mm, S/F = 1:1 and af = 7.5 mm/s.*
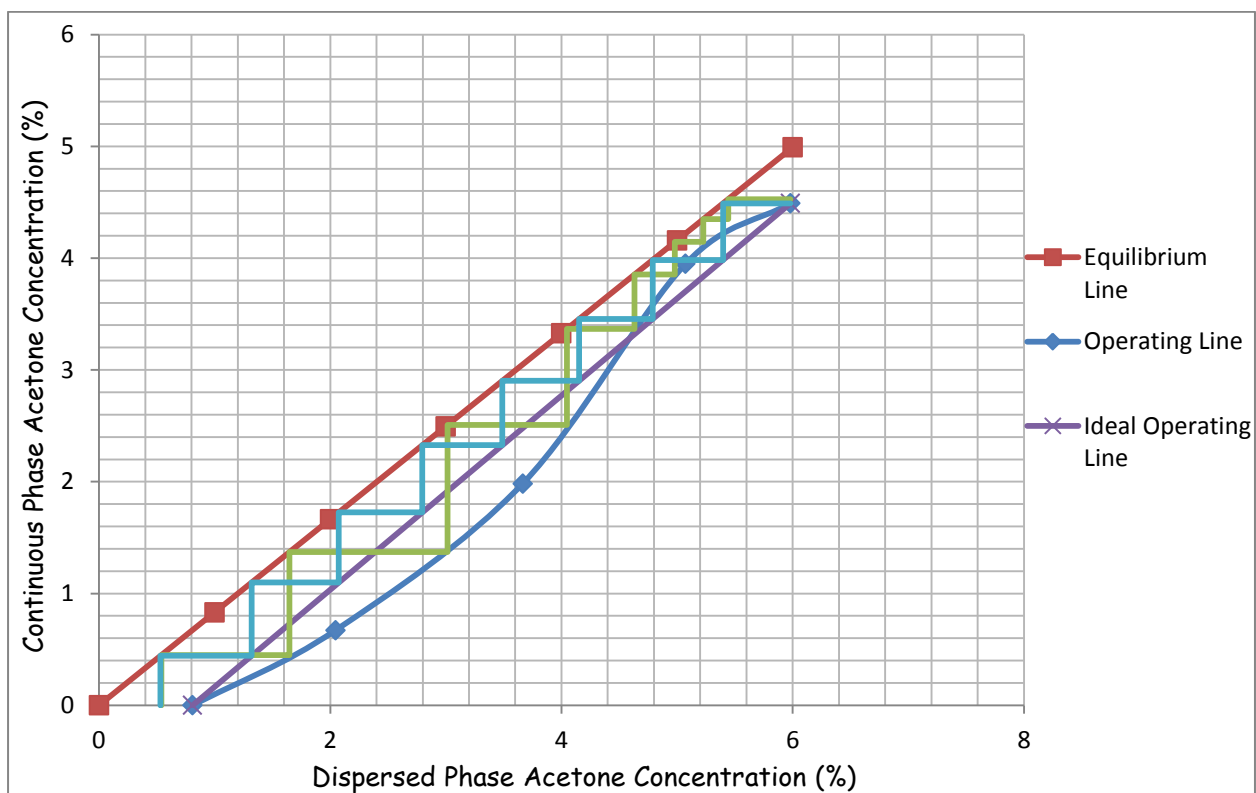
*Figure D 2.2.7: Equilibrium Stages With and Without Backmixing for*
*h = 150 mm, S/F = 2:1 and af = 1.25 mm/s.*
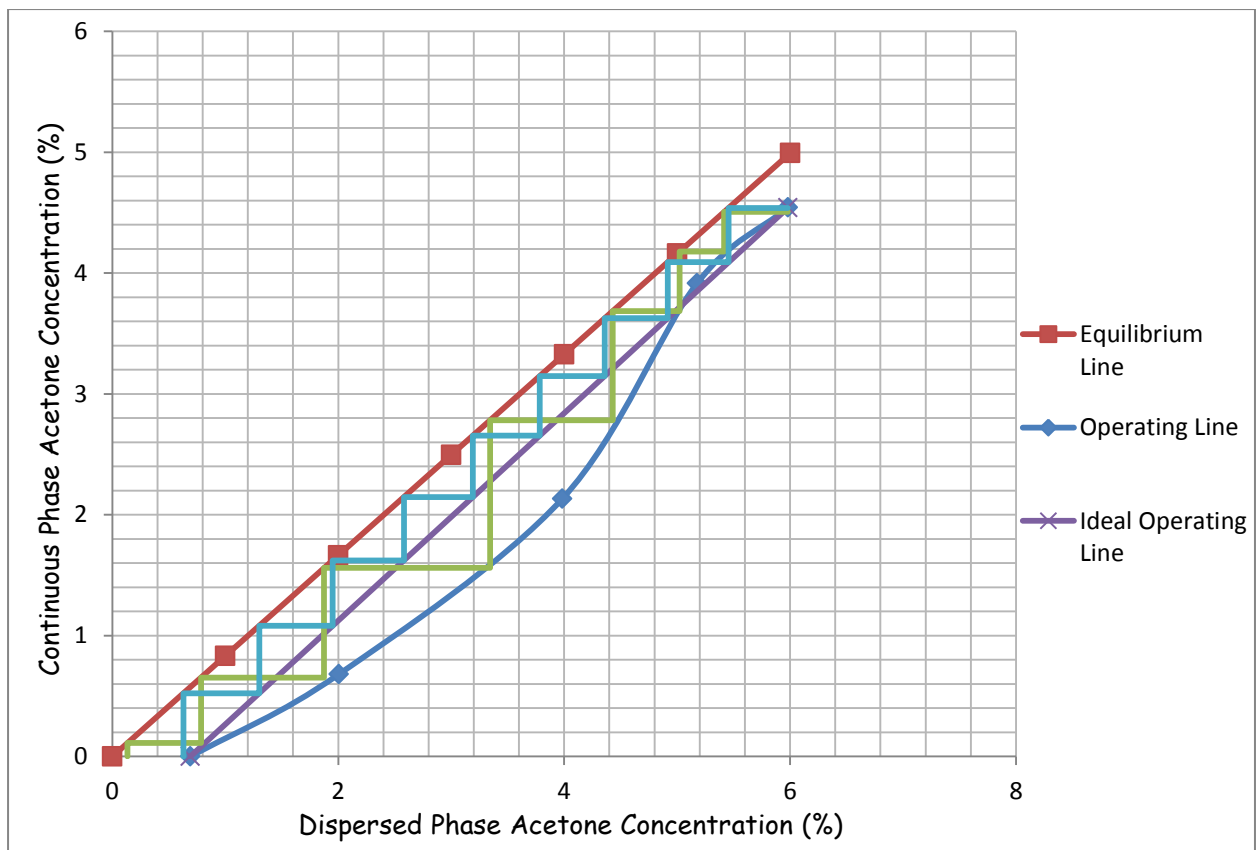


*Figure D 2.2.8: Equilibrium Stages With and Without Backmixing for*
*h = 150 mm, S/F = 2:1 and af = 2.5 mm/s.*

*Figure D 2.2.9: Equilibrium Stages With and Without Backmixing for*
*h = 150 mm, S/F = 2:1 and af = 3.75 mm/s.*
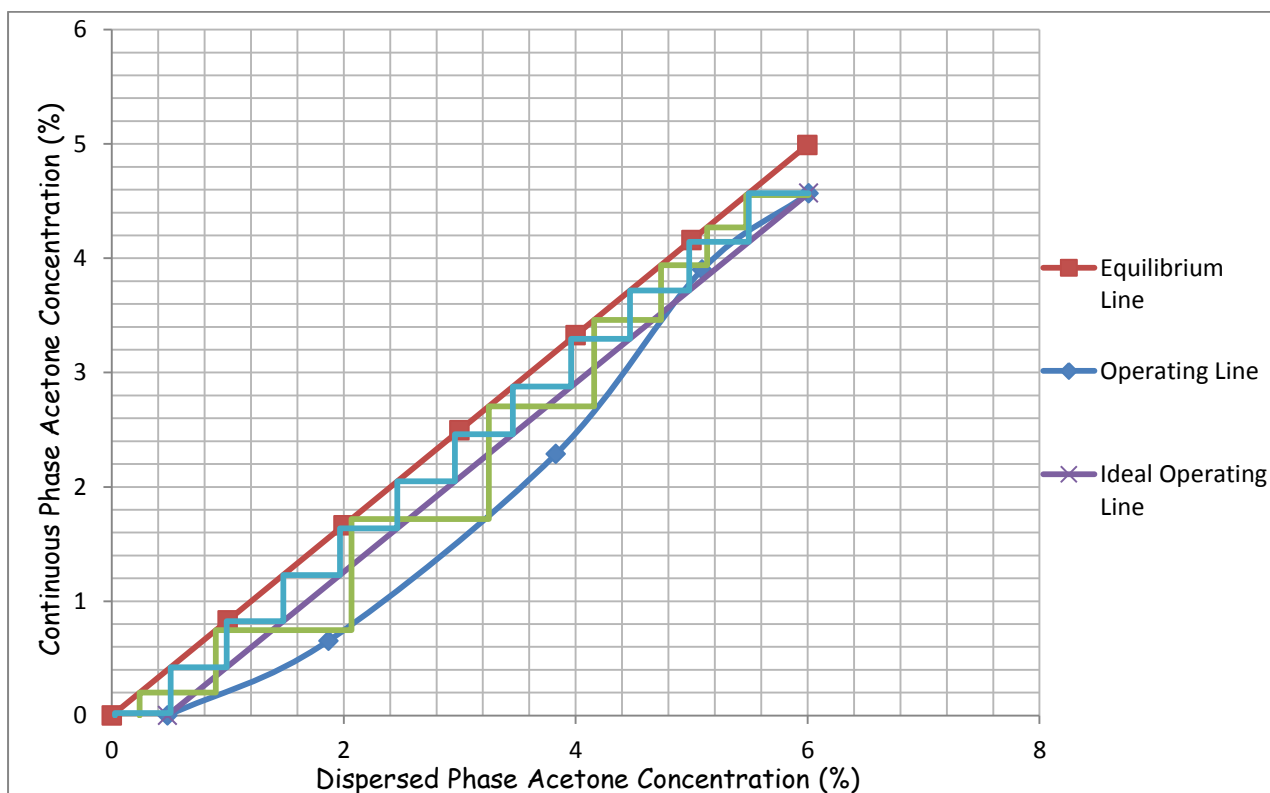


*Figure D 2.2.10: Equilibrium Stages With and Without Backmixing for*
*h = 150 mm, S/F = 2:1 and af = 5 mm/s.*
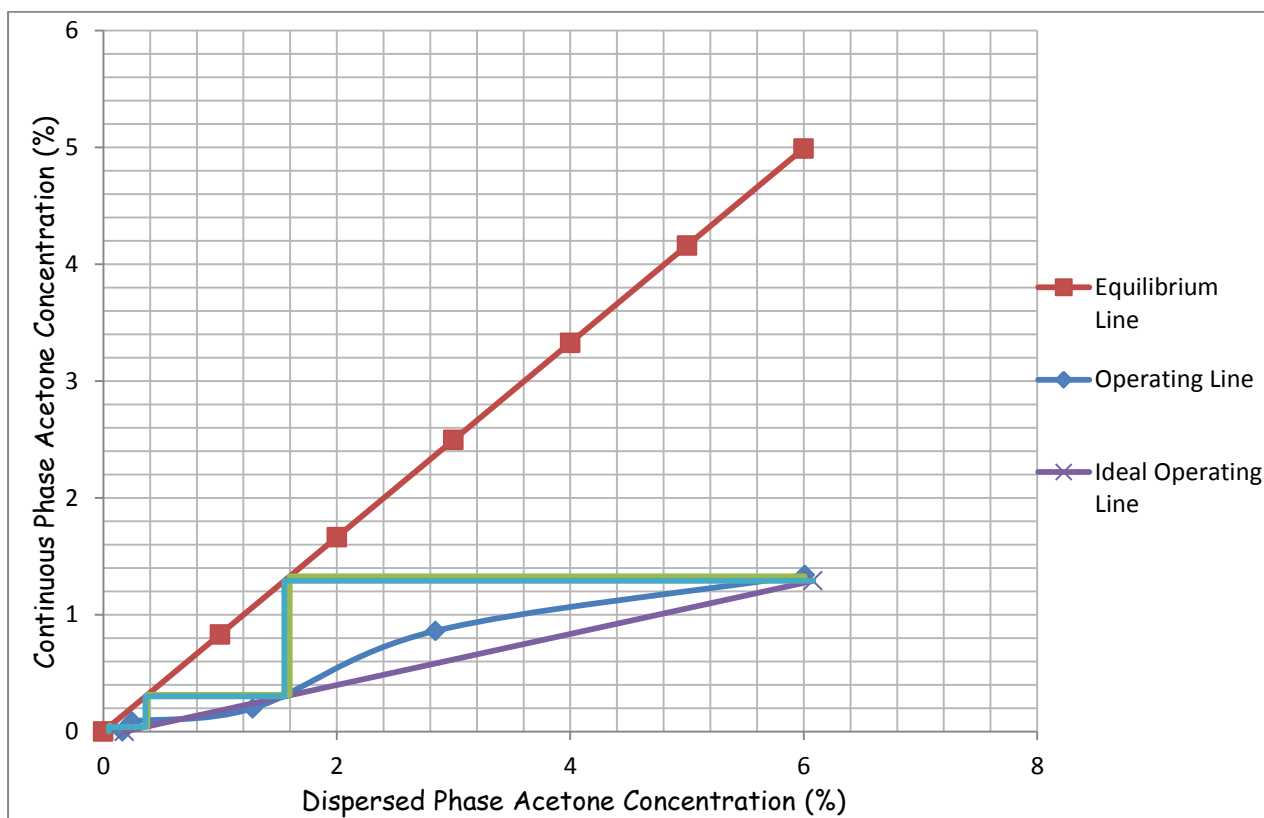
*Figure D 2.2.11: Equilibrium Stages With and Without Backmixing for*
*h = 150 mm, S/F = 2:1 and af = 6.25 mm/s.*



*Figure D 2.2.12: Equilibrium Stages With and Without Backmixing for*
*h = 150 mm, S/F = 2:1 and af = 7.5 mm/s.*

*Figure D 2.2.13: Equilibrium Stages With and Without Backmixing for*
*h = 150 mm, S/F = 1:2 and af = 1.25 mm/s.*



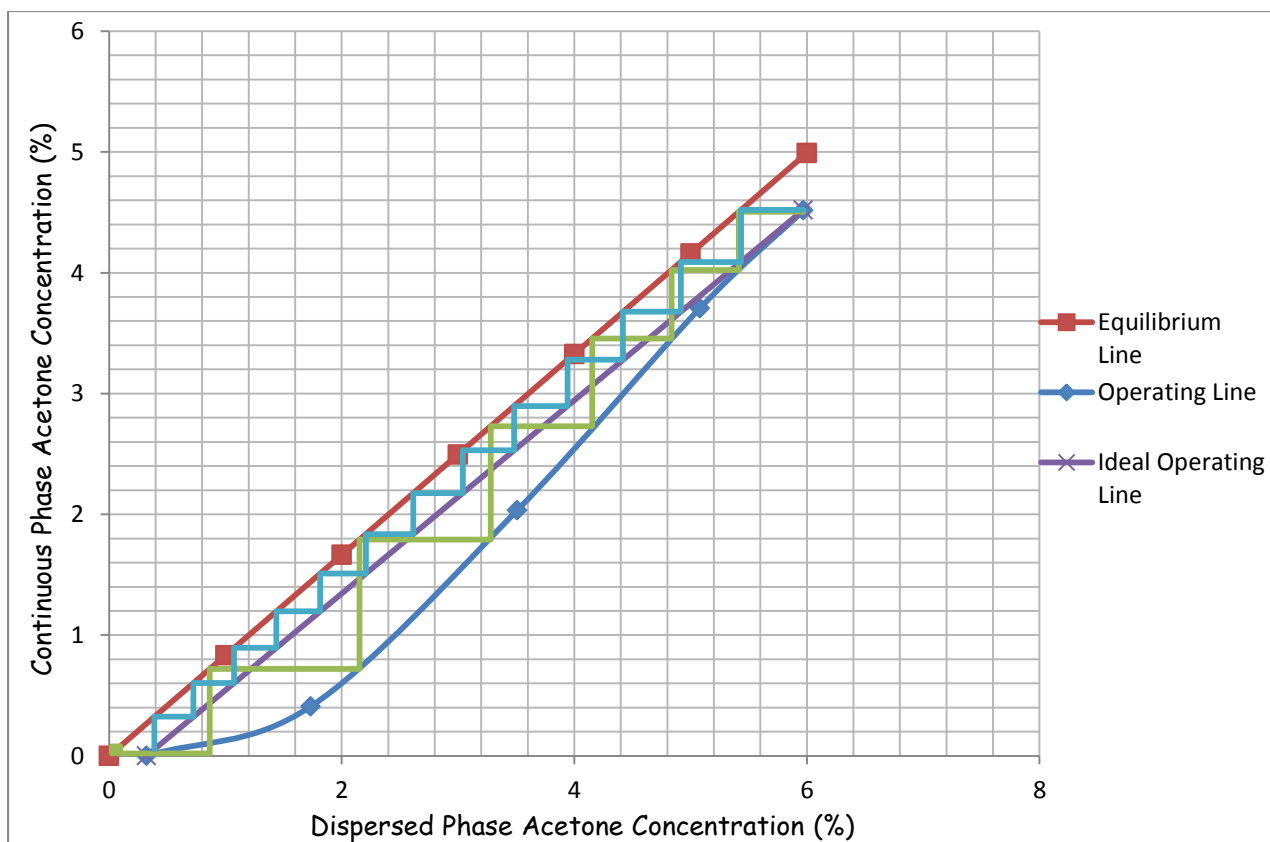*Figure D 2.2.14: Equilibrium Stages With and Without Backmixing for*
*h = 150 mm, S/F = 1:2 and af = 2.5 mm/s.*

*Figure D 2.2.15: Equilibrium Stages With and Without Backmixing for*
*h = 150 mm, S/F = 1:2 and af = 3.75 mm/s.*



*Figure D 2.2.16: Equilibrium Stages With and Without Backmixing for*
*h = 150 mm, S/F = 1:2 and af = 5 mm/s.*
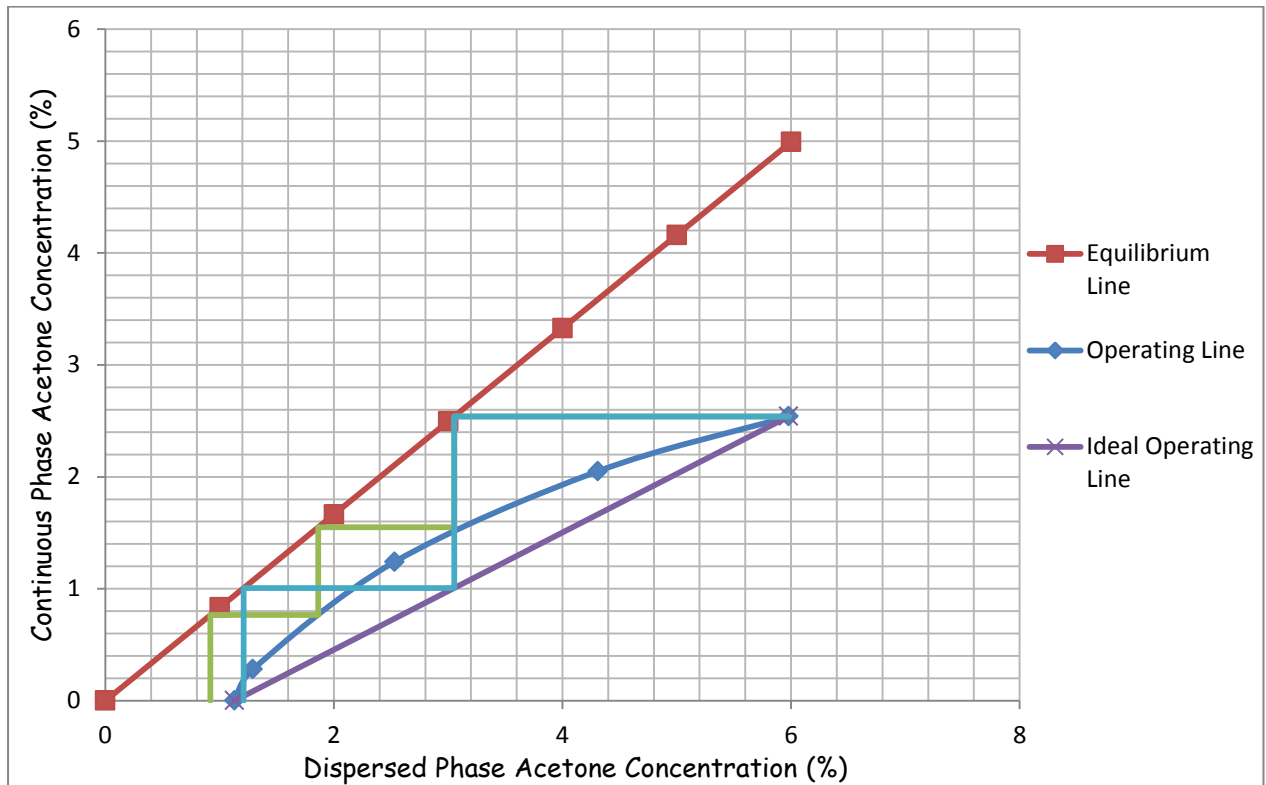
*Figure D 2.2.17: Equilibrium Stages With and Without Backmixing for*
*h = 150 mm, S/F = 1:2 and af = 6.25 mm/s.*
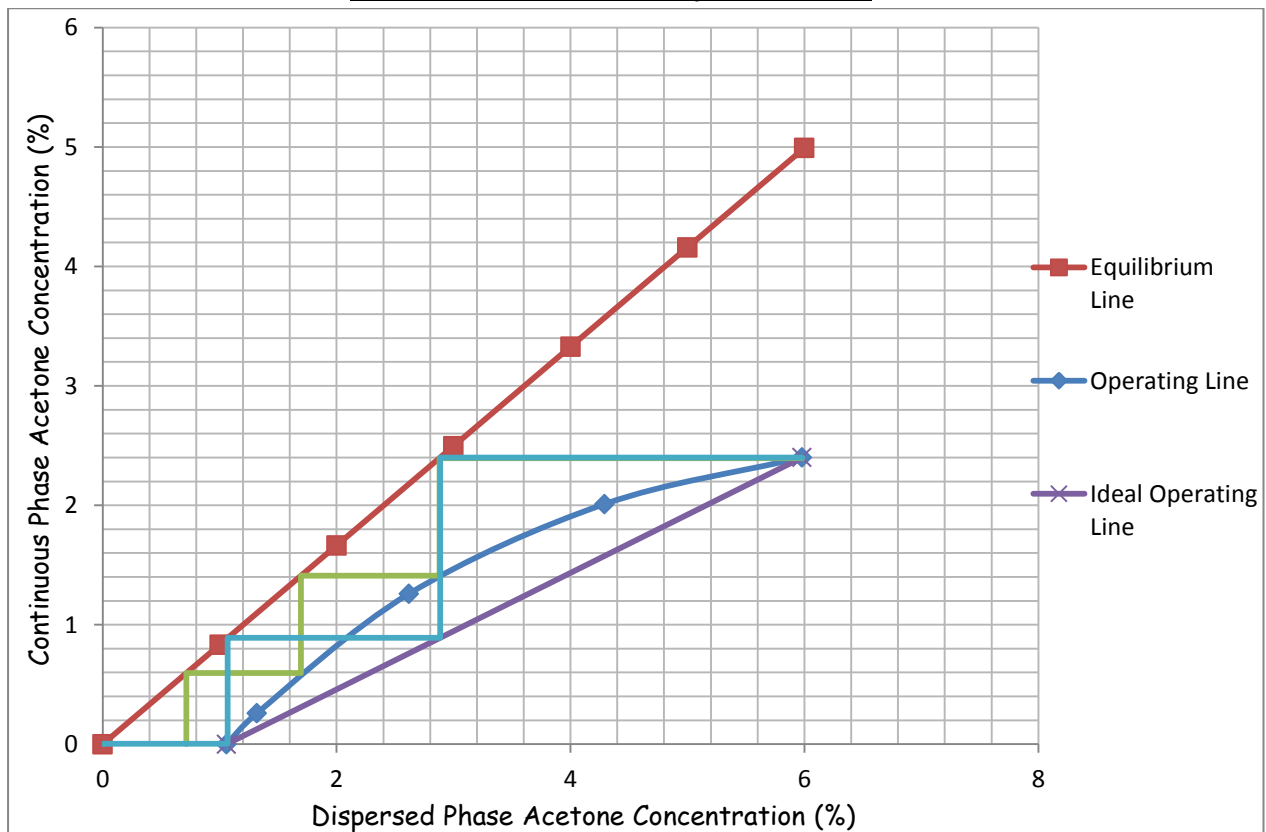


*Figure D 2.2.18: Equilibrium Stages With and Without Backmixing for*
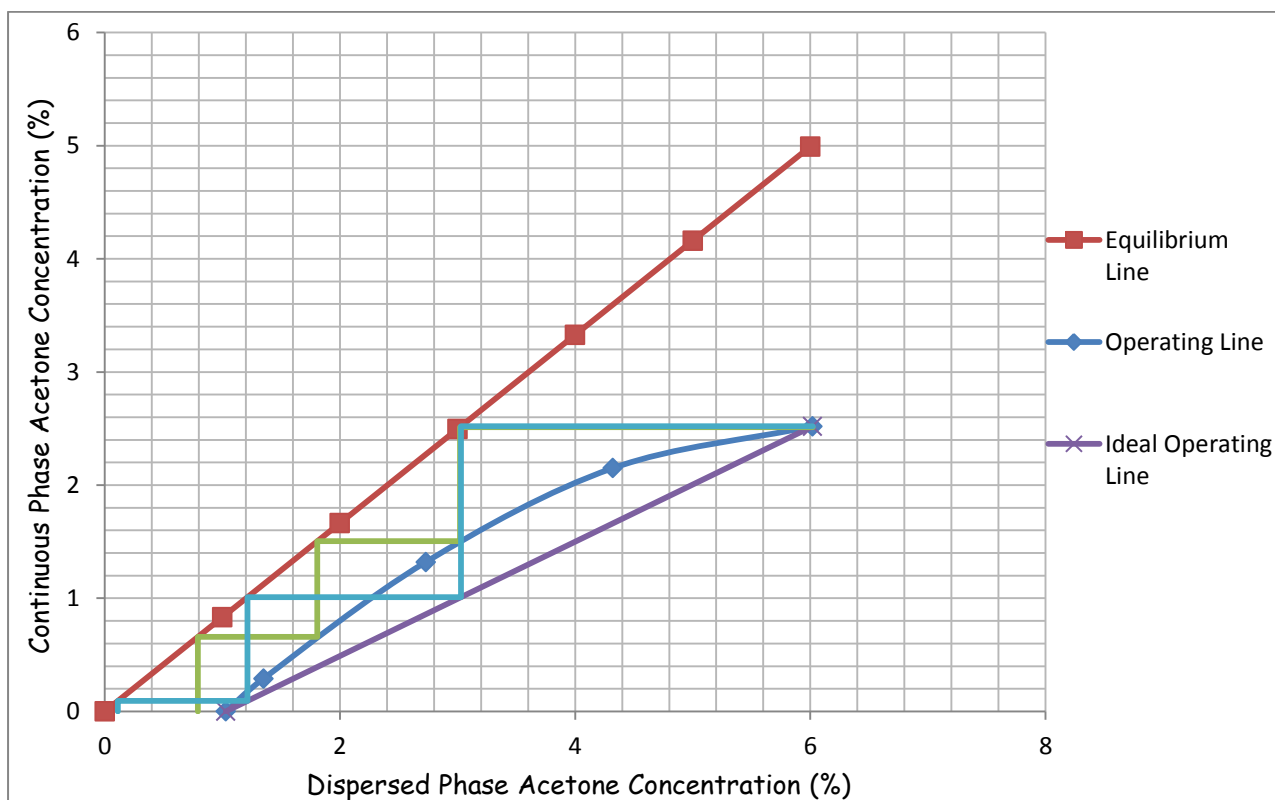*h = 150 mm, S/F = 1:2 and af = 7.5 mm/s.*

**Appendix D 2.3: Stepping-Off Stages for h = 200 mm**



*Figure D 2.3.1: Equilibrium Stages With and Without Backmixing for*
*h = 200 mm, S/F = 1:1 and af = 1.25 mm/s.*



*Figure D 2.3.2: Equilibrium Stages With and Without Backmixing for*
*h = 200 mm, S/F = 1:1 and af = 2.5 mm/s.*

*Figure D 2.3.3: Equilibrium Stages With and Without Backmixing for*
*h = 200 mm, S/F = 1:1 and af = 3.75 mm/s.*
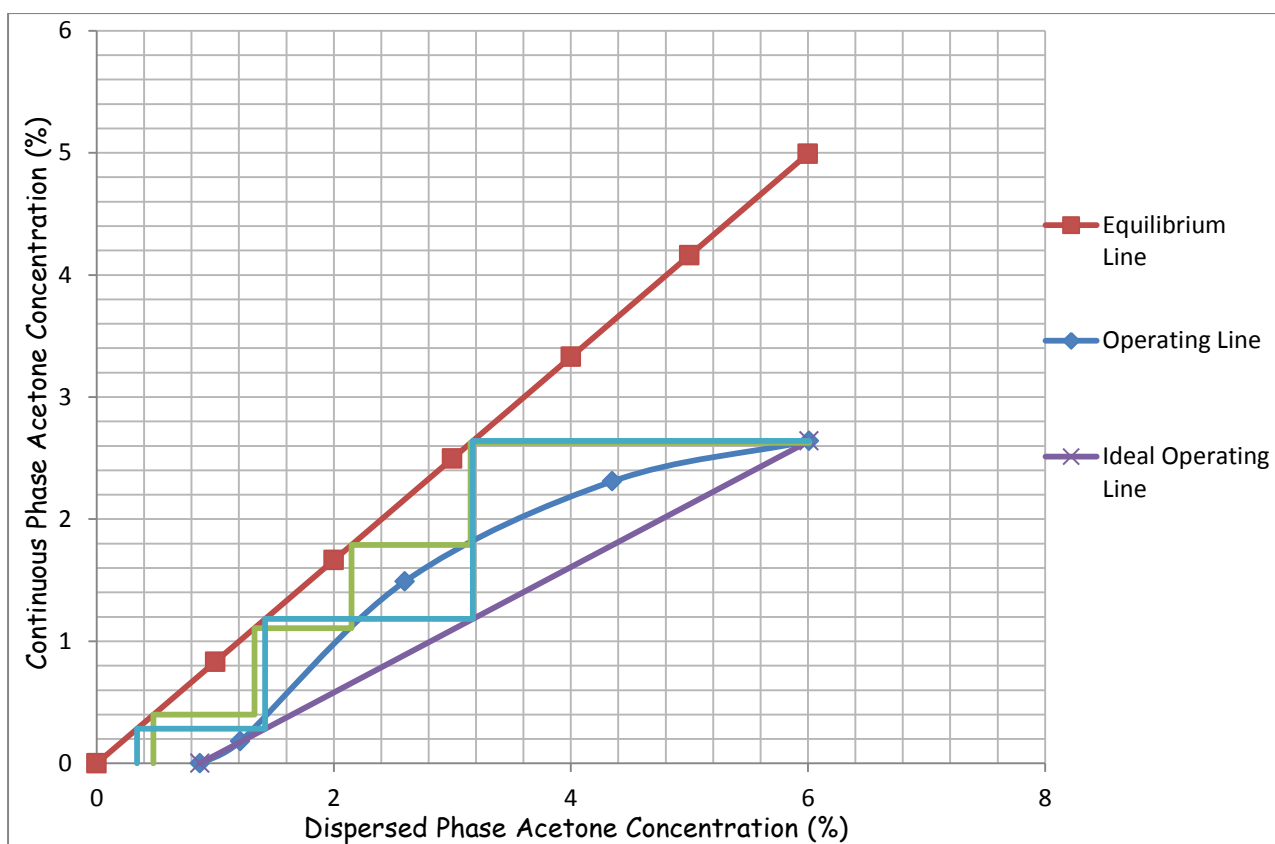


*Figure D 2.3.4: Equilibrium Stages With and Without Backmixing for*
*h = 200 mm, S/F = 1:1 and af = 5 mm/s.*

*Figure D 2.3.5: Equilibrium Stages With and Without Backmixing for*
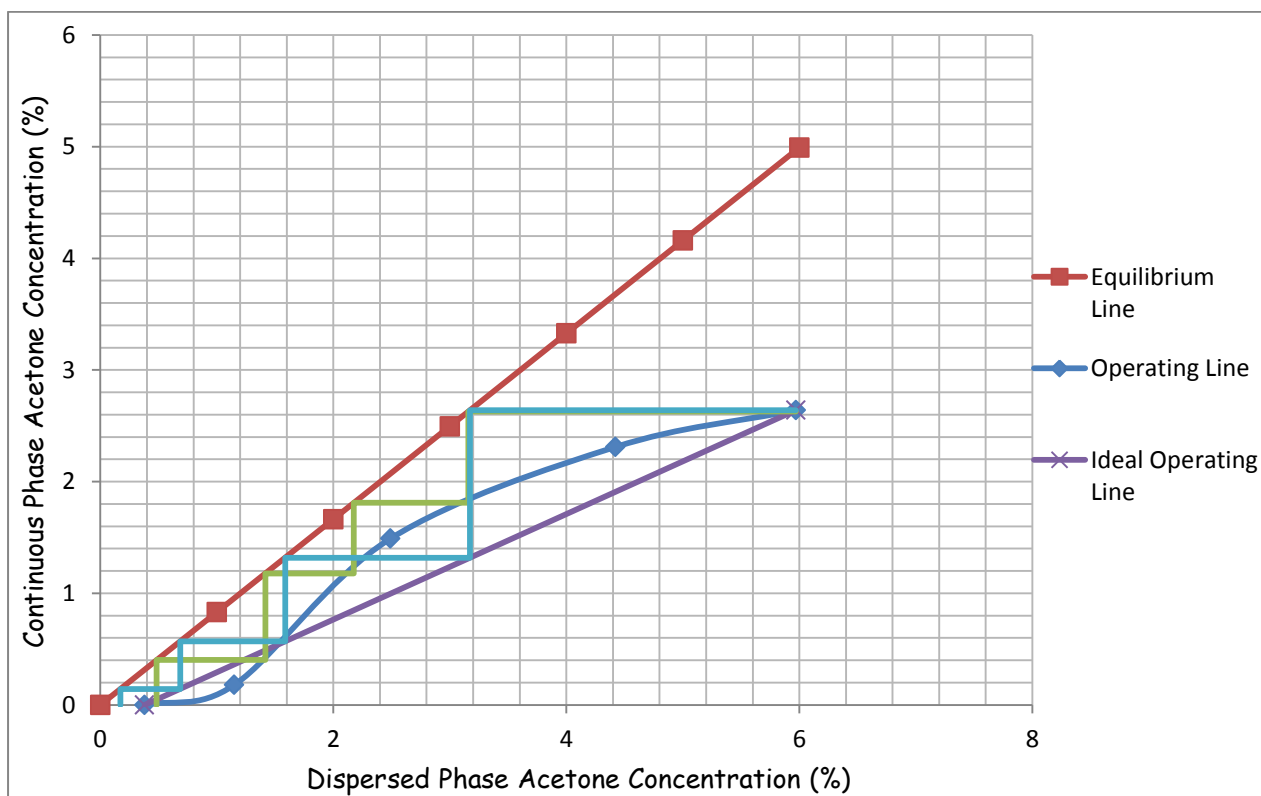*h = 200 mm, S/F = 1:1 and af = 6.25 mm/s.*



*Figure D 2.3.6: Equilibrium Stages With and Without Backmixing for*
*h = 200 mm, S/F = 1:1 and af = 7.5 mm/s.*

*Figure D 2.3.7: Equilibrium Stages With and Without Backmixing for*
*h = 200 mm, S/F = 2:1 and af = 1.25 mm/s.*



*Figure D 2.3.8: Equilibrium Stages With and Without Backmixing for*
*h = 200 mm, S/F = 2:1 and af = 2.5 mm/s.*
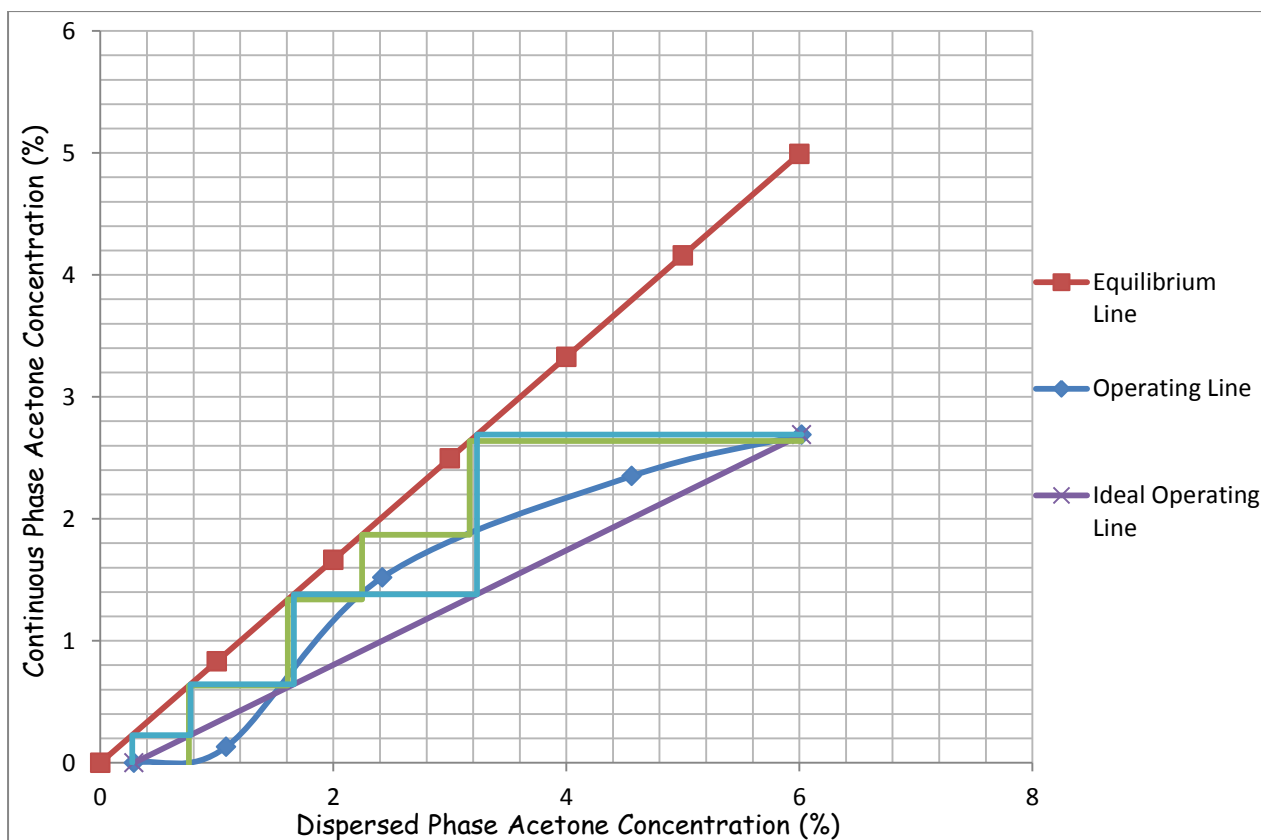
*Figure D 2.3.9: Equilibrium Stages With and Without Backmixing for*
*h = 200 mm, S/F = 2:1 and af = 3.75 mm/s.*
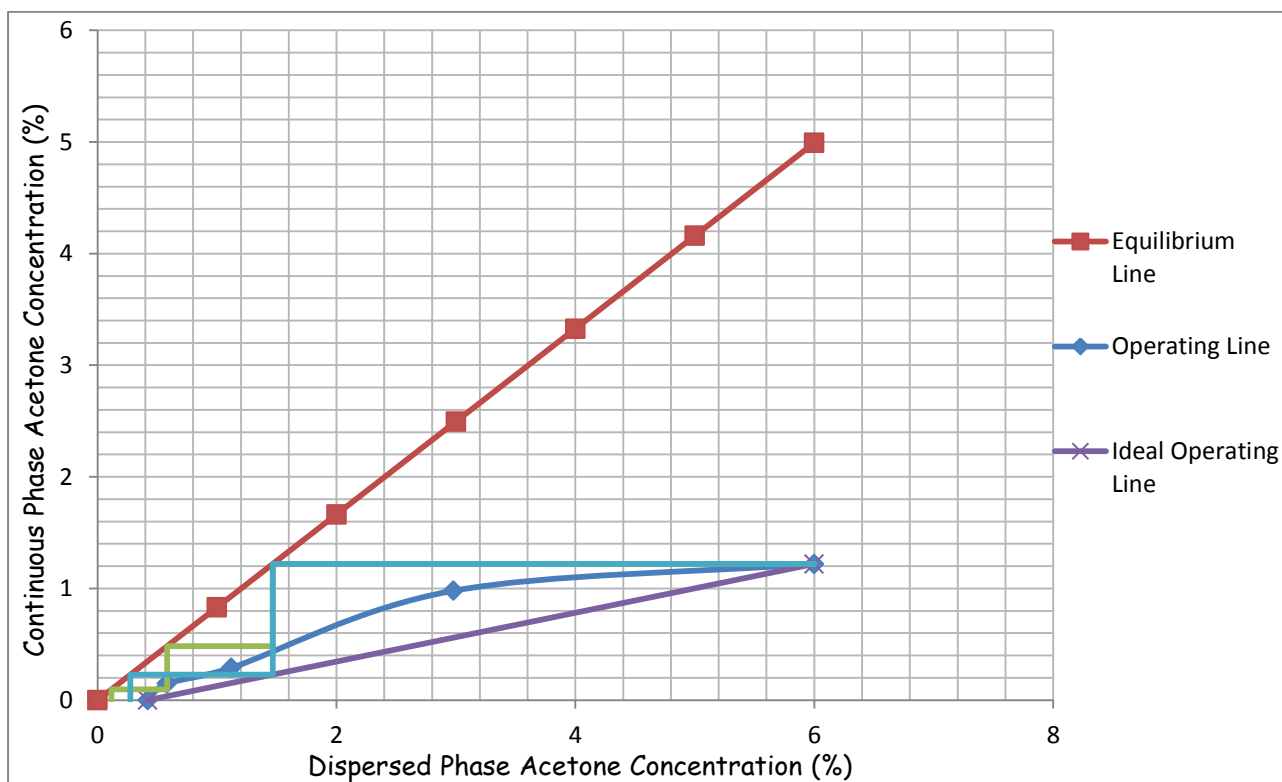


*Figure D 2.3.10: Equilibrium Stages With and Without Backmixing for*
*h = 200 mm, S/F = 2:1 and af = 5 mm/s.*

*Figure D 2.3.11: Equilibrium Stages With and Without Backmixing for*
*h = 200 mm, S/F = 2:1 and af = 6.25 mm/s.*



*Figure D 2.3.12: Equilibrium Stages With and Without Backmixing for*
*h = 200 mm, S/F = 2:1 and af = 7.5 mm/s.*

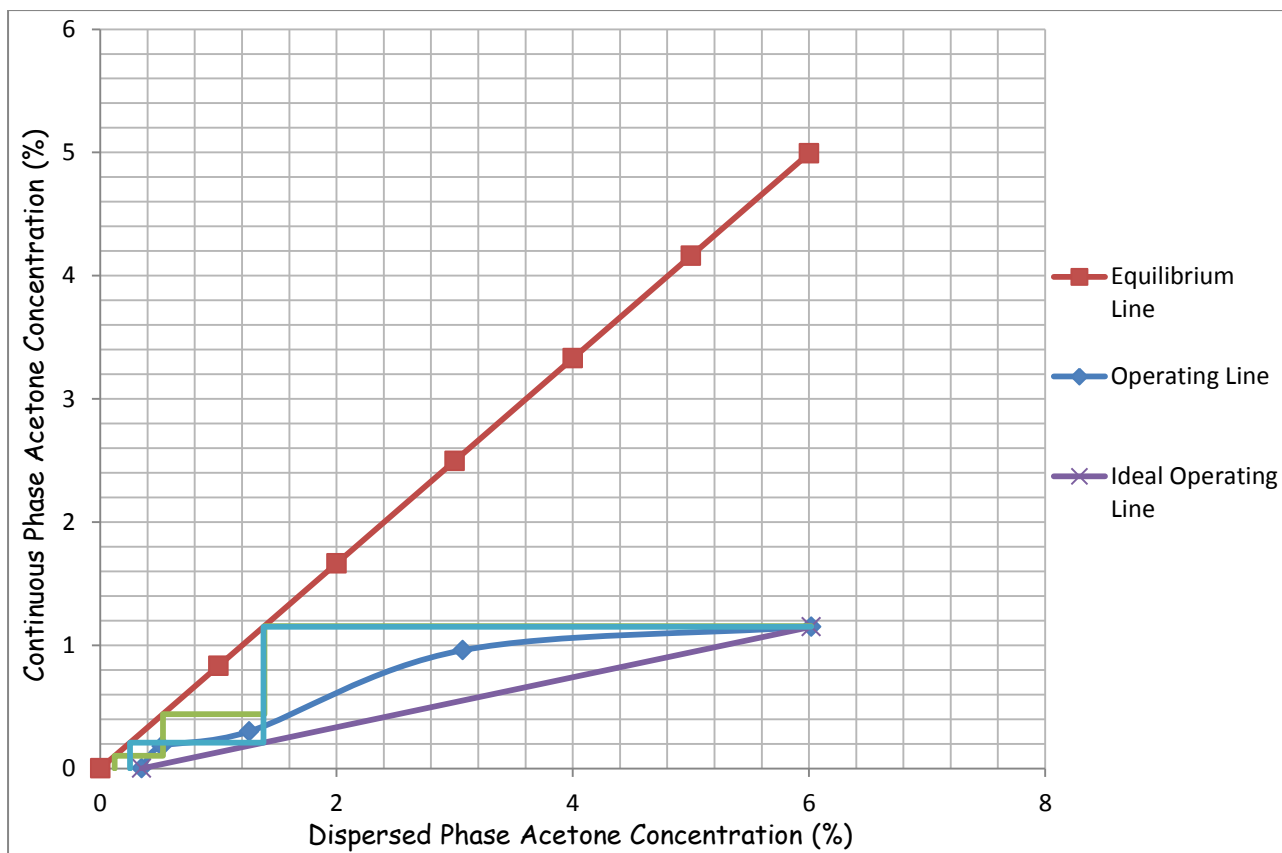***Figure D 2.3.13: Equilibrium Stages With and Without Backmixing for
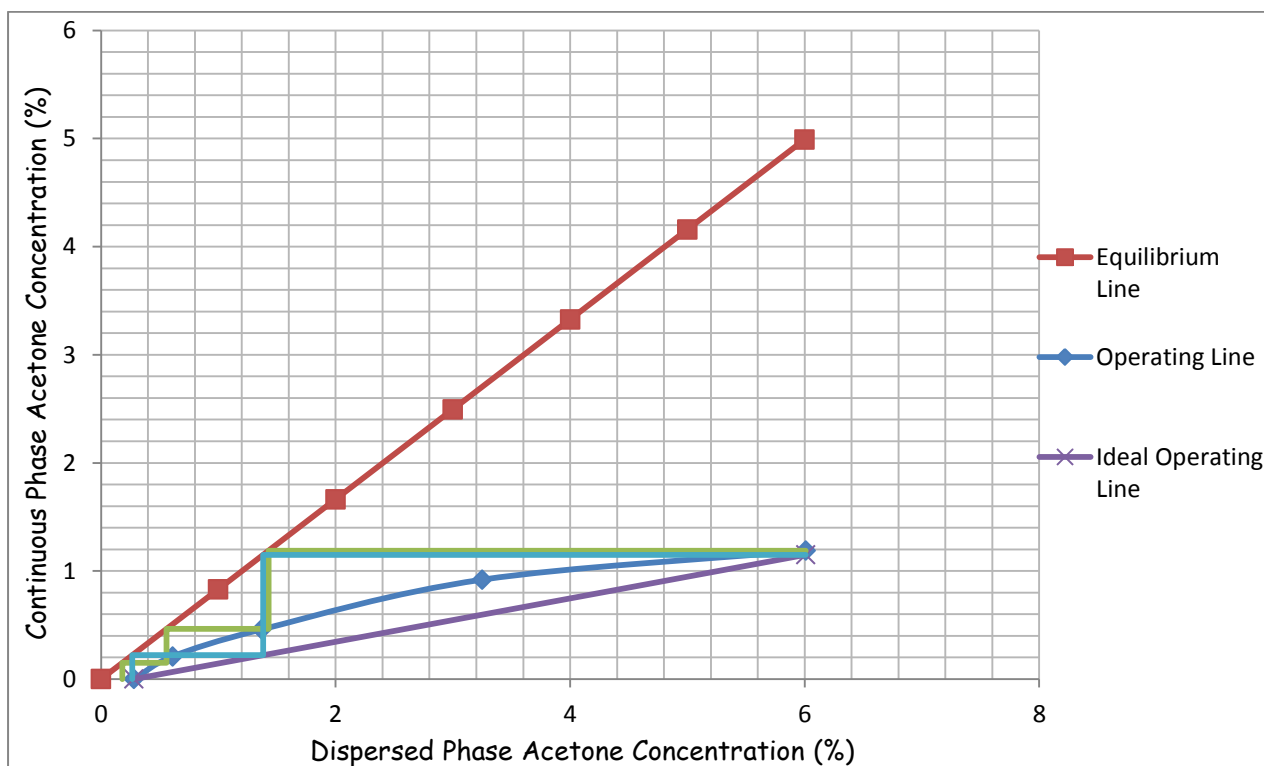h = 200 mm, S/F = 1:2 and af = 1.25 mm/s.***



***Figure D 2.3.14: Equilibrium Stages With and Without Backmixing for
h = 200 mm, S/F = 1:2 and af = 2.5 mm/s.***
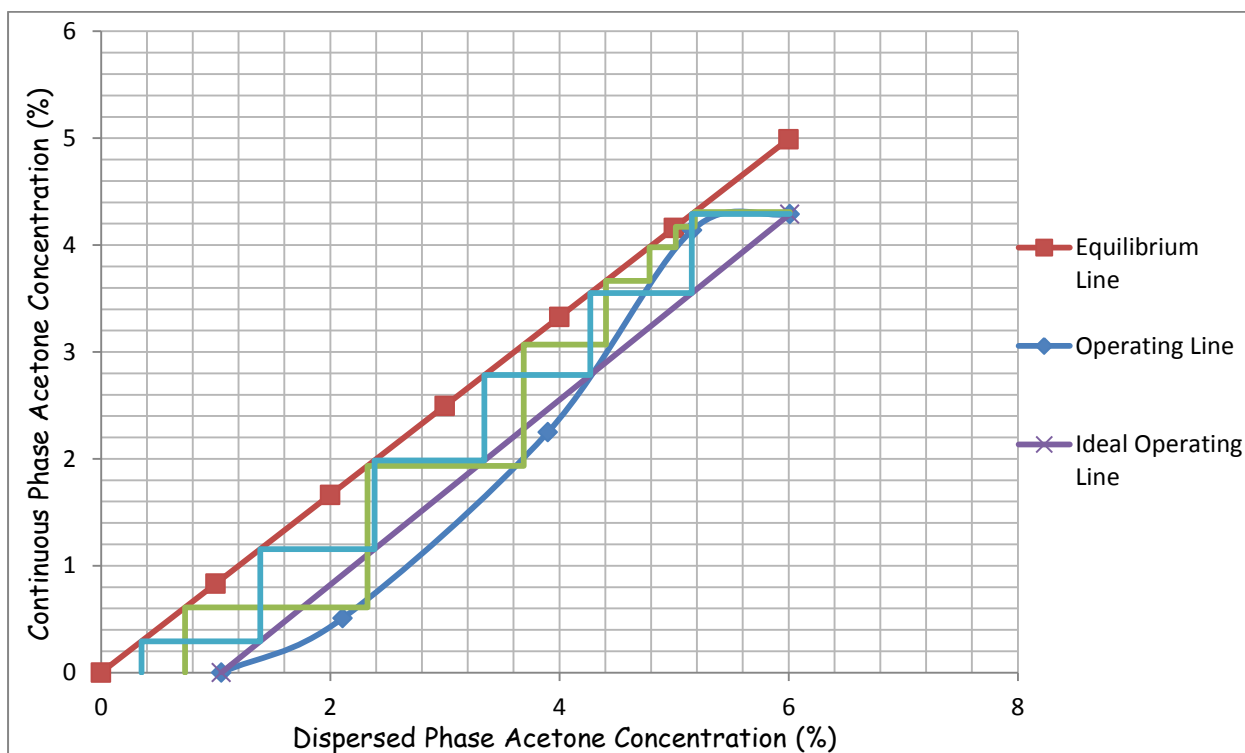
*Figure D 2.3.15: Equilibrium Stages With and Without Backmixing for*
*h = 200 mm, S/F = 1:2 and af = 3.75 mm/s.*
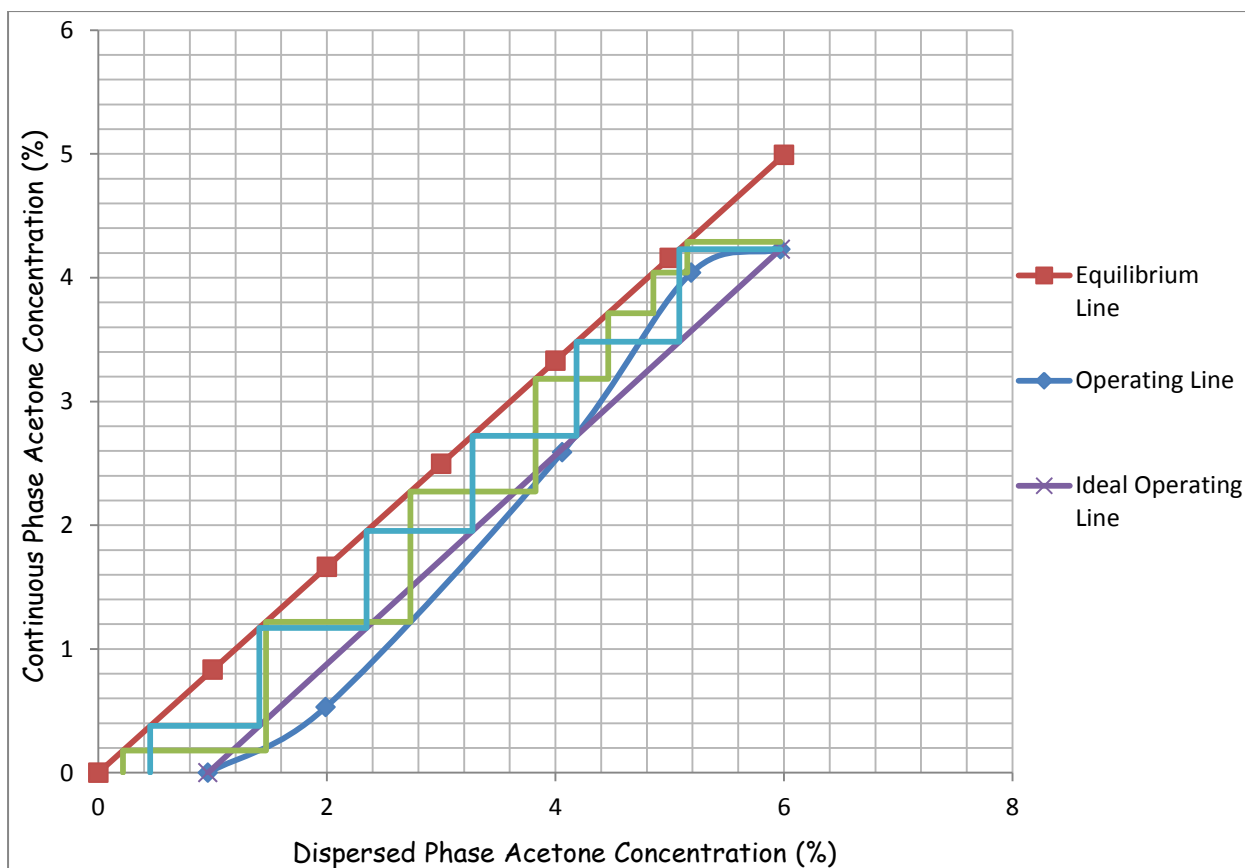


*Figure D 2.3.16: Equilibrium Stages With and Without Backmixing for*
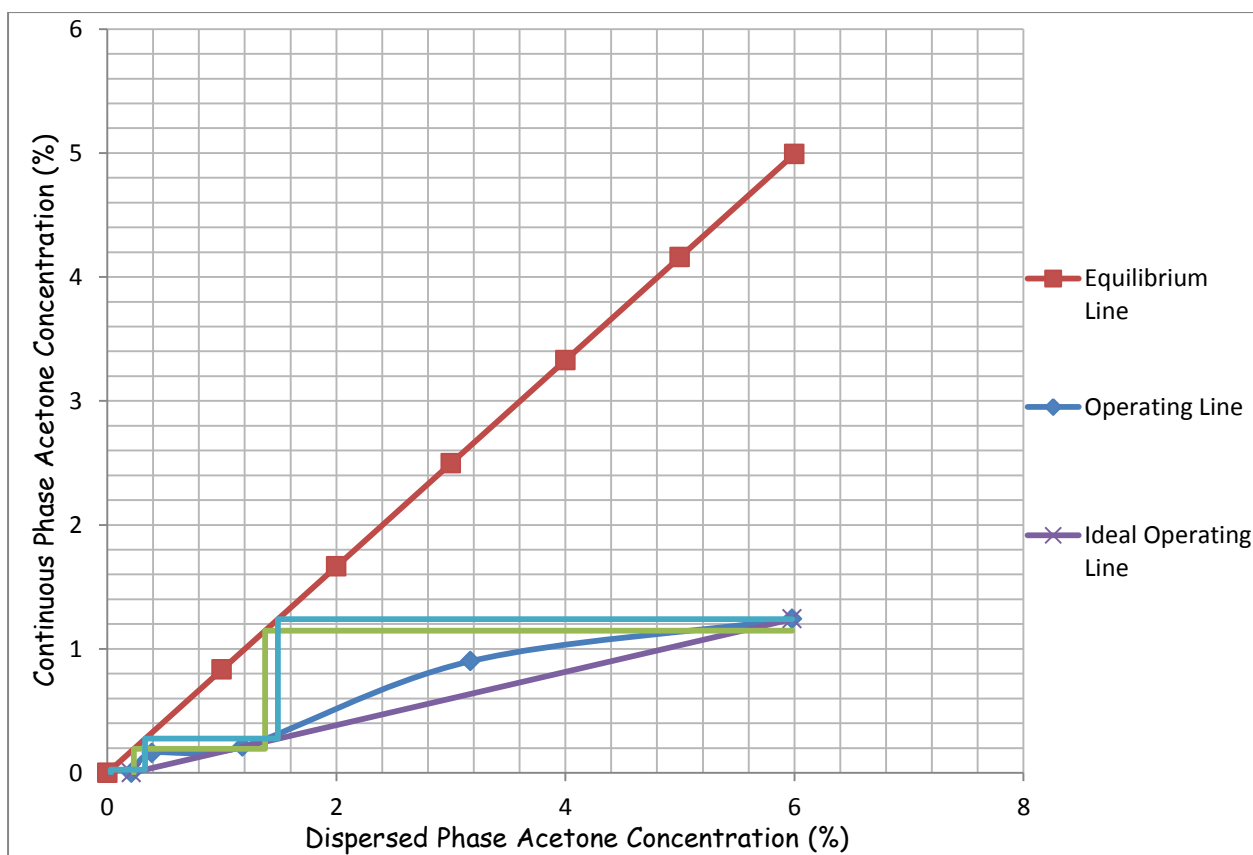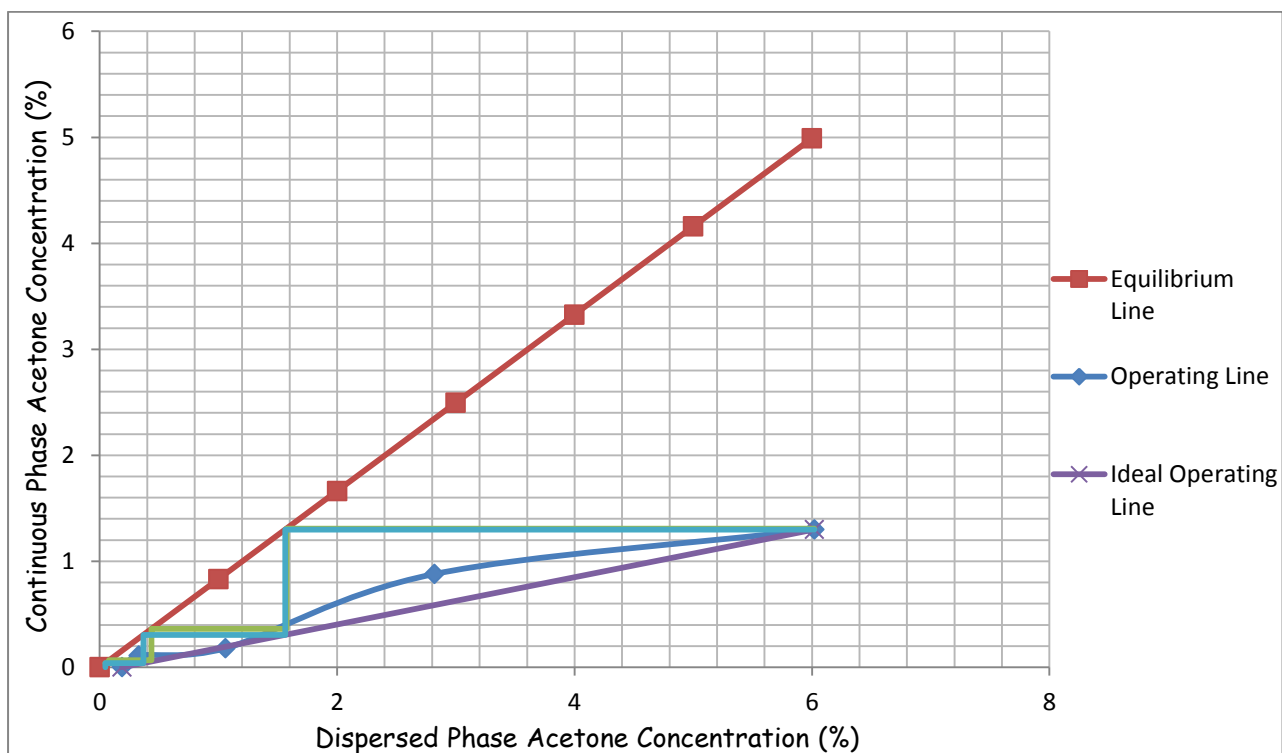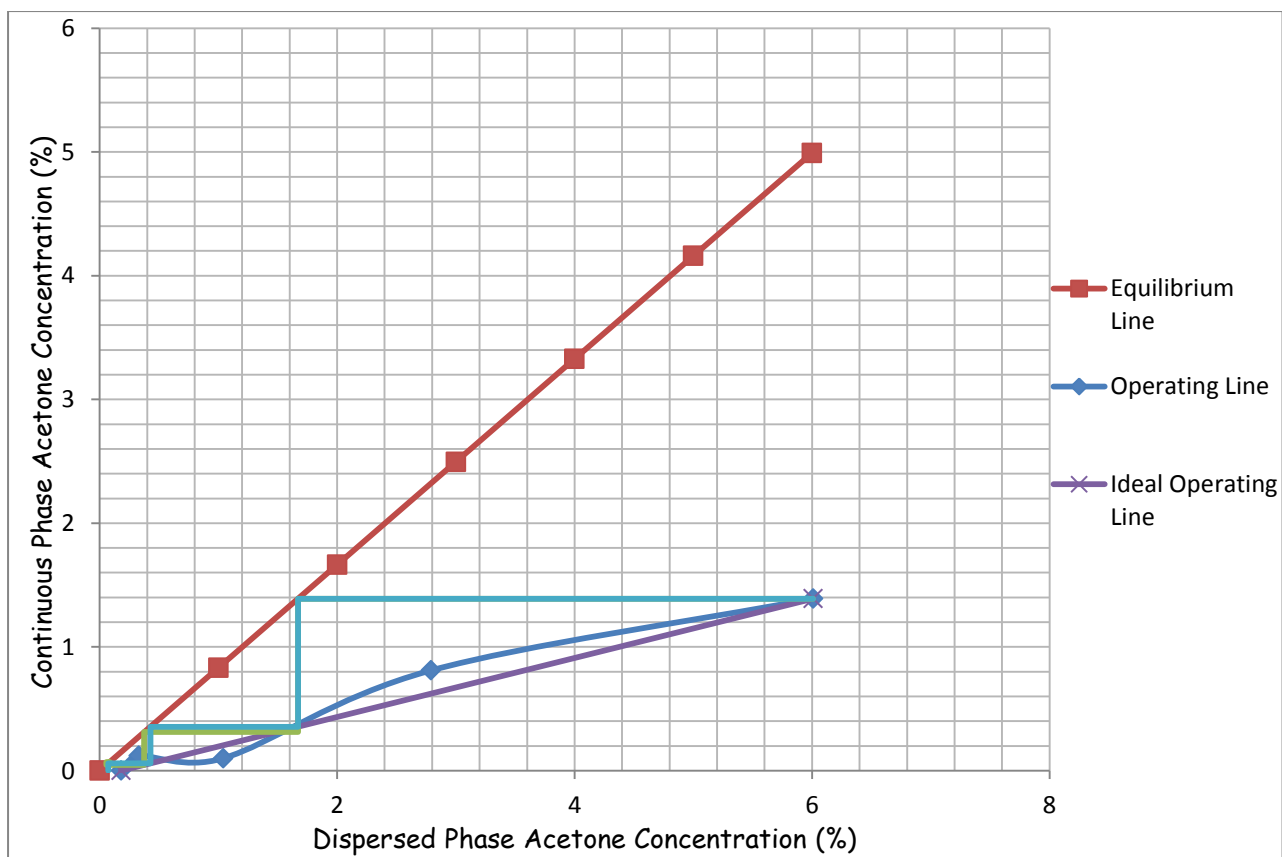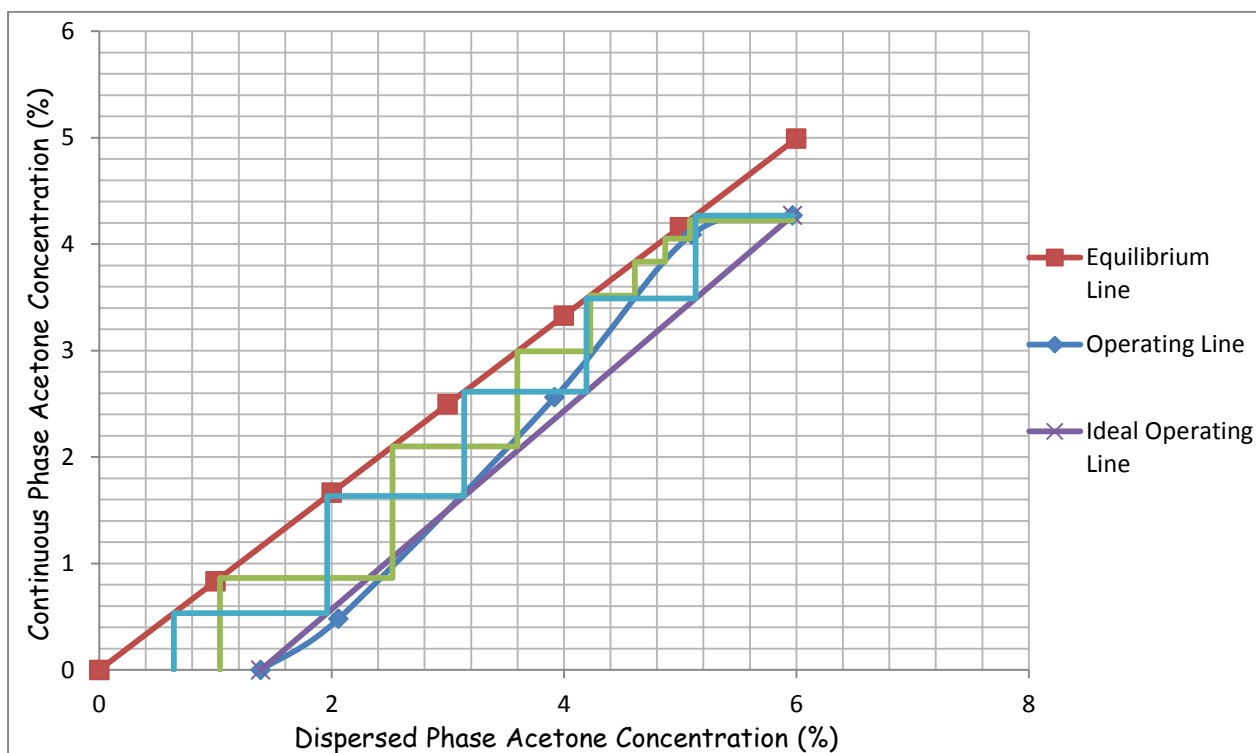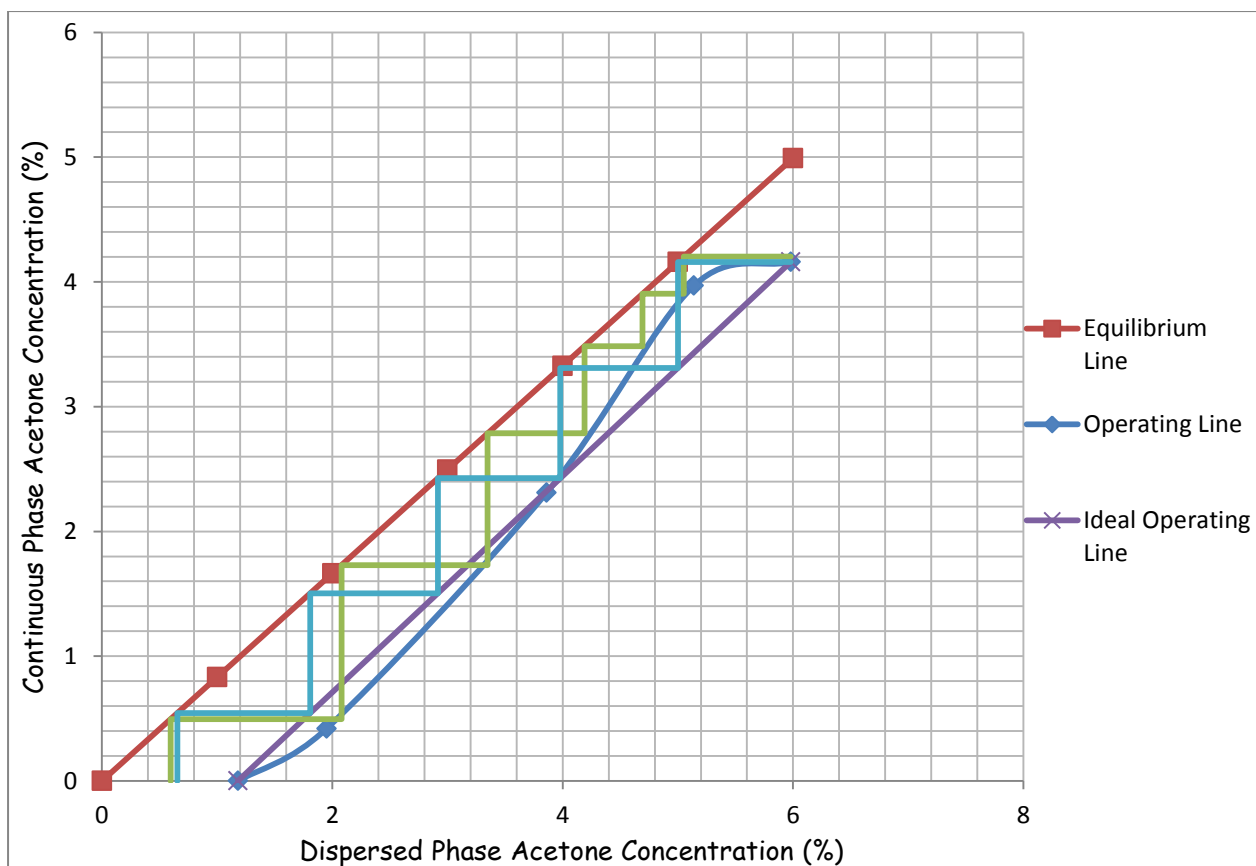*h = 200 mm, S/F = 1:2 and af = 5 mm/s.*
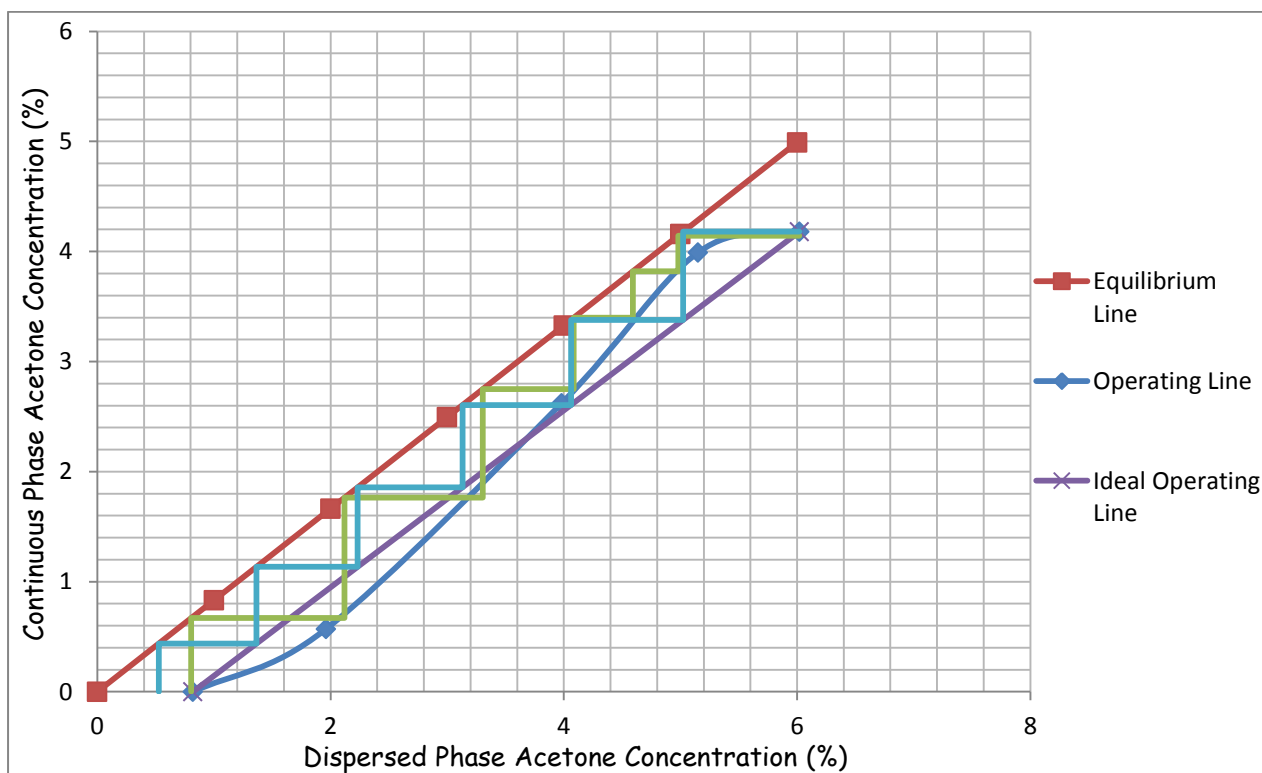
*Figure D 2.3.17: Equilibrium Stages With and Without Backmixing for*
*h = 200 mm, S/F = 1:2 and af = 6.25 mm/s.*
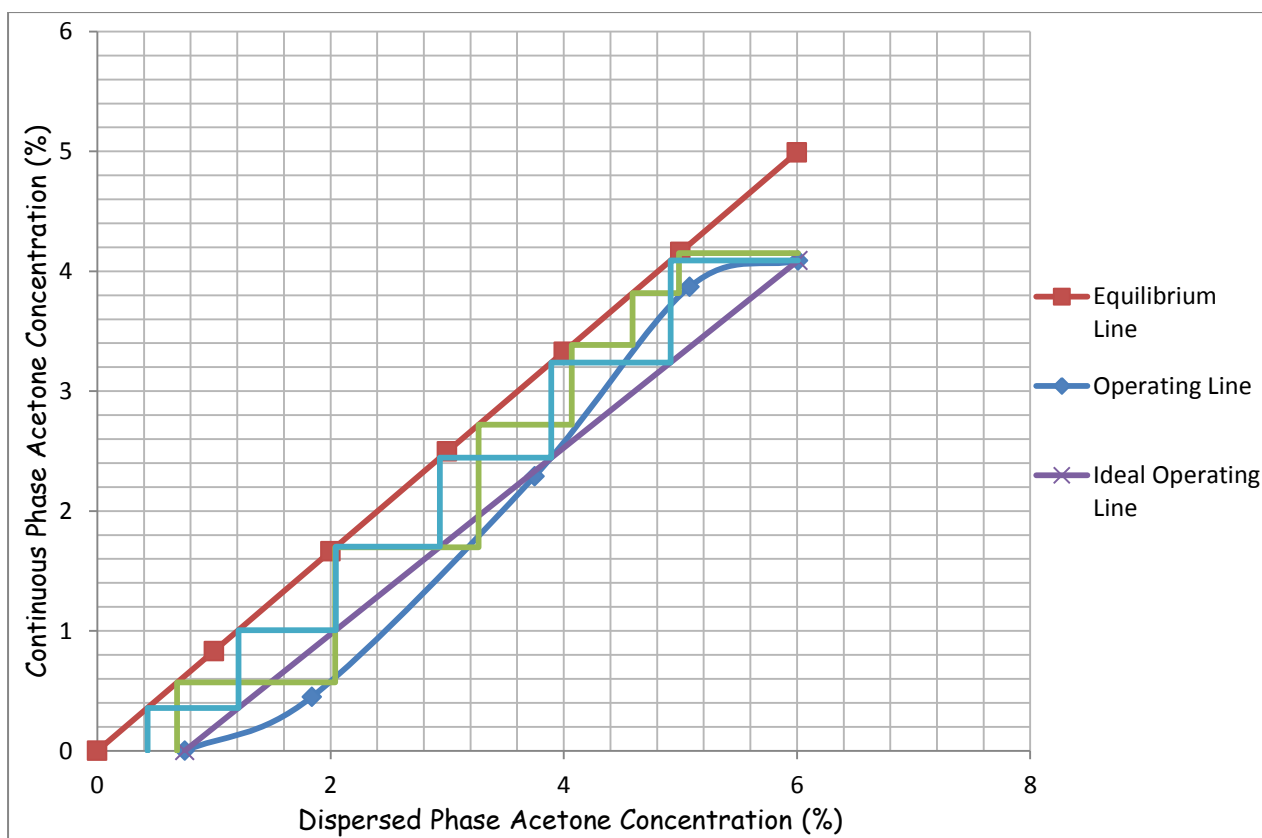


*Figure D 2.3.18: Equilibrium Stages With and Without Backmixing for*
*h = 200 mm, S/F = 1:2 and af = 7.5 mm/s.*

# APPENDIX E: ADDITIONAL INFORMATION

## Appendix E1: Additional Properties of Constituents of the Test System

*Table E 1.1: Fire and Safety Properties of Constituents of the Test System.*

|  | *Acetone* | *Toluene* |
|---|---|---|
| Boiling Point (°C) | 56.5 | 110.4 |
| Melting Point (°C) | -94.6 | -95.0 |
| Flash Point (°C) | -19 | 4 |
| Explosive Limits in Air |  |  |
|    Lower (Vol %) | 2.6 | 1.2 |
|    Upper (Vol %) | 12.8 | 7.0 |
| Ignition Temperature (°C) | 538 | 508 |
| Vapour Density (air = 1) | 2 | 3.14 |
| Vapour Pressure at 20°C (Torr) | 185 | 22 |
| Threshold Limit Value (ppm in air) | 1000 | 200 |
| Threshold Limit Value (mg/m$^3$ of air) | 2400 | 750 |
| Evaporating Rate (ether = 1) | 2.1 | 6.1 |
| Odour Threshold (ppm) | 200 - 450 | 50 |

# APPENDIX F: MATERIAL SAFETY DATA SHEETS

**Appendix F1: Acetone Material Safety Data Sheet** (*Collectioncare.org, 2011*)

| Product Name | Acetone |  |
|---|---|---|
| Molecular formula | $C_3H_6O$ | |

| PHYSICAL AND CHEMICAL PROPERTIES | | | |
|---|---|---|---|
| Physical state | Liquid | Boiling Point | 56.2°C (133.2°F) |
| Colour | Colorless, Clear | Melting Point | -95.35°C (-139.6°F) |
| Odour | Fruity, Mint-like, Fragrant, Ethereal | Critical Temperature | 235°C (455°F) |
| Taste | Pungent, Sweetish | Specific Gravity | 0.79 (Water = 1) |
| Solubility in others | Easily soluble in cold water and hot water | Vapour density | 2 (Air = 1) |
| Molecular weight | 58.08 g/mole | Vapour pressure | 24 kPa @ 20 °C |

| FIRE AND EXPLOSION DATA | |
|---|---|
| Flammability of the product | Flammable |
| Auto-ignition temperature | 465°C (869°F) |
| Flash Points | CLOSED CUP: -20°C (-4°F) OPEN CUP: -9°C (15.8 °F) |
| Flammable Limits | LOWER: 2.6% UPPER: 12.8% |
| Products of Combustion | These products are carbon oxides (CO, $CO_2$) |
| Fire Hazards in Presence of Various Substances | Highly flammable in the presence of open flames and sparks, of heat. |
| Explosive Hazards in Presence of Various Substances | Slightly explosive in the presence of open flames and sparks, of oxidizing, of acids. |
| Fire Fighting Media and Instructions | Flammable liquid, soluble or dispersed in water. SMALL FIRE: Use DRY chemical powder. LARGE FIRE: Use alcohol foam, water spray or fog. |
| Special Remarks on Fire Hazards | Vapor may travel considerable distance to source of ignition and flash back. |

| Special Remarks on Explosion Hazards | Forms explosive mixtures with hydrogen peroxide, acetic acid, nitric acid, nitric acid + sulphuric acid, chromic anhydride, chromyl chloride, nitrosyl chloride, hexachloromelamine, nitrosyl perchlorate, nitryl perchlorate, permonosulfuric acid, thiodiglycol + hydrogen peroxide, potassium ter-butoxide, sulphur dichloride, 1-methyl-1,3 –butadiene, bromoform, carbon, air, chloroform and thitriazylperchlorate. |
|---|---|

## TOXICOLOGICAL DATA ON INGREDIENTS

Acetone: ORAL (LD50): Acute: 5800 mg/kg [Rat]. 3000 mg/kg [Mouse]. 5340 mg/kg [Rabbit]

VAPOR (LC50):  Acute: 50100 mg/m 8 hours [Rat]. 44000 mg/m 4 hours [Mouse]

## HAZARDOUS IDENTIFICATION

POTENTIAL ACUTE HEALTH EFFECTS:
Hazardous in the case of skin contact (irritant), eye contact (irritant), ingestion or inhalation.

POTENTIAL CHRONIC  HEALTH EFFECTS:
DEVELOPMENTAL TOXICITY: The substance is toxic to the central nervous system (CNS). The substance maybe toxic to kidneys, the reproductive system, liver and skin. Repeated or prolonged exposure to the substance can result in organ damage.

## FIRST-AID MEASURES

| Eye Contact | Check for and remove any contact lenses. Immediately flush eyes with running water for at least 15 minutes, keeping eyelids open. Cold water may be used. Get medical attention. |
|---|---|
| Skin Contact | Immediately flush skin with plenty of water. Cover the irritated skin with an emollient. Remove contaminated clothing and shoes. Get medical attention. |
| Serious Skin Contact | Wash with a disinfectant soap and cover the contaminated skin with an anti-bacterial cream. Seek medical attention. |
| Inhalation | If inhaled, remove to fresh air. If not breathing, give artificial respiration. If breathing is difficult, give oxygen. Get medical attention if symptoms appear. |
| Serious Inhalation | Evacuate the victim to a safe area as soon as possible. Loosen tight clothing such as collar, tie, belt or waistband. If breathing is difficult, administer oxygen. If the victim is not breathing, perform mouth-to-mouth resuscitation. Seek medical attention. |
| Ingestion | If swallowed, do not induce vomiting unless directed to do so by medical personnel. Never give anything by mouth to an unconscious person. Loosen tight clothing such as a collar, tie, belt or waistband. Get medical attention immediately. |

## ACCIDENTAL RELEASE MEASURES

SMALL SPILL:
Dilute with water and mop up, or absorb with an inert dry material and place in an appropriate waste disposal container.

LARGE SPILL:
Flammable liquid. Keep away from heat. Keep away from sources of ignition. Stop leak if without risk. Absorb with DRY earth, sand or non-combustible material. Do not touch spilled material. Prevent entry into sewers, basements or confined areas; dike if needed. Be careful that the product is not present at a concentration level above TLV.

## HANDLING AND STORAGE

PRECAUTIONS:
Keep locked up. Keep away from heat. Keep away from sources of ignition. Ground all equipment containing material. Do not ingest. Do not breathe gas/fumes/vapour/spray. Wear suitable protective clothing. In case of insufficient ventilation, wear suitable respiratory equipment. If ingested, seek medical advice immediately and show the container or the label. Avoid contact with skin and eyes. Keep away from incompatibles such as oxidizing agents, reducing agents, acids and alkalis.

STORAGE:
Store in a segregated and approved area (flammables area). Keep container in a cool, well-ventilated area. Keep container tightly closed and sealed until ready for use. Keep away from direct sunlight and heat and avoid all possible sources of ignition (spark or flame).

## EXPOSURE CONTROLS/PERSONAL PROTECTION

ENGINEERING CONTROLS:
Provide exhaust ventilation or other engineering controls to keep the airborne concentrations of vapors below their respective threshold limit value. Ensure that eyewash stations and safety showers are proximal to the work-station location.

PERSONAL PROTECTION:
Splash goggles, lab coat and vapor respirator. Be sure to use an approved/certified respirator or equivalent. Gloves.

PERSONAL PROTECTION IN CASE OF A LARGE SPILL:
Splash goggles, full suit, vapour respirator, boots and gloves. A self-contained breathing apparatus should be used to avoid inhalation of the product. Suggested protective clothing might not be sufficient; consult a specialist BEFORE handling this product.

EXPOSURE LIMITS:
TWA: 500STEL: 750 (ppm) from ACGIH (TLV) [United States], TWA: 750 STEL: 1000 (ppm) from OSHA [United States], TWA: 500 STEL: 1000 [Australia], TWA: 1185 STEL: 2375 (mg/m$^3$) [ Australia], TWA:750 STEL: 1500 (ppm) [United Kingdom, (UK)], TWA: 1810 STEL: 3620 (mg/m$^3$) [United Kingdom, (UK)], TWA: 1800 STEL:2400 from OSHA (PEL) [United States]. Consult local authorities for acceptable exposure limits.

## STABILITY AND REACTIVITY DATA

STABILITY: The product is stable.
CONDITIONS OF INSTABILITY: Excess heat, ignition sources, exposure to moisture, air, or water, incompatible materials.
INCOMPATIBILITY WITH VARIOUS SUBSTANCES: Reactive with oxidizing agents, reducing agents, acids, alkalis.
CORROSIVITY: Non-corrosive in presence of glass.

## TOXICOLOGICAL INFORMATION

ROUTES OF ENTRY: Absorbed through skin. Dermal contact. Eye contact. Inhalation.

**TOXICITY TO ANIMALS:**
WARNING: THE LC50 VALUES HEREUNDER ARE ESTIMATED ON THE BASIS OF A 4-HOUR EXPOSURE. Acute oral toxicity (LD50): 3000 mg/kg [Mouse]. Acute toxicity of the vapor (LC50): 44000 mg/m3 4 hours [Mouse].

**CHRONIC EFFECTS ON HUMANS:**
CARCINOGENIC EFFECTS: A4 (Not classifiable for human or animal.) by ACGIH. DEVELOPMENTAL TOXICITY: Classified
Reproductive system/toxin/female, Reproductive system/toxin/male [SUSPECTED]. Causes damage to the following organs: central nervous system (CNS). May cause damage to the following organs: kidneys, the reproductive system, liver, skin.

**OTHER TOXIC EFFECTS ON HUMANS:**
Hazardous in case of skin contact (irritant), of ingestion, of inhalation. Slightly hazardous in case of skin contact (permeator).

**SPECIAL REMARKS ON CHRONIC EFFECTS ON HUMANS:**
May affect genetic material (mutagenicity) based on studies with yeast (S. cerevisiae), bacteria, and hamster fibroblast cells.
May cause reproductive effects (fertility) based upon animal studies. May contain trace amounts of benzene and formaldehyde which may cancer and birth defects. Human: passes the placental barrier.

**SPECIAL REMARKS ON OTHER TOXIC EFFECTS ON HUMANS:**
Acute Potential Health Effects: Skin: May cause skin irritation. May be harmful if absorbed through the skin. Eyes: Causes eye irritation, characterized by a burning sensation, redness, tearing, inflammation, and possible corneal injury. Inhalation:
Inhalation at high concentrations affects the sense organs, brain and causes respiratory tract irritation. It also may affect the Central Nervous System (behavior) characterized by dizzness, drowsiness, confusion, headache, muscle weakeness, and possibly motor incoordination, speech abnormalities, narcotic effects and coma. Inhalation may also affect the gastrointestinal tract (nausea, vomiting). Ingestion: May cause irritation of the digestive (gastrointestinal) tract (nausea, vomiting). It may also affect the Central Nevous System (behavior), characterized by depression, fatigue, excitement, stupor, coma, headache, altered sleep time, ataxia, tremors as well at the blood, liver, and urinary system (kidney, bladder, ureter) and endocrine system. May also have musculoskeletal effects. Chronic Potential Health Effects: Skin: May cause dermatitis. Eyes: Eye irritation.

| ECOLOGICAL INFORMATION |
|---|
| ECOTOXICITY:<br>Ecotoxicity in water (LC50): 5540 mg/l 96 hours [Trout]. 8300 mg/l 96 hours [Bluegill]. 7500 mg/l 96 hours [Fatthead Minnow]. 0.1 ppm any hours [Water flea].<br><br>PRODUCTS OF BIODEGRADATION:<br>Possibly hazardous short term degradation products are not likely. However, long term degradation products may arise.<br><br>TOXICITY OF THE PRODUCTS OF BIODEGRADATION:<br>The product itself and its products of degradation are not toxic. |

| DISPOSAL CONSIDERATIONS |
|---|
| WASTE DISPOSAL:<br>Waste must be disposed of in accordance with federal, state and local environmental control regulations. |

| TRANSPORT INFORMATION |
|---|
| DOT CLASSIFICATION: CLASS 3: Flammable liquid.<br>IDENTIFICATION: Acetone UNNA: 1090 PG: II |

| OTHER REGULATORY INFORMATION |
|---|
| OSHA: Hazardous by definition of Hazard Communication Standard (29 CFR 1910.1200). EINECS: This product is on the European Inventory of Existing Commercial Chemical Substances.<br><br>PROTECTIVE EQUIPMENT:<br>Gloves. Lab coat. Vapor respirator. Be sure to use an approved/certified respirator or equivalent. Wear appropriate respirator when ventilation is inadequate. Splash goggles. |

**Appendix F2: Toluene Material Safety Data Sheet** (*Sciencelab.com, 2011*)

| Product Name | Toluene | | |
|---|---|---|---|
| Molecular formula | $C_6H_5CH_3$ or $C_7H_8$ | | Health 2 / Fire 3 / Reactivity 0 / Personal Protection H |

| PHYSICAL AND CHEMICAL PROPERTIES | | | |
|---|---|---|---|
| Physical state | Liquid | Boiling Point | 110.6˚C (231.1˚F) |
| Colour | Colorless | Melting Point | -95˚C (-139˚F) |
| Odour | Sweet, pungent, Benzene-like | Critical Temperature | 318.6˚C (605.5˚F) |
| Taste | Not Available | Specific Gravity | 0.8636 (Water = 1) |
| Solubility in others | Soluble in diethyl ether, acetone. Practically insoluble in cold water. Soluble in ethanol, benzene, chloroform, glacial acetic acid, carbon disulfide. Solubility in water: 0.561 g/l @ 25 ˚C | Vapour density | 3.1 (Air = 1) |
| Molecular weight | 92.14 g/mole | Vapour pressure | 3.8 kPa @ 25 ˚C |

| FIRE AND EXPLOSION DATA | |
|---|---|
| Flammability of the product | Flammable |
| Auto-ignition temperature | 480˚C (896˚F) |
| Flash Points | CLOSED CUP: 4.4444˚C (40˚F). (Setaflash) OPEN CUP: 16˚C (60.8 ˚F) |
| Flammable Limits | LOWER: 1.1% UPPER: 7.1% |
| Products of Combustion | These products are carbon oxides ($CO$, $CO_2$) |
| Fire Hazards in Presence of Various Substances | Flammable in presence of open flames and sparks, of heat. Non-flammable in presence of shocks. |
| Fire Fighting Media and Instructions | Flammable liquid, insoluble in water. SMALL FIRE: Use DRY chemical powder. LARGE FIRE: Use water spray or fog. |
| Special Remarks on Explosion Hazards | Toluene forms explosive reaction with 1, 3-dichloro-5, 5-dimethyl-2, 4-imidazolididione; dinitrogen tetraoxide; concentrated nitric acid, sulfuric acid + nitric acid; N2O4; AgClO4; BrF3; Uranium hexafluoride; sulfur dichloride. Also forms an explosive mixture with tetranitromethane. |

| | TOXICOLOGICAL DATA ON INGREDIENTS |
|---|---|

Toluene: ORAL (LD50): Acute: 636 mg/kg [Rat]. DERMAL (LD50): Acute: 14100 mg/kg [Rabbit]. VAPOR (LC50): Acute: 49000 mg/m 4 hours [Rat]. 440 ppm 24 hours [Mouse].

## HAZARDOUS IDENTIFICATION

POTENTIAL ACUTE HEALTH EFFECTS:
Hazardous in case of skin contact (irritant), of eye contact (irritant), of ingestion, of inhalation. Slightly hazardous in case of skin contact (permeator).

POTENTIAL CHRONIC HEALTH EFFECTS:
DEVELOPMENTAL TOXICITY: The substance may be toxic to blood, kidneys, the nervous system, liver, brain, central nervous system (CNS). Repeated or prolonged exposure to the substance can produce target organs damage.

## FIRST-AID MEASURES

| | |
|---|---|
| Eye Contact | Check for and remove any contact lenses. Immediately flush eyes with running water for at least 15 minutes, keeping eyelids open. Cold water may be used. Get medical attention. |
| Skin Contact | Immediately flush skin with plenty of water. Cover the irritated skin with an emollient. Remove contaminated clothing and shoes. Get medical attention. |
| Serious Skin Contact | Wash with a disinfectant soap and cover the contaminated skin with an anti-bacterial cream. Seek medical attention. |
| Inhalation | If inhaled, remove to fresh air. If not breathing, give artificial respiration. If breathing is difficult, give oxygen. Get medical attention. |
| Serious Inhalation | Evacuate the victim to a safe area as soon as possible. Loosen tight clothing such as collar, tie, belt or waistband. If breathing is difficult, administer oxygen. If the victim is not breathing, perform mouth-to-mouth resuscitation. Seek medical attention. |
| Ingestion | If swallowed, do not induce vomiting unless directed to do so by medical personnel. Never give anything by mouth to an unconscious person. If large quantities of this material are swallowed, call a physician immediately. Loosen tight clothing such as a collar, tie, belt or waistband. |

## ACCIDENTAL RELEASE MEASURES

SMALL SPILL:
Absorb with an inert material and put the spilled material in an appropriate waste disposal.

LARGE SPILL:
Toxic flammable liquid, insoluble or very slightly soluble in water. Keep away from heat. Keep away from sources of ignition.
Stop leak if without risk. Absorb with DRY earth, sand or other non-combustible material. Do not get water inside container.
Do not touch spilled material. Prevent entry into sewers, basements or confined areas; dike if needed. Call for assistance on disposal. Be careful that the product is not present at a concentration level above TLV. Check TLV on the MSDS and with local authorities.

## HANDLING AND STORAGE

PRECAUTIONS:
Keep away from heat. Keep away from sources of ignition. Ground all equipment containing material. Do not ingest. Do not breathe gas/fumes/ vapor/spray. Wear suitable protective clothing. In case of insufficient ventilation, wear suitable respiratory equipment. If ingested, seek medical advice immediately and show the container or the label. Avoid contact with skin and eyes. Keep away from incompatibles such as oxidizing agents.

STORAGE:
Store in a segregated and approved area. Keep container in a cool, well-ventilated area. Keep container tightly closed and sealed until ready for use. Avoid all possible sources of ignition (spark or flame).

## EXPOSURE CONTROLS/PERSONAL PROTECTION

ENGINEERING CONTROLS:
Provide exhaust ventilation or other engineering controls to keep the airborne concentrations of vapors below their respective threshold limit value. Ensure that eyewash stations and safety showers are proximal to the work-station location.

PERSONAL PROTECTION:
Splash goggles, lab coat and vapor respirator. Be sure to use an approved/certified respirator or equivalent. Gloves.

PERSONAL PROTECTION IN CASE OF A LARGE SPILL:
Splash goggles, full suit, vapour respirator, boots and gloves. A self-contained breathing apparatus should be used to avoid inhalation of the product. Suggested protective clothing might not be sufficient; consult a specialist BEFORE handling this product.

EXPOSURE LIMITS:
TWA: 200 STEL: 500 CEIL: 300 (ppm) from OSHA (PEL) [United States] TWA: 50 (ppm) from ACGIH (TLV) [United States]
SKIN TWA: 100 STEL: 150 from NIOSH [United States] TWA: 375 STEL: 560 (mg/m3) from NIOSH [United States] Consult local authorities for acceptable exposure limits.

| STABILITY AND REACTIVITY DATA |
|---|

STABILITY: The product is stable.
CONDITIONS OF INSTABILITY: Heat, ignition sources (flames, sparks, static), incompatible materials
INCOMPATIBILITY WITH VARIOUS SUBSTANCES: Reactive with oxidizing agents. CORROSIVITY: Non-corrosive in presence of glass.
SPECIAL REMARKS ON REACTIVITY: Incompatible with strong oxidizers, silver perchlorate, sodium difluoride, Tetranitromethane, Uranium Hexafluoride. Frozen Bromine Trifluoride reacts violently with Toluene at -80 deg. C. Reacts chemically with nitrogen oxides, or halogens to form
nitrotoluene, nitrobenzene, and nitrophenol and halogenated products, respectively.

| TOXICOLOGICAL INFORMATION |
|---|

ROUTES OF ENTRY: Absorbed through skin. Dermal contact. Eye contact. Inhalation. Ingestion

**TOXICITY TO ANIMALS:**
WARNING: THE LC50 VALUES HEREUNDER ARE ESTIMATED ON THE BASIS OF A 4-HOUR EXPOSURE. Acute oral toxicity (LD50): 636 mg/kg [Rat]. Acute dermal toxicity (LD50): 14100 mg/kg [Rabbit]. Acute toxicity of the vapor (LC50): 440, 24 hours [Mouse].

**CHRONIC EFFECTS ON HUMANS:**
CARCINOGENIC EFFECTS: A4 (Not classifiable for human or animal.) by ACGIH, 3 (Not classifiable for human.) by IARC.
May cause damage to the following organs: blood, kidneys, the nervous system, liver, brain, central nervous system (CNS).

**OTHER TOXIC EFFECTS ON HUMANS:**
Hazardous in case of skin contact (irritant), of ingestion, of inhalation. Slightly hazardous in case of skin contact (permeator).

**SPECIAL REMARKS ON TOXICITY TO ANIMALS:**
Lowest Published Lethal Dose: LDL [Human] - Route: Oral; Dose: 50 mg/kg LCL [Rabbit] - Route: Inhalation; Dose: 55000 ppm/40min

**SPECIAL REMARKS ON CHRONIC EFFECTS ON HUMANS:**
Detected in maternal milk in human. Passes through the placental barrier in human. Embryotoxic and/or foetotoxic in animal.
May cause adverse reproductive effects and birth defects (teratogenic). May affect genetic material (mutagenic).

**SPECIAL REMARKS ON OTHER TOXIC EFFECTS ON HUMANS:**
Acute Potential Health Effects: Skin: Causes mild to moderate skin irritation. It can be absorbed to some extent through the skin. Eyes: Cauess mild to moderate eye irritation with a burning sensation. Splash contact with eyes also causes conjunctivitis, blepharospasm, corneal edema, corneal abraisons. This usually resolves in 2 days. Inhalation: Inhalation of vapor may cause respiratory tract irritation causing coughing and wheezing, and nasal discharge. Inhalation of high concentrations may affect behavior and cause central nervous system effects characterized by nausea, headache, dizziness, tremors, restlessness, lightheadedness, exhilaration, memory loss, insomnia, impaired reaction time, drowsiness, ataxia, hallucinations, somnolence, muscle contraction or spasticity, unconsciousness and coma. Inhalation of high concentration of vapor may also affect the cardiovascular system (rapid heartbeat, heart palpitations, increased or decreased blood pressure, dysrhythmia), respiration (acute pulmonary edema, respiratory depression, apnea, asphyxia), cause vision disturbances and dilated pupils, and cause loss of appetite. Ingestion: Aspiration hazard. Aspiration of Toluene into the lungs may cause chemical pneumonitis. May cause irritation of the digestive tract with nausea, vomiting, pain. May have effects similar to that of acute inhalation. Chronic Potential Health Effects: Inhalation and Ingestion: Prolonged or repeated exposure via inhalation may cause central nervous system and cardiovascular symptoms similar to that of acute inhalation and ingestion as well liver damage/failure, kidney damage/failure (with hematuria, proteinuria, oliguria, renal tubular acidosis), brain damage, weight loss, blood (pigmented or nucleated red blood cells, changes in white blood cell count), bone marrow changes, electrolyte imbalances (Hypokalemia, Hypophostatemia), severe, muscle weakness and Rhabdomyolysis. Skin: Repeated or prolonged skin contact may cause defatting dermatitis.

## ECOLOGICAL INFORMATION

ECOTOXICITY:
Ecotoxicity in water (LC50): 313 mg/l 48 hours [Daphnia (daphnia)]. 17 mg/l 24 hours [Fish (Blue Gill)]. 13 mg/l 96 hours [Fish (Blue Gill)]. 56 mg/l 24 hours [Fish (Fathead minnow)]. 34 mg/l 96 hours [Fish (Fathead minnow)]. 56.8 ppm any hours [Fish (Goldfish)].

PRODUCTS OF BIODEGRADATION:
Possibly hazardous short term degradation products are not likely. However, long term degradation products may arise.

TOXICITY OF THE PRODUCTS OF BIODEGRADATION:
The products of degradation are less toxic than the product itself.

## DISPOSAL CONSIDERATIONS

WASTE DISPOSAL:
Waste must be disposed of in accordance with federal, state and local environmental control regulations.

## TRANSPORT INFORMATION

DOT CLASSIFICATION: CLASS 3: Flammable liquid.
IDENTIFICATION: Toluene UNNA: 1294 PG: II

## OTHER REGULATORY INFORMATION

OSHA: Hazardous by definition of Hazard Communication Standard (29 CFR 1910.1200). EINECS: This product is on the European Inventory of Existing Commercial Chemical Substances.

PROTECTIVE EQUIPMENT:
Gloves. Lab coat. Vapor respirator. Be sure to use an approved/certified respirator or equivalent. Wear appropriate respirator when ventilation is inadequate. Splash goggles.